

HYDROGEOLOGY AND HYDROCHEMISTRY OF THE FALLS CITY URANIUM MINE TAILINGS
REMEDIAL ACTION PROJECT, KARNES COUNTY, TEXAS

Charles W. Kreitler
Timothy J. Jackson
Patricia W. Dickerson
Jonathan G. Blount

Prepared for the
Texas Department of Health, Bureau of Radiation Control
under cooperative agreement no. IAC (92-93)-0389

Bureau of Economic Geology
W. L. Fisher, Director
The University of Texas at Austin
Austin, Texas 78713

September 1992

CONTENTS

INTRODUCTION (Section 1)	1
GEOLOGIC SETTING (Section 2)	7
Regional Depositional Environment	7
Surface Geology	7
Stratigraphy	7
Structure	11
Subsurface Geology	12
Distribution of Uranium	15
Summary	15
Uranium ore deposits	15
Radiometric data	17
Surface radiometric measurements	17
Borehole gamma logs	17
Geologic Influences on Ground-Water Movement	20
Geologic Influences on Sediment and Effluent Geochemistry	21
HYDROLOGIC CHARACTERIZATION (Section 3)	33
Methodology	33
Hydrogeology of the Deweesville Aquifer	36
Summary	36
Hydrogeology of the tailings piles and the Deweesville aquifer	36
Hydrogeology of the Conquista Aquifer	41
Summary	41
Hydrogeology of the tailings piles and Conquista aquifer	42
Hydrogeology of the Dilworth Aquifer	46
Summary	46
Background hydrogeology	47

Impact of mining and milling operations on hydrogeology of the Dilworth aquifer	48
HYDROCHEMICAL CHARACTERIZATION (Section 4)	79
Methodology	79
Characterization of the Tailings Solutions.....	81
Summary	81
Uranium ore processing	82
Major element chemistry of the tailings solutions.....	84
Trace element chemistry of the tailings solutions.....	86
Source of the tailings solution acidity	87
Acidity related to aluminum sulfate	88
Chloride-to-bromide ratios	92
Reactions of Tailings Solutions with Sediments.....	93
Summary	93
Neutralization of aluminum sulfate acidity by calcite	94
Neutralization by mixing with alkaline waters.....	96
Neutralization by reactions with aluminosilicates	98
Equilibrium with alunite.....	99
Exchange equilibria.....	100
Hydrochemistry of the Deweesville Aquifer	103
Summary	103
Introduction	104
Geochemical mapping	106
pH.....	106
Aluminum	106
Total dissolved solids	107
Ammonium.....	107
Calcium	107

Sulfate.....	108
Molybdenum in monitoring well 836	111
Chloride	112
Chloride-to-bromide ratios	114
Tritium	114
Cation trace metals	115
Anionic trace metals	117
Uranium	119
Radium	119
Hydrochemistry of the Upper Conquista Clay	120
Hydrochemistry of the Conquista Sand.....	120
Summary	120
Introduction	121
Geochemical mapping	122
pH.....	122
Aluminum	123
Total dissolved solids	123
Ammonium	123
Calcium	123
Calcite and gypsum saturation	124
Carbon dioxide partial pressure.....	125
Sulfate.....	125
Chloride	126
Chloride-to-bromide ratios	126
Tritium	127
Cation trace metals	127
Anionic trace metals	127

Uranium	128
Radium concentrations	128
Hydrochemistry of the Lower Conquista Clay	129
Hydrochemistry of the Dilworth Sandstone	129
Summary	129
Introduction	130
Geochemical mapping	131
Calcite and gypsum saturation	131
Hydrochemistry of the Manning Formation	133
Hydrochemistry along Scared Dog Creek	134
COMPUTER MODEL OF EXCHANGE AND NEUTRALIZATION REACTIONS (Section 5)	205
BATCH LEACH EXPERIMENTS (Core 869) (Section 6)	213
Methods	213
Core Description	214
Batch Leach Results	215
Discussion	217
Pyrite Oxidation	219
Leachate pH Profiles	220
STRATAMODEL (Section 7)	231
Methods	231
Three-Dimensional Views of Contaminant Plumes	232
CONCLUSIONS (Section 8)	237
Geologic Framework	237
Tailings Leakage	238
Tailings Hydrochemistry	239
Reactions of Tailings Solutions with Sediments	240
Delineation of the Contaminant Plumes	242

Deweesville.....	242
Conquista.....	244
Dilworth.....	246
Identification of Background Ground Waters.....	247
Natural Acid-Sulfate Sediments.....	249
Further Study.....	250
ACKNOWLEDGMENTS.....	256
REFERENCES.....	257
APPENDICES.....	265

ILLUSTRATIONS

Figures

1.1. Location of Falls City UMTRA site, Karnes County, Texas.....	4
1.2. Tailings piles and ground-water monitoring wells, Falls City UMTRA site.....	5
2.1. Depositional systems of the Eocene Jackson Group, coastal plain of South Texas.....	22
2.2. Geologic map of the site.....	23
2.3. Stratigraphic column and composite geophysical log of Whitsett and Manning Formations, Jackson Group (Eocene), in the vicinity of the UMTRA site.....	24
2.4. Locations of logged boreholes utilized in interpreting subsurface geology.....	25
2.5. Structure on top of Dilworth Sandstone Member.....	26
2.6. Isopach map of lower Conquista clay, Conquista Clay Member.....	27
2.7. Isopach map of Conquista Sandstone, Conquista Clay Member.....	28
2.8. Isopach map of upper Conquista clay, Conquista Clay Member.....	29
2.9. Isopach map of Deweesville Sandstone Member.....	30
2.10. Uranium mineralization and radiometric anomalies, Falls City UMTRA site.....	31
2.11. Examples of gamma anomalies in Deweesville sandstone and upper Conquista clay.....	32
3.1. Locations of ground-water-monitoring wells, Falls City UMTRA site.....	59

3.2.	Locations of monitoring wells and core holes drilled by Bureau of Economic Geology.....	60
3.3.	Comparison of April 1989 to May 1991 water levels in the same wells	61
3.4.	Potentiometric surface of Deweesville Sandstone Member aquifer.....	62
3.5.	Water elevation versus land-surface elevation for Deweesville aquifer	63
3.6.	Depth to water in boreholes versus land-surface elevation for Deweesville aquifer.....	64
3.7.	Water levels versus top of Deweesville aquifer, indicating whether aquifer setting is confined or unconfined	65
3.8.	Intersections of water level with land surface, indicating approximate elevations of discharge	66
3.9.	Elevation of potentiometric surface of Deweesville/Conquista aquifer around tailings piles.....	67
3.10.	Comparison of water levels in tailings pile 2 to those in SEI monitoring well 2-2	68
3.11.	Comparison of water levels in tailings pile 2 to those in SEI monitoring well 2-5	68
3.12.	Comparison of water levels in tailings pile 2 to those in SEI monitoring well 2-9	69
3.13.	Comparison of water levels in tailings pile 2 to those in SEI monitoring well 7-11	69
3.14.	Potentiometric surface of the Conquista aquifer	70
3.15.	Water level versus land-surface elevation for the three subunits within the Conquista aquifer	71
3.16.	Water levels versus elevation of top of the Conquista aquifer, indicating whether aquifer setting is confined or unconfined	72
3.17.	Water levels versus elevation of top of the Conquista Sand, indicating whether aquifer is confined or unconfined	73
3.18.	Potentiometric surface of the Dilworth aquifer	74
3.19.	Water levels versus elevation of top of Dilworth aquifer	75
3.20.	Water levels versus land-surface elevation, Dilworth aquifer	76
3.21.	Intersection of water level with land surface, indicating possible elevation of discharge	77
4.1.	Aluminum versus pH in ground waters and tailings solutions.....	136
4.2.	Acidity titrations demonstrating pH buffering by aluminum and iron sulfate	137
4.3.	Frequency diagram of ground water and tailings solution pH measurements	138
4.4.	Chloride versus bromide of tailings solutions and natural ground waters.....	139

4.5.	Potassium feldspar and clinoptilolite equilibria diagrams	140
4.6.	Sodium feldspar (albite) equilibrium diagram	141
4.7.	Sodium and calcium-smectite equilibria diagrams	142
4.8.	Alunite equilibrium diagram	143
4.9.	Calcium-strontium and calcium-magnesium exchange equilibria	144
4.10.	Calcium-sodium and calcium-ammonium exchange equilibria	145
4.11.	Locations of Deweesville monitoring wells, tailings piles, and Deweesville sandstone outcrop	146
4.12.	pH of Deweesville ground waters	147
4.13.	Aluminum in Deweesville ground waters	148
4.14.	Total dissolved solids in Deweesville ground waters	149
4.15.	Calcium in Deweesville ground waters	150
4.16.	Sulfate in Deweesville ground waters	151
4.17.	Sulfate versus calcium in Deweesville ground waters and values of tailings solution in piles 4 and 5	152
4.18.	Molybdenum in Deweesville ground waters	153
4.19.	Chloride concentration in ground waters versus depth	154
4.20.	Chloride in Deweesville ground waters	155
4.21.	Chloride versus bromide in Deweesville ground waters and tailings solutions	156
4.22.	Tritium in Deweesville ground waters	157
4.23.	Average normalized cation trace metals in Deweesville ground waters	158
4.24.	Effect of pH on cation trace metal species	159
4.25.	Radium in Deweesville ground waters	160
4.26.	Locations of upper and lower Conquista clay monitoring wells	161
4.27.	Locations of Conquista fossiliferous sandstone monitoring wells	162
4.28.	pH in Conquista fossiliferous sandstone ground waters	163
4.29.	Aluminum in Conquista fossiliferous sandstone ground waters	164
4.30.	Total dissolved solids in Conquista fossiliferous sandstone ground waters	165

4.31.	Calcium, calcite saturation, and carbon dioxide partial pressure in Conquista fossiliferous sandstone ground waters	166
4.32.	Chloride in Conquista fossiliferous sandstone ground waters	167
4.33.	Chloride versus bromide in Conquista fossiliferous sandstone ground waters and tailings solutions in pile 7.....	168
4.34.	Tritium in Conquista fossiliferous sandstone ground waters.....	169
4.35.	Locations of Dilworth Sandstone Member monitoring wells	170
4.36.	Calcite saturation of Dilworth sandstone ground waters.....	171
4.37.	Sulfide in Dilworth sandstone ground waters	172
4.38.	Uranium in Dilworth sandstone ground waters.....	173
4.39.	Locations of monitoring wells in Manning Formation	174
4.40.	Dilute acidic aluminum sulfate plume along Scared Dog Creek.....	175
4.41.	Chloride versus bromide in ground waters near tailings pile 3 (eastern area).....	176
6.1.	pH and water-soluble major elements, core 869	222
6.2.	Water-soluble trace elements, core 869	223
6.3.	Relation of trace metals to pH	224
6.4.	pH of leachates from sediments treated with water	225
7.1.	Geology and topography of Falls City UMTRA site.....	234
7.2.	Aluminum concentration in Deweesville sandstone aquifer	234
7.3.	Calcium in Conquista fossiliferous sandstone aquifer	235
7.4.	Aluminum in Conquista fossiliferous sandstone aquifer	235
8.1.	Identified contaminant plumes, Falls City UMTRA site.....	253
8.2.	Oxidation-reduction fronts in the Dilworth, Conquista, and Deweesville sandstones	254
8.3.	Monitoring wells for ascertaining probable background concentrations	255

Tables

3.1.	Water-level data for the Deweesville aquifer	50
3.2.	Comparison of water levels measured in SEI wells with water levels measured in DOE wells in 1991	52
3.3.	Water-level data for M-2 (pile 2) and monitoring wells near pond 2 during SEI in situ leaching	53
3.4.	Water-level data for the Conquista aquifer	55
3.5.	Water-level data for the Dilworth aquifer	56
4.1.	Tailings water chemistry—lysimeter and well data	177
4.2.	Major constituents of tailings solutions expressed as neutral salts	180
4.3.	Comparison of an average tailings solution to an average shale	181
4.4.	Tailings solution saturation indices for selected solids	182
4.5.	Computer-simulated neutralization of an aluminum sulfate solution by calcium carbonate (calcite)	183
4.6.	Computer-simulated neutralization of an aluminum sulfate solution by a bicarbonate solution	184
4.7.	Water chemistry of the Deweesville sandstone aquifer	185
4.8.	Normalized metals in Deweesville ground waters	188
4.9.	Trace metals in waters associated with uranium mines	189
4.10.	Water chemistry of the upper Conquista clay	190
4.11.	Normalized metals in ground waters of Conquista clays	191
4.12.	Water chemistry of Conquista fossiliferous sandstone	192
4.13.	Normalized metals in ground waters of Conquista fossiliferous sandstone	194
4.14.	Water chemistry of the lower Conquista clay	195
4.15.	Water chemistry of Dilworth sandstone	196
4.16.	Water chemistry of Manning Formation	200
4.17.	Water chemistries in eastern area around tailings pile 3	202

5.1. Model of a reaction in which waters having the composition of sample 625 react to become waters having the composition of sample 914	211
6.1. Results of water-leach experiment, core 869—water-soluble major elements and pH	226
6.2. Results of acid-leach experiment, core 869—water-soluble trace elements	229

INTRODUCTION (SECTION 1)

Oxidized uranium ore deposits were discovered in the Deweesville sandstone (also referred to as the Stones Switch; Bunker and MacKallor [1973]) in the Falls City region in the 1950's. Uranium was mined and milled in the small community of Deweesville by Susquehanna-Western, Inc. (SWI) from April 1961 to August 1973. Tailings composed of sediment residue from the sulfuric acid milling process and residual sulfuric acid solutions were disposed of in six ponds on the outcrop of the Deweesville, within the mined-out uranium pits in the Deweesville, and on the outcrop of the Conquista, creating a set of large tailings impoundments (figs. 1.1 and 1.2). From 1978 to 1982 Solution Engineering, Inc. (SEI) conducted a secondary recovery of the remaining uranium in the tailings piles by in situ leaching. In 1984 the ponds on top of two of the tailings piles were spray evaporated and a clay cap was placed over the piles to prevent additional percolation of water through the piles and into the underlying aquifers. Acidic tailings solutions have been recharging the underlying aquifers since initial tailings disposal and may still be leaking into these aquifers.

Several hydrogeologic investigations have been conducted to assess whether there has been ground-water contamination from the tailings. Early studies were conducted by Turk, Kehle and Associates (1976), and Ford, Bacon & Davis Utah (1978, 1981). Each of these studies included only minor investigations of the hydrogeology and hydrochemistry of the site and, in general, underestimated the extent of contamination from the site. Investigations conducted by the U.S. Department of Energy (DOE) from 1985 to 1991 have since revealed the true extent of contamination (U.S. Department of Energy, 1991).

A Master's thesis by Bryson (1987) summarized some of the early DOE findings:

1. Extensive contaminant plumes existed in the shallow aquifers. Bryson mapped plumes for different contaminants and found no overlap between them. This created a complex and unexplained pattern of contamination.
2. The plumes were migrating at rates fast enough to be of concern and would soon migrate beyond the bounds of the original site. Because of their fast migration rates, remediation strategies should be considered to either clean up or constrain the plumes.

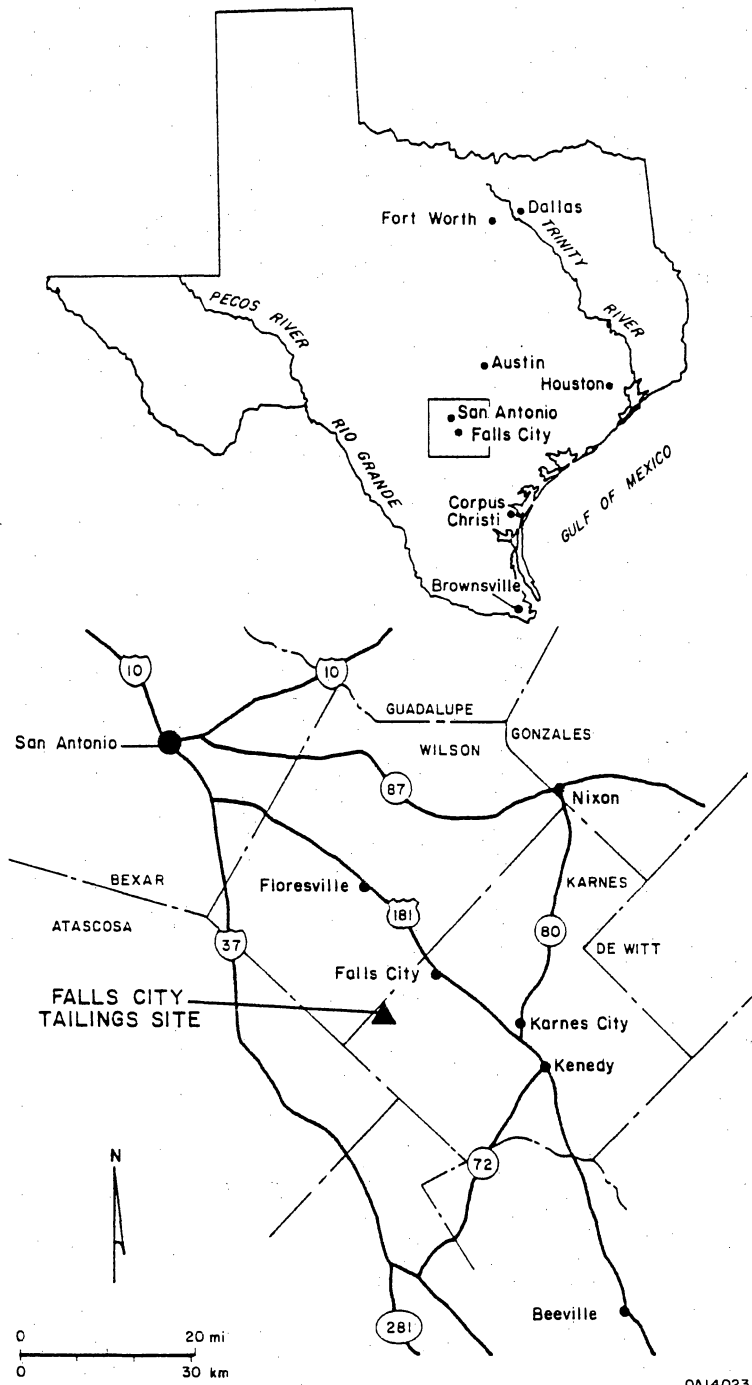
Later studies (U.S. Department of Energy, 1990) raised additional concerns:

1. Differentiating background water chemistry of the aquifers from plume chemistry was impossible. The extent of contamination could not be determined because the chemical signatures of the plumes could not be distinguished from that of background waters.
2. The chemical composition of natural waters could not be determined; it was unknown if the natural ground water was potable. Because of the occurrence of uranium deposits in the aquifers, concentrations of hazardous species in the ground water such as uranium, selenium, arsenic, molybdenum, and radium may have been higher than Environmental Protection Agency (EPA)-allowed concentrations prior to mining. Ground-water quality may be improved beyond the quality of the natural waters as a result of remediation of the plumes.

The Bureau of Economic Geology (BEG), The University of Texas at Austin, proposed a detailed geologic/hydrologic/hydrochemical characterization of the Falls City Uranium Mill Tailings Remedial Action (UMTRA) site in response to the problems recognized by Bryson (1987) and U.S. Department of Energy (1991). This characterization was designed to address the following issues:

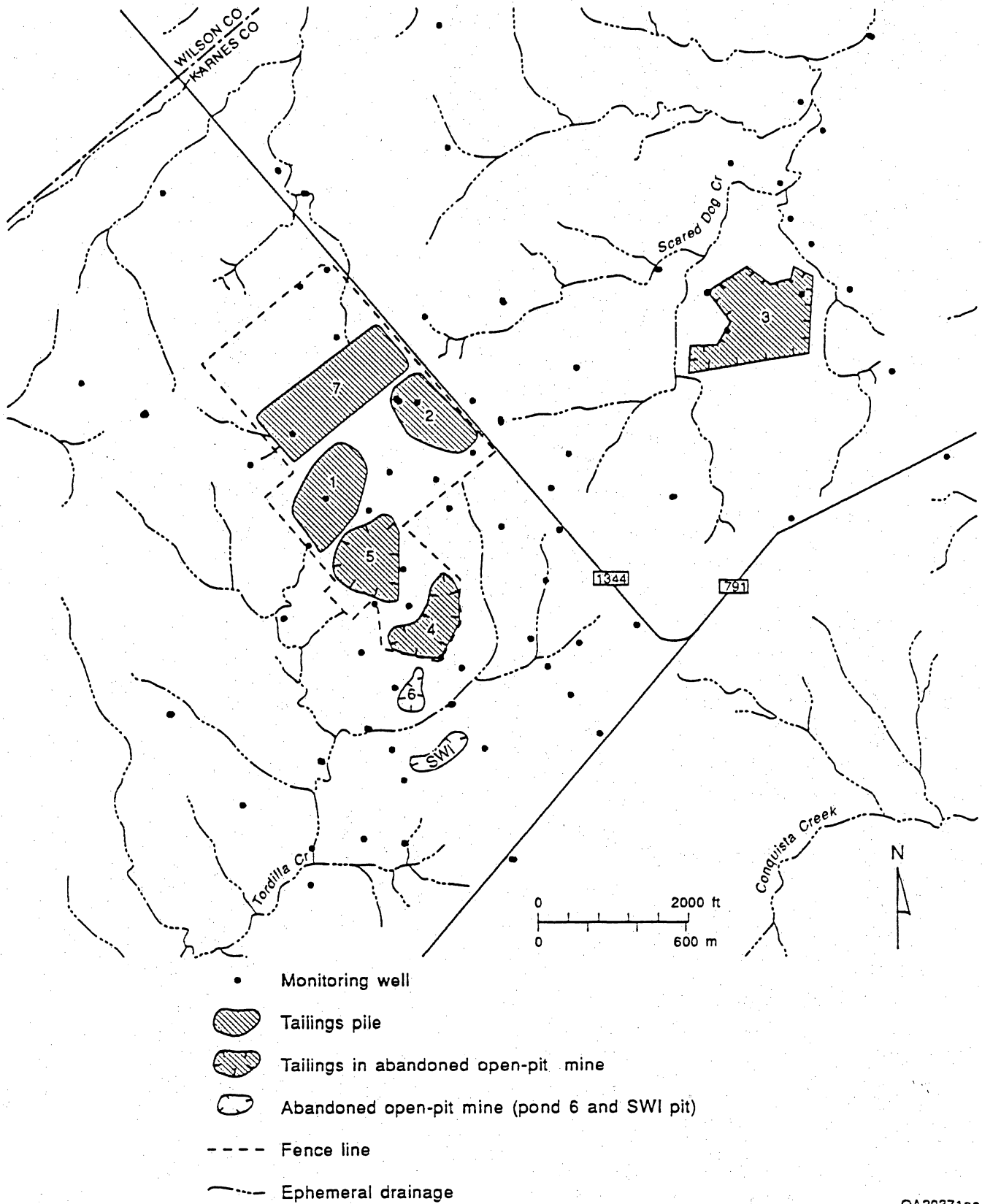
1. Aquifer geology required better definition to permit separation of the different lithologic units within the shallow aquifer (Bryson, 1987).
2. Hydrogeologic conditions of each aquifer (Conquista, Deweesville, and Dilworth) needed to be determined to evaluate ground-water flow directions, zones of recharge and discharge, and the impact of tailings disposal and in situ leaching on the general ground-water conditions.
3. The contaminant plumes unique to each aquifer, if present, should be defined, and the extent and direction of plume migration should be determined.
4. Important geochemical reactions that are altering the chemical composition of the plumes, as well as natural geochemical processes that may be remediating the plumes, need to be identified.
5. Background water chemistry should be defined by determining the chemical composition of the plume waters.

The report that follows addresses these five issues by (1) providing a detailed geologic characterization of the aquifers, (2) mapping the ground-water flow system in each aquifer, (3) delineating the major plumes, (4) describing the chemistry of the tailings solutions and their subsequent geochemical reactions with the rock matrix, and (5) characterizing chemical composition of the natural ground water in the aquifers.



QA14023

Figure 1.1. Location of Falls City UMTRA site, Karnes County, Texas.



QA20371ac

Figure 1.2. Tailings piles and ground-water monitoring wells, Falls City UMTRA site.

GEOLOGIC SETTING (SECTION 2)

Regional Depositional Environment

The Falls City, Texas, UMTRA site is on outcrops of the Eocene Jackson Group. Those strata are elements of the vast siliciclastic wedge of the South Texas Coastal Plain, accumulation of which spanned all Tertiary time. Sand, mud, and lignite of the Jackson part of that major progradational suite attain thicknesses of 1,000 ft.

Strandplain, barrier-bar, shelf, and lagoon systems constitute the depositional mosaic in this part of the coastal plain. Sediments of the Manning and Whitsett Formations near the Falls City mine and mill site are products of strandplain-barrier and probably prodelta sedimentation (fig. 2.1). Summaries of Eocene depositional systems and of the regional geology with respect to uranium ore concentration can be found in Galloway (1979), Eargle and Weeks (1973), and Eargle and others (1975).

Surface Geology

The surficial geology of the mine and mill site (fig. 2.2) has been compiled primarily from publications and open-file materials of the U.S. Geological Survey (USGS) (Bunker and MacKallor, 1973; MacKallor and others, 1962; Eargle and others, 1971; Manger and Eargle, 1967). Lithostratigraphic information from the Crystal City-Eagle Pass sheet of the Geologic Atlas of Texas (Barnes, 1976) and more recent observations from Bryson (1987) and McCulloh and Roberts (1981) were also incorporated.

Stratigraphy

Strata of the upper part of the Jackson Group (Eocene) are exposed at the surface of the site (fig. 2.3). The influence of regional Tertiary depositional systems on uranium ore localization have been studied previously (Folk and others, 1961; Fisher and others,

1970; Galloway, 1979; Henry and others, 1982). Sedimentary units from the Manning Formation upward through the Dubose Member of the Whitsett are elements of a nearshore marine sand/shale sequence.

The Manning Formation is the lowermost unit considered in this investigation. The outcrop belt is as much as 3.5 mi wide and thickness ranges from 250 to 350 ft. Tuffaceous, carbonaceous to lignitic shale is the dominant lithology, with subordinate interbedded sandstone.

Overlying the Manning in the study area are four of the six members of the Whitsett Formation (ascending): Dilworth Sandstone, Conquista clay, Deweesville sandstone, and Dubose Claystone. The Dilworth Sandstone Member consists primarily of fine-grained quartz sandstone with interbedded silt and clay; clay and silt content are more variable in the upper section than in the lower Dilworth. Burrowing is common throughout. A lignite layer generally intervenes between the sandstone of the Dilworth and the overlying lower Conquista clay.

The Dilworth outcrop extends farther south into the northeast corner of the map area (fig. 2.2) than was mapped by previous workers. The revision resulted from field checking and reconciliation of borehole and surface geological relations during this study. Lithologic and geophysical properties of the Dilworth and lower Conquista, relative to ground-water movement, are discussed elsewhere (page 20).

The Conquista clay Member comprises three lithofacies—an upper and a lower claystone and an intervening fossiliferous sandstone. The entire Conquista section in this area is silty and bentonitic, and the lower two units contain calcareous concretions, some as large as 3 by 8 ft. The claystones are generally similar, but the upper interval is siltier whereas the lower is more carbonaceous and contains larger concretions.

The Conquista sand is very fine to medium grained, bentonitic, crossbedded, and fossiliferous; pelecypods (*Corbicula*) are common throughout, with fewer small gastropods. The sand bodies are strike-parallel and change thickness both along strike

and downdip; clay and silt content of the sand varies with the thickness. Geometry, lithology, and fossil content indicate deposition in discontinuous linear nearshore shoals.

The principal uranium-bearing unit in the sequence is the Deweesville Sandstone Member, the thickness of which ranges from 46 ft to an erosional feather edge across the study area. The interval has been described and mapped in its context as a uranium host by several authors (Eargle and Snider, 1957; Moxham and Eargle, 1961; MacKallor and others, 1962; Eargle and others, 1971, 1975; Bunker and MacKallor, 1973; Eargle and Weeks, 1973).

The Deweesville sandstone is interpreted as an upward-coarsening progradational sequence deposited in a barrier-strandplain or possibly delta-front environment (McCulloh and Roberts, 1981; Deweesville = Stones Switch of these authors). It is a tuffaceous, fine- to coarse-grained quartz sand that contains varying amounts of gypsum, lignite and carbonaceous material, clay, volcanic ash, and bentonite. Silicified and carbonate-cemented zones are found throughout the unit.

Bunker and MacKallor (1973) identified three facies (1) sand, (2) intercalated sand and clay, and (3) a clay-filled channel. As did McCulloh and Roberts (1981) we found no evidence of a clay-filled channel, which had been described in considerable detail by USGS geologists. Such a clay body would influence not only ore localization in the Deweesville, as discussed by Bunker and MacKallor (1973), but also ground-water and contaminant movement in the permeable sandstone.

Because of the geohydrologic implications, we carefully reviewed all surface and subsurface (lithologic and log) data across the area where the channel had been mapped. In addition, we reviewed the results of a surface resistivity survey by the Bureau of Radiation Control (Texas) that was conducted to locate the feature; none was found (Price, unpublished report, 1991). This apparent absence of the clay body has

been perplexing because our investigations have been in accord with, and have confirmed many other aspects of, previous interpretations.

Delineation of mined, trenched, backfilled, and otherwise disturbed parts of the site, however, may provide an explanation for the absence of the clay body. The swath of ground occupied by the channel before mining began has since been entirely reworked. Pits have been dug through the zone, probably because exploration drilling confirmed Bunker and MacKallor's (1973) suggestion that ore could be concentrated in the sandstone immediately updip of the clay-filled channel. Some of the pits were backfilled with tailings and surface scrapings, which has further disrupted the stratigraphy. Other areas have been completely recontoured. Thus, the clay-filled channel was either removed or obscured by mining operations, and it is no longer to be considered a factor in the ground-water or contaminant-plume flow at the site.

McCulloh and Roberts (1981) observed within the Deweesville a lower sandstone section overlain by a 2- to 5-ft-thick silty lignitic/organic zone in the middle, and a fine- to coarse-grained sandstone at the top. This character was seen in the Searcy-Niestroy deposit before the pit was reclaimed. Farther updip the Deweesville loses this stratified aspect; the difference may result from pervasive oxidation in outcrop and probably does not reflect a primary facies change.

The Dubose Clay Member consists primarily of bentonitic claystone with tuffaceous and locally carbonaceous siltstone and sandstone; beds are 2 to 5 ft thick. Because of the variable lithology, thin-bedded character, and lack of evidence of brackish-water deposition, this interval is interpreted as a bay-margin to delta-front suite (Bunker and MacKallor, 1973). Thickness ranges from about 50 ft in the southeast to an erosional edge across the site.

Caliche has formed locally at the surface, primarily where more calcareous formations are exposed. Thickness of the caliche zones was not determined. During field reconnaissance we observed caliche on Conquista sandstone outcrops northeast of

tailings pile 7, as well as on Deweesville sandstone south and east of tailings piles 2 and 4.

Structure

Regional strike of Jackson Group strata is northeast (fig. 2.1); dip is southeast from 20 to 60 ft/1,000 ft (1 to 4 degrees), which is less than the regional dip of the Group over most of the coastal plain. The area of investigation is within what Bunker and MacKallor (1973) described as “. . .the warped downthrown block between the ends of two normal northeast-trending en echelon faults. The Falls City fault, north and northeast of the deposits. . . is downthrown to the southeast; the Fashing fault, south and southwest of the deposits, is downthrown to the northwest.” Bunker and MacKallor observed no faults at the site in the course of their surface and subsurface mapping, and none was detected by seismic and resistivity surveying. However, as they pointed out, the lenticular nature and variable facies of the sedimentary strata at the site make detection of small-displacement faults almost impossible.

At the northwest corner of the site (northwest of Bunker and MacKallor's [1973] area of interest) is a northeasterly fault segment that coincides with the Manning–Dilworth contact, as well as with the Karnes–Wilson county line. It parallels the Falls City fault, and displacement is down to the southeast. Roughly 0.5 mi to the east-southeast another parallel fault with the same sense of displacement is inferred to cut the lower Conquista clay.

The only folds that have been mapped in the vicinity are between the SWI pit and Farm Road 791. An anticline and syncline have slightly warped the Deweesville sandstone at the surface; both folds strike west-northwest and are less than 0.5 mi long.

Immediately east of tailings pile 3 and west of the nearby drainage (fig. 2.2) is a 10- to 15-ft-high north-trending scarp, which we examined and sampled during our

reconnaissance of the site. The Deweesville sandstone is brecciated and thoroughly silica-cemented, making the low ridge resistant to erosion. Although Bunker and MacKallor (1973) do not discuss this feature, they do mention north-northeast-trending joints in the northeastern map area, as well as a set that parallels the regional strike and one in the dip direction. Silicification may or may not be related to jointing or faulting, as silicified patches are found in sandier intervals throughout the stratigraphic section over the site.

Subsurface Geology

Thickness, lateral continuity, and both vertical and horizontal lithofacies variability of stratigraphic units were examined to better understand ground-water movement and contaminant distribution at the site. These data were also used in constructing three-dimensional stratigraphic and geochemical models.

Subsurface data, in order of utility and reliability, included (1) core descriptions from BEG stratigraphic boreholes and CONOCO exploration boreholes; (2) cuttings descriptions from Jacobs Engineering Group (JEG/DOE) and BEG water-quality monitoring wells; (3) geophysical logs from JEG and BEG monitoring wells; and (4) geophysical logs from SWI and CONOCO exploration boreholes (fig. 2.4). Objectives of the BEG coring program were to obtain detailed information on lithology and contact relations among strata; to compare units affected by tailings fluids with the same units where unaffected; to ascertain mineralogic changes in the sediments resulting from contact with effluent; and to obtain samples for evaluating the effects of reducing sediments on contaminants.

Geophysical logs for JEG/DOE and BEG wells are of generally good quality; gamma-ray, resistivity, and spontaneous potential traces were recorded. SWI and CONOCO logs consist of gamma-ray and, for most, resistivity traces, but data quality is quite variable.

The principal utility of the geophysical logs is in correlation of stratigraphic units. Little lithologic information could be extracted, especially in the shallower section, for several reasons:

- (1) Because of the presence of radiogenic material, gamma responses in the shallow section, irrespective of lithology, are anomalously high and noisy.
- (2) Because of their greater permeability, sandy intervals at the site commonly contain more radiogenic material than do shales. Gamma readings of shales in typical sand/shale sequences are usually higher than those of sands; in this area that relation may or may not hold, and the two cannot be reliably distinguished on the basis of gamma-log character.
- (3) As natural background radiation levels are higher in the area, some exploration logs were recorded using an elevated gamma-radiation base value. In several instances the change in base level was not noted on the log header.
- (4) Major excursions of all curves—gamma, resistivity, and spontaneous potential—coincided with the top of the water table, as well as with tops of the perched water zones at the site. Where no lithologic descriptions were available, this further complicated interpretation of the lithostratigraphy, particularly before the presence of multiple water-bearing zones at varying depths was recognized.

On the basis of available surface and subsurface data, structure on the top of the Dilworth sandstone was mapped (fig. 2.5); isopach maps of the three Conquista facies and of the Deweesville sandstone were also prepared (figs. 2.6 through 2.9). The entire suite of sands and shales was deposited in a strike-parallel system that transects the site from northeast to southwest, and the relative thicks and thins of each unit are so oriented.

The top of the Dilworth Sandstone Member displays no significant structural disruption, the only trend being gradual regional dip. The lower Conquista clay, which was deposited on that surface, shows thickness variations related to sedimentary processes and differential compaction. The clays and silty clays of this unit range from 20 to 43 ft over most of the site and feather out along the northern erosional limit (fig. 2.6). Only two local anomalies interrupt the otherwise smoothly varying thickness—a thin patch south of tailings pile 3 and a thick one in the north-central part of the map. The thickest portion of this unit constitutes a reasonably continuous belt transecting the northern half of the map area.

The Conquista sand facies shows greater local variation than do the shales of the member; over most of the area, though, the thickness of the entire interval is between 5 and 25 ft (fig. 2.7). It reaches a maximum thickness of 27 ft and thins to nil along the northern outcrop limit; thinning of the unit can also be seen where Scared Dog Creek has cut into the sandstone outcrop. Where thinner, the sand also contains more clay and silt. Strike-parallel thickness and lithologic changes, as well as fossil content, suggest deposition in a nearshore marine setting with linear shoals.

Although the outcrop limit is more complex in the southwestern part of the area, the upper Conquista clay shows few local variations. The interval is generally between 15 and 30 ft thick, with erosion to nil across along drainages in the southwest and along the northern outcrop edge (fig. 2.8). In contrast with the lower Conquista clay, the thickest preserved portion is in the center of the site.

Deweeseville sandstone isopach values vary smoothly across the area of investigation and show the familiar strike-parallel pattern (fig. 2.9). Two small outliers have been preserved from erosion (east-central), and are shown as isolated 15-ft-thick patches. The unit thickens gradually from an erosional feather edge to a maximum of 46 ft, with a broad expanse under most of the site, where the thickness is 25 to 28 ft.

Distribution of Uranium

Uranium mineralization is present in all geologic strata at the site, including the Dubose, Deweesville, Conquista (upper, sand/shell, and lower), and Dilworth. The major commercial-grade uranium ores were predominantly in the Deweesville sandstone and at the top of the upper Conquista clay. Uranium mineralization is also indicated through chemical analysis of sediment/core samples, ground radiometric surveys, and gamma-ray logging (fig. 2.10). The distribution of uranium and of radiometric anomalies in the Falls City area are described in greater detail in the next sections.

Summary

Radiometric anomalies and chemical uranium are widely distributed in the Deweesville and other formations at the Falls City UMTRA site. Remobilization of the ore after its original deposition has further dispersed uranium through the formations. Gamma anomalies recorded in monitoring wells where no tritium was present in the formation waters, as well as those in holes drilled early in the mining operations, indicate that the anomalies are related to ore-forming processes and not to the migration of tailings fluids.

Uranium Ore Deposits

Uranium has been mined from three principal ore deposits in the Deweesville/upper Conquista: the Nuhn ore deposit, the Continental (Lockett) ore deposit, and the Searcy-Niestroy deposit. The Nuhn and Continental deposits, as delineated by MacKallor and others (1962) and described by Bunker and MacKallor (1973), appear to be epigenetic deposits that are composed predominantly of oxidized uranium minerals. The Searcy-Niestroy mine may have exploited what was originally a

roll-front deposit. The latest recorded open-pit mining was by CONOCO in the early 1980's, from a small mine southwest of the SWI pond.

Uranium mineralization in the Deweesville/upper Conquista is not limited to the mined ore bodies. Companies have mined ever-widening halos of lower grade ore away from the earliest operations. In addition to the aureole of uranium surrounding the old pits, significant mineralization still remains in the ground in the region.

McCulloh and Roberts (1981) mapped the distribution of a 2-ft-thick interval bearing 0.03 percent U_3O_8 using core assay data, as well as the distribution of chemical ore for the lower, middle, and upper gamma peaks in the Deweesville. In this area, on the tract south of tailings pile 4, pond 6, and the SWI pit, almost all of the formation contained uranium mineralization (fig. 2.10). In this downdip section of the Deweesville, most of the ore appears to be associated with the lignitic/carbonaceous middle zone. Mining has been primarily from the outcrop of the Deweesville, where the bulk of the ore is in the basal Deweesville and uppermost Conquista. The ore associated with the shallower gamma anomaly appears to have migrated farther downdip than has the ore associated with the deeper high-gamma zone. This may indicate greater oxidation in the shallower and stratigraphically younger sections of the formation, which is to be expected as the oxidizing zone appears to be moving downward from the land surface (McCulloh and Roberts, 1981).

McCulloh and Roberts (1981) identified six ore deposits along a redox boundary within the outcrop (or slightly downdip) of the Dilworth Formation; one outcrop area was mined. Only two of those deposits are shown in figure 2.10. Little information about this mining operation has been located.

Radiometric Data

Review of radiometric data from the Falls City area indicates that radioactive elements (uranium and daughter products) are more widespread than was indicated by the available data for chemical ore. Two types of radiometric data—ground radiometric data and gamma borehole logs—further identify the presence of uranium.

Surface Radiometric Measurements

MacKallor and others (1962) made surface radiometric measurements in the Deweesville area and found high radiometric anomalies over the Nuhn (Climax) deposit. Values as high as 5,000 microrentgen per hour were recorded where ore was exposed at land surface. These measurements include a very small cosmic component of 3 microrentgen per hour. Other anomalous areas are along the northwest end of the Nuhn deposit in the outcrop of the Deweesville, beneath tailings pile 2 in the Deweesville, and in the outcrop of the Conquista sand west of the Nuhn deposit. No radiometric anomaly is indicated over the Continental deposit (fig. 2.10), suggesting that a radiometric survey was not conducted in this region (see MacKallor and others, 1962).

Borehole Gamma Logs

Borehole gamma logging is a common geophysical method in exploration for uranium ore deposits. In normal nonuraniferous sedimentary settings, increased gamma counts are typical for shale strata because of the higher concentration of trace radioactive elements, such as ^{40}K , in shales as compared to sandstones. In uraniferous deposits, increased concentrations of ^{234}U , ^{238}U , ^{232}Th , ^{40}K , ^{222}Rn , ^{226}Ra , ^{228}Ra , ^{214}Pb , and ^{214}Bi result in high gamma counts. Gamma measurements can be empirically compared to chemical analyses of uranium concentrations if radiometric and chemical

uranium data are sufficient. Significant gamma anomalies are observed in the following formations: Dubose, Deweesville, upper Conquista, Conquista sand, lower Conquista, and Dilworth (appendix table 7).

Most major anomalies (greater than 200 cps) are observed in the Deweesville, with progressively fewer and weaker ones in the upper Conquista, Conquista sand, Dubose, lower Conquista, and the Dilworth. Forty-three of 56 wells penetrated at least 1 formation with a gamma anomaly greater than 200 cps. The log for well 863 (fig. 2.11) displays a gamma anomaly at the contact between the Deweesville and upper Conquista clay.

The occurrence of uranium in all strata at the site may indicate that volcanic ash, a possible uranium source, was deposited throughout Jackson Group sediments.

Alternatively, uranium may have been concentrated in the Deweesville, the principal ore-bearing unit, from the outset. The presence of radiogenic uranium in members that crop out updip from the present Deweesville outcrop limit may indicate pre-erosion transport by local ground-water flow. Movement into stratigraphically lower units could have occurred when the Deweesville was more geographically extensive.

The presence of uranium in Tertiary strata other than the Deweesville and some of the radiometric anomalies within the Deweesville might also have resulted from the migration of uranium-rich mill tailings fluids or remobilization and precipitation by acidic mill tailings fluids. The presence of radiometric anomalies in the Dilworth at depths of 100, 105, and 126 ft in well 831 beneath the tailings piles suggests possible downward migration of uranium-rich waters. Waters from this well, however, had a tritium (^3H) concentration of 0.02 tritium units (E. Storm, oral communication, 1991), indicating that the formation water predates any milling operations. This gamma anomaly reflects natural ore-forming processes, not migration of tailings fluids.

Gamma anomalies in a uraniferous geologic setting indicate the presence of uranium near the measured borehole, but a high gamma anomaly does not always

indicate a high concentration of uranium at the exact location of the borehole because of the potential of disequilibrium. A gamma anomaly results primarily from the radioactive buildup of radium and its daughter products ^{214}Pb and ^{214}Bi . This buildup takes approximately 300,000 yr. However, oxidizing ground water can remobilize the uranium from an original deposit and move it down hydrologic gradient within this time, resulting in separation of the mobile uranium from less soluble gamma-emitting radium and daughter products. This separation of the uranium from the gamma emitters is referred to as disequilibrium; estimates of uranium concentration from radiometric logs must be compared with chemical analyses of the host to determine true uranium concentration.

Bunker and MacKallor (1973) compared gamma-log response to chemical analyses of ore-grade mineralization and found evidence of disequilibrium, particularly at lower grades. McCulloh and Roberts (1981) found chemical uranium ore farther downdip than the radiogenic ore in the Deweesville confined beneath the Dubose, suggesting remobilization of uranium by oxidizing ground water. This disequilibrium through remobilization will result in an additional separation of uranium and its daughter products. Uranium and associated trace metals such as Se, Mo, and As may be reconcentrated downdip in more reducing sediments, whereas the radioactive daughter products may remain in the oxidized portions of the original host sediments. Detailed geochemical analyses of the gamma anomalies may indicate that Ra, Pb, and Bi (as examples) are concentrated in the unsaturated section. This may explain the high radioactivity that Bunker and MacKallor (1973) measured from ground geophysical surveys.

Geologic Influences on Ground-Water Movement

Alternating clays and sands function as relative aquitards and aquifers that have permitted perched water-bearing zones to form well above the natural ground-water table at the site. The variable lithology has also affected depth of percolation of oxidizing surface waters, confirming the observations of Bunker and MacKallor (1973). The base of the oxidized zone in both sands and clays generally parallels the original topographic surface before mining but is encountered at varying depths; the base is shallower where less permeable units are at the surface. Tailings have been piled on outcrops of both permeable and less permeable units.

Lithologic properties and geophysical log responses of the lower Conquista, upper Dilworth, and lower Dilworth, were evaluated with respect to possible compositional influences on ground-water movement—specifically whether the lower Conquista and upper Dilworth should be considered as single or separate hydrologic units.

The lower Dilworth is a cleaner and coarser sandstone than the upper. Silt and clay contents are more variable in the upper section, and the upper Dilworth is everywhere sandier than the lower Conquista. The lower Conquista is generally claystone to slightly silty claystone, the silt content of which differs across the area.

Of more than a dozen logs and lithic descriptions examined, only two logs indicated similar physical properties for the lower Conquista and upper Dilworth. In boreholes 969 and 902/903, both units appear clay-rich and silty, and ground-water flow would probably be rather similar through the two. The upper Dilworth in borehole 915 contains slightly more clay and silt, but the interval is still much sandier than is the lower Conquista. Because of areally consistent variations in lithology, we conclude that they should be regarded as separate hydrologic units.

Geologic Influences on Sediment and Effluent Geochemistry

Carbonate content of sediments affects the volume of acidic effluent that may be neutralized within the bedrock. The Conquista sand contains significantly more shell material and calcite cement than does the Deweesville. Both the Deweesville and Conquista sandstones have been contaminated by tailings solutions, but the Conquista has been more effective at neutralizing acidic fluids.

Caliche is developed on the surface in parts of the site, especially on formations such as the Conquista sand that contain more calcium carbonate. Thickness of the caliche horizons was not determined during field reconnaissance, but even the discontinuous caliche patches in other lithologies would provide sufficient carbonate to neutralize acidic effluent in the path of tailings fluid flow.

Clay and bentonite content, and thus cation exchange capacity, are high throughout the stratigraphic section. In the context of evaluating other possible sites for relocation of tailings from this area, Blount and Kreitler (1990) commented on the high clay content and cation exchange capacity of the Manning for sequestering any metals that might be leached from the tailings.

At the request of Pyrih and Associates, Core Laboratories, Inc. conducted analyses of 10 sediment samples of Deweesville sands (5), upper Conquista clays (3), Conquista sand (1), and Dilworth sand (1). All the sands showed higher than usual cation exchange capacities; the highest value of all analyses was for a single Conquista sandstone sample (88.5 milliequivalents [meq]/100 gms). The lowest value obtained was for the Deweesville (7.8 meq/100 gms) at a depth of 11 to 12 ft in borehole 903. The other Deweesville values clustered between 25.9 and 32.1 meq/100 gms, whereas the Conquista clays and the one Dilworth sand yielded values between 53.8 and 57.1 meq/100 gms.

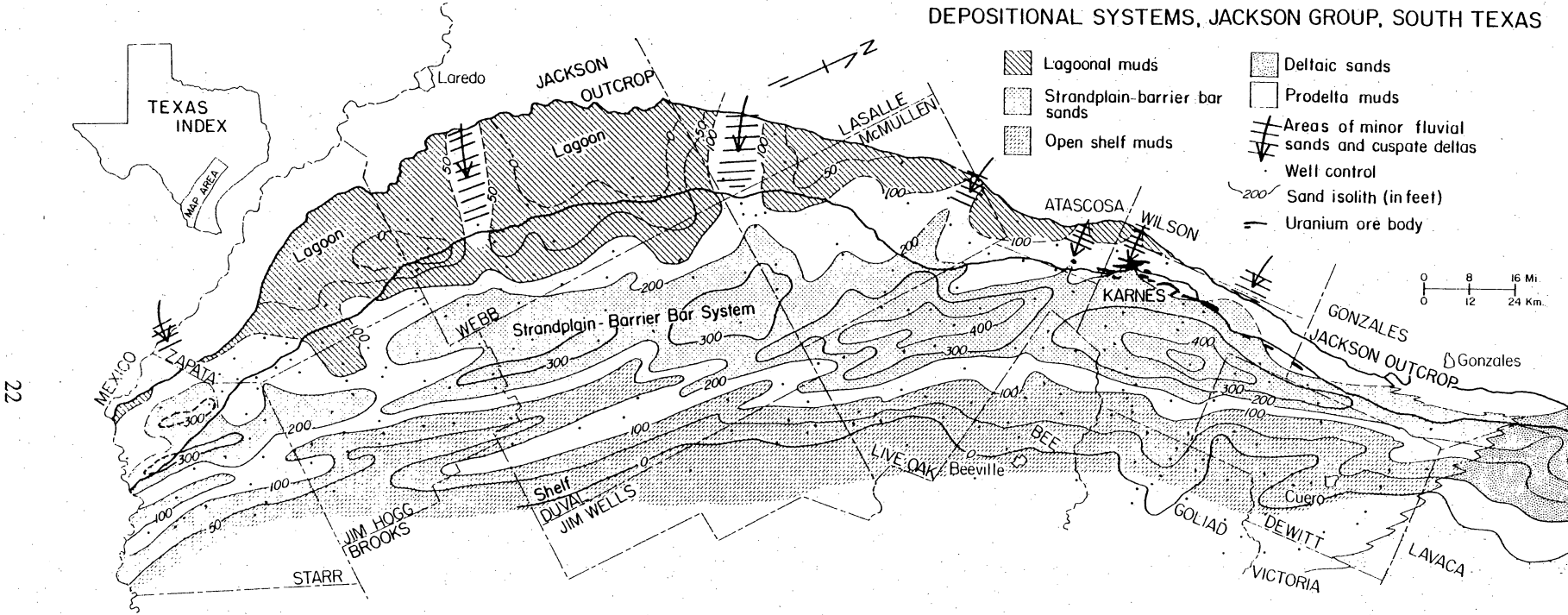
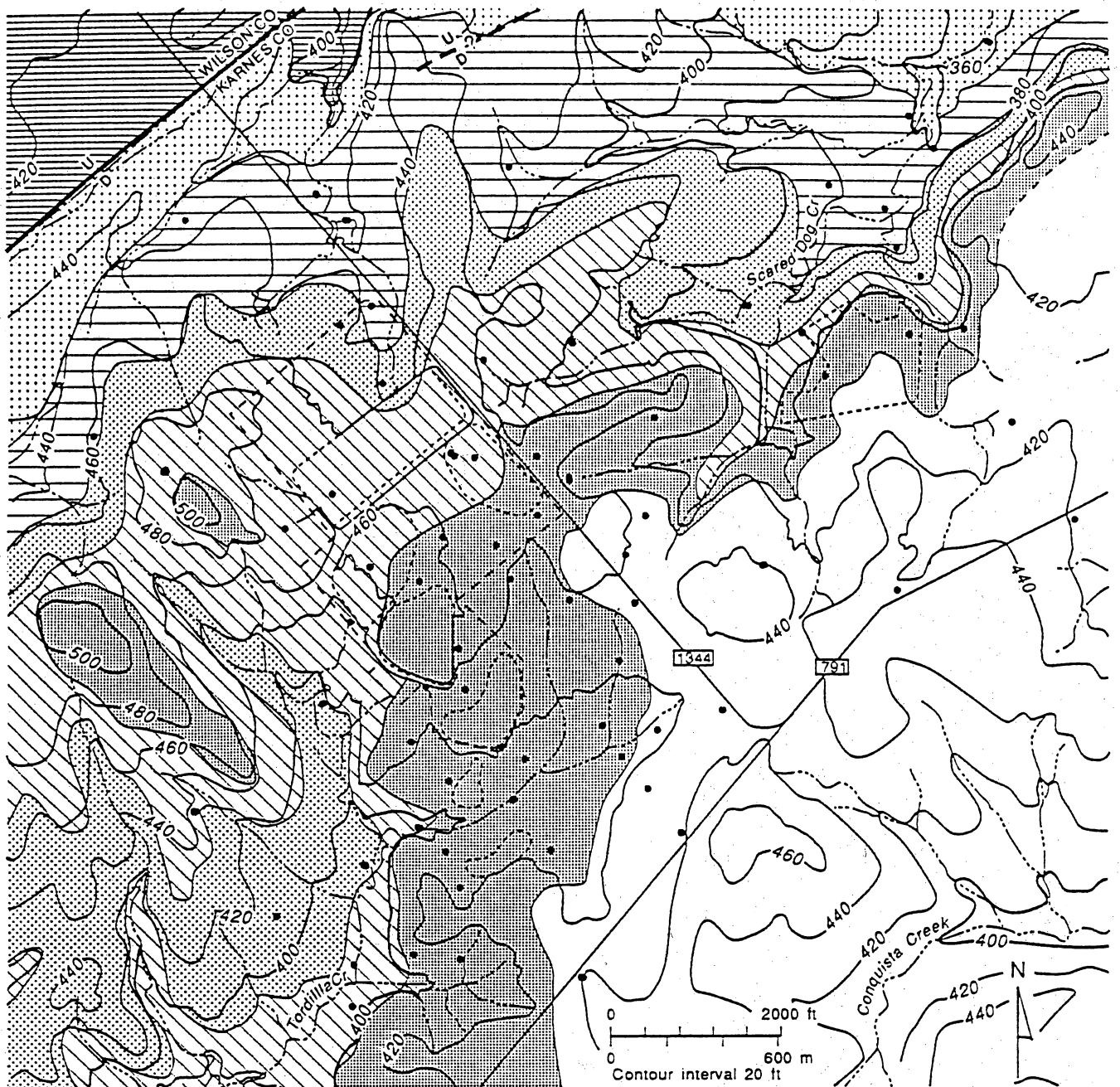


Figure 2.1. Depositional systems of the Eocene Jackson Group, coastal plain of South Texas—a strike-parallel suite of sands, silts, muds and lignites (Fisher and others, 1970).



Jackson Group (Eocene)

- Whitsett Formation
 - Dubose Clay Member
 - Deweesville Sandstone Member
 - Conquista Clay Member
 - upper claystone
 - Conquista fossiliferous sandstone
 - lower claystone

- Dilworth Sandstone Member
- Manning Formation
- 440— Topographic contour in feet above mean sea level
- $\frac{U}{D}$ Fault

- Monitoring well
- Tailings pile, tailings in abandoned open-pit mine and abandoned open-pit mine
- - - Fence line
- · - · - Ephemeral drainage

QA20372bc

Figure 2.2. Geologic map of the site.

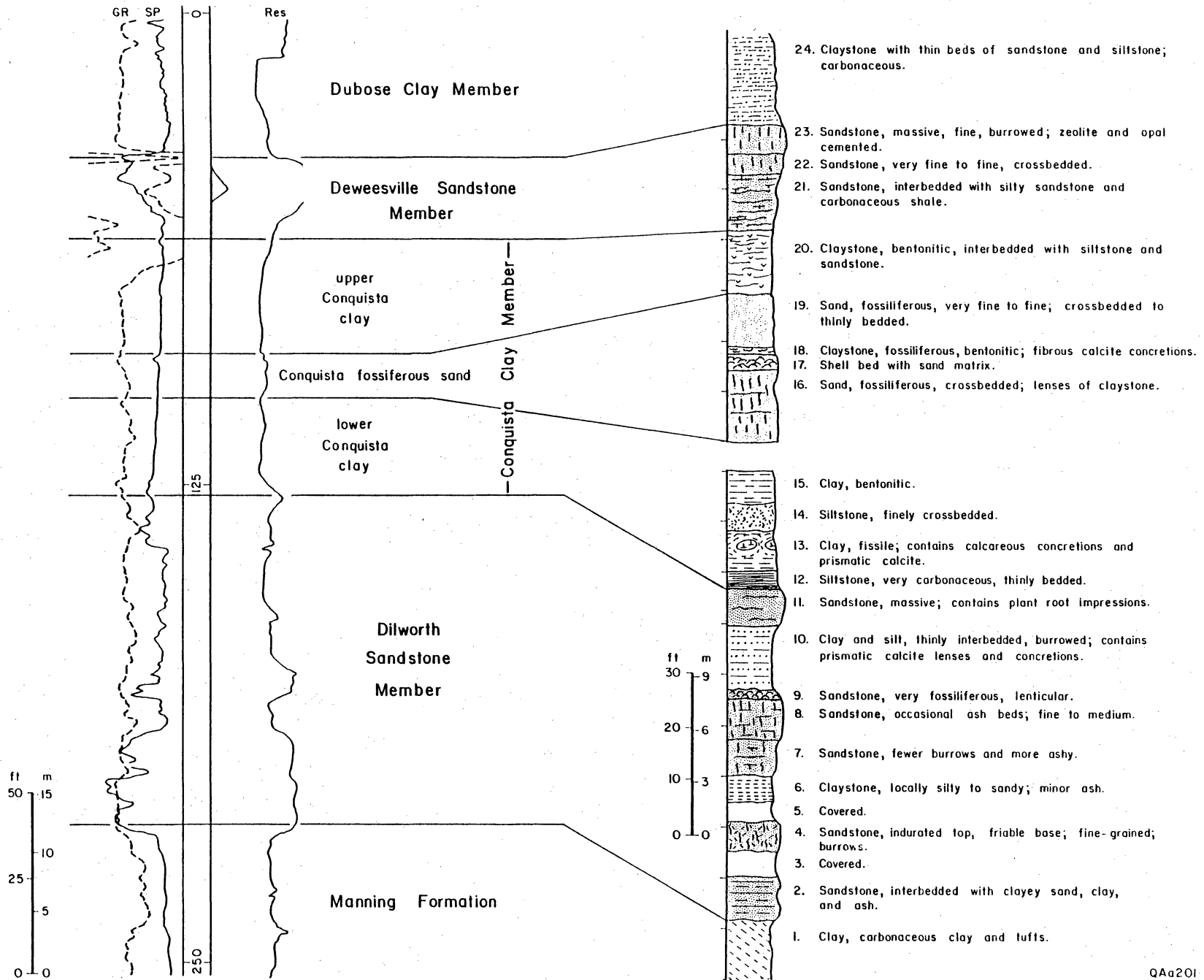
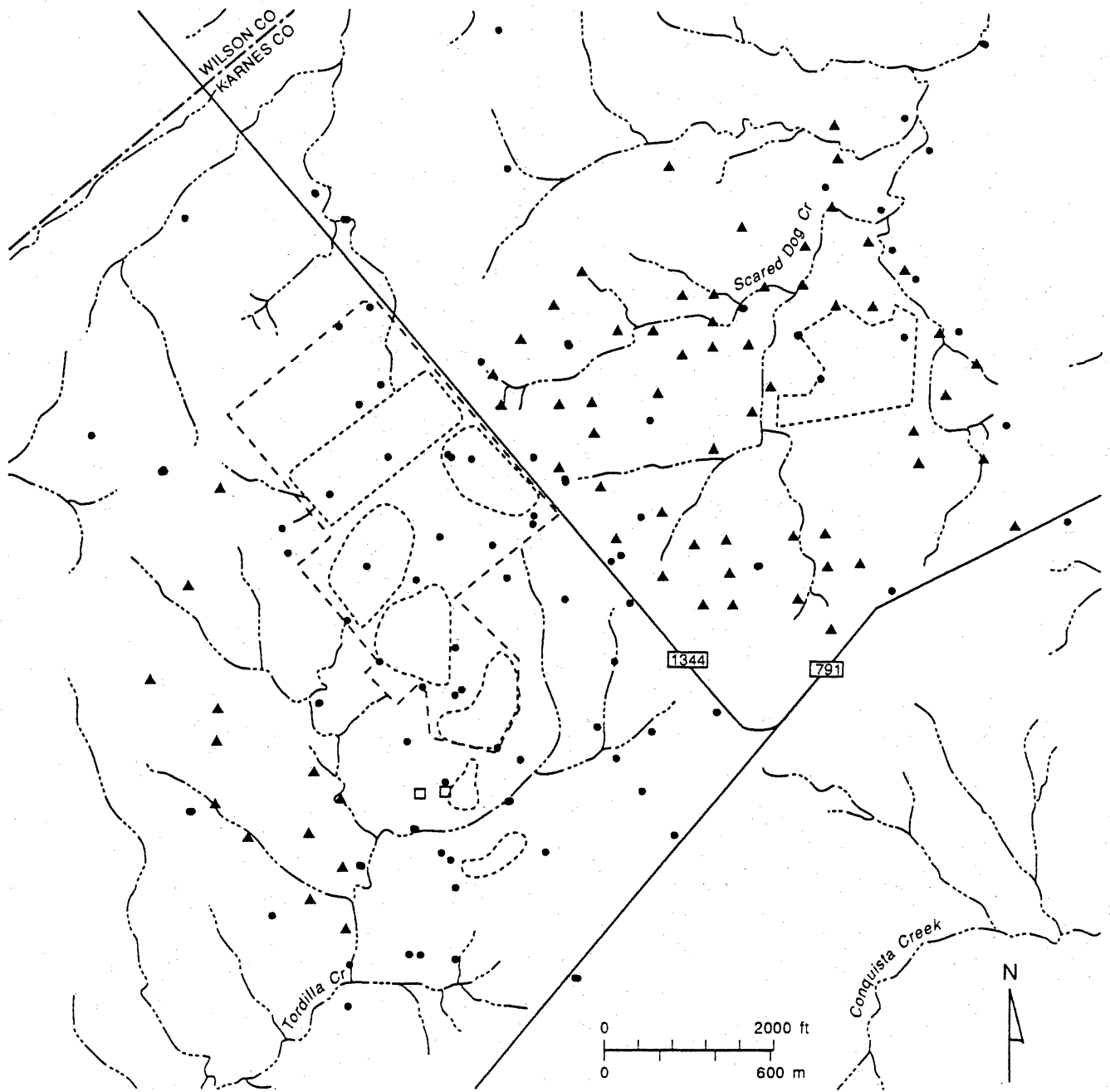


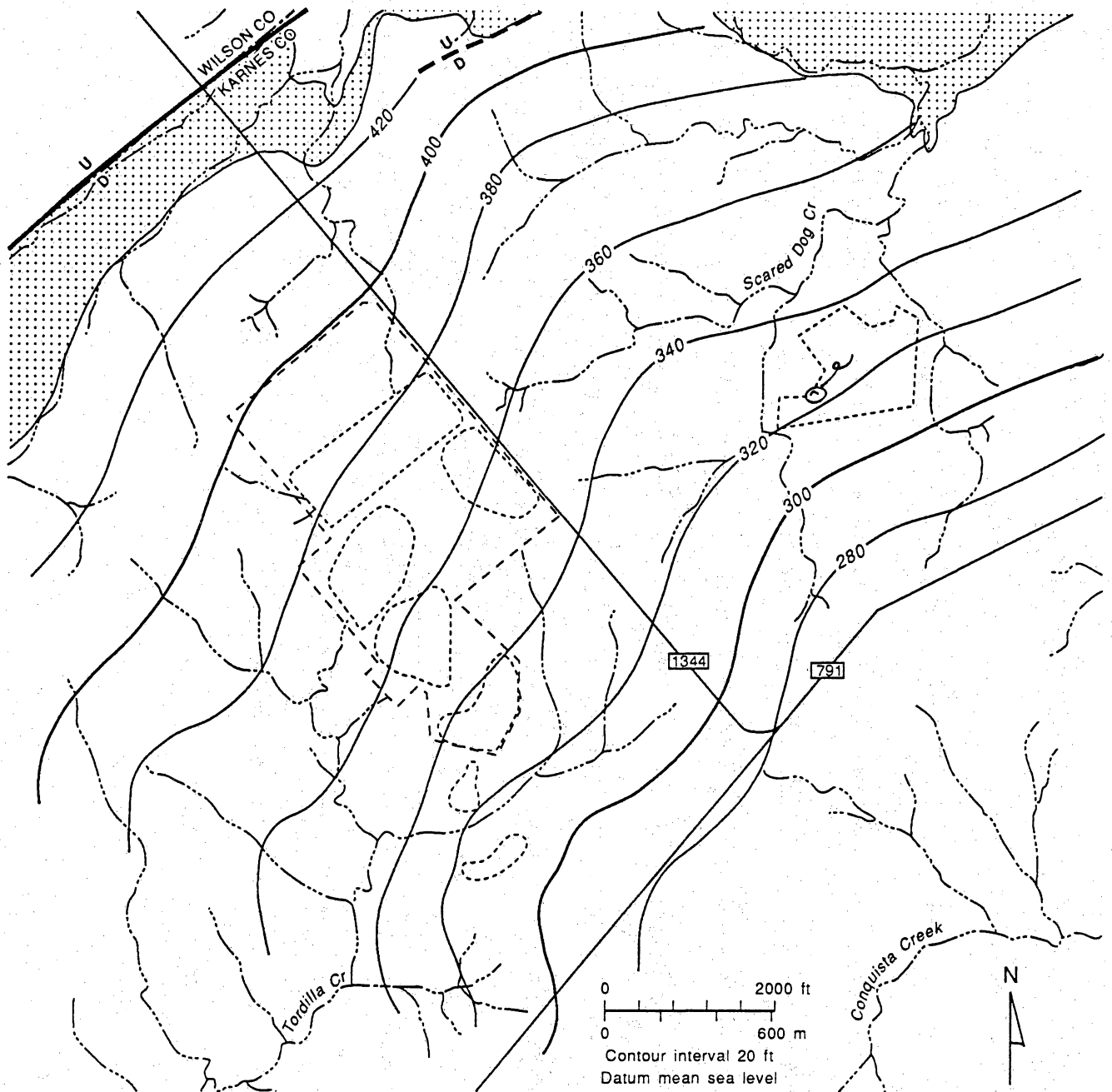
Figure 2.3. Stratigraphic column and composite geophysical log of Whitsett and Manning Formations, Jackson Group (Eocene), in the vicinity of the UMTRA site (modified from Eargle and others, 1971).



- Jacobs Engineering Group and Bureau of Economic Geology monitoring wells and coreholes
- ▲ Susquehanna-Western, Inc., exploration boreholes
- CONOCO exploration boreholes
- Tailings pile, tailings in abandoned open-pit mine and abandoned open-pit mine
- Fence line
- Ephemeral drainage

QAa184c

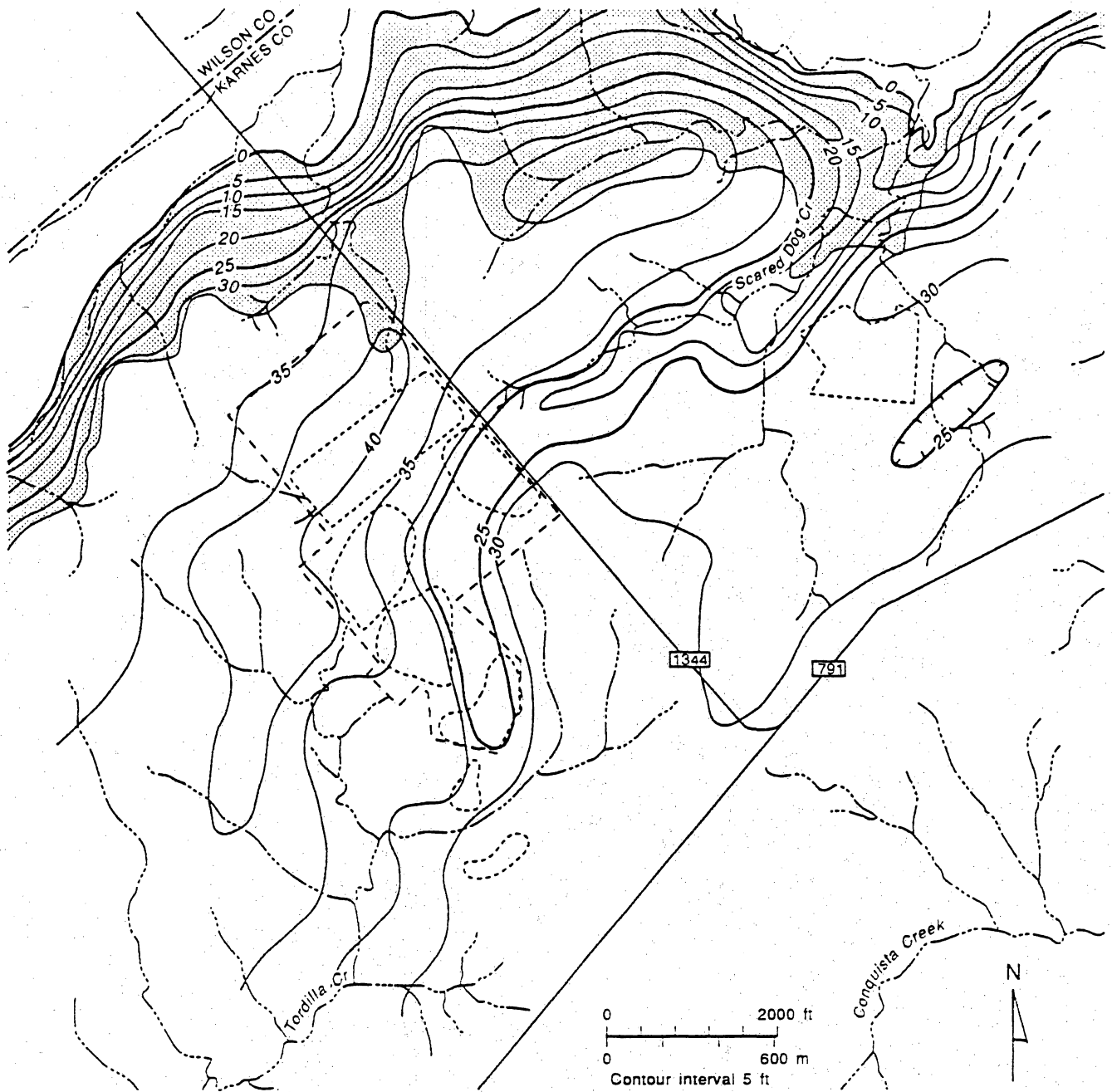
Figure 2.4. Locations of logged boreholes utilized in interpreting subsurface geology.



- 380- Top of Dilworth Sandstone Member, in ft
- Dilworth Sandstone Member outcrop
- Tailings pile, tailings in abandoned open-pit mine and abandoned open-pit mine
- Fault
- Fence line
- Ephemeral drainage

QAa179c

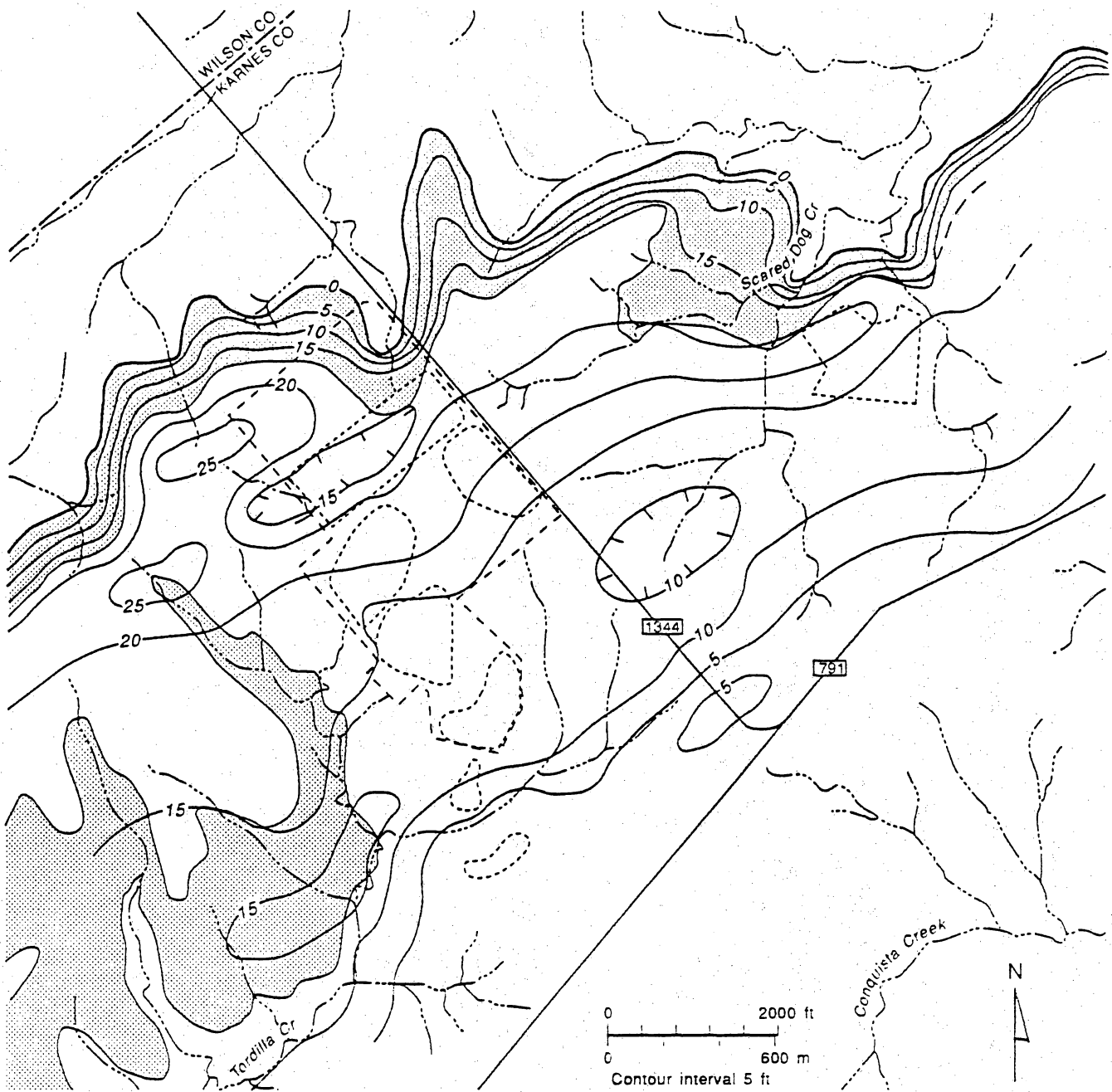
Figure 2.5. Structure on top of Dilworth Sandstone Member.





- 5— Thickness of lower Conquista clay, in ft
- lower Conquista claystone outcrop
- Tailings pile, tailings in abandoned open-pit mine and abandoned open-pit mine
- - - Fence line
- Ephemeral drainage

QAa211c

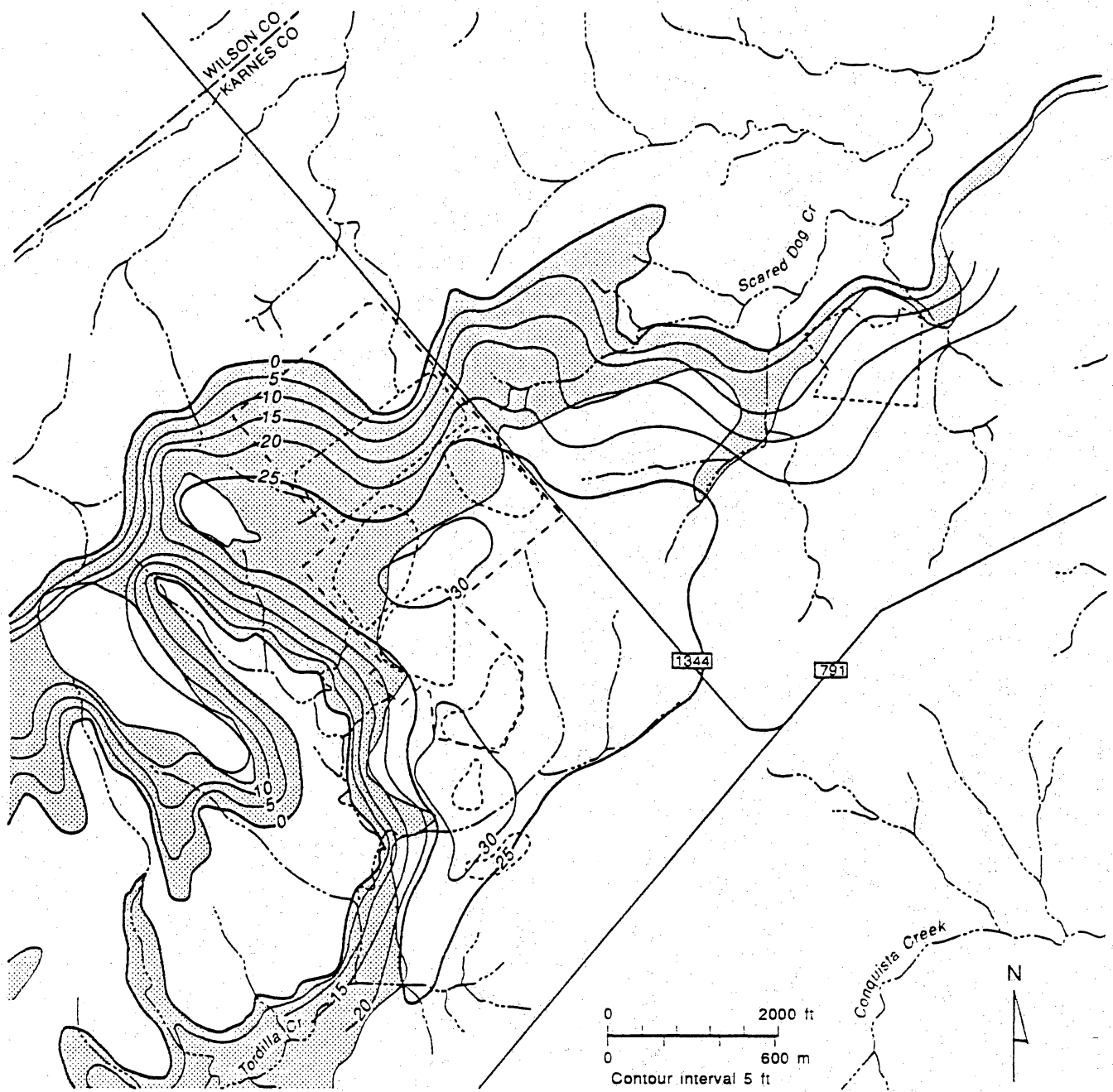
Figure 2.6. Isopach map of lower Conquista clay, Conquista Clay Member.





- 5— Thickness of Conquista fossiliferous sandstone, in ft
-  Conquista fossiliferous sandstone outcrop
-  Tailings pile, tailings in abandoned open-pit mine and abandoned open-pit mine
- - - Fence line
- · - · - · Ephemerical drainage

QAa213c

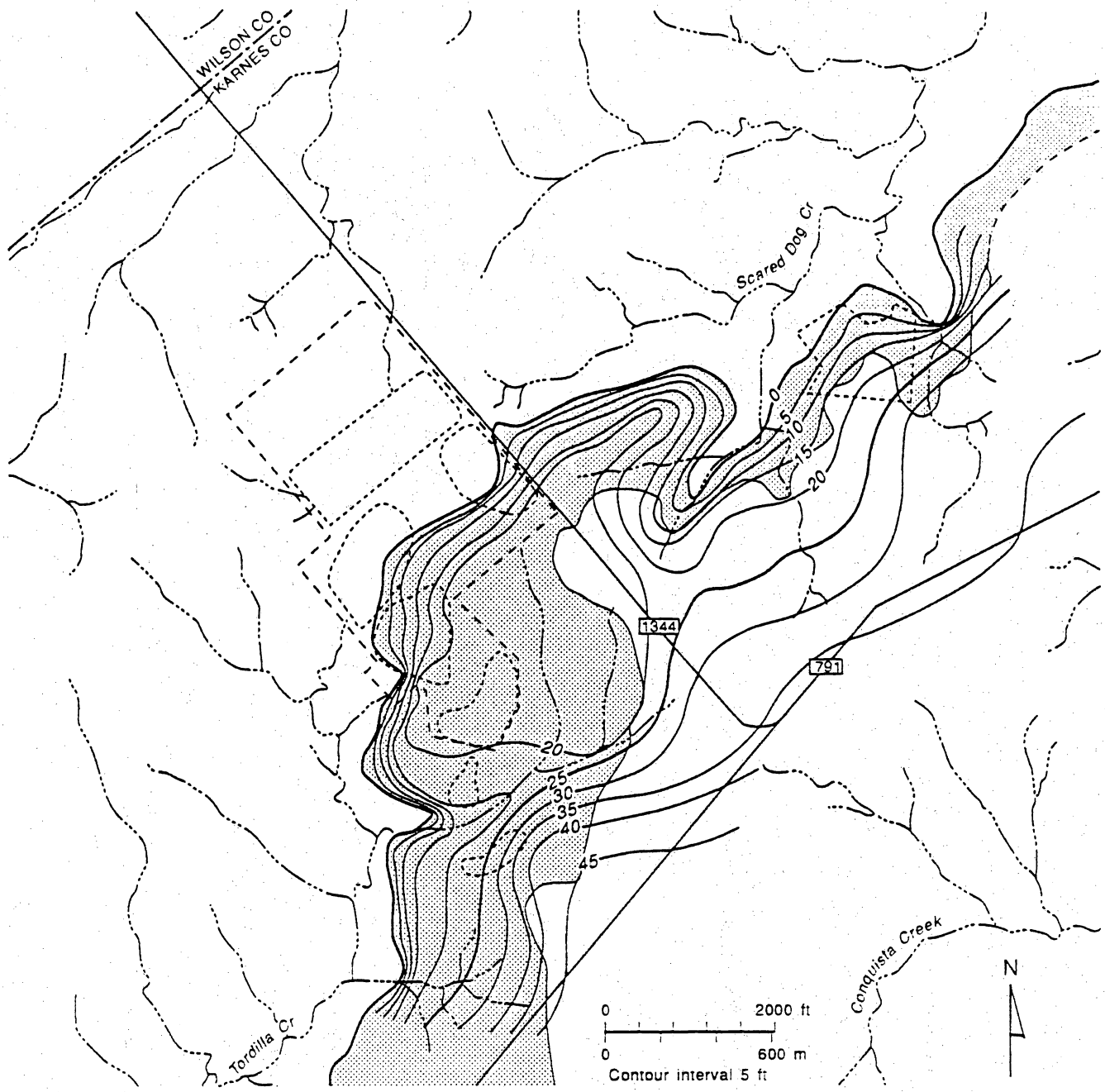
Figure 2.7. Isopach map of Conquista sandstone, Conquista Clay Member.





- 5 — Thickness of upper Conquista clay, in ft
-  upper Conquista claystone outcrop
-  Tailings pile, tailings in abandoned open-pit mine and abandoned open-pit mine
- - - Fence line
- · - · - Ephemeral drainage

QAa2:2c

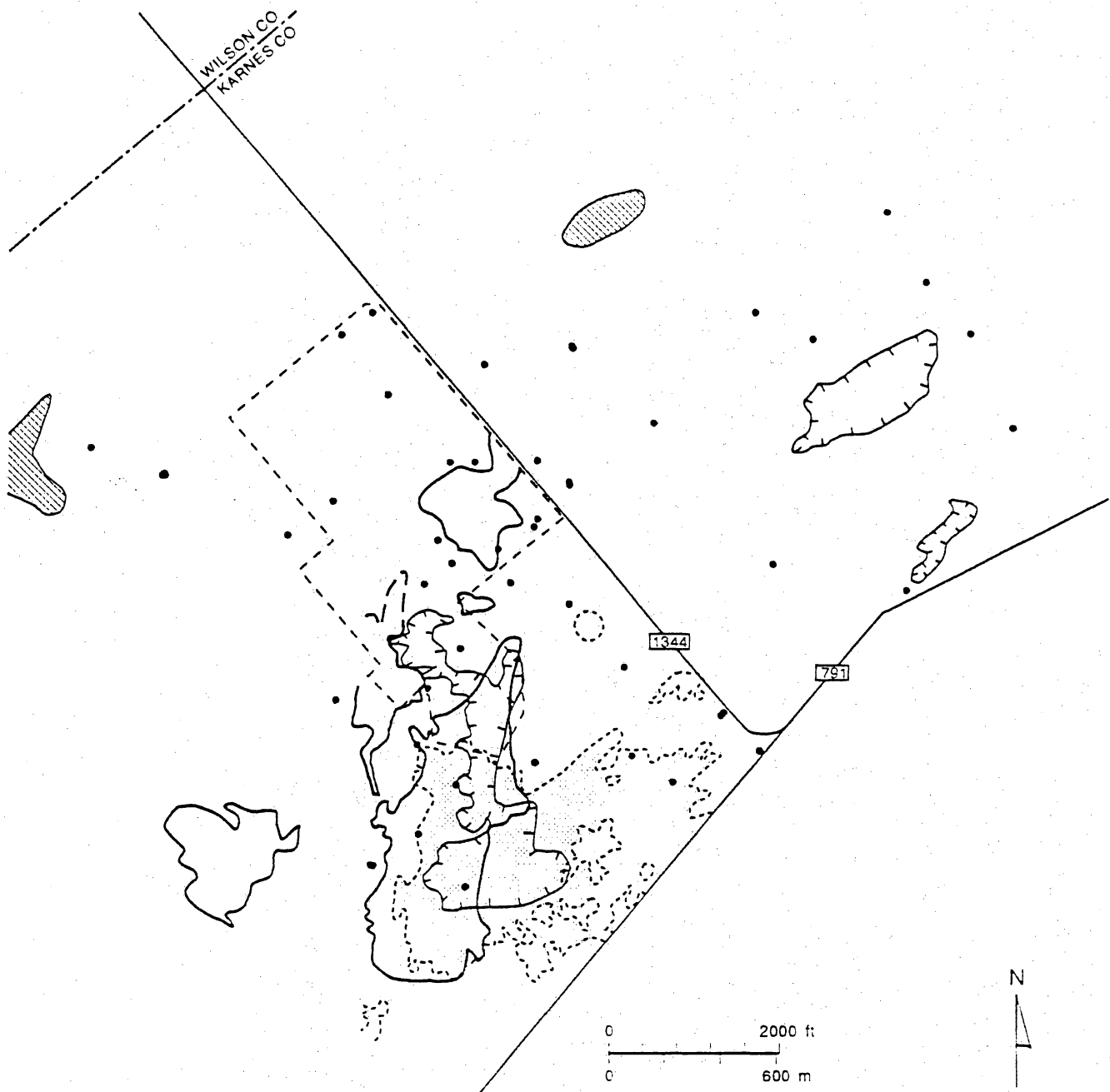
Figure 2.8. Isopach map of upper Conquista clay, Conquista Clay Member.






- 5— Thickness of Deweesville Sandstone, in ft
-  Deweesville Sandstone Member outcrop
-  Tailings pile, tailings in abandoned open-pit mine and abandoned open-pit mine
- - - Fence line
- - - Ephemeral drainage

QAa214c

Figure 2.9. Isopach map of Deweesville Sandstone Member.



- Monitoring well with gamma-log peak >200 cps
- Surface radioactivity, > than 20 microentgens per hour, dashed where inferred
- - - Fence line
- PROVEN URANIUM MINERALIZATION**
-  Mined deposits
-  Mineralization, areas with 2 ft or more of >0.03 percent U_3O_8
-  Unmined deposits in Dilworth

QAa215c

Figure 2.10. Uranium mineralization and radiometric anomalies, Falls City UMTRA site.

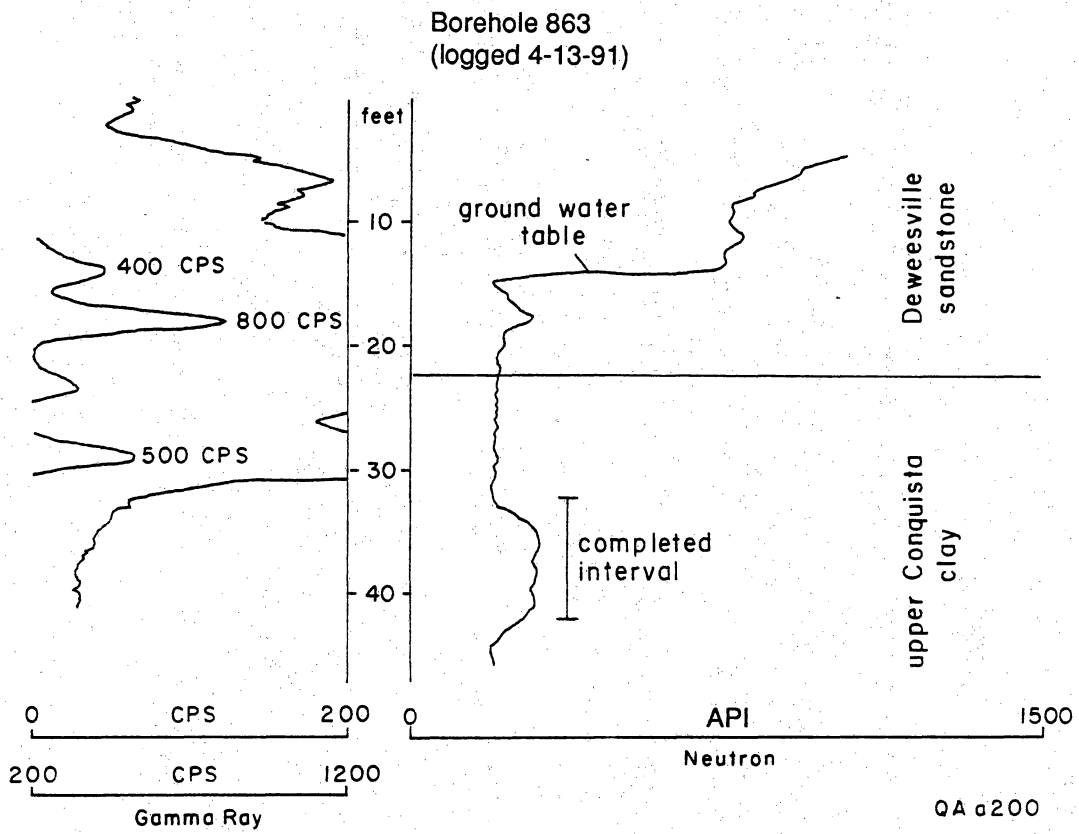


Figure 2.11. Examples of gamma anomalies in Deweesville sandstone and upper Conquista clay.

HYDROLOGIC CHARACTERIZATION (SECTION 3)

Methodology

Potentiometric surface (water level) maps provide valuable information on the general hydrology at the Falls City UMTRA site as well as water-level mounding associated with leakage from tailings piles. Potentiometric maps were constructed for the three important aquifers at the site, the Deweesville, Conquista, and Dilworth aquifers, using data from 80 monitoring wells (fig. 3.1). Lithologic logs, geophysical logs, driller's records, and geologic maps of each well were reviewed to ensure that wells were assigned to proper aquifers. Wells that had been completed across two units were assigned to the more permeable unit. Wells completed across the Deweesville and upper Conquista were assigned to the Deweesville. Wells completed in the lower Conquista and Dilworth were assigned to the Dilworth.

Potentiometric surfaces of each aquifer were mapped by using all available water-level data. Several different sets of monitoring wells have been constructed over the history of tailings disposal, in situ leaching, and site characterization. The BEG recommended the construction of 17 additional wells (fig. 3.2) on the basis of a review of the locations and screened intervals of the existing wells. Most of the recommended wells were screened in the Conquista or Deweesville for better delineation of the extent of the plumes. Wells were constructed by Brothers Engineering under the field supervision of Jacobs Engineering Group/Weston field representatives and a BEG geologist. Water-level measurements and samples were collected for chemical analysis by Jon Blount and Bernd Richter (BEG) between May 25 and June 7, 1991, using BEG Quality Assurance approved methods. (Data are provided in the appendix tables 1-5).

Approximately 75 wells in the 3 aquifers have water-level measurements that can be used for constructing potentiometric surfaces. Water levels were measured at different dates by the DOE (primarily geologists and field technicians affiliated with

Jacobs Engineering Group/Weston) and BEG (see appendices). The potentiometric surfaces were mapped primarily on measurements made by Jacobs Engineering Group/Weston and BEG in the spring of 1991. Water-level measurements from 1989, 1990, and 1991 showed only minor variations (figs. 3.2 and 3.3) and therefore, where 1991 data were missing, earlier data were used for mapping. Each of the aquifers at the site has been geologically divided into more than one subunit. The Deweesville aquifer has been characterized as having an upper and a lower Deweesville unit (McCulloh and Roberts, 1981; fig. 3.4). Previous studies (for example, Bunker and MacKallor, 1973) as well as this study have subdivided the Conquista into a lower Conquista clay, a Conquista sandstone, and an upper Conquista clay. U.S. Department of Energy (1990) differentiated an upper and lower Dilworth. In this study, the hydrologic description treats each aquifer as a single hydrologic unit so that as much data as possible can be used for flow characterization. This level of detail appears to be appropriate for delineating individual plumes in the Deweesville and Conquista aquifers. More detailed hydrologic characterization may be needed if ground-water cleanup programs (such as pump and treatment) are initiated.

Water-level data are also displayed through plots of (1) water level versus land-surface elevation, (2) depth to water versus land-surface elevation, and (3) water elevation versus elevation of the top of the formation (see figs. 3.5 through 3.7 as examples). A plot of water level versus land-surface elevation shows whether ground-water levels follow topography or are independent of topography. When water levels follow topography, water level versus land surface should show a linear relationship, which implies that the aquifer is unconfined. If water levels are independent of land-surface elevation but exhibit their own consistent trend, the aquifer may be confined. Alternatively, water levels do not follow any consistent pattern relative to each other or to overlying topography. Such cases may indicate the effect of changes in elevation of the topography and no recharge to the aquifer, presumably from the presence of an

overlying aquitard. A plot of depth to water versus land-surface elevation is approximately the inverse of a plot of water elevation versus land-surface elevation. If the depth to ground water is constant with varying elevations, the aquifer setting is unconfined and active recharge is occurring along the land surface. If depth to water varies significantly with topographic elevation, then no obvious recharge is occurring.

A plot of water level versus elevation of the top of an aquifer can provide information on the confinement of an aquifer and therefore its hydrodynamics. The terms "confined" and "unconfined" are used in this text to indicate whether water levels rise above the top of the aquifer or not. The term "confined" is not being used to indicate whether the aquifer is overlain by strata of lower permeability. This definition permits the recognition of aquifer settings that are overlain by an aquitard but are not saturated to the top of the aquifer. If water levels rise above the top of the formation, the aquifer becomes confined and indicates resistance to flow further downdip, which may indicate a zone of lower permeability downdip. In contrast, if water levels do not rise to the top of the formation or the base of the overlying aquitard, then there is downdip flow and sufficient discharge to prevent a head buildup within the downdip section of the aquifer. For example, in the downdip section of a typical Gulf Coast Tertiary sandstone aquifer, water levels typically would be above the top of the aquifer, indicating no obvious easy discharge. However, if water levels were below the bottom of the overlying aquitard, discharge would be occurring at least as rapidly as recharge; therefore, this aquifer should contain permeable sediments that continue into the subsurface and connect to a zone of discharge. Plots of water levels versus land-surface elevation, water level versus elevation of the top of the aquifer, and depth to water versus land-surface elevation provide valuable, but commonly qualitative, information for interpreting the hydrodynamics of an aquifer. Integrated use of the potentiometric surface map and these graphical displays of water levels provide an important tool for

understanding the natural and altered ground-water conditions for the aquifers beneath the Falls City UMTRA site.

Hydrogeology of the Deweesville Aquifer

Summary

The Deweesville sandstone crops out across the Falls City site where piles 1, 2, 4, and 5 are located and at pile 3 farther east (fig. 3.4). Most of the tailings piles are located on the Deweesville because it was the host formation for the uranium and for subsequent disposal of tailings back into the abandoned mines. Ground water is recharged at higher elevations, flows down the hydraulic gradient, and discharges to the eastern tributary of Tordilla Creek or continues to flow downdip into the subsurface. Disposal of tailings into the old pits and onto the outcrop of the Deweesville has resulted in a ground-water mound in the Deweesville; water levels rise to 16 ft beneath the piles and to 12 ft downdip in the aquifer. In the outcrop of the Deweesville there may have been very little ground water; before mining, water levels appear to have been at the base of the Deweesville. The mound has developed from the long-term tailings disposal and is not solely the result of the SEI in situ leach operations; it has been relatively stable since 1976. Correlation of changes in water levels in pond 2 and ground-water levels in the Deweesville proximal to pond 2 during the SEI in situ leach operations confirms that there has been leakage from the piles into the underlying aquifers.

Hydrogeology of the Tailings Piles and the Deweesville Aquifer

The outcrop of the Deweesville is almost 0.5 mi wide in the area of tailings piles 1, 2, 4, 5, and 6. In the area of pile 3 the outcrop is much thinner (fig. 3.4). The section of

wide outcrop probably plays a significant role in the natural ground-water flow systems, the location of the oxidized orebodies, and the subsequent contamination of Deweesville ground water. Ground water is recharged by leakage from the tailings piles at higher elevation into the underlying Deweesville and flows down the hydraulic gradient, which is a reflection of the topography (table 3.1; figs. 3.4 and 3.5). Figure 3.5 shows a good correlation between land surface elevation and water levels, indicating strong topographic control and unconfined conditions. Figure 3.5 can be broken into three sections: a steep gradient in the tailings area, the broad valley containing the tributary of Tordilla Creek with a lower potentiometric gradient, and the downdip sections where the water level to land-surface relationship appears random and presumably is affected by overlying topography. The steeper gradient near the tailings piles may result from leakage from the tailings piles and subsequent mounding. The flatter potentiometric surface in the broad valley of the Tordilla Creek tributary may result because it is further from the tailings and therefore does not show the effect of the mounding beneath the tailings piles. Based on the potentiometric surface, this area is also a discharge zone (probably by evapotranspiration) to Tordilla Creek. Figure 3.6, depth-to-water versus land-surface elevation, shows the water table approaching land surface toward the confluence of the tributary with the main northwestern drainage of Tordilla Creek. The dense mesquite vegetation in this area may result from the shallow water table and evapotranspiration. The difference in gradients in the tailings area and the tributary area may result from the water-level mounding between the tailings area (steep gradient) and discharge into the Tordilla Creek tributary (lower gradient).

Part of the ground-water flow is into the deeper subsurface, as evidenced both by the potentiometric surface (fig. 3.4) and by the plot of water level versus top of formation (fig. 3.7). As indicated by cuttings, cores, and geophysical logs, the permeable sands extend into the subsurface. This is in contrast to the Conquista sand, which becomes thinner and less permeable at the approximate location of the drainage way.

Because of the continuity of this sand in the Deweesville, ground water flows into the deeper subsurface and is not forced to exit to Tordilla Creek. The plot of water level to top of Deweesville Formation (fig. 3.7) indicates that the aquifer is unconfined even where the aquifer dips beneath the Dubose clay. These unconfined conditions beneath the Dubose indicate reasonable permeability downdip and a zone of discharge further downdip. Ground-water discharge may be to Conquista Creek, which is southeast of Farm Road 791. A plot of water level versus land surface for the Deweesville suggests that the potentiometric surface will intersect land surface at approximately 340 ft (fig. 3.8), the approximate elevation of Conquista Creek. In figure 3.7, the slight shift of the wells in the vicinity of Tordilla Creek may only be an apparent shift from the regional trend of the rest for the wells. For an unconfined aquifer the top of the formation is also land surface. Erosion will result in a thinning of an aquifer, and a plot of water levels versus the elevation of the top of the formation will suggest an apparent thinning of the saturated section. The Deweesville in this broad valley has been thinned approximately 10 ft by erosion. If the top of the Deweesville (fig. 3.7) is considered to be at least 10 ft higher, there would be a continual trend of the water levels versus top of formation. This trend would show the entire aquifer as unconfined and wells 677, 922, and 953 would not appear anomalous. Part of the ground-water flow therefore continues into the subsurface.

Based on the potentiometric surface (fig. 3.4), ground-water contamination from the tailings area could flow in three directions: to the east away from pile 2, toward the eastern tributary of Tordilla Creek, or down the structural dip of the Deweesville beneath Farm Road 791 and into the deeper subsurface. Mapping of the tailings plumes confirms these flow directions.

The Deweesville potentiometric surface beneath tailings piles 1, 2, 4, and 5 is higher than background water levels. Water levels near the tailings have risen significantly since initial mining. A photograph taken in 1960 from the northern end of

the Nuhn deposit in the Gemblar lease (area of pile 5) (Bunker and MacKallor, 1973) shows no water in the pit and the contact between the Deweesville-Conquista as "dry." Water levels are now 8 to 17 ft above the base of the Deweesville. Downdip from the tailings along the eastern tributary of Tordilla Creek the ground-water levels have also risen. The water table in the Deweesville in 1958 in the vicinity of the SWI pit was at its base, approximately 30 ft below land surface (Manger, 1958, table 23). The saturated section is now 6 to 12 ft thick. Much of the ground water now observed in the Deweesville outcrop and in the vicinity of the tailings, therefore, is tailings fluid.

Before tailings disposal, the Deweesville may have been hydrologically similar to the Dilworth in having a large depth-to-ground water in the outcrop and unconfined conditions extending beneath overlying aquitards. Because of leakage through the tailings piles, the previously dry formation in outcrop is partially saturated with 10 to 15 ft of water.

Mounding in the Deweesville probably started with the initial tailings disposal. A potentiometric surface map constructed from 1976 data (Solution Engineering, Inc., 1976) shows a substantial mounding at that time and predates SEI's injection/in situ leach operations (table 3.2; fig. 3.9). The mound has been there since at least 1976 and water levels from 1976 to 1991 have not changed appreciably. The mound has declined some since maximum SEI water levels in the early 1980's but has not decreased significantly.

Water-level data around pile 2 (fig. 3.9) suggest a discrete ground-water mound around that pile. The aquifer (Deweesville or Conquista) beneath each pile probably has a discrete mound, which results in an overall increase in water levels in the vicinity of the tailings piles. Because of the limited number of monitoring wells, the complexity of the shape of the mound cannot be observed other than as a broad integrated mounded surface (fig. 3.4).

We found hydrologic communication between the tailings piles and the underlying Deweesville or Conquista aquifers. Earlier studies predicted that no significant leakage would occur. Etco Engineers and Associates (1961, 1963a, b, 1966a, b), who engineered the foundation design for the tailings ponds, indicated that the "soils" beneath the ponds were sufficiently impermeable and that no major leakage would occur. Etco Engineers and Associates (1966) also evaluated the potential for leakage through the pits to determine whether the old mines could be used for tailings disposal. They found measurable water loss in some of their boreholes. Leakage presumably was into the Deweesville, because water loss in boreholes deeper than approximately 30 ft was much less than in some of the shallow holes, and they presumably were measuring the difference in permeability between the Deweesville and upper Conquista clay. They concluded that water flow would eventually stop because the tailings themselves would act as an impermeable barrier and disposal of tailings in the old pits would not result in ground-water contamination. Comparison of water-level data for pile 2 (monitoring well M-2) to monitoring wells 2-1, 2-5, 2-9, and 7-11, which are located up to 600 ft away from pile 2, show that water levels in the monitoring wells rise as the water levels in the tailings piles increase, and decline as the water levels in the piles decrease (table 3.3; figs. 3.10 through 3.13), indicating direct hydrologic communication between tailings pile 2 and the Deweesville aquifer.

The increased water levels in the Deweesville raise the issue of how much ground water was in the aquifer before tailings disposal and whether there are any ground waters that have been sampled that represent background (nonmining or nontailings) conditions. There was minimal ground water in the Deweesville from the tailings area down to the tributary of Tordilla Creek. Background conditions may not exist anywhere in the outcrop area of the aquifer. Naturally occurring ground water may only exist where the Deweesville dips beneath the Dubose. Water from wells sampling the Deweesville beneath the Dubose has a nontailings chemistry and no detectable tritium

concentrations (<0.09 tritium units). There is insufficient data in the region of pile 3 to define directions of ground-water flow and contaminant migration associated with pile 3.

Hydrogeology of the Conquista Aquifer

Summary

The Conquista aquifer is composed of three units, an oxidized upper Conquista fractured clay/silt unit, the Conquista sand, and a lower Conquista clay (fig. 3.14). The Conquista sand extends downdip into the subsurface but thins significantly and becomes more silty/shaly. The Falls City site occupies both a natural surface-water and a ground-water divide, which are controlled by Tordilla Creek to the south and Scared Dog Creek to the north. Ground-water flow in the overall Conquista aquifer is under water-table conditions and follows topography. The Conquista sand generally is confined. Recharge occurs both where the Conquista sand crops out and through the fractured, oxidized upper Conquista. Ground water flows in a strike direction toward Tordilla Creek (to the south) and Scared Dog Creek (to the north). Discharge is dominated by evapotranspiration in the region of the creeks.

Emplacement of the tailings piles has resulted in an elevated potentiometric surface in the Conquista. Water levels beneath pile 7 may be as much as 40 ft over background hydrologic conditions. The size of the contaminant mound permits ground-water flow and therefore contaminants from the tailings piles to migrate in all directions, toward the outcrop of the Conquista sand and to the northeast toward Scared Dog Creek. The predominant direction of flow, however, appears to be southeast toward Tordilla Creek. The pinch-out of the sands in the Conquista sand downdip probably further forces the ground water to flow toward Tordilla Creek rather than down the structural gradient into the deeper subsurface.

The updip section of the Conquista sand and upper Conquista clay probably were unsaturated and similar to the "dry" outcrops of the Deweesville and Dilworth. Most water in the updip section of the Conquista, therefore, is tailings fluid and not natural ground waters.

Hydrogeology of the Tailings Piles and Conquista Aquifer

Ground water (and/or tailings fluid) is recharged across the outcrop of the entire Conquista unit and is not restricted to the outcrop of the Conquista sand. Ground water flows predominantly along strike; relatively minor flow occurs down the structural dip into the deeper subsurface. Discharge is considered to be by evapotranspiration in Tordilla and Scared Dog Creeks, the creek alluvium, and the Conquista sand where it crops out in the broad valleys that surround these creeks. The downdip pinch-out of the more permeable sands in the Conquista sand further enhances the strike orientation of ground-water flow toward the streams (fig. 3.14). Although the Conquista sand does not entirely pinch out, the transition from sand to silts and clays as the sand thins results in sufficiently decreased permeabilities to prevent downdip migration of ground water (fig. 2.7).

Ground water is under water-table conditions for the Conquista aquifer. The plot of water level versus land surface (fig. 3.15) shows a linear relationship, indicating unconfined aquifer conditions. Water levels rise into the upper Conquista (fig. 3.16) and are above the top of the Conquista sand (fig. 3.17). Four wells below that trend (fig. 3.15) are located as far downdip as measurements were made. Their anomalous positions off the general trend probably result from increased land-surface elevation from the overlying topography and lack of recharge through the overlying formations. Water levels in two wells in the downdip silty/clayey section of the Conquista sand are below the general water level versus land-surface elevation for the Conquista (fig. 3.15),

suggesting that their heads have not risen to an equilibrated elevation and that they are therefore in a section of low permeability.

The lower Conquista has lower permeabilities than does the upper Conquista or the Conquista sand. The water level of monitoring well 864 in the lower Conquista was significantly below the regional trend (table 3.4), suggesting that the permeability of the lower Conquista is sufficiently low to prevent water levels from rapidly rising to the regional trend. This lower permeability of the lower Conquista prevents natural recharge to the underlying Dilworth, as evidenced by the lower water levels in the Dilworth.

A plot of water level versus top of Conquista aquifer (fig. 3.17) also indicates that most of the aquifer is unconfined. Water levels do not rise above the top of the aquifer (table 3.4). Unconfined areas for the Conquista aquifer include the tailings area, the areas surrounding Tordilla and Scared Dog Creeks, where ground water is discharging by evapotranspiration (figs. 3.14, 3.16, and 3.17). Confined areas are beneath pile 7 and along the downdip extent of the Conquista sand as the sands pinch out (figs. 3.14, 3.16, and 3.17). The locations of these confined and unconfined conditions imply recharge from leaking tailings piles with enough head buildup beneath pile 7 that water levels rise above the top of the Conquista. Ground water flows to the southeast, where it hits the pinch-out of Conquista sand and results in heads above the top of the Conquista, and then flows toward Tordilla Creek, where it discharges predominantly by evapotranspiration and once again results in unconfined conditions.

One hydrologic mound is observed in the Conquista beneath the major disposal area of piles 1, 2, 4, 5, 6, and 7, although additional monitoring wells might reveal localized mounds beneath each tailings pile. The observed mound is elliptical and approximately 40 ft above "background" elevations of the ground water. Forty feet of mounding is estimated by extrapolating water-level contours across the site. The

pretailings potentiometric surface would have been below the base of the Conquista sand.

Confirming that the pretailings water table was below the base of the Conquista sand, and that the sands were unsaturated at the site, is impossible because no field observations or water-level measurements were made at the site before tailings disposal. But an argument can be made that the sands were dry. If the Deweesville aquifer were dry in outcrop (see discussion on Deweesville hydrogeology), the upper Conquista and Conquista sand should also have been unsaturated at outcrop because the base of the Conquista sand is at the same approximate elevation as the base of the Deweesville. Ground water could not occur in the Conquista sand without being present in the Deweesville. If the Conquista aquifer in outcrop were essentially dry, similar to the Deweesville and the Dilworth, much of the ground water currently in the Conquista may be tailings solutions.

The maximum water elevation in the mound is in monitoring well 607 (table 3.4; fig. 3.14). Other wells in the area of tailings piles 1, 2, 4, 5, 6, and 7 also have elevated heads. Although ground-water levels in the Conquista beneath the tailings indicate radial flow away in all directions from the center of the mound, the preferred direction of flow appears to be south-southeast toward Tordilla Creek. The downdip extent of the mound may also be limited by the facies pinch-out of permeable sediments within the Conquista sand.

Recharge occurs through both the upper Conquista and the Conquista sand. The Conquista sand crops out beneath the northern edge of pile 7 and provides a zone for recharge of tailings fluids. Sumps along the flanks of pile 7 may have been important points of recharge. The outcrop probably does not represent the only area where tailings fluids could be leaking into the Conquista. Leakage through the upper Conquista is also occurring. The outcrop of the upper Conquista, should not be treated as an aquitard. The upper Conquista appears sufficiently permeable to permit recharge into

both the upper Conquista and the underlying Conquista sand. The thick oxidized section, the silty nature and numerous limonite-stained (oxidized) joints and fractures in the cores of the upper Conquista, suggest that precipitation and tailings fluids should recharge through the upper Conquista. Water levels (fig. 3.15) in wells screened in the upper Conquista are similar to water levels in the Conquista sand, indicating communication and no perched aquifers in the upper section. In addition, tailings were also disposed of in mined pits beneath piles 4, 5, and 6. Uranium was mined from these pits from the Deweesville and the base of the Conquista. These pits provide additional points for migration of tailings fluids into the Conquista.

The mound in the Conquista probably developed from the initial tailings disposal and was evident before SEI's in situ leach (fig. 3.9). The mound may have been maintained by SEI's in situ leach and ponding of tailings waters on top of the piles until the mid-1980's. Water was ponded over piles 2 and 7 for use in the in situ leach operations. Continual leakage through the tailings piles into the Conquista probably occurred until 1986, when the ponds were spray evaporated and the piles were capped with a few feet of clay to prevent percolation of precipitation.

Waters in the tailings, according to U.S. Department of Energy (1990), represent a perched zone with an unsaturated section between the tailings and the underlying Conquista and therefore no direct hydrologic connection between the two units. This conclusion is partly based on the elevated heads in well 607, a well thought to be in the tailings and not in the underlying Conquista. Bryson (1987), however, assigned well 607 to the upper Conquista. A review of Bryson (1987) and the original logs suggests that the well was screened across the contact between the tailings and the upper Conquista. The tailings piles and underlying formations appear to be hydrologically connected. Waters in the tailings will continue to drain into the underlying formation until the mound has dissipated. This process appears to be ongoing. Water levels in well 607 (beneath or at the base of pile 7) and well 701, north of pile 7, have dropped 18 ft from

1986 to 1991 and 7 ft from 1989 to 1991 (table 3.4), respectively, suggesting that the mound is dissipating. It also indicates a hydrologic connection between the mound and the underlying Conquista and that the emplacement of the cap and the evaporation of the ponds has reduced the leakage of tailings fluids into the underlying ground water.

Hydrogeology of the Dilworth Aquifer

Summary

The Dilworth aquifer, the deepest of the aquifers at the Falls City UMTRA site, is hydrologically separate from the overlying Deweesville and Conquista aquifers. Several observations based on a Dilworth potentiometric surface map and graphs of water level versus land-surface elevation, depth to water versus land-surface elevation, and water level versus top of the aquifer are summarized below.

(1) Recharge appears to occur at the outcrop; ground water flows along strike and discharges along the San Antonio River.

(2) Dilworth water levels are much below water levels in the overlying aquifers and the land surface. These lower heads indicate that the aquifer is more easily discharged than it is recharged.

(3) There appears a north-south-trending band of the potentiometric surface that has a steeper gradient beneath the site. This zone may represent a low-permeability zone created by a redox boundary.

(4) Downdip sections of the aquifer are confined and result from the structural dip of the Dilworth being to the southeast and steeper than the potentiometric surface, not because of decreased permeability downdip.

(5) Water from the shallower Deweesville and Conquista aquifers also could leak into the deeper Dilworth aquifer. Extensive exploration drilling (over 370 holes) by SWI has created the potential for numerous pathways between the overlying aquifers and

the Dilworth. Water levels are abnormally high in the areas that were drilled and are considered as evidence of vertical leakage down the boreholes. Most of the deep SWI drilling that penetrated the Dilworth was peripheral to the mining and to mill tailings disposal; therefore, contamination to the Dilworth may be minor. The water chemistry of the Dilworth aquifer indicates minor contamination from overlying tailings plumes.

Background Hydrogeology

Ground water is recharged in the outcrop of the Dilworth (northwest section of the study area). Ground-water flow is not down the structural dip of the Dilworth, but along strike toward the San Antonio River (fig. 3.18; table 3.5). The San Antonio River, which is incised into the Dilworth outcrop and overlying river alluvium, is a topographic low, and ground water is expected to be discharged either into the San Antonio River or into the lowlands along the river.

The regional potentiometric surface is relatively flat and the regional hydraulic gradient is 4 ft/mi. A north-trending zone of steeper hydraulic gradient (approximately 60 ft/mi) exists beneath the site with relatively flat gradients on the hydrologic updip and downdip sides. This may represent a redox barrier with lower permeabilities. Water chemistry from the outcrop is oxidizing, whereas the downdip waters are more reducing.

Water in the downdip section of the Dilworth appears to be under confined conditions, as indicated by two observations: (1) water levels in many of the wells are above the top of the formation (fig. 3.19) and (2) the water levels do not closely follow the topography (fig. 3.20) in contrast to the Deweesville and the Conquista. Recharge is limited to the outcrop, and there is no natural leakage through the overlying Conquista where it is providing confinement. Dilworth water levels are far beneath land surface and beneath water levels for the overlying Deweesville and Conquista. This is in contrast to previously developed models of coastward dipping Gulf Coast aquifers (for

example, Galloway and others, 1979), in which water levels increase with depth and result in cross-formational upward flow, providing a zone of discharge for the deeper confined ground water. Ground-water flow in the Dilworth, however, is along strike and at water elevations significantly below water levels in overlying aquifers. The intersection of the potentiometric surface with land surface is at approximately 335 ft (fig. 3.21), the approximate land-surface elevation along San Antonio River. The incised San Antonio River may provide a point of discharge for the Dilworth and cause the heads to be lower than in the overlying units which discharge to other stream systems. The flow along strike indicates that ground water can more easily discharge into surface drainage (for example, into the San Antonio River) than flow downdip.

The plot of water levels versus elevation of the top of the aquifer indicates that the updip section is unconfined and the downdip section is confined (fig. 3.19). This relationship results because the top of the Dilworth Formation dips to the southeast and is steeper than the potentiometric surface, which dips to the northeast. The mapped distributions of confined and unconfined conditions are shown in figure 3.18. The 340 ft structure contour on the top of the Dilworth approximately divides confined from unconfined conditions. The potentiometric surface of the Dilworth is relatively flat compared to those of the Deweesville and Conquista, which suggests relatively higher transmissivities for the Dilworth. A potentiometric high where Scared Dog Creek crosses the outcrop of the Dilworth suggests possible recharge to the aquifer from the creek. Ground-water discharge through evapotranspiration may also be occurring along Scared Dog Creek.

Impact of Mining and Milling Operations on Hydrogeology of the Dilworth Aquifer

Shallow ground water from the overlying Deweesville and Conquista aquifers appears to be leaking into the Dilworth aquifer. This is evident from aquifer test data

and the presence of discrete potentiometric highs in the Dilworth. A 10-hr pumping test produced drawdown in well 676 screened in the Deweesville and from pumping well 902 in the Dilworth (U.S. Department of Energy, 1990). Three discrete potentiometric highs (fig. 3.18) are present south, north, and east of the tailings piles and also appear in the water level versus land-surface elevation plot (fig. 3.20). These potentiometric highs occur where there has been extensive deep drilling by SWI. The extensive exploration drilling by SWI (fig. 2.4) typically penetrated through the Dilworth (approximately 300 ft) and among the deepest of the exploration holes at the site. Approximately 370 boreholes penetrated the Dilworth. These boreholes were not backfilled after drilling (James Quinlan, SWI field geologist, personal communication, 1991) although some borehole closure is to be expected from caving of the borehole walls. Other drilling programs, such as CONOCO's (McCulloh and Roberts, 1981) on the Korzekwa tract southeast of the tailings piles, were intensive (1,367 holes were drilled on 100-ft spacings), but holes were typically not drilled below the base of the Deweesville (at an average depth of 65 ft). Only an occasional deeper hole was drilled into the Dilworth. Locations of the orebodies and subsequent tailings piles were not extensively drilled by SWI. The orebodies had already been identified and delineated in the Deweesville and upper Conquista before the SWI exploration program. The most extensive exploration drilling was near pile 7, with approximately 20 holes. The closest Dilworth monitoring well to pile 7, well 878, does not show anomalously high water levels in comparison to the regional potentiometric surface. Because drilling by SWI at the Falls City site was limited to shallow depths, a potentiometric high was not created beneath the site.

The chemical composition of the Dilworth waters shows evidence of contaminants from the shallower aquifers in two wells (monitoring wells 905 and 878). Elsewhere, the water chemistries from the overlying Deweesville and Conquista represent background concentrations that are not significantly different from the water chemistry of the underlying Dilworth waters and therefore are not discernible.

Table 3.1. Water-level data for the Deweesville aquifer.

Well no.	Formation interval	Land-Surface elevation (ft)	Formation top elevation (ft)	Screen depth (ft)	Screen length (ft)	Top of screen elevation (ft)	Bottom of screen elevation (ft)	Location y	x
625	DeweConq	446	436	17	20	429	409	60916	66302
651	DeweConq	431	418	12	20	419	399	58874	64945
676	DeweConq	406	407	10	30	396	366	57483	65997
677	DeweConq	428	388	40	40	388	348	58606	68471
678	DeweConq	410	-	30	30	380	350	56867	66426
799	DeweConq	447	-	20	20	427	407	61567	66297
835	Deweesville	446	446	30	10	416	406	59347	65335
836	DeweConq	461	461	30	10	431	421	60698	65157
851	Deweesville	432	424	25	10	407	397	59878	67425
852	Deweesville	438	437	29	10	410	400	59902	66685
853	Deweesville	415	410	23	10	392	382	58403	67051
854	Deweesville	410	405	15	10	395	385	57716	65231
855	Deweesville	412	411	9	10	403	393	55580	65392
879	Deweesville	422	368	51	10	361	351	57626	67601
904	DeweConq	399	399	16	10	383	373	57171	64875
914	DeweConq	434	434	9	10	425	415	61382	66677
918	DeweConq	403	403	6	5	397	392	56864	65175
922	Deweesville	441	393	69	10	372	362	57057	67961
953	DewDubose	415	394	21	20	394	374	62029	71914

Table 3.1 (cont.)

Well no.	Water levels (ft) (5/89)	Water levels (ft) (1/90)	Water levels (ft) (5/90)	Water levels (ft) (4/91)	Water levels (ft) (5/91)	Water levels composite (ft)	Depth to water (ft)	Comments
625	-	427	426	428	-	428	18	Water level data for 5/89, 1/90, 5/90, and 4/91 measured by Jacobs Engineering
651	-	414	-	413	-	413	18	
676	400	398	399	400	-	400	6	
677	368	367	368	369	-	369	59	
678	-	396	400	403	-	403	7	Water-level data for 5/91 measured by Bureau of Economic Geology
799	-	-	-	448	-	-	-	
835	-	428	427	427	-	427	19	Composite data primarily for 4/91 and 5/91, filled in with data from other periods when 4/91-5/91 data unavailable
836	-	439	440	440	-	440	21	
851	-	-	-	-	406	406	26	
852	-	-	-	-	415	415	23	
853	-	-	-	-	399	399	16	
854	-	-	-	-	398	398	12	
855	-	-	-	dry	-	-	-	
879	-	-	-	-	387	387	35	
904	395	-	395	396	-	396	3	
914	420	417	418	-	-	417	17	
918	396	395	-	399	-	399	4	
922	378	376	377	377	-	377	64	
953	377	377	376	dry	-	377	38	

Table 3.2. Comparison of water levels in SEI wells measured in 1976, 1978, 1982, and 1984 with water levels measured in DOE wells in 1991.

SEI well no.	Water level (ft) (1976)	Water level (ft) (1978)	Water level (ft) (1980)	Water level (ft) (1982)	Water level (ft) (1984)	Comparable DOE Well No.	Water level (ft) (1991)	Formation
1-4	427					617	419	Conquista
2-2	434	438	449	441				
2-5	432	436	441	440	437	625	428	Deweeseville
3-4	399							
3-5	399							
3-6	398							
3-10	392							
3-11	382							
3-12	382							
3-13	383							
4-5	422							
5-1	421					651	413	Deweeseville
5-2	424							
6-1	399					676	400	Deweeseville
7-1	433	433	434	438	433			
7-2	442	445	446	448	445	607	456	Conquista
7-6	445							
7-7	435							
7-8	431	431	433	436	431			
7-9	423	424	426	428		709	427	Conquista
7-10	432					701	423	Conquista
7-11	429	429	434	436	431			
7-12	418					712	411	Conquista
7-13	433	436	433	439		713	434	Conquista

See figure 3.9 for monitoring well locations.

Table 3.3. Water-level data for M-2 (pile 2) and monitoring wells near pond 2 during SEI in situ leaching.

Measurement date	Tailings well M-2 (ft)	Well 2-2 (ft)	Well 2-5 (ft)	Well 2-9 (ft)	Well 7-11 (ft)
10/30/78	442	438	436	442	429
11/30/78	442	439	437	442	430
12/27/78	442	437	435	441	430
1/23/79	443	439	437	443	430
2/25/79	444	440	438	445	431
3/30/79	445	440	438	444	436
4/27/79	446	441	439	447	431
5/30/79	446	441	439	445	432
6/30/79	447	442	440	445	432
7/31/79	448	441	441	445	433
8/27/79	448	441	439	445	433
9/24/79	448	441	439	445	432
10/29/79	449	440	439	447	433
11/29/79	450	440	438	447	433
12/28/79	450	441	438	447	433
1/31/80	450	441	439	447	433
2/29/80	451	442	440	448	434
3/31/80	451	441	440	443	434
4/25/80	450	439	440	443	433
5/30/80	451	442	440	447	434
6/30/80	451	442	440	443	433
7/28/80	455	443	440	445	433
8/30/80	455	443	441	446	433
9/29/80	454	445	442	448	434
10/30/80	454	449	441	447	434
11/29/80	453	444	442	450	434
12/31/80	453	443	441	448	435
1/30/81	454	444	442	448	435
2/28/81	453	444	442	450	436
3/31/81	452	444	442	448	436
4/30/81	452	444	442	440	436
5/29/81	452	443	441	448	436
6/30/81	453	446	444	451	437
7/63/81	452	444	443	448	438
8/31/81	451	443	442	449	438
10/2/81	452	443	441	448	438
10/30/81	451	444	442	449	437
12/1/81	451	444	442	448	438
12/31/81	451	443	441	447	437
1/29/81	450	440	441	447	437
3/1/82	451	445	443	449	437
3/31/82	451	444	442	447	438
4/28/82	451	443	442	447	438
5/28/82	452	444	442	448	438

Table 3.3 (cont.)

Measurement date	Tailings well M-2 (ft)	Well 2-2 (ft)	Well 2-5 (ft)	Well 2-9 (ft)	Well 7-11 (ft)
6/28/82	451	443	441	445	437
7/28/82	450	442	440	445	437
8/27/82	450	442	441	445	436
9/30/82	450	441	439	444	436
10/29/82	450	441	440	445	436
11/26/82	449	441	440	445	436
12/28/82	449	441	439	444	436
1/27/83	449		439	445	436
2/25/83	468		440	447	436
3/30/83	450		441	447	436
4/26/83	451		440	446	437
5/24/83	451		440	446	437
6/28/83	450		439	445	437
7/26/83	450		438	444	436
8/29/83	450		438	444	435
9/29/83	449		439	445	435
10/31/83	449		439	444	435
11/25/83	449		439	444	435
12/29/83	449		438	443	435
1/24/84	449		439	444	435
2/29/84	449		438	444	435
4/30/84	449		437	443	434
5/31/84	448		437	442	434
10/29/84	446		436	441	431
11/30/84	448		437	442	433

See figure 3.9 for SEI monitoring well locations.

Table 3.4. Water-level data for the Conquista aquifer.

Well no.	Formation interval	Land-surface elevation (ft)	Formation top elevation (ft)	Screen depth (ft)	Screen length (ft)	Top of screen elevation (ft)	Bottom of screen elevation (ft)	Location y x	
607	Conquista	482	454	19	20	463	443	61182	63800
617	Conquista	433		18	20	415	395	59670	64000
701	Conq Sand	439	439	18	20	421	401	62506	64500
709	Conquista	446	446	18	20	428	408	63214	63900
712	Conq Sand	433	405	19	20	414	394	62807	65700
713	Conq Sand	469	448	19	20	450	430	60773	63300
856	Conq Sand	458	458	39	10	420	410	61631	65300
857	Conq upper	442	414	42	10	400	390	60451	67300
858	Conq Sand	442	442	40	10	402	392	60184	65900
859	Conq Sand	426	399	32	10	395	385	58209	64800
860	Conq Sand	420	375	64	10	357	347	58362	67700
861	Conq Sand	415	392	48	10	367	357	56467	65300
863	Conq Sand	416	394	33	10	384	374	57986	66100
864	Conq lower	416	372	89	10	328	318	58029	67300
865	Conq Sand	415	404	33	10	382	372	55660	64800
906	Conq Sand	418	418	14	15	404	389	58671	63800
913	Conq upper	423	398	29	10	394	384	59086	67200
916	Conq Sand	419	394	9	10	410	400	62973	66700
919	Conq lower	400	400	9	10	391	381	56737	64200
921	Conq Sand	434	394	46	10	388	378	61389	66700
924	Conquista	395	395	29	10	366	356	55042	64000
940	Conquista	424		28	10	396	386	62587	69700
951	Conquista	436	380	79	10	357	347	60335	69000
954	Conq Sand	410	360	38	20	372	352	63163	71300
957	Conq Sand	390	380	9	5	381	376	63435	68800
961	Conq Sand	382	382	20	20	362	342	63815	70800
962	Conq Sand	373		7	15	366	351	64140	70500
963	Conquista	369	369	9	10	360	350	64640	70400

Well no.	Water level (ft) (5/89)	Water level (ft) (1/90)	Water level (ft) (5/90)	Water level (ft) (4/91)	Water level (ft) (5/91)	Water-level composite (ft)	Depth to water (ft)	Comments
607	460	461	458	456	-	456	26	Water-level data for 5/89, 1/90, 5/90, and 4/91 measured by Jacobs Engineering Group
617	-	419	419	419	-	419	14	
701	-	430	429	423	-	423	16	
709	428	427	427	427	-	427	19	Water-level data for 5/91 measured by Bureau of Economic Geology
712	-	411	411	411	-	411	22	
713	-	435	435	434	-	434	35	
856	-	-	-	-	427	427	31	
857	-	-	-	-	408	408	34	
858	-	-	-	-	424	424	18	
859	-	-	-	-	400	400	26	
860	-	-	-	-	381	381	39	
861	-	-	-	-	390	390	25	
863	-	-	-	-	403	403	13	
864	-	-	-	321	325	-	-	Conquista aquifer includes upper Conquista, Conquista Sand, and lower Conquista
865	-	-	-	-	380	380	35	
906	406	404	405	406	-	404	14	
913	-	402	401	401	-	401	22	
916	-	-	-	dry	-	-	-	
919	391	390	390	393	-	393	7	
921	413	412	411	410	-	410	24	
924	378	376	378	379	-	379	16	
940	397	396	396	396	-	396	28	
951	371	371	371	-	-	371	65	
954	371	370	371	372	-	372	38	
957	380	379	380	381	-	381	9	
961	-	366	366	366	-	366	16	
962	-	359	359	374	-	359	14	
963	359	358	358	358	-	358	11	

Table 3.5. Water-level data for the Dilworth aquifer.

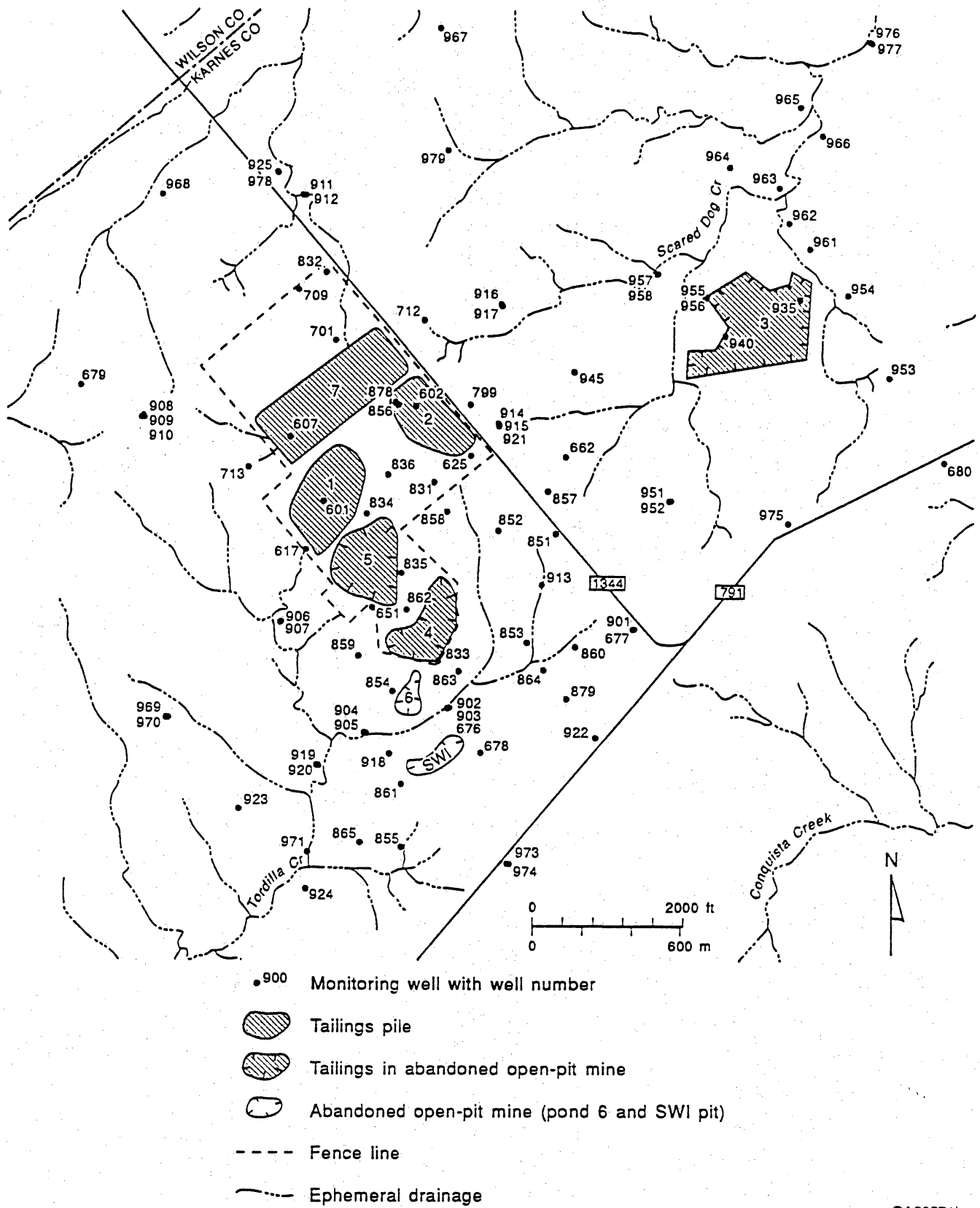
Well no.	Formation	Land-surface elevation (ft)	Formation top elevation (ft)	Screen depth (ft)	Screen length (ft)	Top of screen elevation (ft)	Bottom of screen elevation (ft)	Location y	Location x
664	Dilworth	-	-	-	-	-	-	-	-
679	Dilworth	453	361	130	30	323	293	61878	60978
831	Dil/Conq	445	-	-	-	-	-	-	-
832	Dilworth	436	420	122	30	314	284	63440	64332
834	Dilworth	465	346	122	31	343	312	60165	64893
862	Dilworth	437	330	118	10	319	309	58817	65416
878	Dilworth	458	-	116	10	342	332	61660	65241
901	Dilworth	428	303	124	20	304	284	58598	68462
902	Dilworth	407	317	119	20	288	268	57504	65984
905	Dilworth	399	339	59	15	340	325	-	-
907	Dilworth	418	369	57	20	361	341	58659	63745
910	Dil/Man	494	-	-	-	-	-	-	-
915	Dilworth	434	346	94	15	340	325	61372	66688
917	Dilworth	418	394	69	20	349	329	62980	66715
920	Dil/Conq	395	347	40	10	355	345	56731	64229
925	Dilworth	415	409	90	30	325	295	64843	63664
945	Dilworth	438	343	118	20	320	300	62071	67688
958	Dilworth	385	385	60	20	325	305	63430	68800
964	Dilworth	378	357	88	25	290	265	64926	69745
965	Dilworth	367	367	11	10	356	346	65774	70673
966	Dilworth	369	369	23	15	346	331	65378	70988
967	Dilworth	430	430	83	20	347	327	66837	65846
968	Dilworth	434	418	58	30	376	346	64511	62106
969	Dilworth	440	373	86	20	354	334	57396	62190
971	Dilworth	390	322	73	20	317	297	55530	64106
974	Dilworth	-	291	-	-	-	-	55371	66813
975	Dilworth	452	265	185	22	267	245	60037	70541
976	Dilworth	359	282	80	100	279	179	66684	71637
977	Dilworth	361	346	30	40	331	291	66668	71652
979	Dilworth	419	378	-	-	-	-	65119	65945

Table 3.5 (cont.)

Well no.	Water level (ft) (5/89)	Water level (ft) 1/90)	Water level (ft) (5/90)	Water level (ft) (4/91)	Water level (ft) (5/91)	Water-level composite (ft)	Depth to water (ft)	Comments
664	314	310	-	-	-	310	-	Water-level data for 5/89.
679	364	363	373	366	-	366	87	1/90, 5/90, and 4/91 measured by Jacobs Engineering Group
831	-	-	-	-	-	-	-	
832	350	353	351	351	-	352	84	
834	361	360	360	361	-	361	104	Water-Level data for 5/91
862	-	-	-	357	321	357	80	measured by Bureau of
878	-	-	-	-	350.4	350	108	Economic Geology
901	375	373	374	374	-	373	55	
902	354	354	354	355	-	355	52	Composite data composed
905	-	-	-	383	-	383	16	primarily of 4/91-5/91 data,
907	373	372	371	371	-	371	47	filled in with data from other
910	-	-	-	364	-	364	130	periods when 4/91-5/91 data
915	378	378	379	378	-	378	56	not available
917	367	366	366	366	-	366	52	
920	373	373	373	373	-	373	22	
925	363	363	363	364	-	363	52	
945	345	-	-	dry	-	345	93	
958	342	342	342	345	-	345	40	
964	339	338	339	339	-	339	39	
965	-	353	353	353	-	353	14	
966	358	355	357	357	-	357	12	
967	346	347	347	347	-	347	83	
968	373	373	372	372	-	372	62	
969	365	365	365	366	-	366	74	
971	361	361	362	362	-	362	28	
974	350	350	350	350	-	350		
975	342	344	342	342	-	342	110	
976	336	335	336	336	-	336	23	
977	339	339	339	339	-	339	22	
979	344	344	344	-	-	344	75	

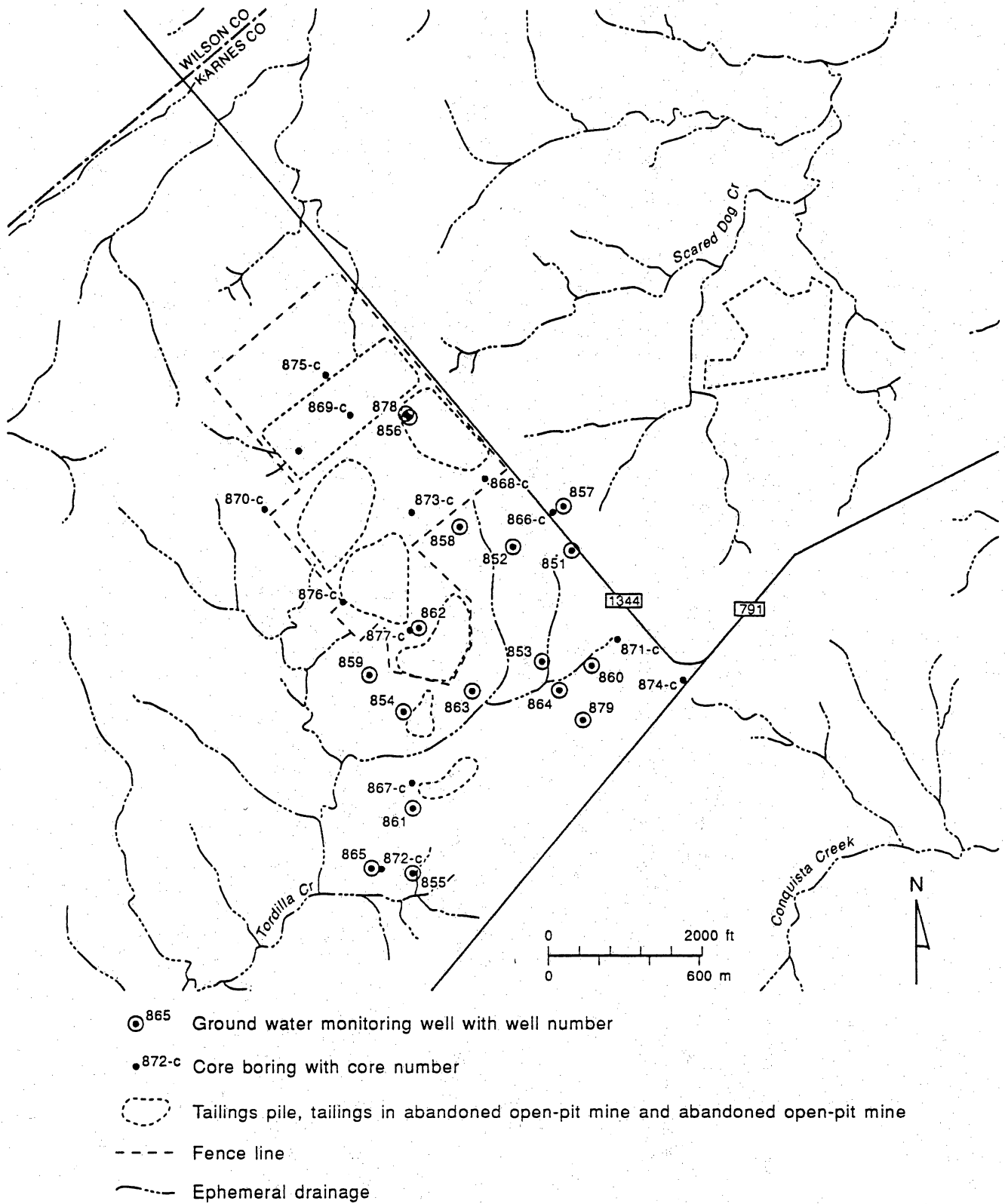
Table 3.5 (cont.)

Well no.	Water level (ft) (5/89)	Water level (ft) 1/90)	Water level (ft) (5/90)	Water level (ft) (4/91)	Water level (ft) (5/91)	Water-level composite (ft)	Depth to water (ft)	Comments
664	314	310	-	-	-	310	-	Water-level data for 5/89.
679	364	363	373	366	-	366	87	1/90, 5/90, and 4/91 measured by Jacobs Engineering
831	-	-	-	-	-	-	-	
832	350	353	351	351	-	352	84	
834	361	360	360	361	-	361	104	Water-Level data for 5/91
862	-	-	-	357	321	357	80	measured by Bureau of Economic Geology
878	-	-	-	-	350.4	350	108	
901	375	373	374	374	-	373	55	
902	354	354	354	355	-	355	52	Composite data composed primarily of 4/91-5/91 data, filled in with data from other periods when 4/91-5/91 data not available
905	-	-	-	383	-	383	16	
907	373	372	371	371	-	371	47	
910	-	-	-	364	-	364	130	
915	378	378	379	378	-	378	56	
917	367	366	366	366	-	366	52	
920	373	373	373	373	-	373	22	
925	363	363	363	364	-	363	52	
945	345	-	-	dry	-	345	93	
958	342	342	342	345	-	345	40	
964	339	338	339	339	-	339	39	
965	-	353	353	353	-	353	14	
966	358	355	357	357	-	357	12	
967	346	347	347	347	-	347	83	
968	373	373	372	372	-	372	62	
969	365	365	365	366	-	366	74	
971	361	361	362	362	-	362	28	
974	350	350	350	350	-	350		
975	342	344	342	342	-	342	110	
976	336	335	336	336	-	336	23	
977	339	339	339	339	-	339	22	
979	344	344	344	-	-	344	75	



QA20371bc

Figure 3.1. Locations of ground-water-monitoring wells, Falls City UMTRA site.



QAa202c

Figure 3.2. Locations of monitoring wells and core holes drilled by Bureau of Economic Geology.

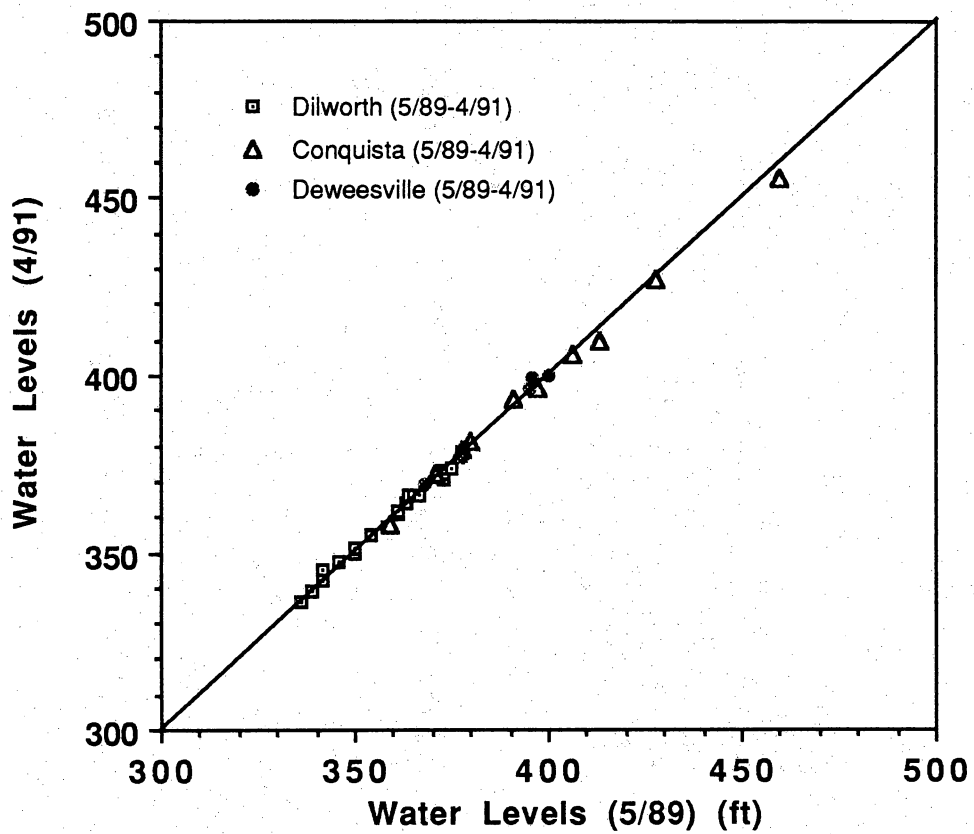
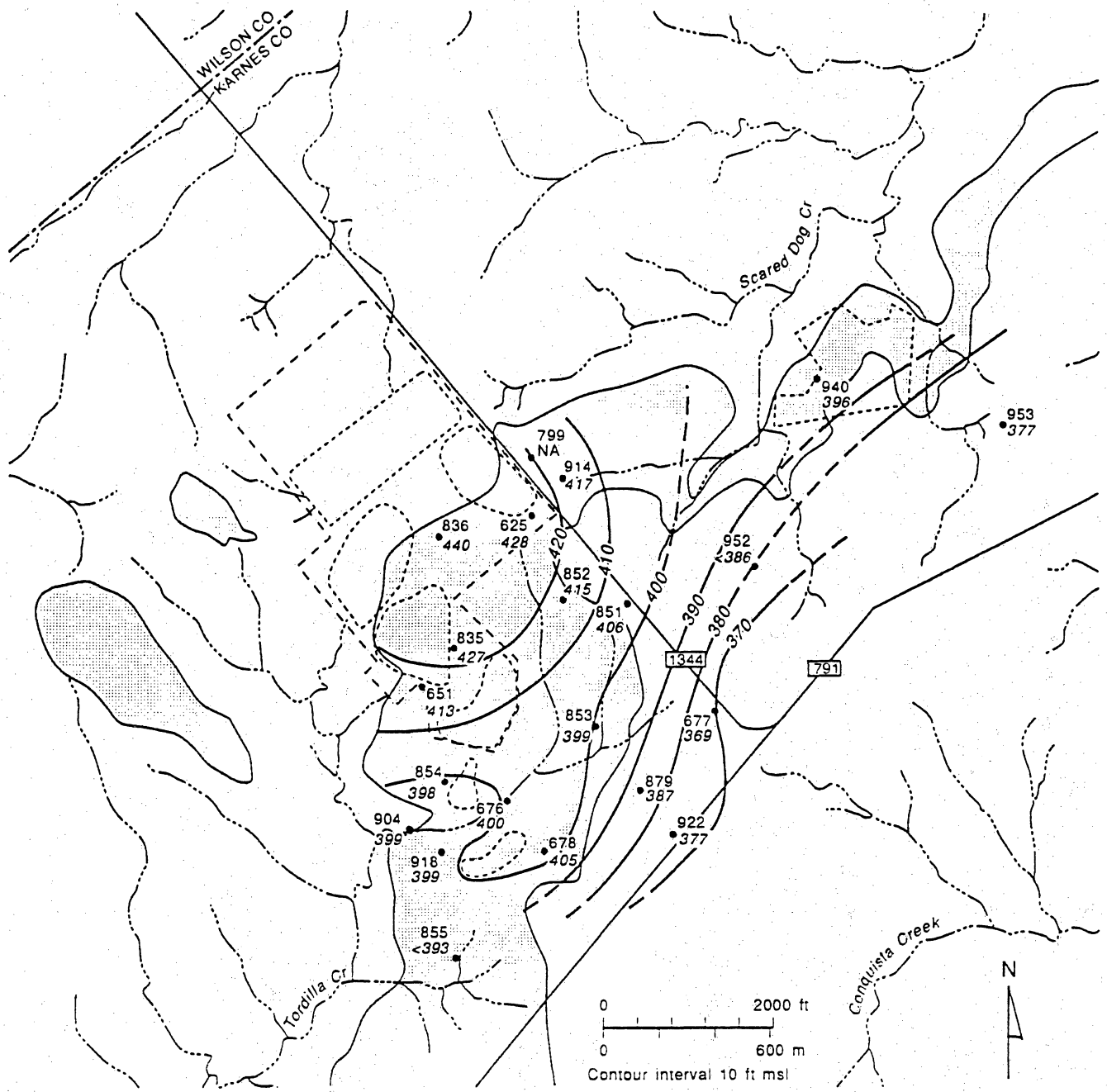


Figure 3.3. Comparison of April 1989 to May 1991 water levels in the same wells.



-420- Potentiometric (water level) contour for Deweesville aquifer (ft msl), dashed where inferred

Deweesville Sandstone Member outcrop

Well No.
 Monitoring well
 Water level

Tailings pile, tailings in abandoned open-pit mine and abandoned open-pit mine

- - - Fence line

Ephemeral drainage

QAa186c

Figure 3.4. Potentiometric surface of Deweesville Sandstone Member aquifer.

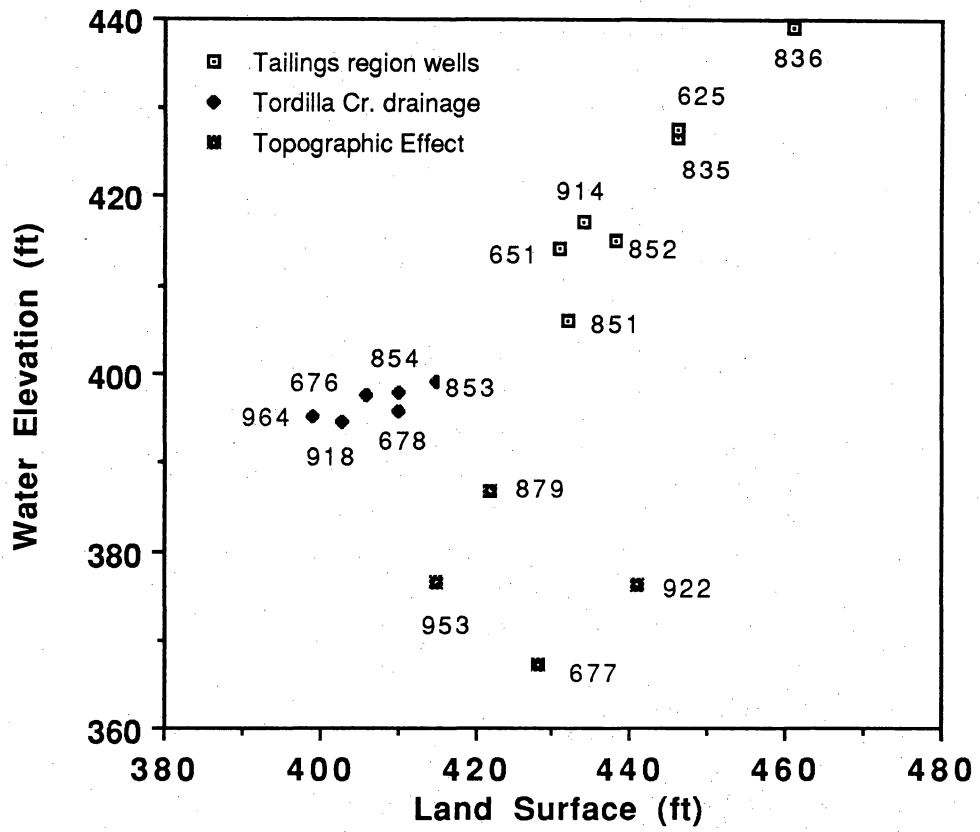


Figure 3.5. Water elevation versus land-surface elevation for Deweesville aquifer.

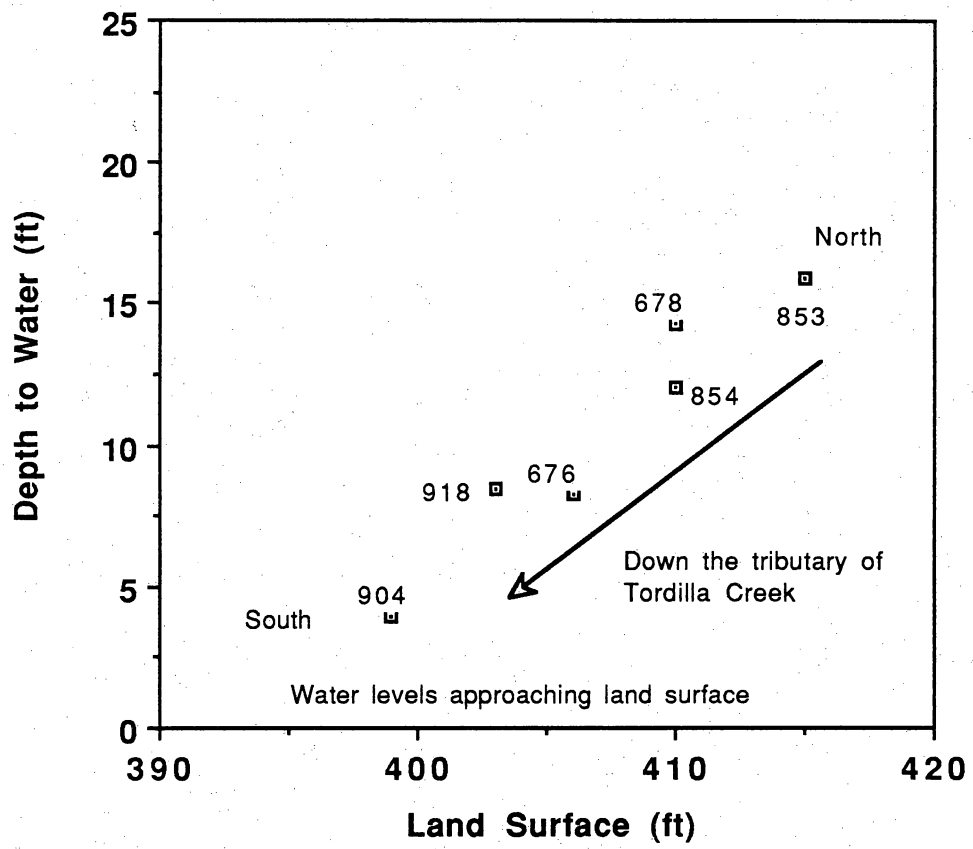


Figure 3.6. Depth to water in boreholes versus land-surface elevation for Deweesville aquifer.

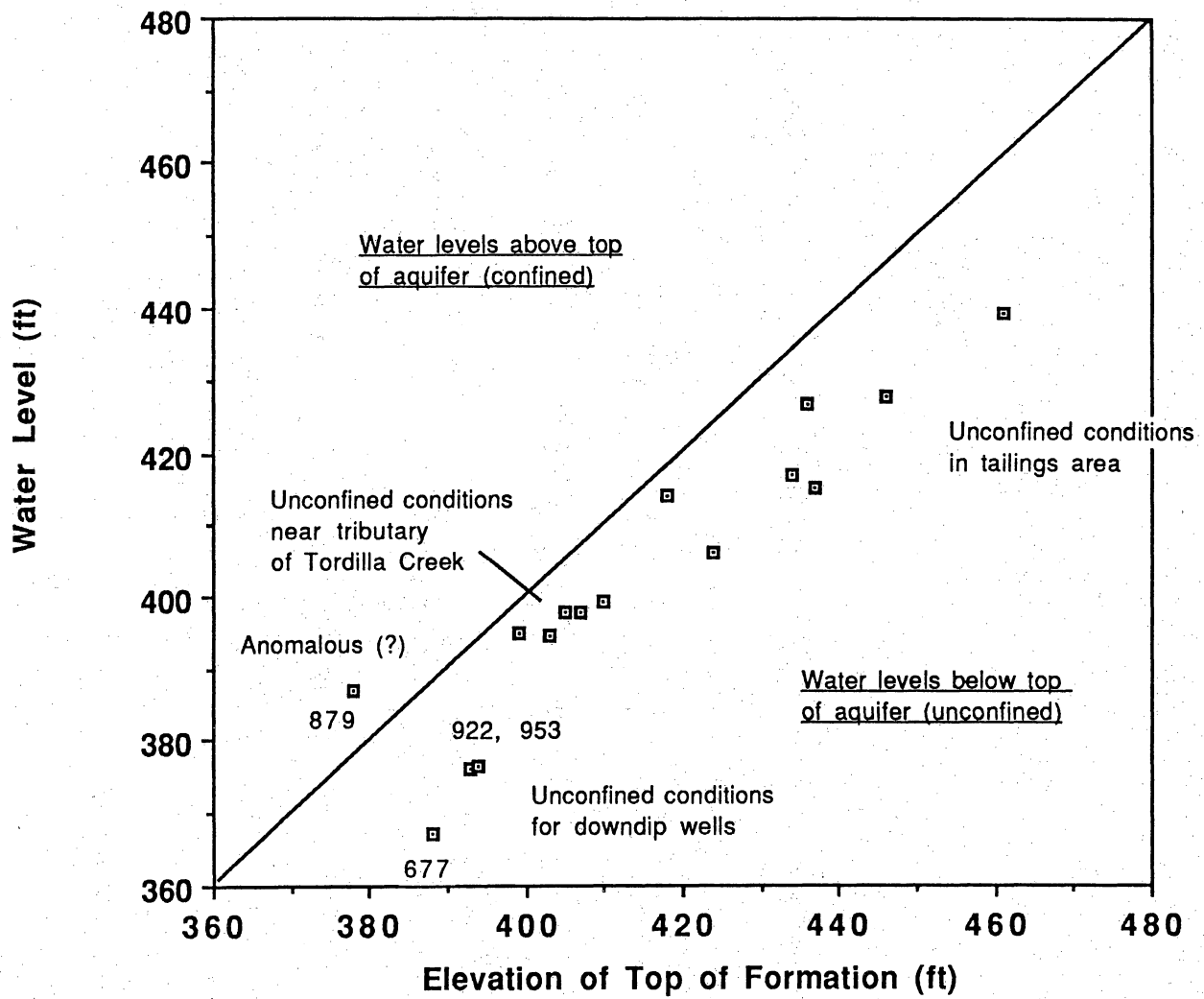


Figure 3.7. Water levels versus top of Deweesville aquifer, indicating whether aquifer setting is confined or unconfined.

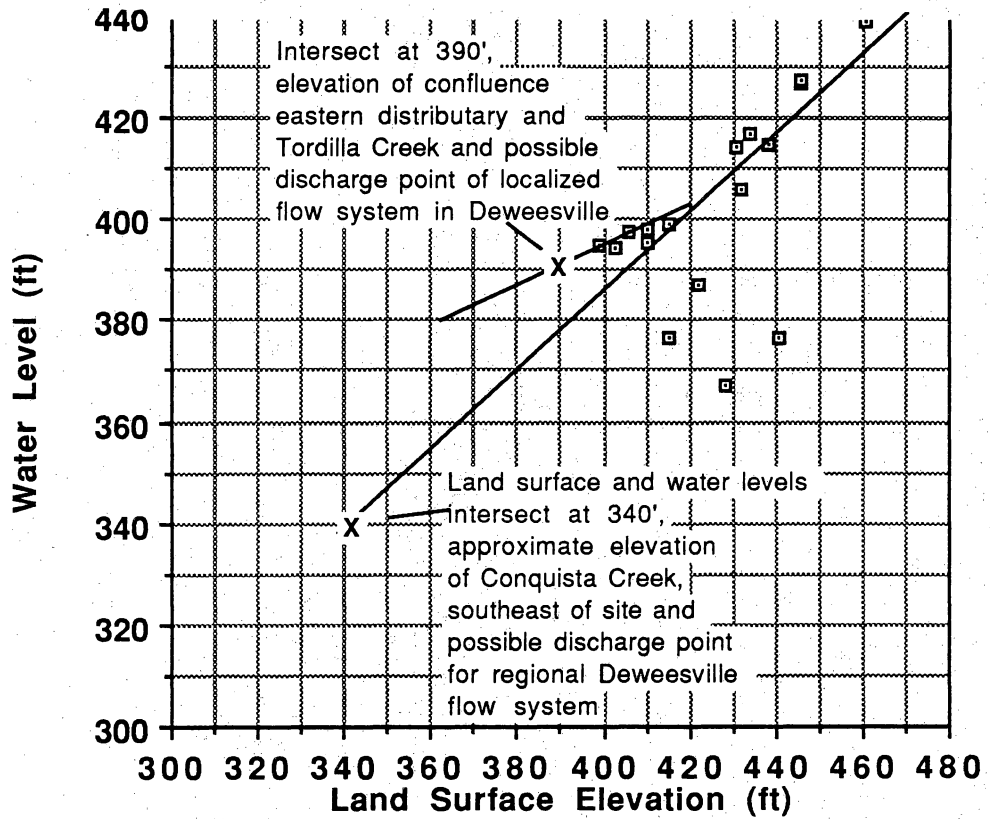
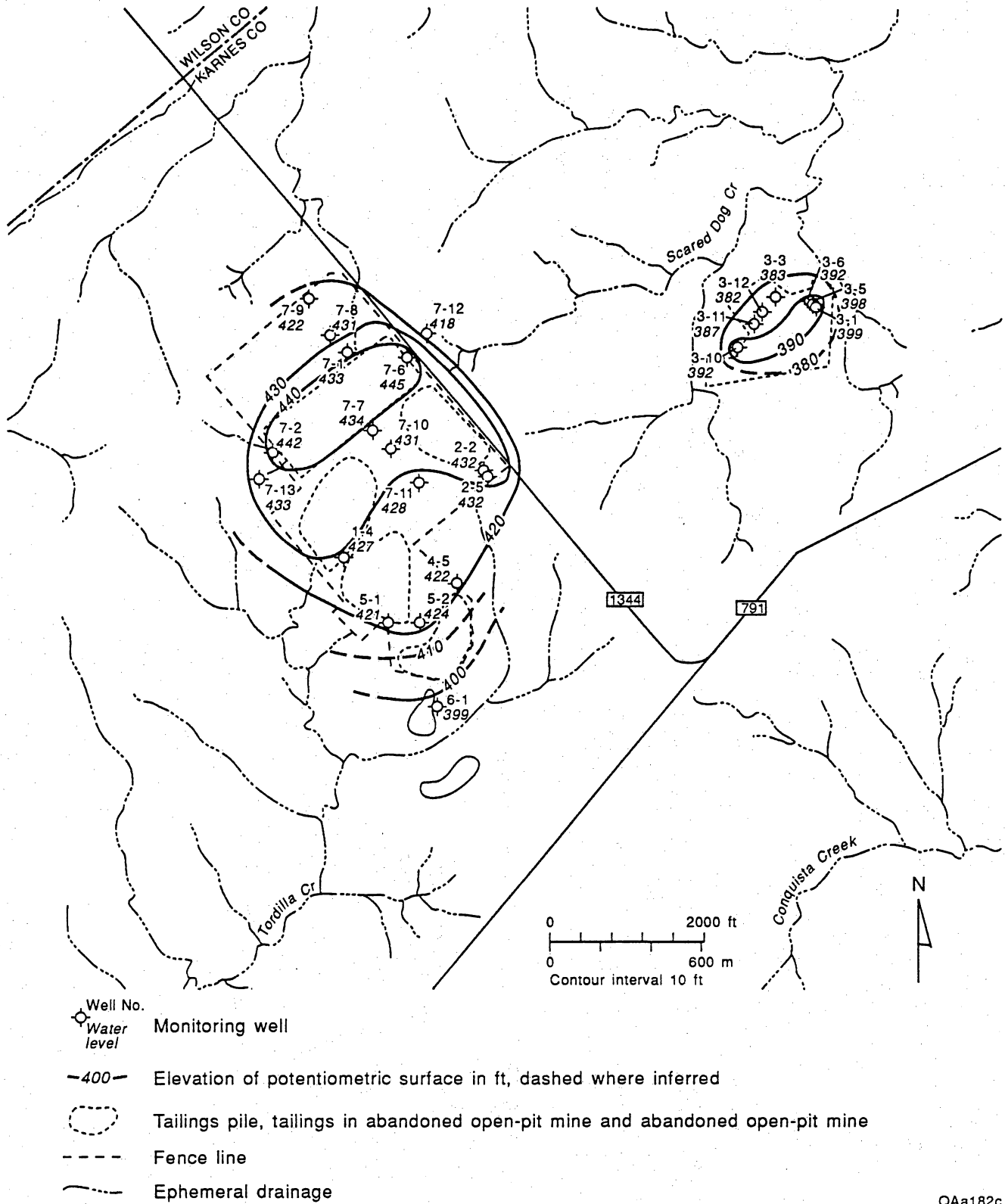


Figure 3.8. Intersections of water level with land surface, indicating approximate elevations of discharge.



QAa182c

Figure 3.9. Elevation of potentiometric surface of Deweesville/Conquista aquifer around tailings piles (August 1976).

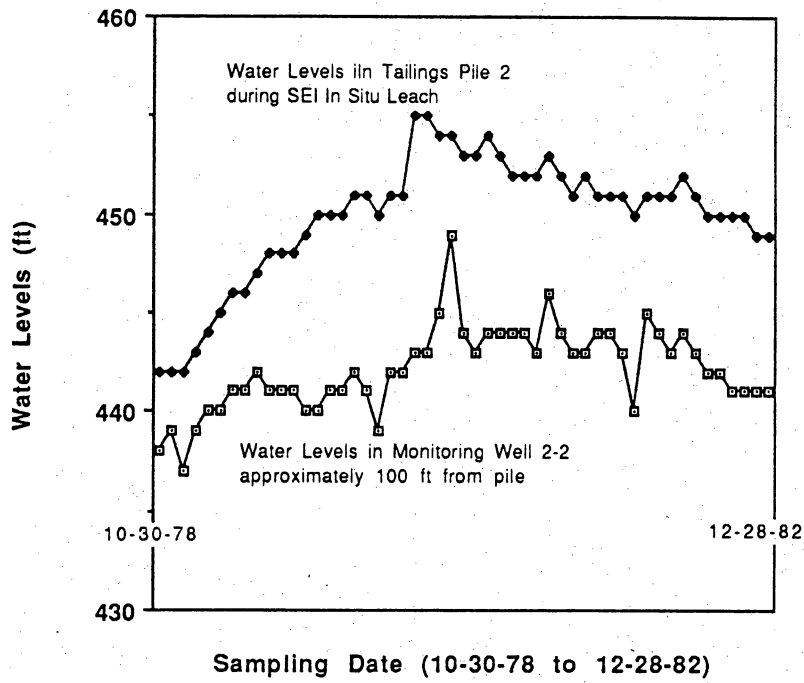


Figure 3.10. Comparison of water levels in tailings pile 2 to those in SEI monitoring well 2-2.

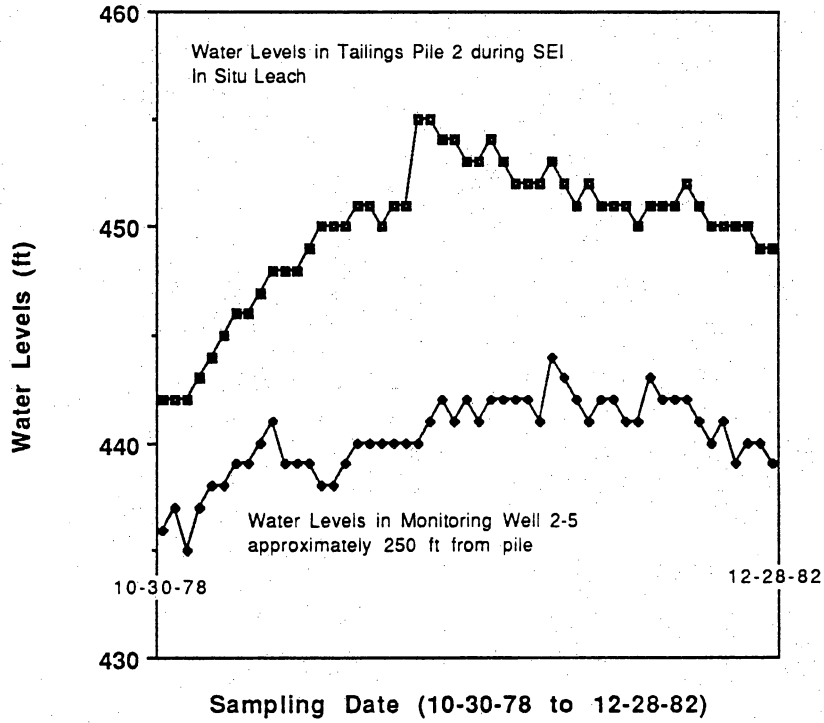


Figure 3.11. Comparison of water levels in tailings pile 2 to those in SEI monitoring well 2-5.

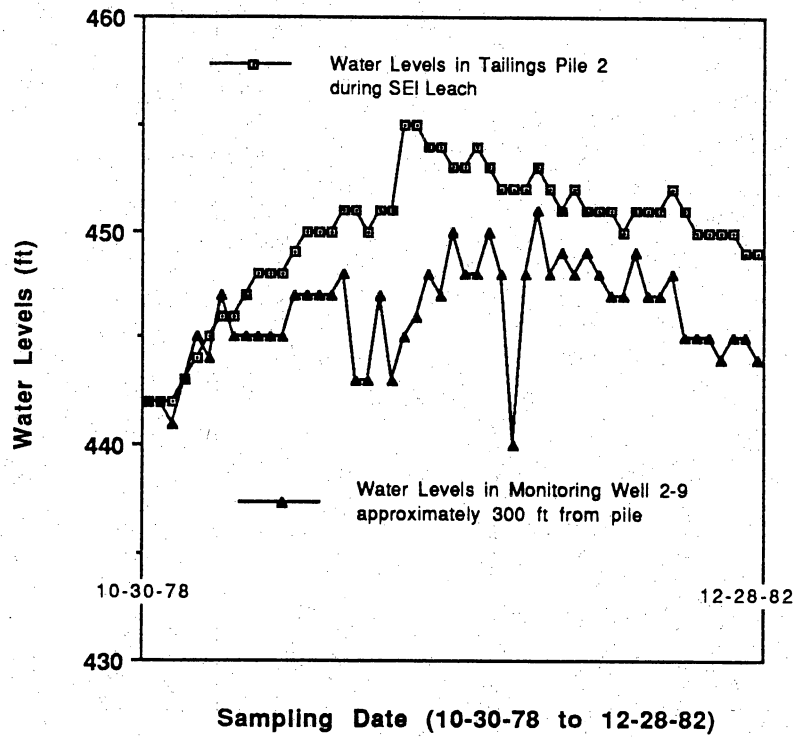


Figure 3.12. Comparison of water levels in tailings pile 2 to those in SEI monitoring well 2-9.

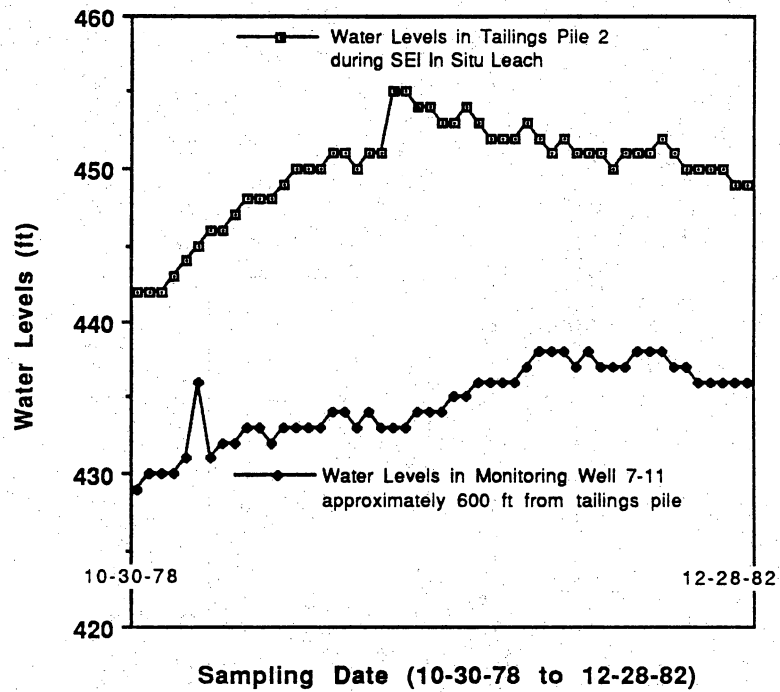


Figure 3.13. Comparison of water levels in tailings pile 2 to those in SEI monitoring well 7-11.

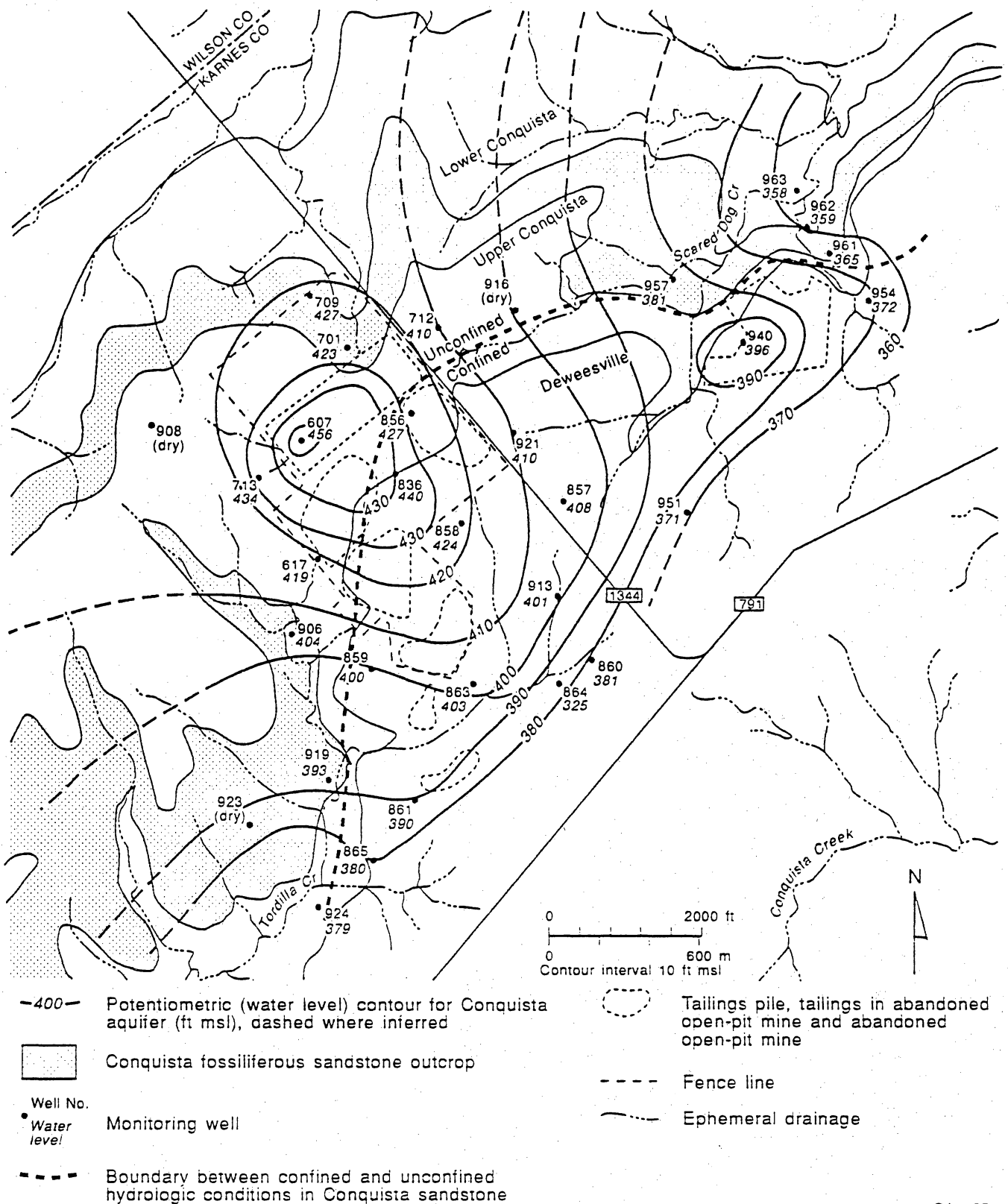


Figure 3.14. Potentiometric surface of the Conquista aquifer.

QAa185c

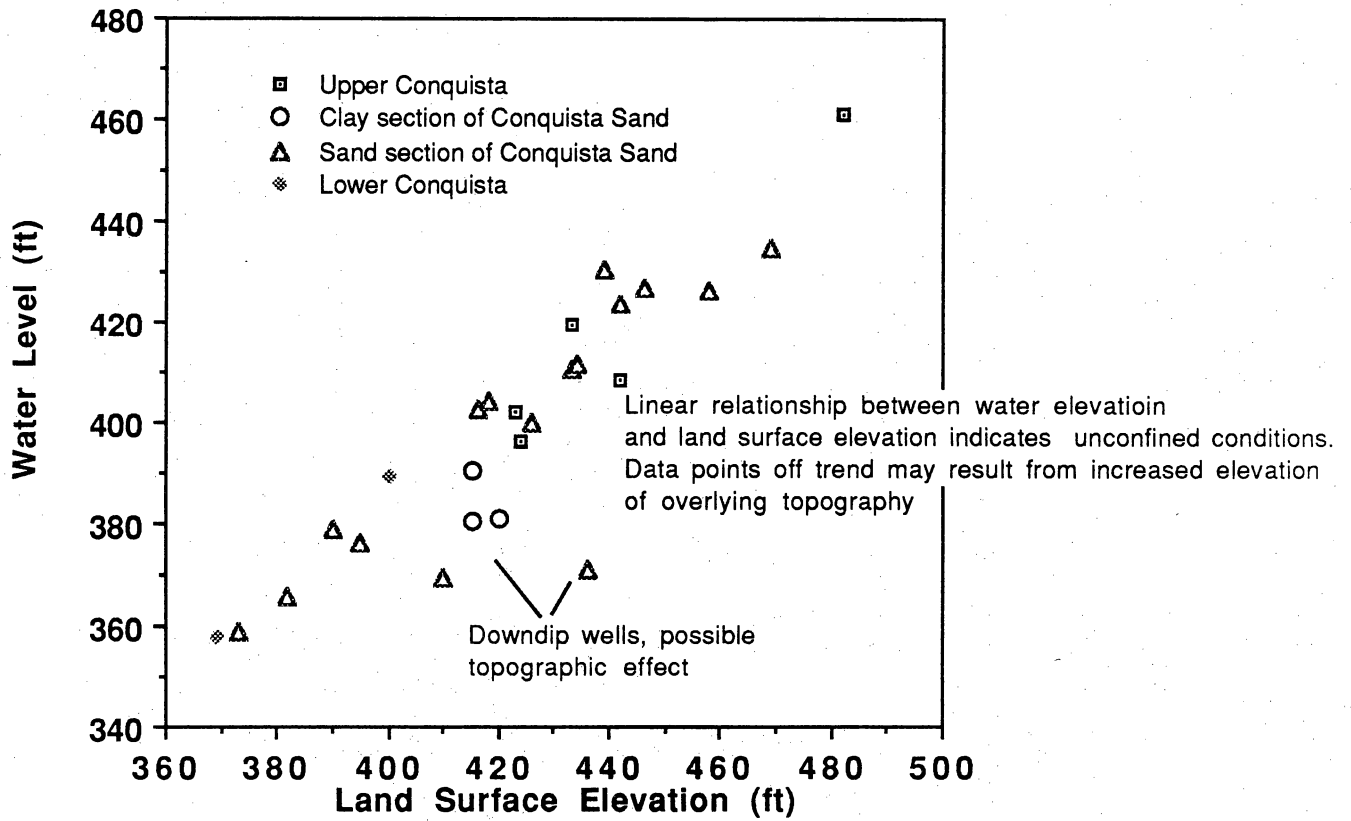


Figure 3.15. Water level versus land-surface elevation for the three subunits within the Conquista aquifer.

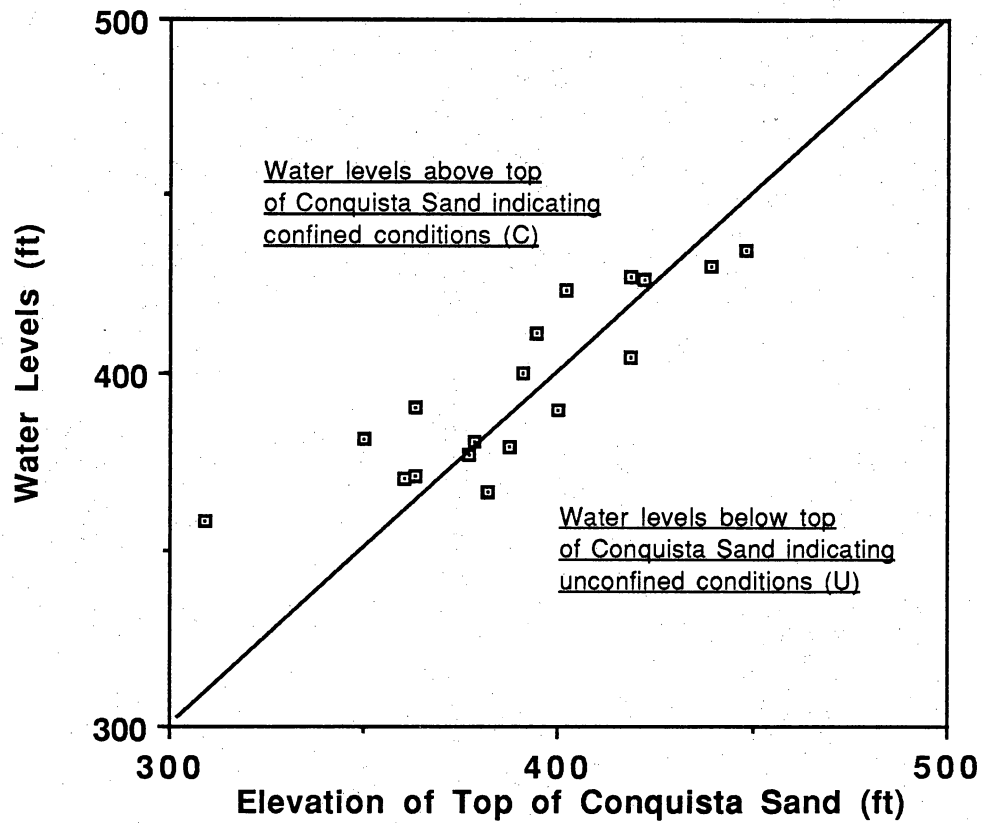


Figure 3.16. Water levels versus elevation of top of the Conquista aquifer, indicating whether aquifer setting is confined or unconfined.

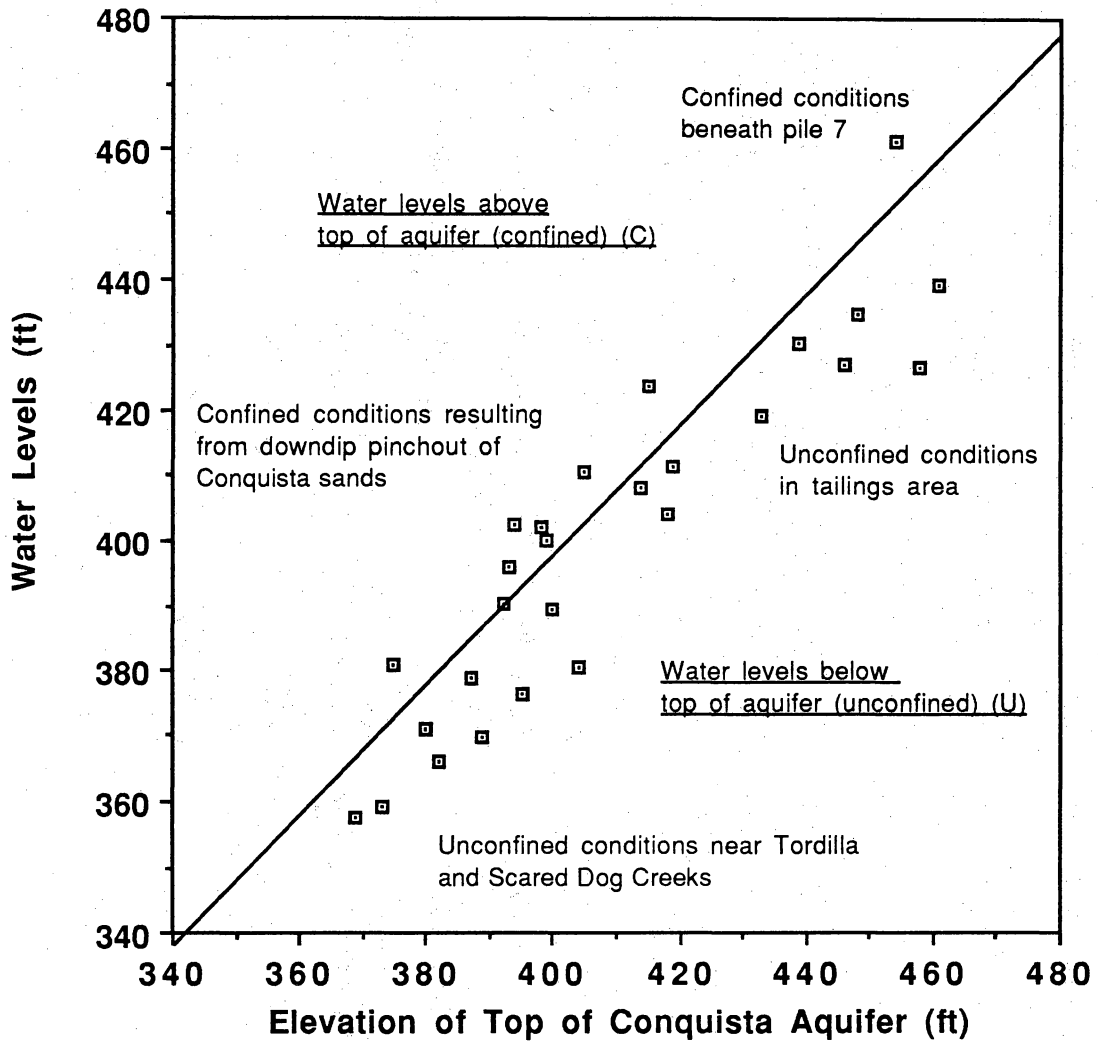
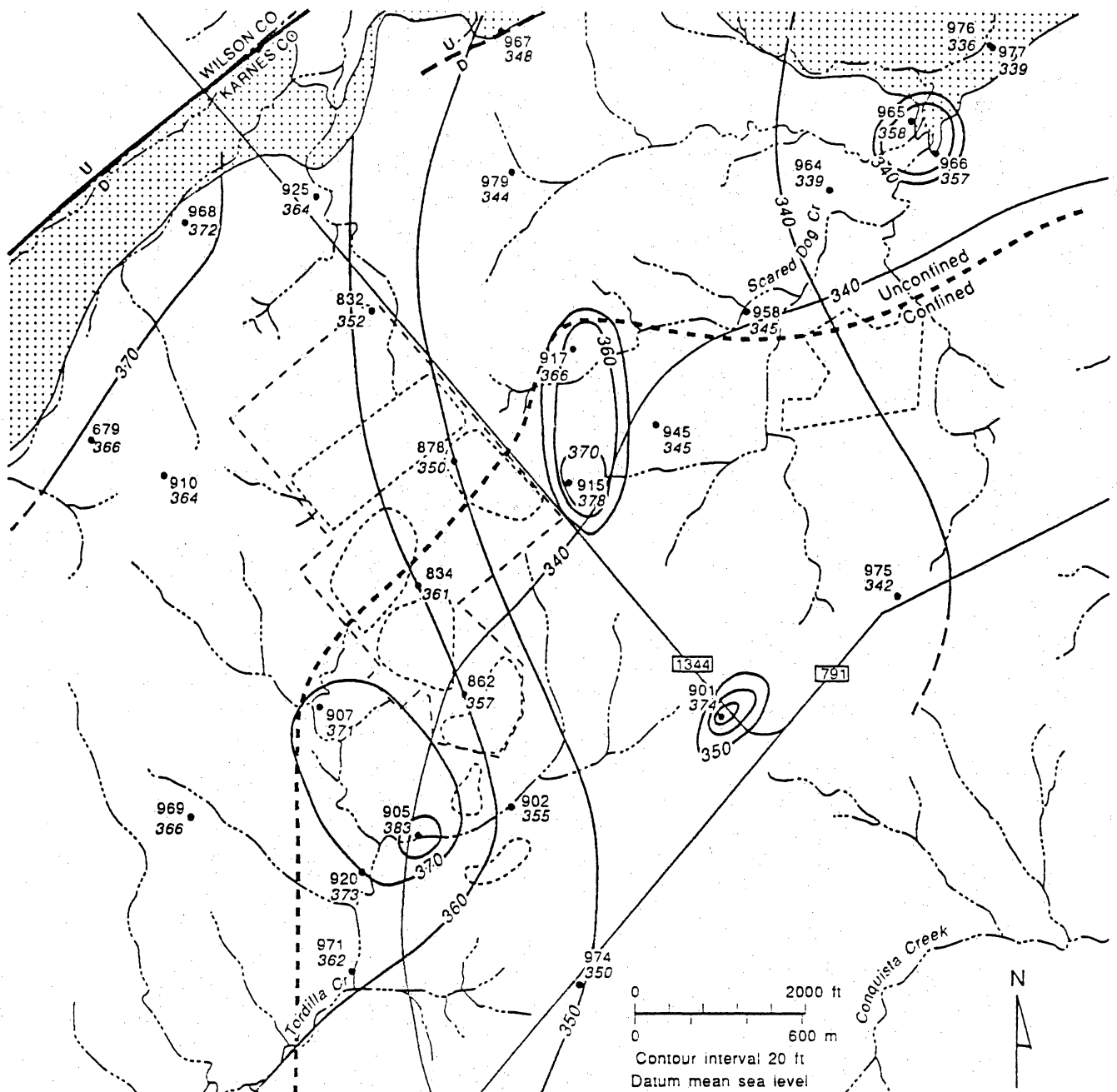


Figure 3.17. Water levels versus elevation of top of Conquista sandstone, indicating whether aquifer is confined or unconfined.



- 360- Potentiometric (water level) contour, in ft, for Dilworth aquifer
- 340- Top of Dilworth structure contour, in ft
- - - Boundary between confined and unconfined hydrologic conditions
- Well No.
• Water level Monitoring well
- [Stippled Box] Dilworth Sandstone Member outcrop

- [Dashed Oval] Tailings pile, tailings in abandoned open-pit mine and abandoned open-pit mine
- $\frac{U}{D}$ Fault
- - - Fence line
- [Wavy Line] Ephemeral drainage

QAa183c

Figure 3.18. Potentiometric surface of the Dilworth aquifer.

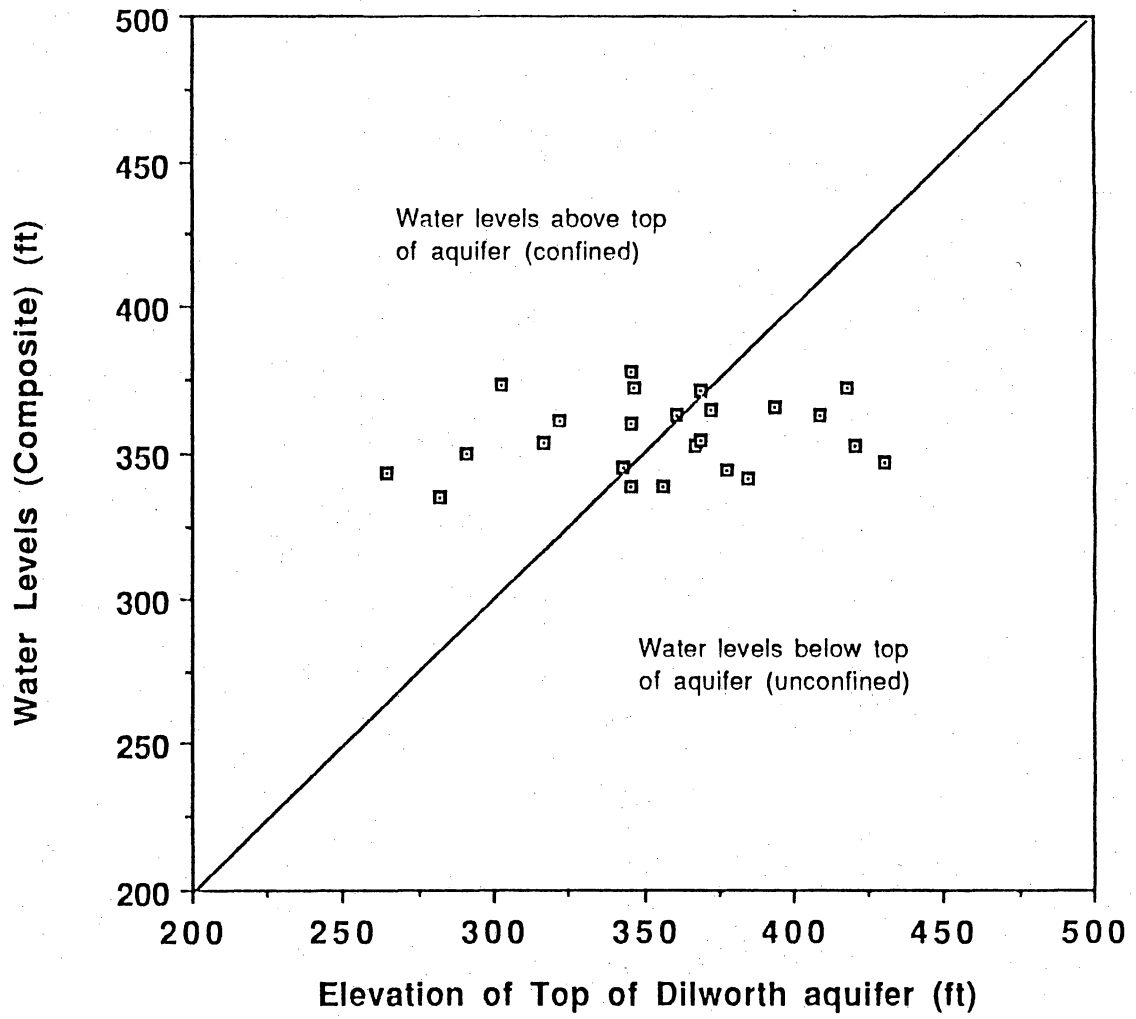


Figure 3.19. Water levels versus elevation of top of Dilworth aquifer.

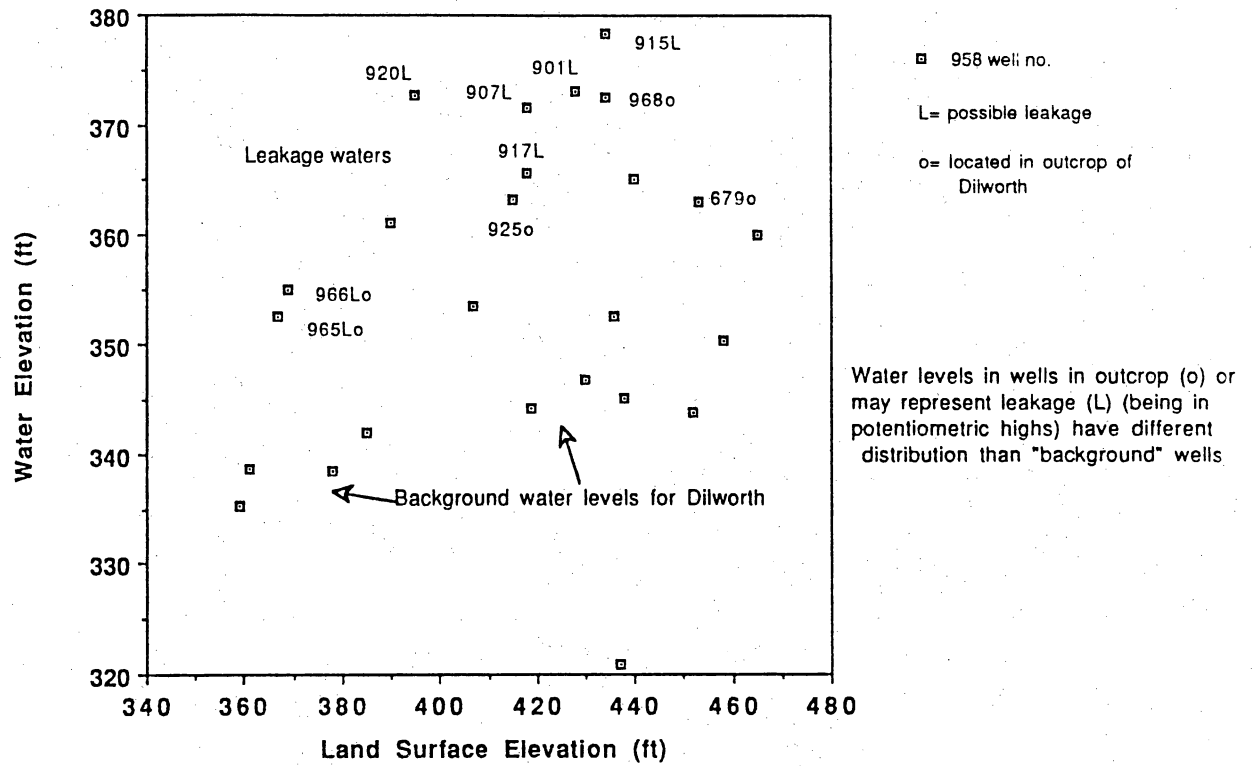


Figure 3.20. Water level versus land-surface elevation, Dilworth aquifer.

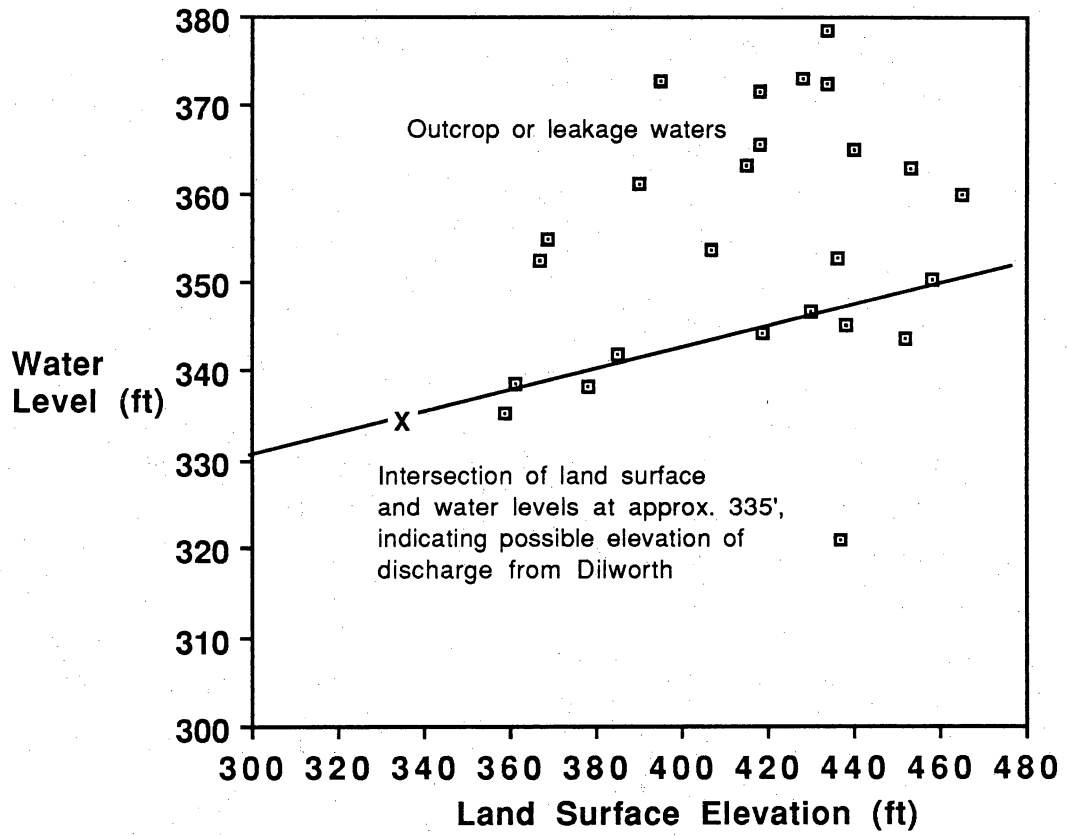


Figure 3.21. Intersection of water level with land surface, indicating possible elevation of discharge.

HYDROCHEMICAL CHARACTERIZATION (SECTION 4)

Methodology

Questions addressed by this portion of the study are: What are the contaminants? What is the extent of contamination? What reactions are affecting the contaminants as they migrate? Where are the contaminant plumes headed? What is not contaminated? Answering these questions requires a thorough and careful analysis of the data and an understanding of the geochemical processes that modify the tailings solutions as they migrate through the sediments below and beyond the tailings piles.

The method we used entailed the following steps:

1. Sort data according to hydrogeologic unit and geographic location.
2. Characterize tailings-solution contaminants and their chemical properties.
3. Identify the parameters indicative of contamination by the tailings solutions.
4. Compare the ground waters in each unit to the contaminant parameters, and map their distributions.
5. Determine the extent of contamination.
6. Determine the reactions and processes affecting the contaminants.
7. Identify parameters indicative of contamination and reactions, and organize the data base to reflect the extent and types of contamination.
8. Identify uncontaminated waters.

Hydrochemical data were collected from monitoring wells and lysimeters during May 1991 by Jacobs Engineering Group (fig. 3.1). In addition, data collected from 1976 through 1991 were used to confirm the 1991 analyses and identify recent changes in water chemistry. The May 1991 data were first sorted according to the hydrogeologic units sampled. Where the monitoring-well completions straddled two units, the data

were assigned to the more permeable unit. Data from the eastern area (pile 3) were compiled separate of data from the western portion of the site (tailings piles 1, 2, 4, 5, and 7; see the section on hydrochemistry along Scared Dog Creek for data relating to the eastern area).

Chemistry of the tailings solutions was characterized using data from lysimeters and monitoring wells completed in the tailings piles and data from batch leach studies of dried tailings conducted by Jon Blount at the BEG. Acid pH buffering by aluminum sulfate was investigated in the laboratory to provide quantitative data on the acidity of the tailings solutions and tailings leachates. In general, analysis and interpretation of the tailings solution chemistry provided the basic chemical information for recognizing contamination of the aquifers, identifying changes in contaminant chemistry due to geochemical reactions, and quantifying those reactions.

Geochemical reactions and processes affecting contaminants during migration through the aquifers include dilution, evaporation, cation exchange, acid neutralization by reaction with calcium carbonate, and acid neutralization by mixing with alkaline background waters. These reactions were investigated using a computer program with the capability of modeling reactions of minerals with solutions (SOLMINEQ.88; Kharaka and others, 1988; Perkins and others, 1990).

Maps of chemical parameters were prepared for each hydrologic unit at the site (the Deweesville Sandstone Member, upper Conquista clay, Conquista fossiliferous sandstone, lower Conquista clay, Dilworth Sandstone Member, and Manning Formation). Those maps, in conjunction with potentiometric surface maps and geochemical models of tailings solutions reacting with calcite, were used to delineate the contaminant plumes and to identify background ground waters in each hydrologic unit.

Water-chemistry data, sorted by hydrologic unit, were also sorted first by aluminum concentration and then, for waters with no detectable aluminum, by calcium concentrations. Waters with no detectable aluminum and with calcium below 900 mg/L

were tentatively considered as background waters, and chloride-to-bromide ratios supported this identification. Sorting the data in this way demonstrates covariance of other parameters, especially the hazardous constituents, with pH, aluminum, and calcium.

Although many different trace metals are associated with the tailings solutions and plumes, our analysis of the data found that these metals tend to occur and vary together. In order to reduce the number of parameters, clarify the pH dependence of these parameters, and relate these parameters to the tailings solution values, a single parameter was developed for both the cationic and anionic trace metals. That parameter is computed by subtracting the detection limit from the trace metal value (to assign a zero value to all values below detection), dividing by the average concentration of the metal in the tailings solutions (to normalize the different ranges of trace metals to a value between zero and one) and averaging those ratios for both anion and cation trace metals. These two averages greatly reduce the quantity of data and allow easier identification of the effects of reactions on the concentrations of trace elements.

No single parameter identifies contaminants in the aquifers. Only an understanding of the chemistry of the contaminants and chemical processes affecting the contaminants provides a clear delineation of the plume geometries.

Characterization of the Tailings Solutions

Summary

Tailings solutions are composed of dissolved neutral sulfate salts and sodium chloride. The predominant sulfate salts are aluminum and ammonium sulfate; lesser amounts of iron, calcium, magnesium, and potassium sulfate also exist. Ammonium, chloride, and sulfate were introduced as processing reagents, the latter as sulfuric acid. Reactions of sulfuric acid with aluminosilicates and oxides in the ores produced the

aluminum, iron, calcium, magnesium, and potassium sulfates. These dissolution reactions also produced soluble salts of trace metals including those occurring as cation species (beryllium, cadmium, cobalt, copper, nickel, radium, thallium, and zinc) and metals occurring as anion species (arsenate, chromate, molybdate, selenate, uranyl, and vanadate). Trace metals that form relatively insoluble oxidized chloride or sulfate salts (barium, silver, mercury, and lead) are generally below detection in the tailings. Metals commonly enriched in uranium deposits (uranium, radium, molybdenum, and arsenic), as well as those often associated with pyrite (thallium and cadmium), are enriched in the tailings solutions relative to amounts expected from dissolution of an average shale. The other metals are present in amounts typical of dissolution of an average shale.

Hydrolysis of aluminum sulfate produces the acid pH (pH 3 to 4) of the tailings solution. At least 1 mg/L aluminum sulfate must be present to generate an acid solution by hydrolysis. Also, aluminum sulfate is a strong pH buffer and controls the acidity of the solutions. This buffer explains the cluster of tailings and ground waters in the pH range of 3 to 4. A second cluster in the pH range of 6 to 7 is due to buffering by bicarbonate.

Bromide concentrations of the tailings solutions are variable, but those with higher chloride concentrations are relatively depleted in bromide when compared to natural ground waters. Thus, a high chloride-to-bromide ratio, probably related to the addition of chloride reagents during processing, serves as a tracer for tailings solutions in the aquifers.

Uranium Ore Processing

The tailings pile solutions derive from raffinates created during processing of uranium ores by SWI, between 1961 and 1973. According to records of process chemicals bought in 1967, reagents included sulfuric acid, sodium hydroxide, sodium chlorate, anhydrous ammonia, and ammonium chloride. In addition, calcium chloride and

hydrochloric acid were incorporated in a molybdenum extraction circuit, and sodium carbonate was used in the uranium precipitation circuit.

Uranium was extracted from ores by acid leaching of calcined ore (dried at 600° to 800°F). Dried, ground ore was diluted to about 45 percent solids with process water that included recycled raffinates. According to records from 1960, water used in processing was produced from an 800-ft-deep well. The pH of the slurry was adjusted to 1.0 by addition of concentrated sulfuric acid (Merritt, 1971). Records of process chemicals indicate that a small amount of oxidant (sodium chlorate) was added to the solution, although 95 percent recovery of uranium from some ores was obtained without adding oxidant (Merritt, 1971).

The acid leachate was separated from solids (tailings) in a countercurrent washing circuit in which sand and clay solids were first separated then washed using raffinates from the solvent extraction circuit. Polyacrylamide-type flocculant was used to flocculate and separate the clay solids from the pregnant liquor. The pregnant solution was stripped of uranium using an immiscible organic solvent composed of 7.5 percent Tertiary amine and 2.5 percent isodecanol in kerosene. Once stripped of uranium and separated from the loaded organic, the resulting raffinate (acid solution stripped of uranium) was either recycled through the leach circuit or pumped to ponds within the tailings piles (Merritt, 1971).

The loaded organic was stripped of uranium using 10 percent sodium carbonate solution or acidified sodium chloride. This pregnant strip solution was separated from the organic and then treated with sodium hydroxide to a pH of 7 to precipitate sodium diuranate. Molybdenum, which generally follows uranium through the circuit, does not precipitate, and remains in the neutralized, sodium sulfate solution (Merritt, 1971). As will be discussed, monitoring well 836, located near the old sludge pits just north of the mill, contains molybdenum-rich, bicarbonate-rich, sodium sulfate solutions produced by the uranyl precipitation stage.

The tailings were disposed of in tailings piles located in unmined areas (piles 1, 2, 3, and 7) or within abandoned open-pit mines (piles 4 and 5). Each tailings pile had a settling pond on top. The pH of the fluids in these ponds varied from 1 to 2, indicating that a large amount of sulfuric acid remained in the solutions. With time, this acid has reacted with the minerals in the tailings to produce the solutions of sulfate and chloride salts now sampled from the tailings piles.

Major Element Chemistry of the Tailings Solutions

The tailings solutions were sampled by lysimeters and monitoring wells (table 4.1). The major constituents are aluminum, ammonium, calcium, iron, magnesium, potassium, sodium, chloride, and sulfate (table 4.1). These constituents can be expressed as a mixture of sodium chloride and neutral sulfate salts in constant relative proportions dissolved in varying amounts of water (table 4.2). On average, the tailings solutions contain a mix of salts comprised of (in chemical equivalent percent, not weight percent) sodium chloride (17 percent) and neutral sulfate salts (83 percent), including aluminum sulfate (31 percent), ammonium sulfate (11 percent), iron sulfate (11 percent), calcium sulfate (13 percent), magnesium sulfate (10 percent), sodium sulfate (5 percent), and potassium sulfate (2 percent). These salts account for nearly 100 percent of the total dissolved solids in the tailings solutions. Other elements are present in minor or trace amounts.

Ammonia was added to the processes solutions during ore processing. Reaction of the ammonia with sulfuric acid produced ammonium sulfate. The remaining sulfate salts were created by reaction of sulfuric acid with the aluminum silicates present in the ores. Dissolution of the aluminosilicates is reflected in the composition of the tailings solution, as indicated by a comparison of an average shale composition to the average tailings solution chemistry (table 4.3). To make this comparison, it is necessary to

normalize the data to a component common to both the solid (an average shale) and the liquid (the average tailings solution). Aluminum is used for that purpose. When normalized to aluminum, the major element composition of the tailings solution (boron, calcium, fluoride, iron, magnesium, manganese, phosphate, potassium, and strontium) is found to be similar to an average shale (table 4.3).

Elements that are depleted in the tailings solutions (relative to an average shale) are those that form relatively insoluble sulfates or oxides. These are barium (which has precipitated as barium sulfate), phosphate (which appears to be controlled by precipitation of ferric phosphate), and silica (which precipitates as amorphous silica). Computation of saturation indices (using SOLMINEQ.88) indicates that all of the tailings solutions are saturated with barium sulfate (barite) and ferric phosphate (strengite) and near saturation with amorphous silica (table 4.4).

Elements enriched in the tailings solutions are sodium, chloride, bromide, and sulfate. Sulfate was added as sulfuric acid. Bromide is associated with chlorides and may have been added to the solutions as a component of the sodium chloride reagents. Or, both the chloride and bromide may be naturally abundant in the ores. The ores are supergene deposits formed near the ground-water table. Studies by the U.S. Geological Survey (1958) found that the Falls City ores were associated with relatively high chloride concentrations due to evapotranspiration of ground waters at and above the ground-water table. Rainwater, a possible source of the ground-water chloride, is enriched in bromide relative to chloride and the high bromide-to-chloride ratio of the tailings solutions (1 to 500) may reflect evaporative concentration of rainwater chloride and bromide in the uranium ores. Regardless, the major element chemistry of the tailings solution certainly reflects, in large part, dissolution of an average shale by sulfuric acid.

Trace Element Chemistry of the Tailings Solutions

The dissolution of an average shale is also the source of many of the trace metals present in the tailings solutions. Uranium ores may or may not be enriched in many of these metals, depending on the type of deposit (Galloway and others, 1982). At the Falls City site, no enrichment (relative to an average shale) is required to explain the presence of most trace metals in the tailings solutions, as demonstrated by a comparison of an average shale to trace metals present in an average tailings solution from the site (normalized to the aluminum). Dissolution of an average shale explains the concentrations of the antimony, beryllium, cobalt, nickel, selenium, silver, vanadium, and zinc (table 4.3). Chrome, copper, and lead are quite depleted relative to an average shale. These three metals are present, but their low concentrations in the tailings solutions suggests that they are either present in naturally low amounts, precipitated out as insoluble solids, or sorbed by the tailings. Chrome forms an oxidized anionic complex (chromate), which is likely to be sorbed under acid conditions or coprecipitated with ferric hydroxides as chromite (FeCr_2O_4 ; Hem, 1977). Lead sulfate is a relatively insoluble salt and the tailings solutions are near saturation with lead sulfate (table 4.4). Copper may simply be present in low concentrations in the ores. Analyses of copper in soils at the Falls City site (Henry and Kapadia, 1980) indicate that copper averages 5 ppm, which is about 0.1 of the copper content of an average shale (57 ppm).

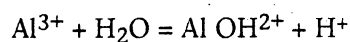
Arsenic, molybdenum, and uranium are greatly enriched in the tailings solutions. All are commonly associated with uranium ores. Also, cadmium and perhaps thallium are enriched, and both are associated with sulfides, including pyrite. The oxidation and destruction of pyrite was an important natural process in formation of the uranium ore, and the enrichment in cadmium and thallium may reflect that process. One line of evidence that supports this supposition is a semiquantitative analysis of an amorphous manganese dioxide deposit collected from the lower Conquista clay. That analysis

indicated the presence of thallium, as well as barium, strontium, yttrium, lanthanum, cerium, uranium, and abundant cobalt.

Uranium in the tailings solutions is equivalent to a shale with 0.04 weight percent uranium or 21 percent of the reported 0.19 weight percent uranium in the ores (Merritt, 1971). Radium-226 concentrations in the tailings solutions average 300 pCi/L or 0.43 pCi per ppm Al. Assuming that the ^{226}Ra in the original uranium ore was in secular equilibrium with its parent U-238 and that the initial ore contained 0.19 percent total uranium (equivalent to 64,600 pCi ^{238}U per 100 grams ore) then the ^{226}Ra concentration in the ore would have been 64,600 pCi per 100 grams of ore, or 1.4 pCi per ppm aluminum. Thus, the tailings solutions are only slightly depleted in radium relative to the initial ores.

Source of the Tailings Solution Acidity

Although the sulfuric acid added to the raffinates was consumed by reactions with the ore, the tailings solutions remain very acid, having pH values of 2.8 to 3.9. This acidity is due to the presence of aluminum sulfate and, to a lesser extent, iron sulfate in the tailings pile salts and solutions. Aluminum sulfate ($\text{Al}_2[\text{SO}_4]_3$) and alums (sodium or potassium aluminum sulfates) are soluble, hydrolyzing salts. When dissolved in water, aluminum ions form a complex with hydroxyl ions, leaving free hydrogen ions.



In effect, the aluminum ions compete with hydrogen ions in the water for the hydroxyls. As a result, the activity of the hydrogen ion increases, which is measured as a decrease in the pH (the negative log of the hydrogen ion activity). Thus, aluminum sulfate salts are weak acids.

The relation between dissolved aluminum and pH of tailings solutions and ground waters at the Falls City site is such that, for a given aluminum content, most of the acid

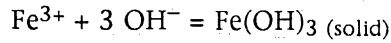
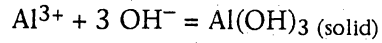
waters are in a pH range expected for aluminum sulfate solutions (fig. 4.1). In waters containing appreciable iron, such as those at the Falls City site, precipitation of iron hydroxides will also cause a decrease in pH. Further, the Falls City tailings solutions and ground waters are oversaturated with respect to alunite, and its precipitation would also tend to decrease the pH. In general, the relation between aluminum and pH in Falls City site acid waters is consistent with aluminum sulfate being the major cause of low pH with a secondary contribution from iron sulfate. The Falls City site solutions do not contain unreacted sulfuric acid.

At least 1 mg/L aluminum sulfate must be present to generate an acid solution by hydrolysis. This is based on the following reasoning. If acid is defined as having a pH of 4 or less, then hydrolysis of at least 0.33×10^{-4} moles per liter of aluminum (as aluminum sulfate) or 0.9 mg/L must occur to produce an acid solution. Thus, in plots of aluminum concentrations in ground waters, waters with more than 1 mg/L aluminum generally correspond to acid ground waters. If the tailings solutions are evaporated to dryness, aluminum sulfate and other neutral salts precipitate. Redissolving the sulfate salts will simply reconstitute an acid solution. The sulfate salts are acid anhydrides. This explains why batch leaching of dried tailings using distilled water produces acid leachates. Drying the tailings will not reduce the capacity of the tailings to produce acid solutions when wetted.

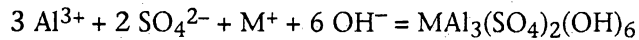
Acidity Related to Aluminum Sulfate

A second important effect of the dissolved aluminum sulfate is that it is the major source of acidity in uranium mill tailings impoundments (Longmire and others, 1990). Acidity of a solution is its quantitative capacity to react with a strong base to a designated pH (American Public Health Association, 1985). The acidity of tailings solutions can be

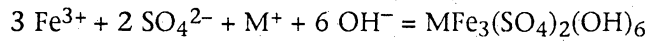
much greater than indicated by pH due to reaction of the aluminum (and iron) with bases to produce basic aluminum and iron salts. Simplified reactions are



where dissolved aluminum and iron react with an added base to form hydroxide precipitates. Precipitation of basic sulfate salts of aluminum and iron sulfate (alunites and jarosites, respectively) will have the same general effect of consuming a base—



(alunites, where M^{+} may be K^{+} , Na^{+} , NH_4^{+}).



(jarosites, where M^{+} may be K^{+} , Na^{+} , NH_4^{+}).

Regardless of which basic salts are precipitated, the precipitation of aluminum and iron consumes added bases and preserves the pH (hydrogen ion activity) of the solution until the aluminum and iron are exhausted. The aluminum-hydroxide ion species that produce acid pH values involve about 10 percent of the total aluminum in an aluminum sulfate solution. The remaining 90 percent aluminum is present as free aluminum or aluminum-sulfate species; these species provide an aluminum “reserve” for reaction with bases. Thus, aluminum and to a lesser extent iron buffer the pH of the tailings solutions to acid values. This is demonstrated by acidity titrations performed in the laboratory.

A graph of an acidity titration of an aluminum sulfate solution prepared in the laboratory (fig. 4.2) provides a typical buffer curve for an aluminum sulfate solution. Initially, the pH is poorly buffered, rising from an initial pH value of 3.8 to a value of 4.1 with the addition of a small amount of strong base. Then, from pH 4.1 to 4.6, the change in pH is gradual (buffered), requiring considerable base to increase the pH. It is over this range that visible basic aluminum salt precipitation occurs (X-ray diffraction indicates that these salts are amorphous). At pH 4.6, aluminum in solution is nearly exhausted and

pH increases rapidly with the further addition of base. At high pH values, greater than 8.3, redissolution of the aluminum hydroxides again buffers pH (although not shown in fig. 4.2).

An acidity titration of surface waters from pond 6 (fig. 4.2) also displays the influence of aluminum on acidity. The acidity, to a pH of 7, is 17 meq base per liter of solution, 34 times that indicated by the initial pH (3.3). Analyses of the pond 6 water indicate minor iron (2 mg/L) but 168 mg/L aluminum. Precipitation of that aluminum as $\text{Al}(\text{OH})_3$ would require 18.6 meq base per liter, agreeing with the measured acidity (17 meq/L). Also, the form of the acidity titration curve closely matches that of the aluminum sulfate solution titration curve consistent with aluminum precipitation as the source of acidity.

A tailings solution was prepared by leaching 20 grams of dried tailings from pile 7 (core 869, 35–37 ft) in 40 ml of distilled water. The filtered leachate was oxidized (using hydrogen peroxide to oxidize all iron to the ferric state) and then subjected to an acidity titration (fig. 4.2). The procedure is a standard method used to measure solution acidity (American Public Health Association, 1985). The titration curve of the tailings solution is similar to that of the aluminum sulfate acidity titration, but with some differences. First, there is minor buffering of pH in the range of 3 to 4 due to ferric hydroxide precipitation. Strong buffering occurs in the pH range of 4 to 4.6 (due to basic aluminum hydroxide precipitation), then all buffer capacity is lost and pH rises rapidly (fig. 4.2), indicating depletion of aluminum and iron from the solution. The total measured acidity of the tailings solution (to a pH of 7) was 205 meq base per liter of solution, equivalent to a 0.2 normal acid. The initial pH of the solution (after oxidizing the iron) was 2.45, equivalent to a strong (highly dissociated) acid with a normality of 0.0035. Thus, the measured acidity is 56 times that indicated by the initial pH.

Relative to dried tailings weight, neutralization of the leachate requires 410 meq base per kilogram tailings (fig. 4.2). Based only on this one measurement, neutralization

of tailings by adding a solid base, such calcium carbonate, requires mixing tailings with about 2 weight percent calcite.

Iron also provides a source of acidity, and oxidation of ferrous iron and its precipitation as iron hydroxides (ferrolysis) may produce solutions with low pH. At the Falls City site the dominant source of acidity in the tailings solutions and contaminated ground waters is aluminum, but iron plays an important secondary role, accounting for about 25 percent of the total acidity. In contrast, iron sulfate, rather than aluminum sulfate, may be a major source of natural acidity in sediments at the site. One example is a leachate of a lower Conquista claystone from core 870. This claystone is at an oxidation-reduction boundary 75 ft below the surface. Oxidation of pyrite has produced iron sulfate. Leaching that clay produced a solution with a pH of 3.0. After oxidizing the leachate with hydrogen peroxide, pH decreased to 2.4 due to precipitation of ferric hydroxide. The absence of aluminum in this solution is evident in the acidity titration curve, which is not buffered (fig. 4.2). The total acidity to a pH of 7 was 45 meq base per kilogram of clay, or about 0.1 that of the tailings. (These data are discussed further in the section on batch leach experiments.)

The presence of acid sediments at the Falls City site is indicated by batch leach data, as well as in other studies (U.S. Geological Survey, 1958). The difference in the form of the titration curves could be useful in recognizing whether acid pH soils and sediments contain aluminum or iron sulfate salts, perhaps discriminating between tailings contamination versus natural acid soils. The method is cheap, simple, and rapid and provides semiquantitative information on the source of soil acidity.

The general importance of the aluminum-sulfate pH buffer is evident in the distribution of pH in tailings solutions and ground waters at the Falls City UMTRA site. The pH values are generally in the range of 3 to 4 or 6 to 7 (fig. 4.3). This distribution, including the general lack of waters with pH values between 4.6 and 5.6, indicates the

presence of two different pH buffers. As discussed, aluminum sulfate is the acid pH buffer. Ground-water analyses indicate that bicarbonate is the high pH buffer.

Chloride-to-Bromide Ratios

Chloride-to-bromide ratios appear to be useful as supportive data for ground-water contamination by tailings solutions. Chloride-to-bromide ratios are useful as tracers in waters undergoing extensive reactions because both ions are unaffected by those reactions and remain in constant proportion. Chloride-to-bromide ratios are therefore used to discriminate solutions having different sources. The ratio is fixed in both seawater and solutions derived directly from seawater, such as connate (depositional) waters in sediments and rainwater (the salts in rainwater coming from aerosols). These sources have chloride-to-bromide ratios of about 300, a ratio that is common in shallow ground waters. Other sources of chloride, such as chemical reagents, are likely to have much higher chloride-to-bromide ratios (being depleted in bromide). Chloride may have been added in large amounts to at least some of the ore process solutions, as indicated by the relation between chloride and bromide in the tailings solutions (fig. 4.4). About half of the sampled tailings solutions have chloride-to-bromide ratios significantly greater than seawater. For comparison, ground waters in the Dilworth aquifer, which are generally uncontaminated, have chloride-to-bromide ratios similar to seawater (fig. 4.4). One water from the Dilworth (sample 905) has high chloride to bromide, anomalous chloride, anomalous calcium, and an anomalously high potentiometric surface—data indicating contamination by tailings-derived solutions.

Thus, high chloride-to-bromide ratios may serve as indicators of contamination. However, low ratios (similar to seawater) are not necessarily indicative of uncontaminated ground waters since some tailings solutions have seawater ratios (fig. 4.4). Also, at low chloride and especially low bromide concentrations, analytical errors can

result in spurious chloride-to-bromide ratios. Chloride-to-bromide ratios must be used in conjunction with other data to determine contamination or lack of contamination of ground water.

Reactions of Tailings Solutions with Sediments

Summary

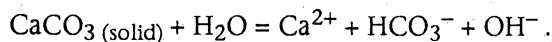
Neutralization of the tailings solutions is predominantly a reaction of aluminum sulfate with a base to produce a basic aluminum salt. Neutralization by calcite produces high partial pressures of carbon dioxide (one atmosphere). A mere 0.05 volume percent of calcite will neutralize an average tailings solution migrating through sediment. The reactions will have a negligible effect on porosity and permeability.

In contrast, neutralization of a tailings solution by mixing with a typical alkaline bicarbonate water requires a large volume of alkaline water (>90 percent) due to the buffering capacity of aluminum sulfate. Thus, pH is a sensitive indicator of small amounts of contamination and aluminum is a direct indicator of the remaining acidity of the contaminant. The tailings solutions and acid ground waters are equilibrated with the common aluminosilicates in both sediments and tailings and will not significantly react with those minerals.

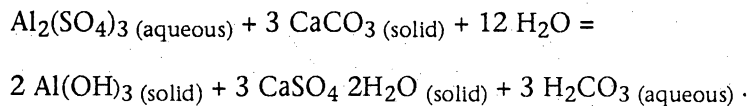
Ground waters at the site appear to be in equilibrium with cation exchangers, predominantly calcium smectite. Exchange reactions between these smectites and migrating tailings solutions probably result in the near-total removal of ammonia and large decreases in sodium, magnesium, and potassium. These ions are probably exchanged for calcium, which then precipitates as gypsum, resulting in a decrease in sulfate concentrations. These postulated exchange reactions could be proved with further study of available core.

Neutralization of Aluminum Sulfate Acidity by Calcite

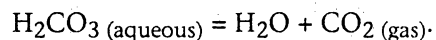
The natural neutralization of contaminant ground-water plumes at the site appears to be due to reaction of dissolved aluminum and ferric sulfate with either solid calcium carbonate or alkaline ground waters. Calcium carbonate is a base which, when dissolved in water, produces free hydroxyls by complexing of the carbonate ion with hydrogen ions. The reaction is



When an acid aluminum sulfate solution encounters solid calcium carbonate, the pH of the solution increases due to the loss of aluminum from the solution by the reaction



Carbonic acid (H_2CO_3) is created by this reaction and, in part, the reaction simply replaces one acid (aluminum sulfate) with another (carbonic acid). The pH of the solution will increase to about 6 because carbonic acid is a weakly dissociated acid. However, while the pH is relatively high the acidity is still equal to the initial acidity unless the carbonic acid is lost by degassing of the solution



From a practical standpoint, the pH, not acidity, controls the adsorption or precipitation of trace metals; thus, increased pH is an important effect of reaction with calcite. Relatively high partial pressure of the CO_2 (P_{CO_2}) values are good indicators of reactions with calcite.

Computer modeling of neutralization of an aluminum sulfate solution (with an aluminum content equal to that of an average tailings solution—714 mg/L aluminum, table 4.3) reacting with calcite (calcium carbonate) indicates that the P_{CO_2} generated is equal to 1 atmosphere (table 4.5). Carbon dioxide partial pressure in the atmosphere is 0.0003 atmosphere. Thus, there is a strong tendency for the evolved CO_2 to escape to

the atmosphere. Computations of the P_{CO_2} in ground waters at the site indicate that, near the ground-water table, the P_{CO_2} values are in the range of 0.5 to 0.1 atmosphere. This is significantly greater than P_{CO_2} values commonly reported for shallow ground-water systems and soil waters (0.1 to 0.01; Drever, 1982), and it will be shown in later sections that some of the highest values of ground-water P_{CO_2} , on the order of 0.4 atmosphere, are due to the reaction of the tailings solutions with calcite.

Despite the seemingly large acidity of the tailings solutions, the amount of calcite required to neutralize an average tailings solution is actually quite minor. The stoichiometry of the reaction indicates that an average tailings solution with 714 mg/L aluminum (26.4 mmoles/L) will be neutralized by the addition of 4.0 g/L of calcite (39.7 mmoles/L calcium carbonate). Computer modeling of the reaction gives a slightly greater value (4.7 g/L calcite) due to changes in the solution chemistry during the reaction, primarily the increase in bicarbonate. The 4.7 grams of calcite per liter of solution is equivalent to 1.7 cc of calcite per liter of solution. Assuming that the sediments at the site have a porosity of 33 percent (a liberal estimate), 3 L of sediment would contain 1 L of pore space. If that 1 L of pores were contaminated by tailings solution, only 1.7 cc of calcite per 3 L of sediment would be required to neutralize the solution. In other words, 0.058 volume percent calcite in the sediments is all that is required to neutralize tailings solutions entering the sediments.

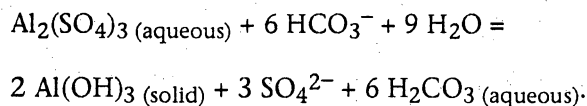
If calcite is present, these reactions will certainly occur. And, the existence of acid ground waters in the Deweesville sandstone at the Falls City site indicates that the Deweesville near outcrop contains virtually no calcium carbonate. A few analyses of neutralization potentials of sediments at the site support this; four of five Deweesville sandstone samples had less than 0.05 weight percent calcium carbonate (Pyrih and Associates, 1986).

Relative to the sediment bulk volume, the reaction consumes 0.058 volume percent calcite and produces 0.056 percent gypsum and 0.023 percent aluminum

hydroxide (boehmite). These small amounts of precipitates are difficult to detect, and attempts to identify such precipitates in the sediments surrounding the tailings piles were generally fruitless. X-ray diffraction of a high-pH sediment from beneath tailings pile 7 did identify calcite and gypsum occurring together in small nodules (as discussed in the section on batch leach experiments). Also, the net volume of precipitate (0.021 volume percent, equal to the precipitated volume less dissolved volume) will have a negligible effect on porosity and permeability of the sediments. Reactions of the tailings solutions with the sediments will not significantly increase or decrease the porosity or permeability of the sediments.

Neutralization by Mixing with Alkaline Waters

In the absence of calcite, neutralization of contaminant plumes will occur when acid aluminum sulfate waters mix with alkaline bicarbonate waters, provided that such waters are present. The reaction is



At the Falls City site, waters with pH values in the range of 5.8 to 7.0 have bicarbonate concentrations (alkalinity) ranging from 37 to 1061 mg/L as calcium carbonate. The average is 308 mg/L (\pm 195) as calcium carbonate or 375 mg/L as bicarbonate (6.16 mmoles/L). For the purposes of modeling neutralization by mixing, a water based on the chemistry of water from the Deweesville sandstone (monitoring well 677) was used. That water has an alkalinity of 268 mg/L as bicarbonate (4.4 mmoles/L). Assuming that the above reaction approximates the stoichiometry of the neutralization of aluminum sulfate, computation of the amount of mixing required to neutralize the aluminum sulfate in an average tailings solution is derived from the relation

$$2 X (\text{Al}) - 6 (1-X) \text{HCO}_3^- = 0$$

where X is the fraction the aluminum sulfate solution in the mix, 1-X is the fraction of bicarbonate solution in the mix, Al is the concentration of aluminum (in mmoles/L) in the aluminum sulfate solution, and HCO_3 (in mmoles/L) is the concentration of bicarbonate in the alkaline solution. Using the values 714 mg/L aluminum (26.6 mmoles/L) and 268 mg/L bicarbonate (4.4 mmole/L), X is found to be 0.076. That is, neutralization of the aluminum sulfate will require a mixture of about 92 percent alkaline ground waters with 8 percent tailings solution. Computer modeling of the mixing of two such solutions indicates that to increase the pH to 6.0 would require 99 percent alkaline ground water and 1 percent tailings solution (table 4.6). In this model the solution is first saturated with respect to gypsum (as are all of the tailings solutions), then brought to equilibrium with boehmite ($\text{Al}[\text{OH}]_3$). The reaction simply exchanges some of the initial aluminum for hydrogen ions; the acidity does not change. Then the solution is mixed with the bicarbonate solution (also at gypsum saturation) and equilibrated with boehmite. Both the above computation and the computer model illustrate that as little as 10 percent tailings solution mixed with an alkaline water typical of that occurring at the site will produce acid waters (with a pH of 4 or less).

Conversely, mixing less than 10 percent of tailings solutions with an alkaline water will produce acid (pH <4) ground waters. Thus, pH is a sensitive measure of contamination by acid tailings solutions. However, pH, in itself, is not a measure of acidity of contaminated water. Waters with pH values of 3 to 4 vary in aluminum content (and iron) by as much as two orders of magnitude (fig. 4.1), and it is the aluminum and iron that control the acidity, not pH. Thus, in mapping the extent of contaminant plumes, aluminum is used as an indicator of the acidity of the contaminant. The smaller the aluminum and iron content of a solution, regardless of pH, the greater the probability that reaction with calcite or mixing with alkaline waters will neutralize the solution.

Neutralization by Reactions with Aluminosilicates

Reactions with aluminosilicates will not neutralize the tailings solutions because the solutions are already near equilibrium with the aluminosilicates due to the very high concentrations of aluminum, silica, and alkalis. Aluminum silicates and silica are the predominant constituents of both sediments and tailings at the site. The silica occurs as detrital quartz, diagenetic opal, and diagenetic chalcedony. The tailings solutions are oversaturated with respect to all of these silica polymorphs, and saturated with respect to amorphous silica (table 4.4). Thus, the tailings solutions will tend to precipitate, not dissolve, silica as they migrate through the sediments beneath the tailings piles.

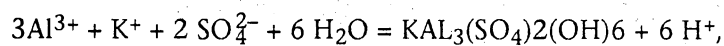
Common potassium-bearing aluminosilicates at the site include potassium feldspars and potassium clinoptilolite. Equilibria diagrams for these two minerals indicate that both the acid tailings solutions and the acid ground waters at the site are near saturation with respect to potassium feldspar and near to slightly oversaturated with respect to clinoptilolite (fig. 4.5). The more basic waters (pH of 5 to 7.5) tend to be oversaturated with respect to both potassium-bearing phases.

Plagioclase feldspars are common in the sediments at the site. The most stable of these is albite, which may not occur as a pure mineral at the site. X-ray diffraction data indicated that most of the plagioclases are solid solutions. However, the acid tailings solutions and acid ground waters are essentially saturated with respect to albite (fig. 4.6). The more basic ground waters are oversaturated with respect to albite and the more calcic plagioclases.

Smectites are very common at the site, in both the sedimentary shales and sands and within the tailings piles (as slimes). Equilibrium diagrams for both calcium- and sodium-smectite indicate that the acid tailings solutions and acid ground waters are essentially saturated with respect to these phases, while the more basic waters are oversaturated (fig. 4.7).

Equilibrium with Alunite

In general, the acid tailings solutions are near saturation with jarosite, a phase that has been identified in air-dried tailings by X-ray diffraction. All tailings and ground-water solutions at the site (in which aluminum was detected) are oversaturated with respect to potassium-alunite (fig. 4.8). Note that, unlike the aluminosilicates, the degree of oversaturation remains relatively constant over the entire pH range. The variability in the logs activities of silica, sodium, potassium, calcium, and sulfate are all relatively small over the pH range of the ground waters at the site. But pH is strongly related to changes in aluminum activity such that, as for every unit of increase in pAl, the pH increases by 2 units. This relation is consistent with the aluminum concentrations and pH being controlled by alunite precipitation and dissolution.



$$6 \text{pH} = -\log K_{\text{equil}} + 3\text{pAl} + \text{pK} + 2\text{pSO}_4.$$

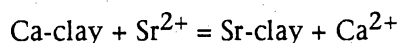
If the pSO₄ and pK are relatively constant, then alunite saturation will result in a relationship in which the change in pH is twice the change in pAl, as is observed in waters at the site. This provides indirect evidence of alunite precipitation. Attempts to identify alunite in the tailings and in sediments below the tailings were unsuccessful, which may be due to the very small amount of alunite that would precipitate during neutralization. Alunite does occur at the site, but naturally, as rinds surrounding calcium concretions in the lower Conquista clay.

Oversaturation of the solutions with respect to alunite indicates that the alunite (and aluminum) are being precipitated, not dissolved, in response to some acid-consuming reaction. Also, as the pH increases, the solutions become oversaturated with aluminosilicates. Thus, some reaction other than aluminosilicate dissolution is consuming the acids. The most likely acid-consuming mineral in the sediments is calcite.

Exchange Equilibria

Certain relations provide evidence that cation exchange occurs when tailings solutions invade sediments beneath the tailings piles. Data indicate that the cation exchangers in the sediment, smectites and zeolites (clinoptilolite), buffer the ratios of major cations in the ground-water solutions. In general, the tailings solutions are enriched in ammonium, magnesium, sodium, and potassium relative to ground waters, and exchange reactions produce decreases in these ions as the tailings solutions migrate into the sediments. The sandstones and clays at the site have relatively high cation-exchange capacities, averaging 38 meq/100 g for clayey sandstones (Pyrih and Associates, 1986), and measurements of exchangeable cations indicate that the dominant cation is calcium, accounting for 62 equivalent percent of the exchange capacity (Pyrih and Associates, 1986). Thus, ammonium, sodium, magnesium, and potassium are exchanged for calcium. Because the tailings solutions and ground waters are both equilibrated with gypsum, exchange for calcium results in gypsum precipitation and a decrease in contaminant sulfate concentrations. The mass balance of these reactions is discussed in the section on reaction path models.

Relations between pCa versus pSr and pCa versus pMg indicate cation exchange influence. Exchange equilibria between Ca and Sr are given by the equations



$$p\text{Sr} - p\text{Ca} = \log (X_{\text{Ca}}/X_{\text{Sr}}) - \log K_{\text{equil}}$$

where pSr and pCa are the negative logs of their respective activities in the solution, XCa and XSr are the equivalent fractions of those cations on the exchange sites, and K_{equil} is the equilibrium constant, also referred to as the selectivity coefficient. Selectivity coefficients in smectites are commonly near 1 (Farrah and Pickering, 1979; Drever, 1982) and thus, at equilibrium, the ratio of the activity of Ca-to-Sr is equal to the ratio of the activity of those cations on the exchange sites of the smectite. If the latter

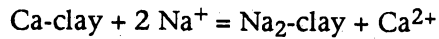
ratio is relatively constant over the site, then the Ca-to-Sr ratios in the ground waters will tend to be buffered to a constant ratio. Also, pCa and pSr will vary in one-to-one correspondence. A plot of pCa versus pSr indicates that this is the case (fig. 4.9). In the ground waters, pCa and pSr vary in one-to-one correspondence (slope of 1 on a pCa versus a pSr plot) and the intercept at pCa = 0 is 2.3, equivalent to the log of the ratio of Ca to Sr on the clays at the site. That is, the ratio of Ca to Sr in the clays at the site appears to be about 200 to 1.

Although the Ca-to-Sr ratios of many ground waters are buffered by exchange, most tailings solutions have lower Ca-to-Sr ratios (40 to 1) and thus greater pCa-to-pSr ratios (fig. 4.9). The Sr in the tailings tends to vary independently of Ca, such that whereas pCa tends to remain fairly constant, pSr varies between celestite saturation at low pSr (high Sr activity) and exchange equilibria (low Sr activity). The interpretation is that, as the tailings enter the sediments, cation exchange causes about a 50-percent decrease in the Sr concentrations relative to Ca due to adsorption of Sr onto the clays and release of Ca to the solutions. However, the effect is small, and Sr concentrations generally only vary from a high of 21 ppm in the tailings to a low of about 2.5 ppm in the ground waters.

Relations between Ca and Mg are similar to those between Ca and Sr. Again, the slope of the pCa versus pMg relation is near 1 (fig. 4.9), as expected for exchange with clays having a relatively constant composition. The intercept at pCa = 0 is 0.4, meaning that the ratio of calcium to magnesium is $10^{-0.4}$ or 0.4. Measurements of exchangeable cations in sandstones and clays at the site gave Ca-to-Mg ratios ranging from 0.55 to 0.13, the average being 0.18 ± 0.08 (Pyrih and Associates, 1986). This is very good agreement considering the scatter in ground-water data.

Exchange relations between calcium and sodium show more scatter than those between calcium, magnesium, and strontium. Nonetheless, there is a relation (fig. 4.10), and the slope of the ground-water data (0.42) is close to that expected (0.5) for

divalent-monovalent cation exchange equilibria with a selectivity coefficient of 1. The exchange equilibria is given as



$$2 \text{pNa} - \text{pCa} = \log (\text{XCa}/\text{XNa}) + \log K_{\text{equil}}$$

where pNa and pCa are the negative logs of activities, and XCa and XNa are the mole fractions of Ca and Na on the exchanger. Given that XCa/XNa is relatively constant and that the selectivity coefficient (K_{equil}) is approximately 1, then

$$\text{pNa} = 0.5 \text{pCa} + 0.5 \log (\text{XCa}/\text{XNa}).$$

Regression through the ground-water data (fig. 4.10) gives a slope of 0.42 and an intercept of 0.58, equivalent to a low Ca/Na ratio of 2.5. Measured values average a Ca/Na equivalent ratio of 6.1 (Pyrih and Associates, 1986). The difference in values is within the scatter of both data sets.

Ammonium displays no relation to sodium (fig. 4.10) or other major cations because ammonium is not a major natural ion either in ground waters or in cation exchangers. Thus, there is probably no set amount of ammonium on natural exchange sites sufficient to buffer ground-water chemistries to a constant value. About three orders of magnitude difference exist between ammonium in tailings solutions and ammonium in ground waters. In the absence of significant ammonium on the exchange sites in the sediments and assuming that the amount of ammonium in a tailings solution is small compared to the number of exchange sites, then nearly all ammonium in a contaminant solution will be exchanged for calcium. The critical question is whether the amount of ammonium is negligible relative to the number of exchange sites.

Sandstones at the site have an average cation exchange capacity of 380 meq/kg (Pyrih and Associates, 1986) or approximately 950 meq/L of solids (at a specific gravity of 2.5). Ammonium in tailings solutions averages 23.7 meq/L of solution. At 33 percent porosity, therefore, the ratio of ammonium to exchange sites is 23.7 to 1,900, or 0.012. Thus, cation exchange will have a negligible effect on the exchange site chemistry

except in volumes of sediment immediately adjacent to the tailings piles, volumes through which large amounts of tailings solution have passed. The same holds true of other cations (sodium, magnesium, calcium, and potassium) that appear to be exchanged for calcium as the tailings solutions migrate through the sediments. One question for future investigation is how much of the sediment surrounding the tailings piles contains significant amounts of exchanged ammonium. This has implications for ground-water remediation because ammonium is difficult to remove from ground water once a large reserve of ammonium has been sorbed into the sediment.

Hydrochemistry of the Deweesville Aquifer

Summary

Aluminum, pH, and total dissolved solids (TDS) indicate two sources for two acid plumes in the Deweesville—tailings pile 2 and tailings piles 4 and 5. Decreases in aluminum concentrations and increases in Ca concentrations away from tailings piles 4 and 5 indicate partial to complete neutralization of the plumes 500 to 2,000 ft from these sources. Concurrent increases in chloride indicate evaporative concentration along flow paths of the acid plume. Low-chloride concentrations indicate a local freshwater recharge point associated with the water-filled SWI pit.

There is good agreement between the extent of the geochemical plumes, the extent of the ground-water mound in the Deweesville, the hydrologic potentials for flow, and observed areal trends in contaminants. Notably, both hydrologic flow potentials and geochemical trends indicate eastward, southeastward, and southwestward migration of contaminants from the tailings piles toward Scared Dog, Conquista, and Tordilla Creeks, respectively.

Total dissolved solids, aluminum, pH, calcium, and tritium indicate that three of the monitoring wells (852, 851, and 677) are not contaminated by tailings solutions. The

earliest (1989) data for monitoring well 922 could also be used as possible background values, but more recent changes (1991) in pH and calcium data provide some evidence for recent contaminant influx. However, these data are not consistent with decreasing chloride concentrations over the same period.

Data in the area of pile 3 are too few to map. However, aluminum, TDS, and calcium concentrations suggest that a plume may extend about 1,000 ft from the tailings pile.

Total dissolved solids, sodium, sulfate, bicarbonate, and molybdenum indicate a small, nonacid, sodium-sulfate-sodium bicarbonate contaminant with high molybdenum content located near monitoring well 836. The source is probably a sludge pit located just north of the old mill site and adjacent to monitoring well 836. Water chemistry indicates that the solutions dumped in this pit were from the uranium precipitation stage of processing.

Introduction

The Deweesville sandstone is the stratigraphically highest aquifer on the site, and the unit mined for uranium ores. The sandstone outcrop underlies portions of tailings piles 1 and 2 which were built on the surface during the early stages of mining. Later, as pits 3, 4, and 5 (within the Deweesville) were abandoned, tailings were placed in those pits. Thus, tailings in piles 1, 2, 3, 4, and 5 are in direct contact with the Deweesville sandstone and there is a considerable potential for contamination of the Deweesville.

Monitoring wells used in determining the chemistry of the Deweesville ground waters include all monitoring wells with at least a portion of the completed interval intersecting the Deweesville (table 4.7 and fig. 4.11). In many of these wells, the completed intervals extend into the upper Conquista clay (table 4.7).

Chemical analyses of the Deweesville ground waters in the western area of the site are provided in table 4.7. The wells with detectable aluminum (greater than 0.05 mg/L) are sorted from highest to lowest aluminum concentration, reflecting decreasing acidity. Wells with no detectable aluminum are sorted by highest to lowest calcium concentration, reflecting whether these waters are neutralized tailings solutions (high calcium) or possible background waters (low calcium). In addition to wells completed in the Deweesville, chemical data from monitoring well 904 has been included on the maps. Well 904 is completed in a surficial sand, thought to be alluvium of Tordilla Creek, and within the underlying upper Conquista clay. Chemical trends indicate that this well is within a near-surface plume migrating from the Deweesville outcrop into the alluvium of the creek. Chemical data for well 904 are included in the section pertaining to the upper Conquista clay. Chemical data for monitoring wells completed in the Deweesville in the eastern area of the site, near pile 3, are presented in a separate table in the section pertaining to the plumes along Scared Dog Creek.

Core from the Deweesville contains no calcite, and the paucity of calcium carbonate is reflected in the ground-water chemistry. Only 3 of 15 samples are equilibrated with calcite. Most are equilibrated with gypsum (table 4.7). Two Deweesville ground-water samples from the CONOCO Conquista project (monitoring wells 668 and 667; not shown on fig. 4.12), are located south of the site within the reduced portion of the Deweesville. Both are equilibrated to calcite and undersaturated with respect to gypsum, consistent with their being in the reduced zone of the aquifer. Water chemistries from these two wells may not be representative of natural waters in the oxidized portion of the Deweesville, the portion affected by contamination.

Geochemical Mapping

pH

The most acid pH values are immediately adjacent to piles 2 and 5 (monitoring wells 625 and 835, respectively, fig. 4.12). Acid pH values of 4 or less delineate a small plume centered on the south side of pile 2 and a much larger plume extending south of piles 4 and 5. This larger plume has two tongues. One tongue extends southwest toward Tordilla Creek and includes the ground water exposed in pond 6 (an abandoned mine pit). Pond 6 water has a pH of about 3.6, similar to that in adjacent monitoring wells. The second tongue extends southwest toward Conquista Creek. The leading edge of the latter tongue is between monitoring wells 879 and 922. In monitoring well 922, the pH decreased steadily from 6.2 in October 1987 to 5.8 in May 1991. This decrease suggests that the acid plume is slowly migrating toward the southeast.

Aluminum

Aluminum concentrations indicate the acidity of the contaminant plumes. The greatest aluminum concentrations (essentially that of the tailings solutions themselves) are immediately adjacent to tailings piles 2 and 5. (No monitoring well is located adjacent to pile 4.) Aluminum concentrations decrease to low values (<1 ppm) within a 1,000-ft radius of pile 2. Aluminum also decreases away from piles 4 and 5, but waters with greater than 2 ppm aluminum extend as much as 2,000 ft away from pile 4 (fig. 4.13).

As with pH, aluminum concentrations in the acid plume surrounding piles 5 and 4 indicate two tongues extending southwest and southeast. The southwest tongue has relatively high acidity (>10 ppm aluminum) and extends southwest about 1,000 ft from pile 4. This southwest tongue of the piles 4 and 5 plume appears to be discharging

waters with 7 ppm aluminum into the alluvium and upper Conquista clay beneath Tordilla Creek (monitoring well 904) and is a source of contamination into the Conquista sand (as will be discussed). The tongue of the contaminant plume extending toward the southeast has high acidity (100 ppm aluminum) about 1,000 ft southwest of pile 4, decreasing to 10 ppm aluminum 2,000 ft from pile 4. To date, aluminum has not been detected further southeast, in monitoring well 922.

Total Dissolved Solids

The tailings solutions are high in TDS, averaging 11,600 mg/L. In the Deweesville, TDS values again reflect the sources of contamination, being highest in wells adjacent to piles 2 and 5 and extending as two tongues southeast and southwest from pile 4. In well 922, TDS is relatively low (5,640 mg/L) and has displayed no significant change since 1989 (fig. 4.14).

Ammonium

Ammonium concentrations similar to the tailings occur only in monitoring wells 625 and 835, immediately adjacent to piles 2 and 5. Elsewhere, ammonium is generally low (between 2 and 0.2 mg/L) indicating that ion exchange for calcium rapidly removes the ammonium from the contaminant plumes. Further study would document this buildup of ammonium in sediments adjacent to the tailings piles.

Calcium

Calcium concentrations indicate ion exchange and partial to complete neutralization of the contaminant plumes by calcium carbonate. Both the tailings solutions and background ground waters have relatively low calcium concentrations

(<900 mg/L calcium). In the Deweesville, waters with anomalously high calcium concentrations (1,000 to 1,750 mg/L calcium) are found within the plumes (as delineated by pH and aluminum) in a position between the tailings piles and the edge of the plumes (fig. 4.15). In the plume associated with pile 2, the calcium concentration increases from 494 mg/L adjacent to the tailings pile to 1,370 mg/L about 500 ft to the east (monitoring well 914, fig. 4.15). In the contaminant plume extending southwest of pile 4, calcium concentrations increase from about 560 mg/L to 1,480 mg/L. And in the tongue extending toward the southeast, the calcium concentrations increase from 560 mg/L in tailings pile 4 (table 4.7) to 1,750 mg/L, 1,000 ft to the southwest (monitoring well 853), and then decrease to 1,130 mg/L in monitoring well 922. As with pH, the calcium concentration in well 922 has increased over time, but the increase occurred over a shorter period (from 795 mg/L in December 1990 to 1,130 mg/L in May 1991).

Sulfate

Sulfate concentrations are essentially those of a tailings solution (~10,000 mg/L) in monitoring wells 835 and 625, adjacent to tailings piles 5 and 2, respectively. Sulfate concentrations are also high in monitoring well 836 (9,400 mg/L) due to solutions derived from the molybdenum pit (to be discussed).

Much like ammonia, sulfate concentrations rapidly decrease away from the tailings piles, to values of 2,500 mg/L or less (fig. 4.16). The sulfate shows an inverse relation to calcium such that the solutions remain in equilibrium with gypsum, a mineral that occurs both in the tailings and within the shallow portions of the Deweesville. The saturation indices for gypsum (computed using SOLMINEQ.88) indicate that all tailings solutions and all but three of the ground waters (wells 678, 852, and 851) are at gypsum equilibrium (table 4.7). The decrease in sulfate and increase in calcium are due to cation exchange of ammonium, sodium, magnesium, strontium, and potassium for calcium,

reactions of aluminum and iron sulfate with calcium carbonate, and precipitation of gypsum.

A plot of calcium versus sulfate discriminates between three types of waters present in the Deweesville on the site (fig. 4.17). The first type is low in calcium (about 500 mg/L) and high in sulfate (ranging from 9,000 to 14,000 mg/L sulfate). These solutions have molar sulfate-to-calcium ratios significantly greater than the one due to the presence of aluminum, iron, magnesium, and potassium sulfates in the solutions. The tailings solutions and ground waters adjacent to the tailings piles (monitoring wells 835 and 625) comprise this type of water.

The second type of water in the Deweesville is high in calcium (from 1,200 to 1,750 mg/L) and relatively low in sulfate (1,600 to 2,300 mg/L), with a molar sulfate-to-calcium ratio of one or less than one (fig. 4.17). In the Deweesville, four of the high-calcium waters are acid (monitoring wells 853, 854, 979, and 676) and one is not (well 914). In all of these waters, chloride is an important constituent. All of these waters are equilibrated with gypsum and one, 914, is also equilibrated with calcite.

The third type of water is relatively low in both calcium (300 to 750 mg/L) and sulfate (500 to 2,600 mg/L). These waters have molar sulfate-to-calcium ratios approaching 1. None are acid. Some are saturated with respect to gypsum, some are undersaturated. These waters are may be indicative of background.

The high sulfate-to-calcium ratio is due to the presence of aluminum, ammonium, iron, and other sulfate salts besides calcium sulfate. Decreases in the amount of sulfate as a result of dilution or precipitation of aluminum and iron sulfate salts while calcium concentrations remain constant are a result of gypsum buffering the water chemistry. As sulfate decreases or increases, equilibrium with gypsum tends to buffer the calcium to a constant value. The general effect is the result of the chemical divide principle:

whenever a binary salt is precipitated during evaporation, and the effective ratio of the two ions in the salt is different from the ratio of the

concentrations of these ions in solution, further evaporation will result in an increase in the concentration of the ion present in greater relative concentration in solution, and a decrease in the concentration of the ion present in lower concentration (Drever, 1982).

In the tailings solutions, the binary salt is gypsum, and the effective molar ratio of the salt is one-to-one. The tailings solutions have a sulfate-to-calcium ratio greater than one-to-one, and thus, sulfate tends to increase relative to calcium during evaporation and decrease relative to calcium during dilution or precipitation of aluminum and iron sulfates. If activity corrections are neglected, the concentration of calcium is predicted to decrease during evaporation (Drever, 1982). However, if activities are taken into consideration, it is found (by computer modeling) that calcium concentrations remain constant while sulfate decreases or increases during dilution, evaporation, or precipitation of aluminum and iron sulfate, provided that the initial solution calcium-to-sulfate ratio is less than one and that gypsum is present.

If a solution calcium-to-sulfate ratio becomes greater than 1 by some process such as cation exchange for calcium coupled with aluminum sulfate precipitation, and gypsum is present, then evaporation or further reactions that increase calcium in the solution will result in an increase in calcium relative to sulfate. Computer modeling indicates that these reactions result in relatively constant sulfate concentrations (about 2,000 mg/L) over a range of calcium concentrations of between 900 and 2,500 mg/L, such as observed in figure 4.17. Thus, the relation between calcium and sulfate in the ground waters and tailings solutions (fig. 4.17) are due to dilution, evaporation, and chemical reactions in the presence of gypsum.

Molybdenum in monitoring well 836

Monitoring well 836 has very high sulfate but is not a tailings solution (fig. 4.18). The predominant salt is sodium sulfate, the pH is high (6.8), the alkalinity is very high (1,036 mg/L bicarbonate), and other major elements, associated with the acid-sulfate tailings solutions, are relatively low (including aluminum, ammonium, iron, potassium, magnesium, and fluoride; table 4.7). In addition, monitoring well 836 contains the greatest molybdenum concentration of any water on the site (54 mg/L). Bryson (1987) attributed this water to contamination from a pit, located 500 ft north of the monitoring well, that had been used to store spent resins from the molybdenum extraction circuit at the mill. The large amount of sodium and bicarbonate in the water sample from monitoring well 836 suggests that the solution derives from acid solutions used to strip uranium from the loaded organics that were treated with sodium hydroxide to a pH of 7 to precipitate sodium diuranate. Sludges from this process were apparently buried in trenches within the upper Conquista clay (Texas Department of Health, Bureau of Radiation Control, 1984).

Bryson (1987) failed to differentiate the molybdenum in this sodium-sulfate-bicarbonate water from molybdenum in both tailings piles and acid-ground waters and thus mapped a large molybdenum plume radiating out 1,000 to 2,000 ft from monitoring well 836. This plume does not exist. Molybdenum is sporadically distributed among wells on the site (fig. 4.18) and is high in a number of wells, some showing no major element evidence for contamination (including wells 851, 852, and 677). The molybdenum in these latter three wells is probably natural, associated with identified uranium mineralization (fig. 2.10).

Chloride

Chloride is a chemically conservative parameter in ground waters as it is unaffected by reactions between the solutions and the sediments. Variations in chloride serve as an indicator of evaporation or dilution, provided that a baseline can be established.

Chloride is one of the few parameters for which some premining baseline data exist.

The USGS made a study of the chlorinity, porosity, and water content of sediments from core in the Deweesville area (U.S. Geological Survey, 1958) and computed a chloride content of the ground waters in both unsaturated and saturated sediments. Their results indicate a decrease in chlorinity with depth with chloride concentrations of up to 5,200 mg/L 10 ft above the ground-water table (at ~30 ft of depth) to about 500 mg/L chloride below the ground-water table (fig. 4.19). This is in good agreement with the general trend in chloride with depth for all monitoring wells at the site (fig. 4.19). The tailings solutions display considerable variation in chlorinity (from 570 to 3,040 mg/L), which is primarily due to evaporative concentration. Also, chlorinities in monitoring wells 851, 852, and 677 are in this range (~2,000 mg/L chloride). There is no evidence of contamination of ground waters from these three wells. Chloride, by itself, cannot be used as an indicator of contamination by tailings solutions. In the Deweesville, chloride in monitoring wells adjacent to tailings piles 2 and 5 are 1,740 and 1,400 mg/L, respectively, essentially that of an average tailings solution (fig. 4.20). The background wells (852 and 851) have slightly higher chlorinities (1,960 and 1,880 mg/L, respectively) and are consistent with the results of the U.S. Geological Survey (1958) study (fig. 4.19).

Anomalously high chloride concentrations are associated with both the southeast and southwest tongues of the plume extending from piles 4 and 5 (fig. 4.20). These high chloride concentrations may indicate (1) threefold evaporative concentration of the tailings solutions in the tailings ponds and piles before entering the aquifer,

(2) evaporative concentration of the tailings solutions after entering the aquifer, (3) mixing with high chloride background waters in the unsaturated zone of the aquifer as the tailings solutions enter the aquifer, or (4) mixing of tailings solution with chloride salts in the unsaturated zone after entering the aquifer.

Pond 6, which intercepts the ground-water table, provides one area for seasonal evaporative concentration of the plume solutions; evaporites, primarily gypsum but with some halite and jarosite, have been observed in pond 6 when it is dry. The eastern tributary drainages of Tordilla Creek, which run from Farm Road 1344 to south of pond 6, may be the sites of evapotranspiration for the plume extending from pile 4 to the southwest. These tributaries, especially near monitoring well 853, have eroded into the Deweesville such that the ground-water table is closer to the surface (to within 16 ft), increasing the potential for evapotranspirative discharge of ground water. The thick stand of mesquite that has overgrown these tributaries since 1983 may contribute to evapotranspiration.

Chloride concentrations southwest of monitoring well 853, decrease to 1,130 mg/L in monitoring well 922, which is approximately at background level. Unlike calcium, the chloride concentration in well 922 is actually lower than concentrations measured from 1989 to 1990.

Anomalously low chloride concentrations are found in monitoring wells 918 and especially 678 (653 and 158 mg/L, respectively). Both wells are adjacent to the abandoned, water-filled SWI pit (fig. 4.20) and are probably receiving fresh-water recharge from that pit. Thus, there is a potential mixing zone of high-TDS tailings solutions with low-TDS surface recharge waters along the southern boundary of the contaminant plume north of the SWI pit.

Chloride-to-bromide ratios

Chloride-to-bromide ratios support the idea that waters with high calcium concentrations (>900 mg/L) are reacted tailings solutions. As discussed in the section on tailings solutions, some tailings solutions have higher chloride-to-bromide ratios than expected for natural ground waters. All high-calcium and -chloride waters in the Deweesville also have high chloride-to-bromide ratios (fig. 4.21). One low-calcium water with a pH of 5.4 (monitoring well 651) has very low bromide relative to chloride, and this well is immediately adjacent to tailings pile 4. It may be contaminated with diluted, partially reacted tailings solution. Two samples thought to be natural waters (monitoring wells 852 and 851) are also somewhat depleted in bromide (fig. 4.21). There is no major element evidence of tailings solution contamination of these two wells. But, this does introduce uncertainty in using chloride-to-bromide ratios for identifying contamination by tailings solutions. Other data must be used in conjunction with chloride-to-bromide ratios.

Tritium

The greatest tritium (4.0 tritium units) is found in monitoring well 854, adjacent to pond 6 and about 500 ft southeast of pile 4 (fig. 4.22). Lower but significant tritium values (0.7 and 0.4 tritium units) occur in monitoring wells 853, 879, and 922, associated with the contaminant plume to the southeast. Monitoring wells 852 and 851 show no major element chemical evidence of contamination by tailings solutions, and these have tritium values below the level of detection (<0.09 tritium units), which is consistent with being background waters that have not received significant recharge since the early 1950's. However, the make-up water used for ore processing was taken from a well completed at an 800-ft depth. This water would have no tritium. Thus, tritium is only useful in identifying recent recharge (post 1950's), and the absence of tritium is not, in

itself, indicative of background waters. Tritium solutions from tailings piles are as great as 8.5 tritium units (table 4.1), which may reflect recharge into the tailings by recent rainwater.

Cation trace metals

Trace metals that occur as cations include antimony, beryllium, cadmium, cobalt, copper, lead, mercury, nickel, silver, thallium, tin, and zinc. Of these, only six, beryllium, cadmium, cobalt, copper, nickel, and zinc, occur in measurable amounts within the tailings solution and the ground waters. Antimony, lead, mercury, thallium, and silver are generally below the lower levels of detection. The six metals which do occur in appreciable amounts are those which form relatively soluble sulfate or bicarbonate salts (Krauskopf, 1967) which are present in appreciable amounts within an average shale. These six metals are chemically similar and occur together in waters at the site. If one of the six is detected, so are the others, usually in proportions similar to that within an average shale.

A single parameter can thus be abstracted from analyses of these six metals. That parameter is the average of cation trace metals concentrations normalized to the tailings pile concentrations, hereafter called the average normalized trace metal concentration. It is computed by (1) subtracting the parameter's lower level of detection from the measured parameter (for each of the six cation trace metals), (2) dividing the result by the parameter's average in the tailings solutions, then (3) taking those results for all six parameters and averaging them (table 4.8). Thus, values below detection are expressed as zero, and each parameter is normalized to a tailings solution value. For example, the beryllium normalized trace metal concentration in monitoring well 625 is 2.5. Thus, beryllium in sample 625 is 2.5 times that of the average tailings solution (table 4.8). The average for all six cation trace metal ratios is 1.13, indicating that trace metal

concentrations in sample 625 are about the same as that in the tailings. A similar parameter is computed for the anion trace metals and for uranium, radium-226, aluminum, iron, and manganese (table 4.8).

The distribution of the normalized cation trace metal concentrations in the Deweesville is the same as that of the acid plumes mapped using the major elements, TDS and pH (fig. 4.23). Cation trace metal concentrations adjacent to the tailings piles are the same as those within the tailings piles (monitoring well 625). Further away, the metals decrease. In the southeast plume, cation trace metal concentrations are about 50 percent of those in the tailings piles. In the southwest plume, concentrations are 20 to 15 percent of those in the tailings piles. Background concentrations in waters are 2 percent or less of the tailings pile concentrations. In general, pH is the major control on the cation trace metals (fig. 4.24). At pH values of 4 or less, metals concentrations are significant, whereas at higher pH values, trace metals are generally 2 percent or less of the tailings concentrations.

Comparison of the decrease of trace metals to the decreases in iron and aluminum indicates that the trace metals are not as strongly attenuated along flow paths. Iron and aluminum decrease by two orders of magnitude along the southwest plume whereas the metals remain at 50 percent of the tailings concentrations. These data suggest that the trace metals are not coprecipitated with or sorbed by aluminum and iron hydroxide precipitates so long as the pH remains at or below 4. This is in agreement with experimental studies of cation trace metal sorption by iron and aluminum hydrous oxides (Shuman, 1977; Watzlaf, 1988) and clays (Farrah and Pickering, 1979; Farrah and others, 1980). These studies have demonstrated that at pH values of less than 4, cation exchange and sorption are inhibited by competition with hydrogen ions for sorption sites.

Ground water in monitoring well 914 is a calcite-neutralized tailings solution. Comparison of the average normalized cation trace metal concentration in samples from

monitoring well 625 (an acid tailings solution) and well 914 indicates that neutralization of the tailings solutions has reduced the trace metals to an average of 2 percent of that of a tailings solution.

Anionic trace metals

Trace metals that exist as anions (under the oxidizing conditions at the site) are arsenic, chrome, molybdenum, vanadium, and selenium. The average normalized anion trace metal concentrations are also provided in table 4.8. The anion trace metal concentrations are similar to those in the tailings solutions in ground waters with an acid pH (4 or less), and commonly low in waters of higher pH. There are, however, a number of high-pH waters with significant anion trace metals. The highest average normalized concentration of anion trace metals (nine times that of an average tailings solution) is in monitoring well 836. This well is contaminated with an anomalous sodium sulfate water with very high molybdenum (45 times that of a tailings solution). The source is probably the molybdenum disposal pit 500 ft to the north. Other high-pH waters contain large amounts of molybdenum, selenium and/or arsenic, including waters having no evidence of major element contamination (monitoring wells 678, 677, and 852). Molybdenum, selenium, and arsenic are commonly concentrated in or near uranium deposits, and these three metals may be naturally occurring in the ground waters at the site in concentrations similar to that of a tailings solution. The one high-pH water thought to be a neutralized tailings solution (monitoring well 914) contains virtually no anion trace metals (table 4.8).

The range of molybdenum in the Deweesville high-pH waters is from less than 0.01 to 0.82 mg/L. The latter value is associated with relatively dilute ground water adjacent to the flooded SWI pit (monitoring well 678). That well is also located on the Deweesville sandstone redox boundary, and the high molybdenum (and arsenic) may be

due to oxidation of pyrite by the influx of oxidizing waters. A similar situation was reported in the Oakville Sandstone, George West uranium district, where a ground-water molybdenum concentration of 700 mg/L was reported (Henry and others, 1982). However, in that report, molybdenum in regional Oakville ground waters was generally in the range of less than 0.0001 to 0.050 mg/L. Data from Jackson Group uranium mines, however, demonstrate that high molybdenum concentrations are associated with ground water or leachates developed in uranium deposits (table 4.9). These data, sampled, analyzed, and reported in 1973—are from company files of SWI. The data are for Karnes County mine waters from the Sickenius, Galea, and Butler uranium open-pit mines, which are a few miles from the Falls City Mill. In mine waters with a pH of about 7.6, molybdenum ranged from 0.48 to 24 mg/L (table 4.9).

Selenium ranges from less than 0.01 to 0.8 mg/L in the high-pH ground waters, and arsenic ranges from less than 0.01 to 0.25 mg/L. The highest concentration reported in the regional ground waters in the Oakville Sandstone uranium districts was 0.028 mg/L selenium. In the Karnes County mine waters, selenium ranged from 0.007 to 0.053 mg/L. Thus, a few waters herein tentatively designated as background Deweesville ground waters have anomalously high selenium compared to Oakville uranium district ground waters and Karnes County mine waters.

In the high-pH ground waters at the site, arsenic ranges from less than 0.01 to 0.25 mg/L. Some values are high compared to Oakville uranium district ground waters (with a maximum of 0.098) but are within the range displayed by Karnes County mine waters (<0.01 to 0.63 mg/L, table 4.9). Overall, it is possible that molybdenum, selenium, arsenic, and also zinc, nickel, and lead concentrations may be fairly high in ground waters or leachates associated with the Karnes County uranium deposits, but more study of ground waters from within uranium deposits is required to demonstrate this.

Uranium

Uranium concentrations in both the tailings and the ground waters are erratically distributed. Acid-pH ground waters generally contain considerable uranium (0.1 to 3 times that in the average tailings solution, table 4.8) but high-pH waters also contain significant uranium, including waters thought to be background waters. Uranium ranges from less than 0.01 to 25 mg/L in the high-pH waters. The latter value is very high compared to regional ground waters in other uranium districts, where uranium concentrations generally range from less than 0.001 to 0.040 mg/L (Henry and others, 1982). However, major element chemistry does not indicate contamination of some of the ground waters containing high uranium and/or anion trace metals. No uranium data are available for Karnes County mine waters (table 4.9).

Radium

Radium-226 averages 304 picocuries per liter (pCi/L) in the tailings solutions. The acid waters in the Deweesville contain about 10 percent of the radium-226 in the tailings solutions. Nearly all high-pH waters have radium-226 concentrations of less than 5 percent of the tailings solutions (<15 pCi/L). There are two exceptions: one is the molybdenum pit monitoring well (836), which has waters of 25 pCi/L; the other is monitoring well 918. Monitoring well 918 appears to be at a ground-water boundary between saline waters migrating toward Tordilla Creek from pile 4 and pond 6, and fresh waters from the abandoned SWI uranium pit. Well 918 may also be within mine backfill. The relatively high radium (30 percent of a tailings solution) is anomalous when compared to radium values upgradient, toward pond 6, and piles 4 and 5 (fig. 4.25), which suggests a local source. This radium may be leached from the sediments in this area, including uranium mine backfill. The process by which this is occurring is unknown and bears further investigation.

Hydrochemistry of the Upper Conquista Clay

Three monitoring wells are completed exclusively in the upper Conquista clay (table 4.10 and fig. 4.26): wells 857, 863, and 913. In addition, monitoring well 904 is thought to be completed in sandy alluvium (or Deweesville) and upper Conquista clay. The driller's log identified the upper sand as Conquista sandstone, which is not consistent with geologic mapping by MacKallor and others (1962). Monitoring well 617 was reportedly completed in the upper Conquista clay (Bryson, 1987). However, geologic mapping suggests that this well is completed in the lower Conquista clay and perhaps also in the Conquista sand.

Aluminum, pH, chloride, and calcium concentrations all suggest that waters in monitoring wells 863, 904, and 913 are contaminated. These wells have relatively high concentrations of cation trace metals and also selenium, uranium, and radium (Table 4.11). The solution chemistries closely resemble those of waters in the adjacent Deweesville sandstone. In monitoring well 913, there is only 2 ft of clay between the top of the completed interval and the Deweesville. Vertical leakage of Deweesville solutions into the upper Conquista clay is the most likely flow path of the contaminant solution into the clay.

Hydrochemistry of the Conquista Sand

Summary

Concentrations of pH, TDS, and chloride indicate at least two sources of groundwater contamination of the Conquista sand by tailings solutions. One source is located along the north edge of tailings pile 7 (near monitoring well 701) and a second source is located at the confluence of the north and east tributaries of Tordilla Creek (near monitoring well 919; fig. 4.27). The latter is discharge from the southwest-trending

plume in the Deweesville into the alluvium and upper Conquista clay subcrop beneath Tordilla Creek, down the creek as underflow, and into the Conquista sand, where it subcrops beneath the alluvium. This interpretation is based upon consistent trends in pH, aluminum, TDS, calcium, and chloride along this proposed flow path. The ultimate sources of this southwest-trending plume are piles 4 and 5.

A large plume within the Conquista sand is associated with tailings pile 7. This is a plume comprised of tailings solutions neutralized by calcite, an interpretation strongly supported by the spatial distributions of TDS, pH, aluminum, calcium, chloride, selenium, carbon dioxide partial pressures, calcite saturation indices, and gypsum saturation indices. In addition to an increase in calcium and decrease in sulfate associated with the neutralization reaction, there are major decreases in other chemical parameters, especially ammonium but also potassium and magnesium, due to cation exchange for calcium. Cation trace metals also decrease to near background levels, as do radium, molybdenum, vanadium, chrome, arsenic, and uranium. Selenium, however, remains in solution. As with the Deweesville, there is good agreement between the extent of the geochemical plumes and the extent of the ground-water mounds in the Conquista.

Introduction

The Conquista sand is a 30-ft-thick sandstone that thins and becomes finer grained toward the south portion of the site, down the structural dip. The outcrop underlies a portion of tailings pile 7 and is exposed to the northeast of pile 7 (fig. 4.27). Also, outcrops occur along Tordilla Creek and in the upper reaches of Scared Dog Creek (fig. 4.27).

Along the lower reaches of Scared Dog Creek, the Conquista forms a slope on the face of a cuesta dipping to the south (MacKallor and others, 1962). Below and north of

this slope, driller's logs incorrectly identified Dilworth sandstone as Conquista sandstone along the downstream portions of Scared Dog Creek (in monitoring wells 965, 966, 976, and 977). Those four wells are discussed in a later section on ground waters in the eastern area of the site, near the Searcy mine and tailings pile 3.

Unlike in the Deweesville sand, calcite in the Conquista is commonly encountered in the core of the Conquista sand. The chemistry of ground waters in the Conquista sand reflects the presence of calcite: 7 of 15 samples are in equilibrium with calcite, and all but 2 are equilibrated with gypsum (table 4.12).

Geochemical mapping

pH

In general, Conquista sandstone ground waters have pH values of 6.0 to 6.8. Four acid-pH waters identify point sources of acid tailings solutions into the Conquista sand. All four are located at the outcrop of the Conquista sand. One is associated with the intersection of pile 7 and the Conquista sand outcrop (monitoring well 701, fig. 4.28). A second acid water is located in the Conquista sand outcrop in the upper reaches of Scared Dog Creek, below tailings pile 3 (monitoring well 957), and two are located at the outcrop of Conquista sandstone along Tordilla Creek (monitoring wells 906 and 919, fig. 4.28). Monitoring well 906 is only slightly acid (pH of 5.4) whereas monitoring well 919 is very acid (3.7). Monitoring well 919 is downstream and down the ground-water gradient from well 906, but its lower pH suggests that the source of acid in well 919 is unrelated to that in well 906. Comparison to Deweesville sandstone pH and aluminum data (figs. 4.13 and 4.28) suggests that the acid water in well 919 is a continuation of the southwest-trending plume in the Deweesville (which includes monitoring wells 904, 902, and 854). Other chemical data (chloride, calcium, and normalized trace metals) are consistent with this interpretation.

Aluminum

Aluminum concentrations in the Conquista sand are relatively low compared to aluminum concentrations in the Deweesville and upper Conquista shales, even in areas with acid pH (fig. 4.29). The exception is probably monitoring well 701, which has very high sulfate but which has not been analyzed for aluminum. The highest measured aluminum concentration, in monitoring well 919, is 4.3 mg/L, which is near the lower limit for acidity buffering by aluminum. Iron, which contributes to acidity, also has low concentrations at the outcrop and in the subsurface (table 4.12). The acid waters in the Conquista sand, except that in monitoring well 701, therefore have low acidity and high potential for neutralization down gradient (fig. 4.29).

Total Dissolved Solids

In the Conquista, TDS values reflect the sources of contamination being highest in the well adjacent to pile 7 (monitoring well 701) and in well 919 located down gradient from the Deweesville plume that extends southwest of pile 4. Overall, the TDS displays the same pattern as calcium and pH (fig. 4.30).

Ammonium

Ammonium in all Conquista sandstone monitoring wells is at background levels (<1 ppm). None of the Conquista waters have elevated ammonium concentrations.

Calcium

Calcium concentrations in the Conquista sand, in conjunction with the pH and aluminum, delineate a large plume of waters with high calcium concentrations, in excess of 1,000 mg/L (fig. 4.31). This plume centers on tailings piles 1, 2, and 7, extending out

about 1,000 ft from these potential sources. A second high-calcium plume may be associated with tailings pile 3, but there are too few data to truly delineate a plume.

Unlike the Deweesville high-calcium waters, none of the high-calcium waters in the Conquista sand are acid; all have pH values of 5.4 to 6.0. The high calcium concentrations are thought to be due to neutralizing reactions between tailings solutions and calcium carbonate, and this is supported by the distribution of calcite saturation indices and partial pressures of carbon dioxide (P_{CO_2} ; fig. 4.31).

Calcite and gypsum saturation

The Deweesville ground waters are generally undersaturated with respect to calcite and saturated with respect to gypsum, but about half of the Conquista sand wells are saturated with respect to calcite, and most are saturated with respect to gypsum (table 4.12). Few of the high-calcium waters are at calcite saturation (fig. 4.31), but the one water with the highest calcium concentration, located near piles 2 and 7 (monitoring well 856), is both calcite and gypsum saturated. Likewise, monitoring wells 712 and 921, located northeast and southeast of 856, are also saturated with both phases. Saturation with both gypsum and calcite is the expected endpoint of neutralization of aluminum and iron sulfate waters by calcite, and finding high-calcium waters saturated with both phases close to the expected source of aluminum sulfate waters supports the model for generating high-calcium waters by calcite neutralization of acid plumes.

Waters undersaturated with gypsum are downdip. These are calcite saturated and are located within the reduced portion of the Conquista sand (monitoring wells 861, 860, and 951; fig. 4.30). Logging of wells 861 and 860 confirms the presence of calcite in the Conquista sand from these wells and from adjacent core borings. Background waters from the oxidized portion of the Conquista sand may be saturated with respect to calcite and gypsum. Water from monitoring well 865 appears to be such a water (fig. 4.30).

Carbon dioxide partial pressure

Neutralization of acid-sulfate waters by calcium carbonate will produce carbon dioxide, potentially with partial pressures in excess of one atmosphere. Partial pressures of carbon dioxide (P_{CO_2}) in the Conquista sand show a high of 0.38 atmosphere in monitoring well 856, the well with the highest calcium concentration, and relatively high P_{CO_2} values in other high-calcium waters (monitoring wells 921, 906, and 712; fig. 4.30). These relatively high P_{CO_2} values lend more support to the calcite neutralization model. Monitoring well 865, thought to be a background well in the oxidized Conquista, has a P_{CO_2} of 0.16 atmosphere. Waters from the reduced Conquista sandstone have lower P_{CO_2} values (0.06 atmosphere.)

Sulfate

Sulfate indicates an aluminum sulfate water adjacent to pile 7 (monitoring well 701). The chemical analysis of monitoring well 701 water is incomplete, but its pH, TDS, and sulfate all indicate that it contains relatively unreacted tailings solution, consistent with this area as a point source of contamination into the Conquista sand.

Otherwise, sulfate displays no significant trends. Sulfate concentrations are controlled by gypsum saturation. In the presence of gypsum (calcium sulfate), variations in both calcium concentrations and ionic strength result in variations in sulfate (from 1,110 to 2,890 mg/L). The lower sulfate concentrations are, in some cases, associated with the high-calcium waters (monitoring wells 856, 921, and 906) that define a reacted plume surrounding piles 1, 2, and 7. In contrast, relatively high sulfate is associated with low-TDS waters and low calcium concentrations, in equilibrium with gypsum. The lowest sulfate concentration is in monitoring well 951, located within the reduced Conquista sandstone. That water is undersaturated with respect to gypsum because of the lack of

gypsum in the reduced sections of the aquifer. Sulfate is not a consistent indicator of contamination by tailings solutions.

Chloride

Chloride concentrations are consistent with two major sources of contamination, one near piles 1, 2, and 7, and one in Tordilla Creek down gradient from the southwestern Deweesville plume (fig. 4.32).

Chloride-to-bromide ratios

The best example of the distinction between chloride-to-bromide ratios in natural ground waters, tailings solutions, and neutralized tailings solutions is from the Conquista sand (fig. 4.33). The tailings solutions are those sampled from tailings pile 7 and adjacent monitoring well 701.

Waters tentatively identified as natural ground waters, based on their lack of aluminum, high pH, and relatively low calcium (<950 mg/L), all have relatively high bromide content, and a consistent chloride-to-bromide ratio of 330 to 1, close to that expected for natural ground waters. The relation extrapolates to about 0 bromide at 0 chloride, as expected for any dilution/evaporation curve for a set of solutions with the same Cl/Br ratio.

Waters identified as neutralized tailings solutions all have chloride-to-bromide ratios that are lower than that of the background and similar to that of some of the high-chloride tailings solutions (fig. 4.33). These form a unique population of data and support the idea that these are not high-calcium background waters but rather tailings solutions that have reacted with calcite.

Tritium

Tritium decreases with decreasing calcium concentrations with well 856 having the highest tritium concentration (3.0 tritium units, fig. 4.34). The general trend indicates that the Conquista is receiving recent (post 1950's) recharge from the area around tailings pile 7, and possibly from Tordilla Creek (near monitoring well 924). Low chloride, low TDS, and high pH also indicate recent recharge of relatively dilute, uncontaminated water near well 924, possibly floodwaters. Tritium values below detection (<0.09 tritium units) are found in the downdip portions of the Conquista sand. These low values are consistent with major element data suggesting that these downdip wells are background (monitoring wells 860 and 861), having received no recharge since the early 1950's.

Cation trace metals

Normalized anion trace metal concentrations in the Conquista sand indicate that neutralization of the tailings solutions has caused nearly complete loss of the cation trace metals. Cadmium appears to be the most mobile (at about 4 percent of the tailings solution value, or 0.01 mg/L). Even monitoring well 919, which has a pH of 3.7, has relatively low cation trace metal concentrations (4 percent of the average tailings; table 4.13).

Anionic trace metals

The average normalized anion trace metal concentrations (table 4.13) correlate with the high-calcium waters representing neutralized tailings solutions. Waters having high calcium (>900 mg/L) generally have a high normalized cation metal averaged due to the elevated concentration of one metal, selenium (table 4.13). Selenium is 1.65 to 8.2

times more concentrated in the high-calcium waters than it is in the tailings solutions. One possible explanation is that the neutralization reaction with calcite releases selenium from the sediment matrix, but a more likely explanation is that earlier tailings solutions contained more selenium than at present. Over time, adsorption of selenium within the acid environment of the tailings has lowered selenium concentrations in leachates. Outside of the tailings piles, selenium was not as strongly sorbed due to alkaline conditions.

Unlike those in the Deweesville, molybdenum concentrations are generally low in the Conquista (<2 percent of that in the tailings), which tends to support the idea that molybdenum in the high-pH Deweesville ground waters is related to the uranium deposits in that unit and is not necessarily contamination derived from tailings solutions.

Uranium

Uranium concentrations in both the tailings and the ground waters are erratically distributed, but the only two ground waters with significant uranium (from wells 856 and 712) are high-calcium waters. Monitoring well 856 waters are oversaturated with respect to uranyl carbonate (rutherfordine). This is the only ground water at the site that is saturated with respect to a uranium mineral.

Radium concentrations

Radium concentrations in the Conquista sand are all 2 percent or less of that in the tailings, that is, all below 7 pCi/L. Neutralization of the tailings solutions by calcite effectively attenuates radium concentrations, as has been observed in other studies of uranium mill tailings (for example, Markos and Bush, 1982).

Hydrochemistry of the Lower Conquista clay

Two monitoring wells on the site are completed in the lower Conquista clay (monitoring wells 617 and 864; refer to fig. 4.26). Aluminum concentrations, where detectable, are less than 1 mg/L and pH values are 6.2 and 6.5, respectively (table 4.14). Calcium concentrations are near 900 mg/L, and the chloride concentration is close to that of an average tailings solution in sample 617. Anions from monitoring well 864 were not determined. The data provide no evidence of contamination by tailings solutions, and the chloride-to-bromide ratio of sample 617 (352 to 1) is similar to that of a natural water.

Hydrochemistry of the Dilworth Sandstone

Summary

Hydrologic data indicate localized vertical leakage of both tailings solutions and background waters from overlying units into the Dilworth. Geochemical data also indicate localized vertical leakage of tailings solutions into the Dilworth, notably near monitoring wells 878 and 905. In both cases, the solutions have been neutralized by calcite. With the exception of monitoring well 905, chloride-to-bromide ratios in the Dilworth are generally those expected for natural waters rather than contaminants. Some waters with natural chloride-to-bromide ratios are high in uranium or radium, and these uranium or radium anomalies appear to be natural.

Geochemical data also indicate contamination of the Dilworth where it crops out along the lower reaches of Scared Dog Creek. These data are discussed in a separate section.

Introduction

The Dilworth sandstone outcrop is located about 3,000 ft north of the tailings piles (fig. 4.35). Potential paths for contaminant migration into the Dilworth are vertical leakage through the Conquista member or recharge at the Dilworth outcrop from contaminated surface runoff in drainages that flow north from the tailings area (fig. 4.35). Chemical and hydrologic data suggest that the surface runoff along Scared Dog Creek has resulted in contamination of the Dilworth at its outcrop in the northeast corner of the site. This area will be discussed in a later section. Local ground-water elevation highs (section 3) suggest that vertical leakage into the Dilworth is occurring. Ground-water chemistry confirms this, especially in monitoring well 905.

Monitoring wells used in determining the chemistry of the Dilworth ground waters include all monitoring wells with at least a portion of the completed interval intersecting the Dilworth (table 4.15). In many of these wells, the completed intervals extend into the overlying lower Conquista clay or underlying Manning Formation claystone (table 4.15).

Chemical analyses of the Dilworth ground waters from the western area of the site are provided in table 4.15. Data from the eastern area, near pile 3, are presented in the next section. None of the Dilworth samples in the western area have detectable aluminum (>0.05 mg/L). The samples are sorted from highest to lowest calcium concentrations which, in overlying units, reflects whether those ground waters are neutralized tailings solutions (high Ca) or background waters (low Ca). The greatest calcium concentration, 745 mg/L, is in monitoring well 878, and that value is not indicative of a calcite-neutralized tailings solutions. The next largest concentration is in monitoring well 905 (660 mg/L). However, this 1991 analysis is thought to be in error, and the actual calcium concentration is probably 3 times this value (1,980 mg/L) as will

be discussed. Thus, monitoring well 905 does contain ground water indicative of a neutralized tailings solution source.

Geochemical Mapping

Calcite and gypsum saturation

The ground-water chemistry indicates that about two-thirds of the Dilworth sand is calcite saturated and only two sands are saturated with gypsum. The distribution of the calcite-saturated and undersaturated ground waters (fig. 4.36) indicates that most ground waters near the outcrop are undersaturated with respect to calcite, whereas ground waters downdip are saturated. This probably reflects leaching of calcite from the Dilworth by ground waters recharged at the outcrop. Partial pressures of carbon dioxide are also relatively high near the outcrop (~0.1 atmosphere versus 0.05 atmosphere downdip). Downdip, pyrite is present in the Dilworth, and reducing conditions associated with the lower P_{CO_2} values and calcite-saturated ground waters are indicated by detectable hydrogen sulfide and very low sulfate values (1 mg/L) in the ground waters (table 4.15; fig. 4.37). Waters with very low Eh (<0 mmvolts) are associated with high dissolved sulfide (>100 mg/L, table 4.15).

Two areas of outcrop, near monitoring wells 925 and 976, stand out as anomalous. Both have calcite-saturated waters (fig. 4.36). Also, uranium concentrations in those two ground waters are high, especially in monitoring well 925 (1.2 mg/L; fig. 4.38). Downdip, monitoring wells 878, 834, and 905 are anomalous as samples are saturated with respect to gypsum, which may indicate leakage of tailings solutions contaminants through the Conquista into the Dilworth. This is supported by detectable tritium in monitoring well 878 (0.7 tritium units) and the high ground-water elevations in monitoring well 905 relative to those in surrounding wells. However, the tritium, ground-water elevation,

and gypsum saturation could also indicate poor well completion allowing some leakage along the well bore from the overlying Conquista or Deweesville sandstones.

Another anomaly is the chloride content of monitoring well 905 (table 4.15). Well 905 has 4,400 mg/L chloride, which is at least four times higher than any other sample from the Dilworth. In addition, the chloride-to-bromide ratio is greater than that expected for a natural water (590 versus about 330 for a natural water, refer to fig. 4.4). The electrical balance of the ground water sampled from this well was very poor (anions having about twice the charge of cations), but the conductivity and TDS were consistent with a saline water, and earlier analyses (in 1987) replicated the high chloride. Calcium was not replicated, being twice as great in 1987 (1,550 mg/L in 1987 versus 655 mg/L in 1991), and the 1987 data were electrically balanced to within 2 percent of the cations. The 1987 sample was saturated with respect to gypsum and oversaturated with calcite and contained detectable aluminum (0.4 mg/L). Thus, the 1987 data indicate neutralized tailings solutions within the Dilworth sandstone in the vicinity of monitoring well 905. Also, in 1987, some metals were detectable (table 4.15). Ground-water elevations also suggest leakage into the Dilworth near monitoring well 905.

With the exception of monitoring well 905, chloride-to-bromide ratios of the Deweesville are generally those of a natural water (fig. 4.4) although with the low chloride and bromide values, small errors (0.4 mg/L) in the bromide may give spurious chloride-to-bromide ratios, and the utility of the ratio is limited at lower concentrations.

Locally high uranium values (for example, samples 925, 971, and 974; fig. 4.37) are associated with natural chloride-to-bromide ratios, low trace metals concentrations, and normal major element chemistry. Thus, these uranium-bearing waters probably represent natural waters associated with uranium mineralization. The Dilworth is locally mineralized at its outcrop (McCulloh and Roberts, 1981). Also, there is an apparent north-south permeability barrier (indicated by the closely spaced potentiometric contours in fig. 3.19) that roughly coincides with a northerly trend of ground waters

saturated with calcite and enriched in uranium and sulfide (figs. 4.36 through 4.38). This may represent a mineralized front within the Dilworth. Cementation along this front might explain the permeability barrier and the lack of producible ground water in monitoring well 833 (fig. 4.35).

Both anion and cation trace metals are generally below detection in all Dilworth samples, although zinc does occur at detectable concentrations. Zinc is a naturally abundant and soluble cation trace metal (Krauskopf, 1967), and its occurrence at low concentrations (0.017 mg/L) is to be expected in natural waters.

Concentrations of ^{226}R are generally low in the Dilworth sandstone (about 1 pCi/L). The one exception is monitoring well 975, which has 20 pCi/L ^{226}R and 59 pCi/L ^{228}R . The latter, a thorium decay-series daughter product, does occur at elevated concentrations in the tailings solutions (because of wholesale dissolution of rock with normal thorium content). But there are no other major element or trace element indicators of tailings solution contamination in monitoring well 975, and these elevated radium concentrations may be natural.

Hydrochemistry of the Manning Formation

The Manning Formation crops out about 4,000 ft northwest of the Falls City UMTRA site. Four wells were completed in the Manning downdip of this outcrop (fig. 4.39; table 4.16). All four wells were completed in claystone, and monitoring well 903 also intersects lignites. Monitoring well 903 has a very high pH (9.67), for reasons that are not understood, whereas monitoring wells 973, 970, and 978 have near-neutral pH.

The monitoring well closest to outcrop (978) has relatively high chloride (1,160 mg/L), suggesting concentration by evapotranspiration. This well is located in a drainage that may be a discharge point. Uranium in monitoring well 978 is also high

(1.05 mg/L), suggesting mineralization, and it is on the possible mineralization trend within the Dilworth. The chloride-to-bromide ratio is normal (351). The adjacent monitoring well in the Dilworth (well 925) also had anomalous uranium (25 mg/L), a normal chloride-to-bromide ratio, but lower chloride concentrations (440 mg/L). Other than uranium, all trace metals are below detection, and radium concentrations are low (table 4.16). There is no evidence for contamination of the Manning by tailings solutions.

Hydrochemistry along Scared Dog Creek

Analysis of the geochemical and geologic data indicated a zone of shallow, acid ground-water contamination extending along Scared Dog Creek north and northeast of tailings pile 3 (fig. 4.40). This zone horizontally crosses lithologic boundaries, indicating that it is either a ground-water plume migrating as underflow beneath Scared Dog Creek, surface recharge from contaminated surface waters flowing within the creek, or leachates of tailings deposited in the sediments along Scared Dog Creek. Data from all geologic units in this eastern area near tailings pile 3 are compiled in table 4.17.

Chloride concentrations are variable, with relatively low concentrations (393 to 621 mg/L) within the Scared Dog Creek drainage. The greatest chloride is in monitoring well 940, which is completed in the Deweesville below the tailings. Chloride-to-bromide ratios are generally low (fig. 4.41) and close to the expected value for natural waters (292). The highest chloride-to-bromide ratio, 456, is also in monitoring well 940. The low chloride-to-bromide ratios, coupled with low chloride, indicate that ground waters in this area consist of tailings solutions diluted by natural ground waters, rain or runoff. Ammonium is low (0.5 mg/L), indicating ion exchange with the sediments. All waters but one in this area (monitoring well 977) are saturated with gypsum, which buffers the

calcium and sulfate concentrations to relatively constant values, although waters with higher aluminum contain higher sulfate (table 4.17).

The aluminum concentrations (92 mg/L, well 962) are greatest in the Scared Dog Creek drainage immediately downstream from the northeast corner of tailings pile 3. Seepage, drainage, or windblown tailings from tailings pile 3 are possible sources of the contamination. Calcium concentrations are not elevated, indicating that the aluminum is not being neutralized by calcite. Instead, aluminum and iron are probably being diluted through mixing with natural waters and are partially neutralized by bicarbonate in those natural waters. Further dilution may explain the decrease in aluminum downstream, from 92 mg/L in monitoring wells 962 and 963 to 1 mg/L in monitoring well 977. Thus, the acidity of the contaminant plume is decreasing downstream due to dilution by background waters and at monitoring well 977, the well farthest downstream, the pH buffering capacity of the aluminum sulfate is nearly exhausted. Thus, monitoring well 977 is, at present, near the edge of the contaminant plume.

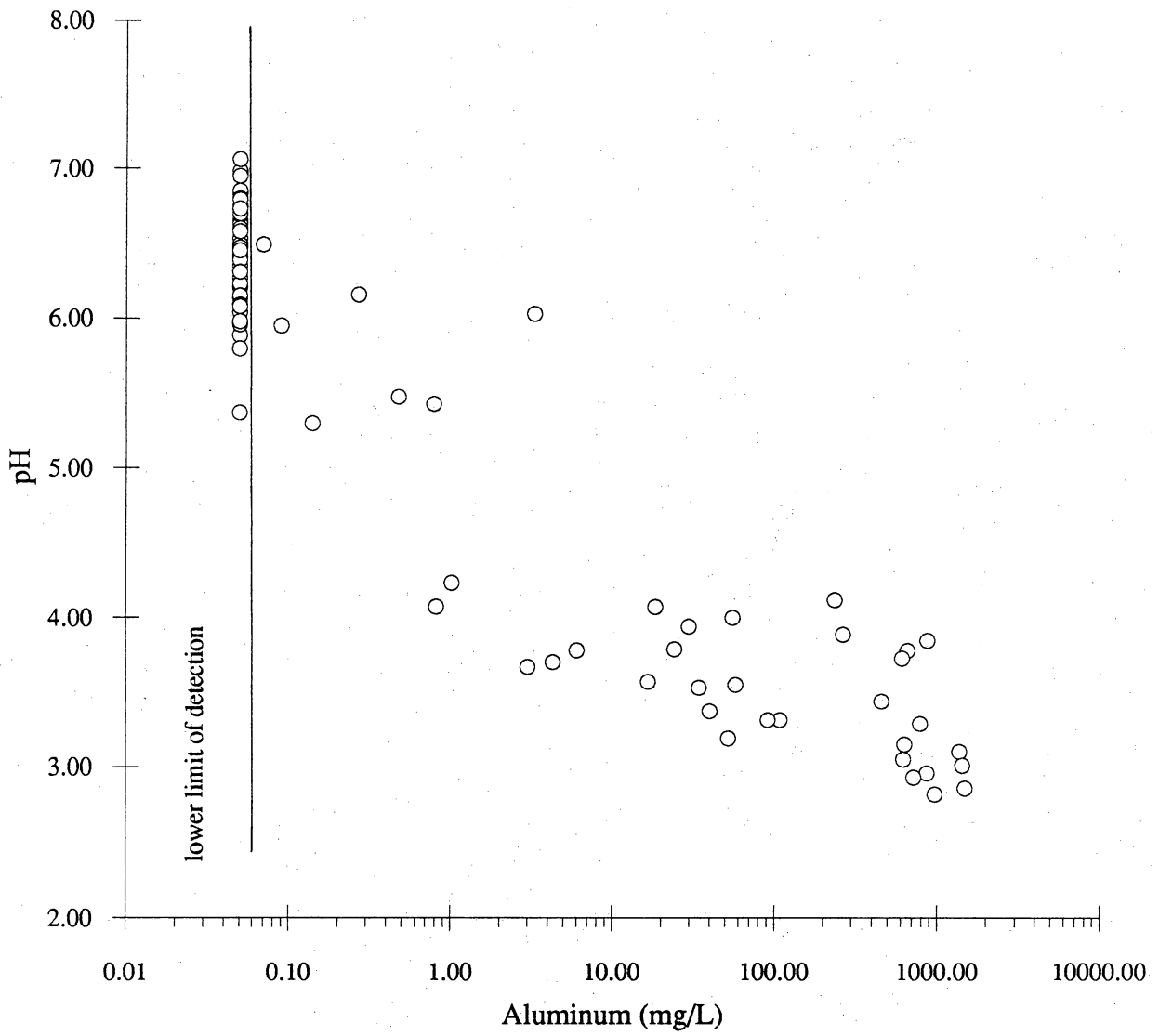


Figure 4.1. Aluminum versus pH in ground waters and tailings solutions.

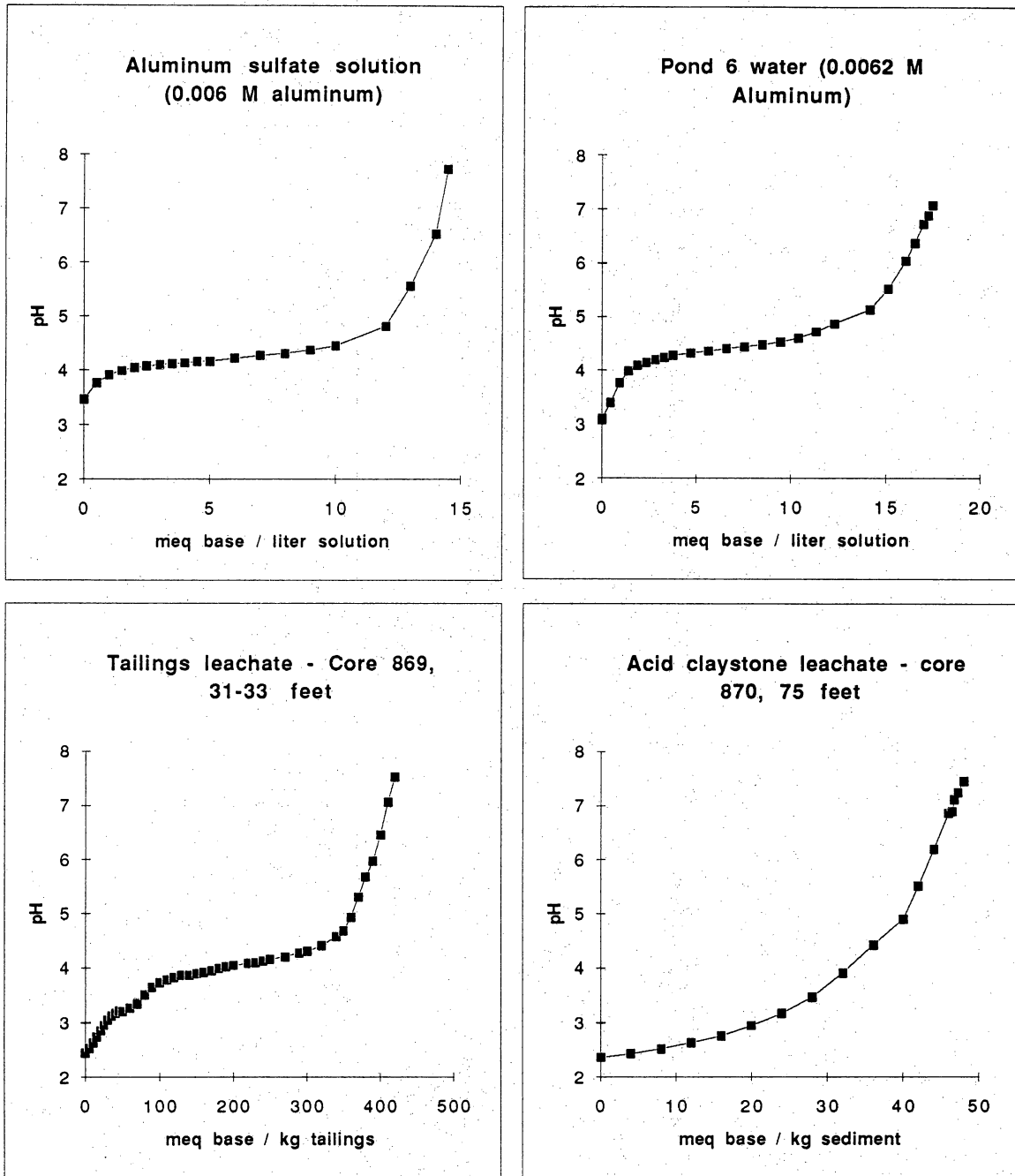


Figure 4.2. Acidity titrations demonstrating pH buffering by aluminum and iron sulfate. Aluminum sulfate and pond 6 waters with similar aluminum concentrations are acidic, and strongly buffered by aluminum hydroxide precipitation to pH values between 4 and 4.6. A tailings leachate pH is buffered by ferric hydroxide precipitation at a pH of 3.2 and aluminum hydroxide precipitation at a pH of 3.8 to 4.5. An acid leachate of a partially oxidized pyrite-bearing claystone has about 0.1 the acidity of the tailings and no pH buffer.

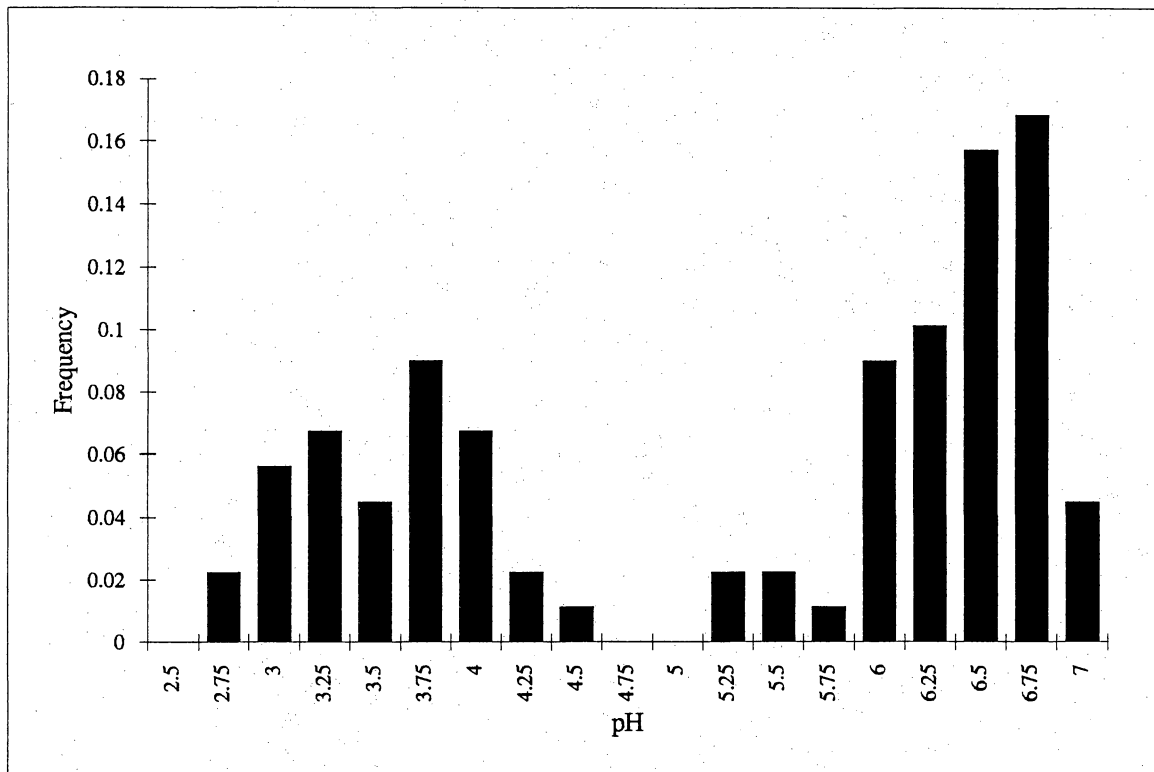


Figure 4.3. Frequency diagram of ground-water and tailings solution pH measurements (May 1991 data). Bimodal distribution indicates two pH buffers.

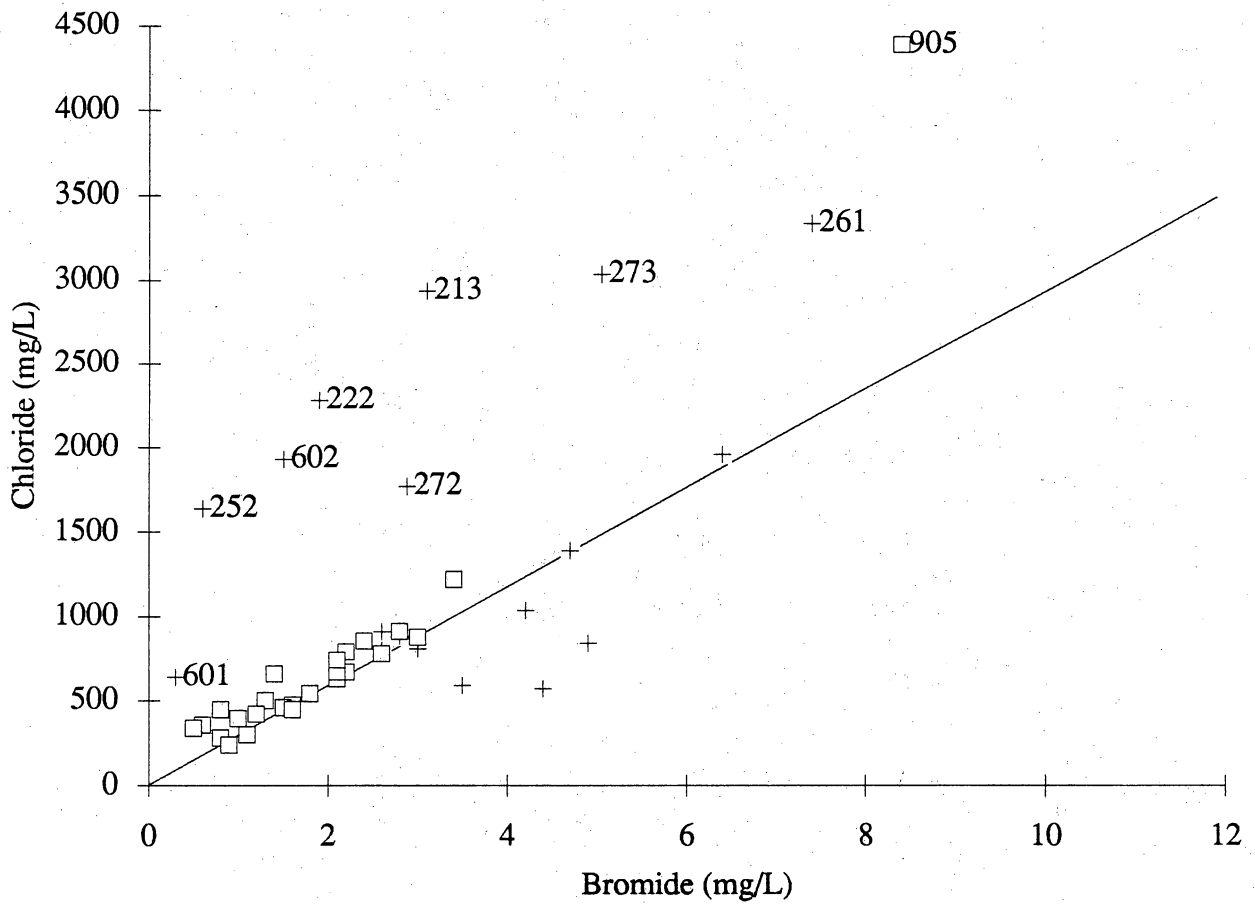


Figure 4.4. Chloride versus bromide of tailings solutions and natural ground waters. Line is that expected for natural waters, including connate water and rainwater. Uncontaminated Dilworth ground waters (squares) fall along that line, as do some tailings solutions (crosses). Other tailings solutions (and one Dilworth ground water) that fall significantly above that line probably contain chloride from bromide-depleted ore-processing reagents. Numbers are wells with bromide-depleted waters.

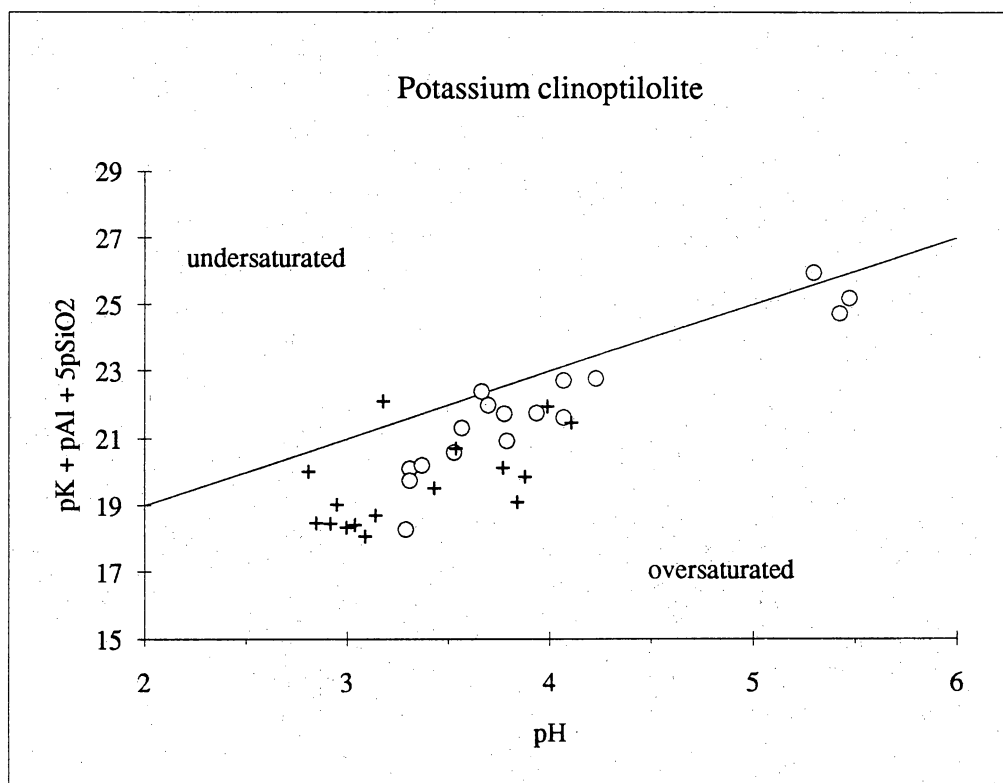
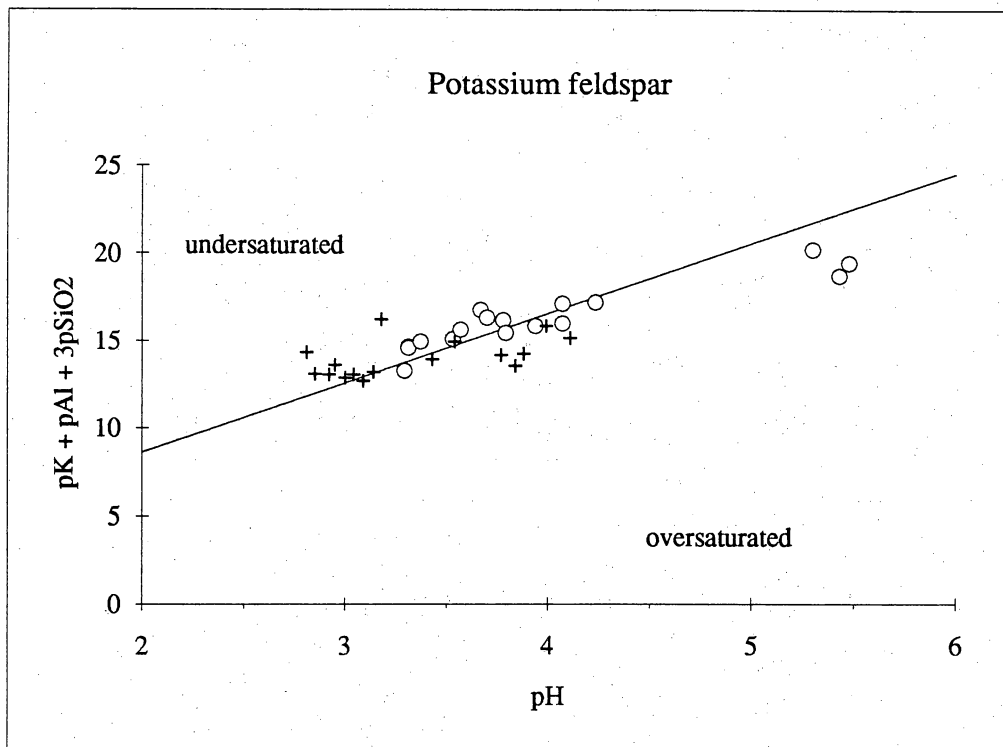


Figure 4.5. Potassium feldspar and clinoptilolite equilibria diagrams. Circles are ground waters; crosses are tailings solutions; lines are saturation (equilibria), with feldspar or clinoptilolite. Waters are saturated with potassium feldspar and oversaturated with clinoptilolite.

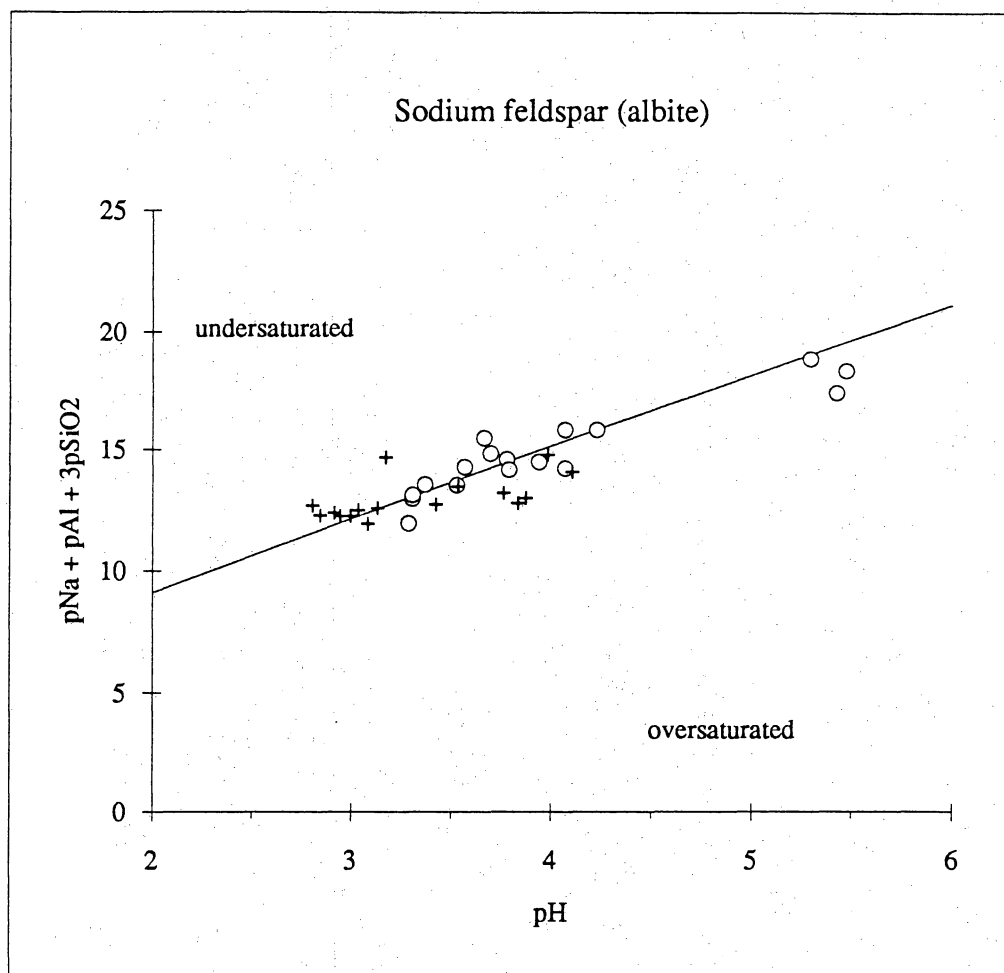


Figure 4.6. Sodium feldspar (albite) equilibrium diagram. Circles are ground waters; crosses are tailings solutions; line is saturation (equilibrium) with albite.

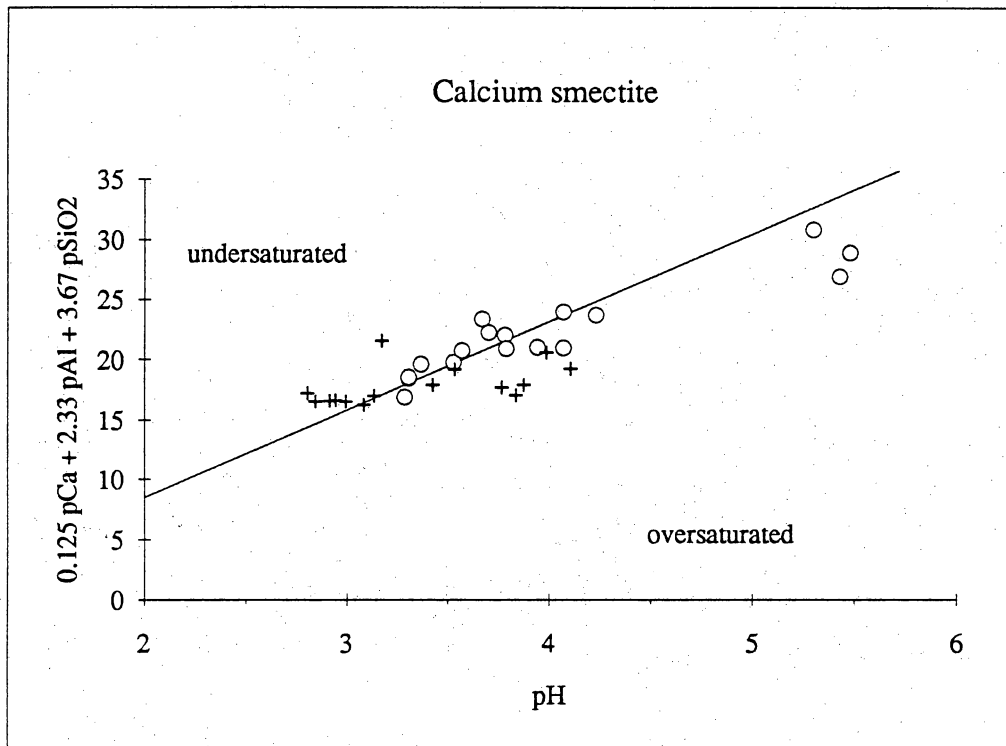
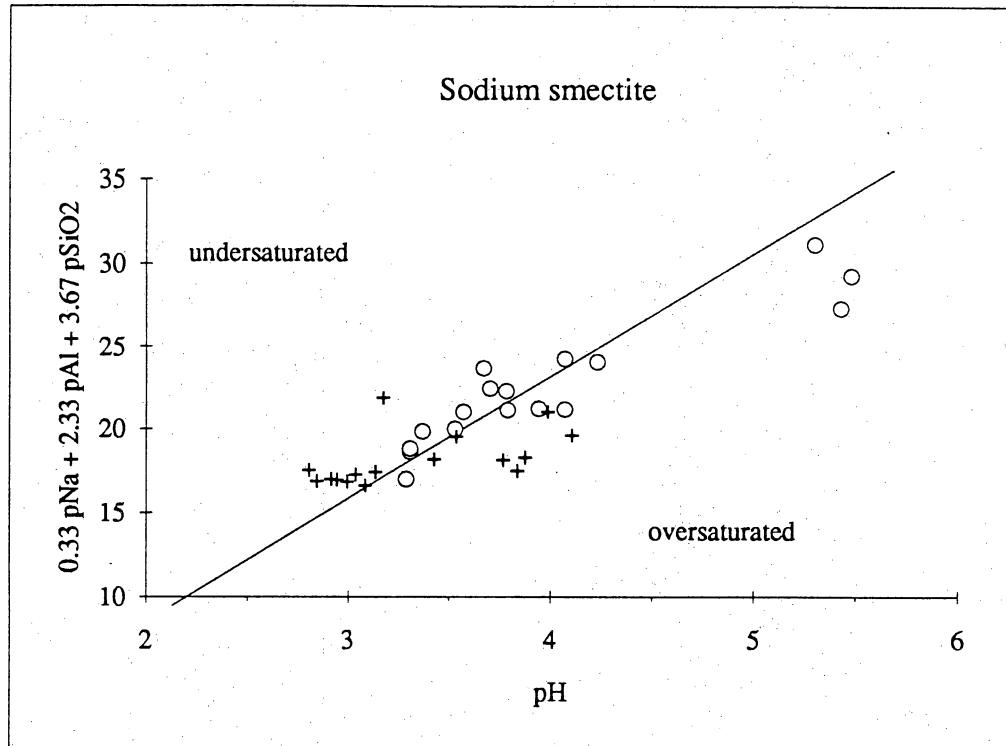


Figure 4.7. Sodium and calcium smectite equilibria diagrams. Circles are ground waters; crosses are tailings solutions; lines are saturation (equilibria) with smectites.

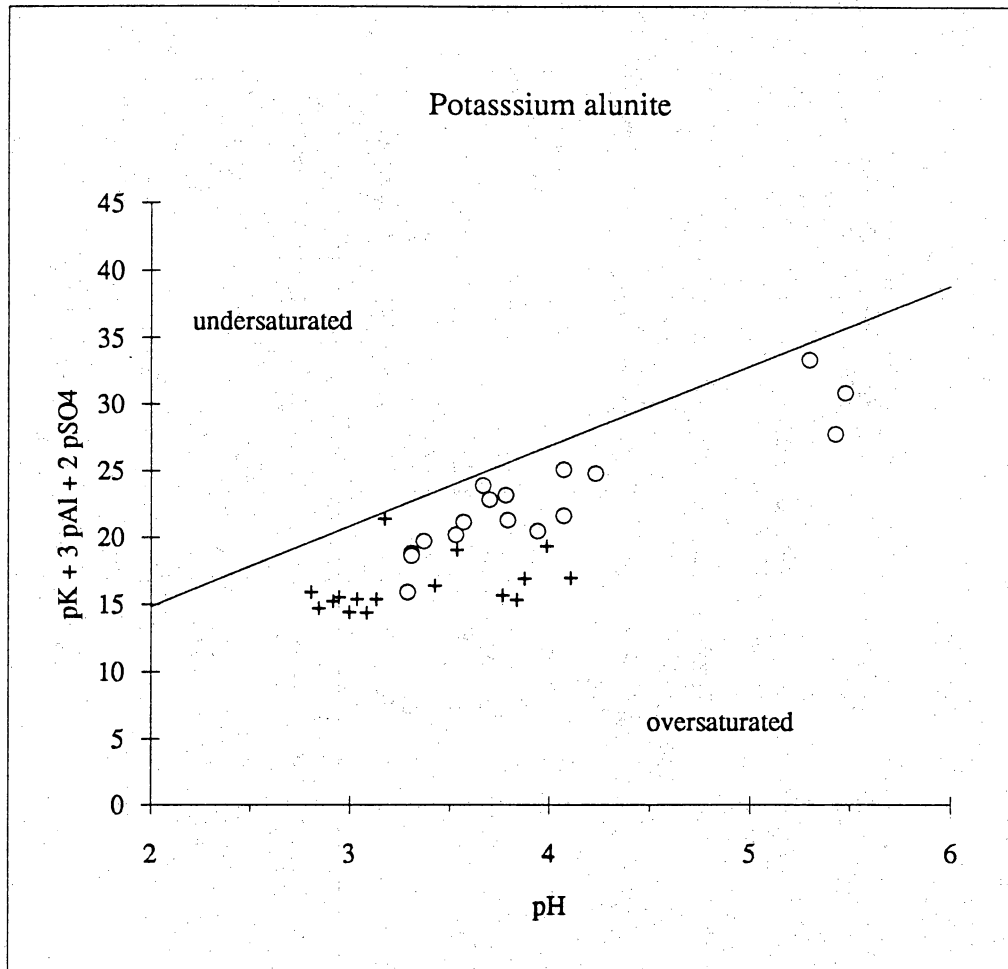


Figure 4.8. Alunite equilibrium diagram. Circles are ground waters; crosses are tailings solutions; line is saturation (equilibrium) with alunite. Most samples are oversaturated.

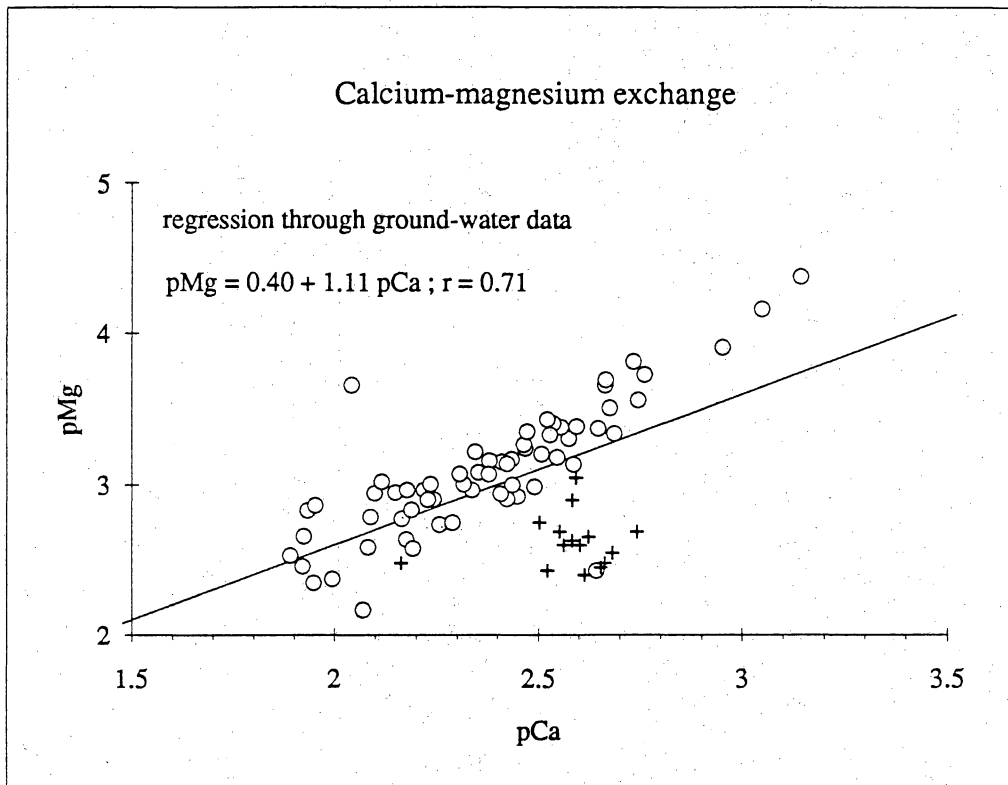
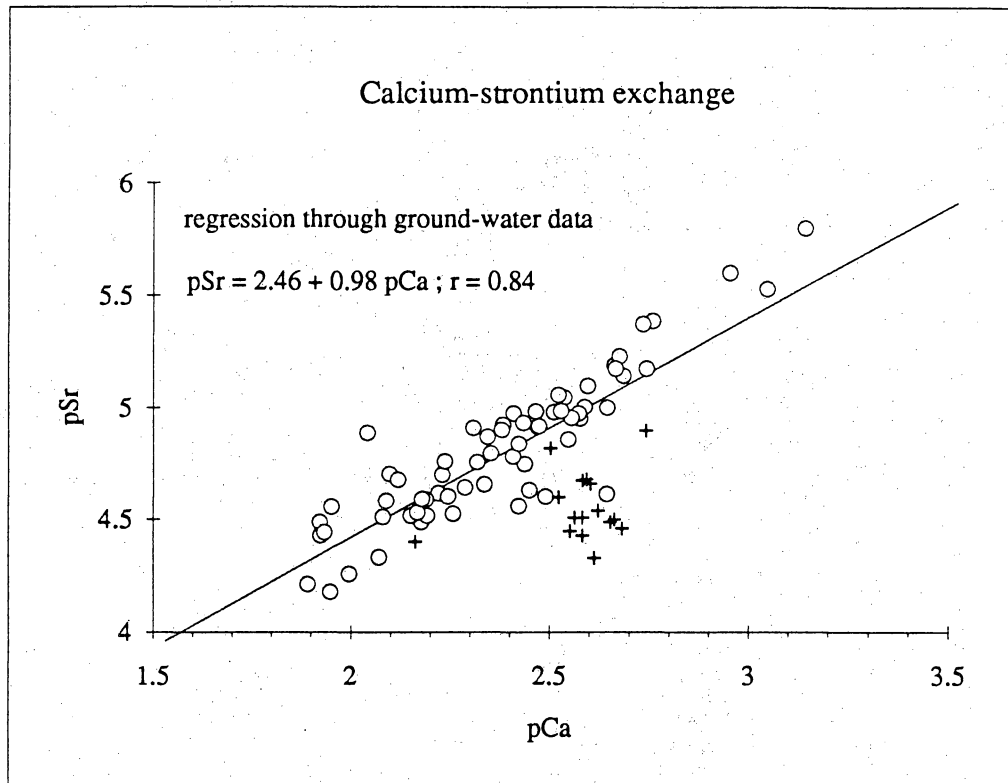


Figure 4.9. Calcium-strontium and calcium-magnesium exchange equilibria. Circles are ground waters; crosses are tailings solutions. See text for discussion of regression lines.

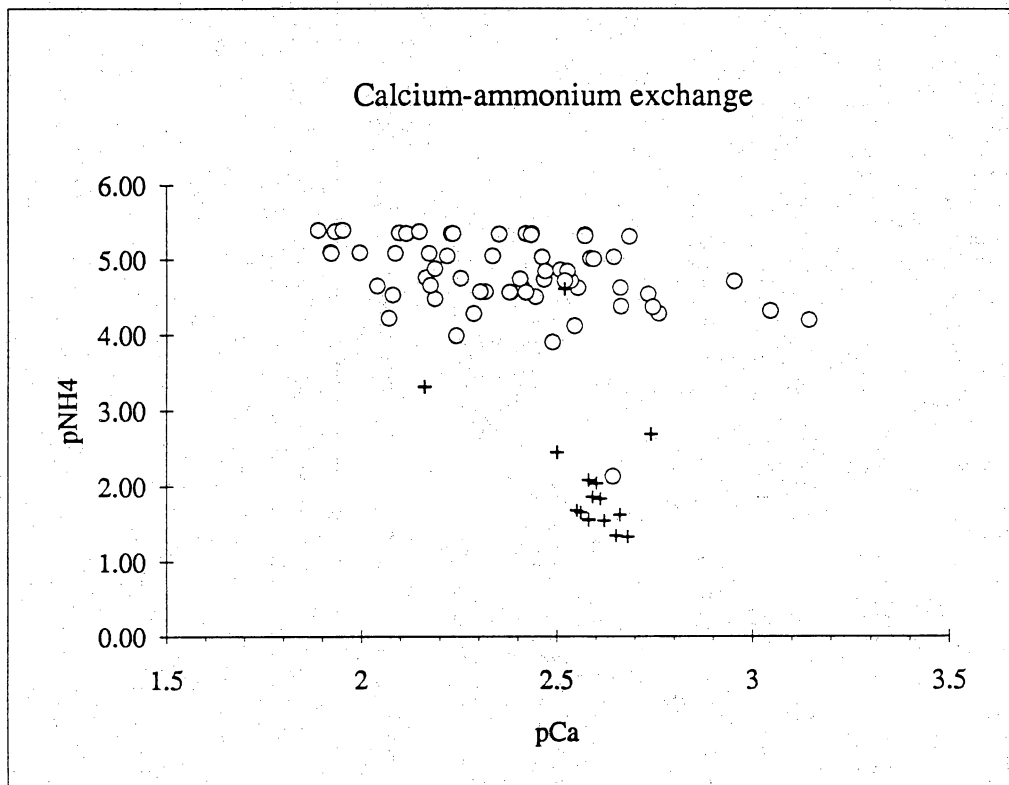
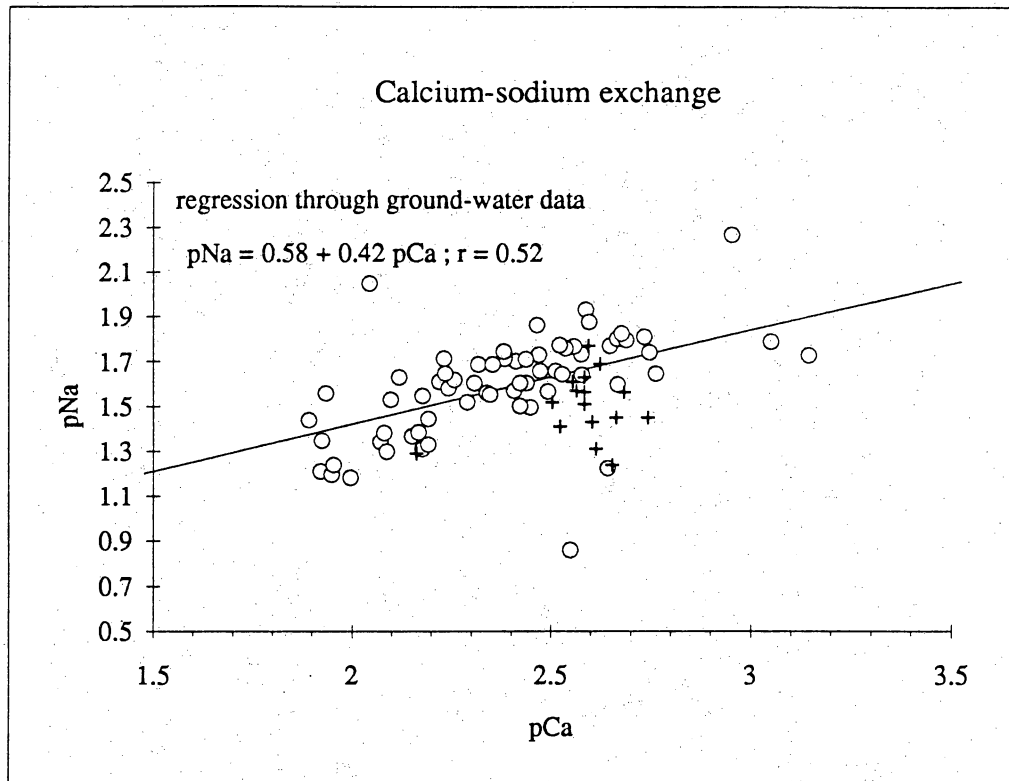
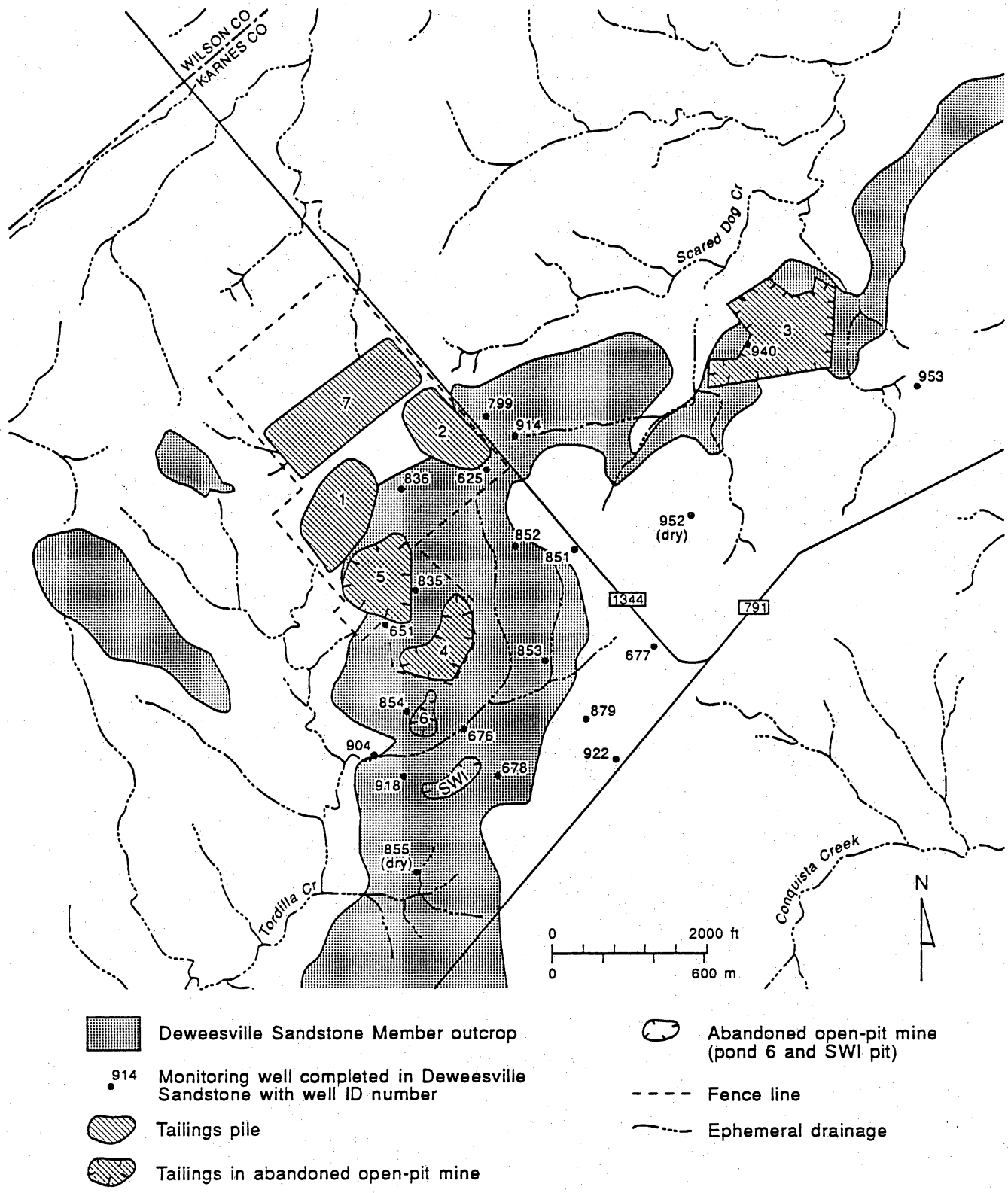


Figure 4.10. Calcium-sodium and calcium-ammonium exchange equilibria. Circles are ground waters; crosses are tailings solutions.



QA20373c

Figure 4.11. Locations of Deweesville monitoring wells, tailings piles, and Deweesville sandstone outcrop.

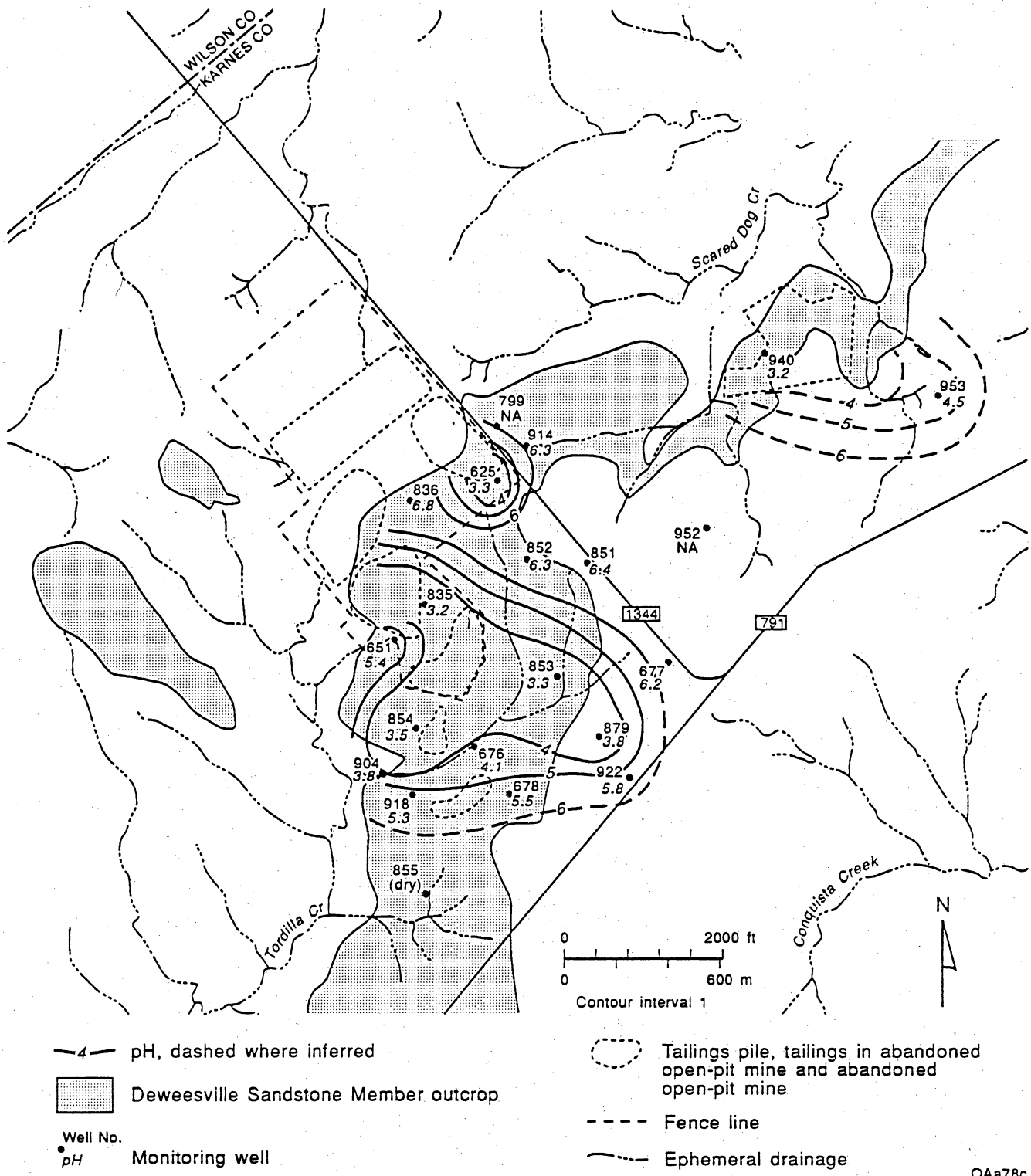


Figure 4.12. pH of Deweesville ground waters.

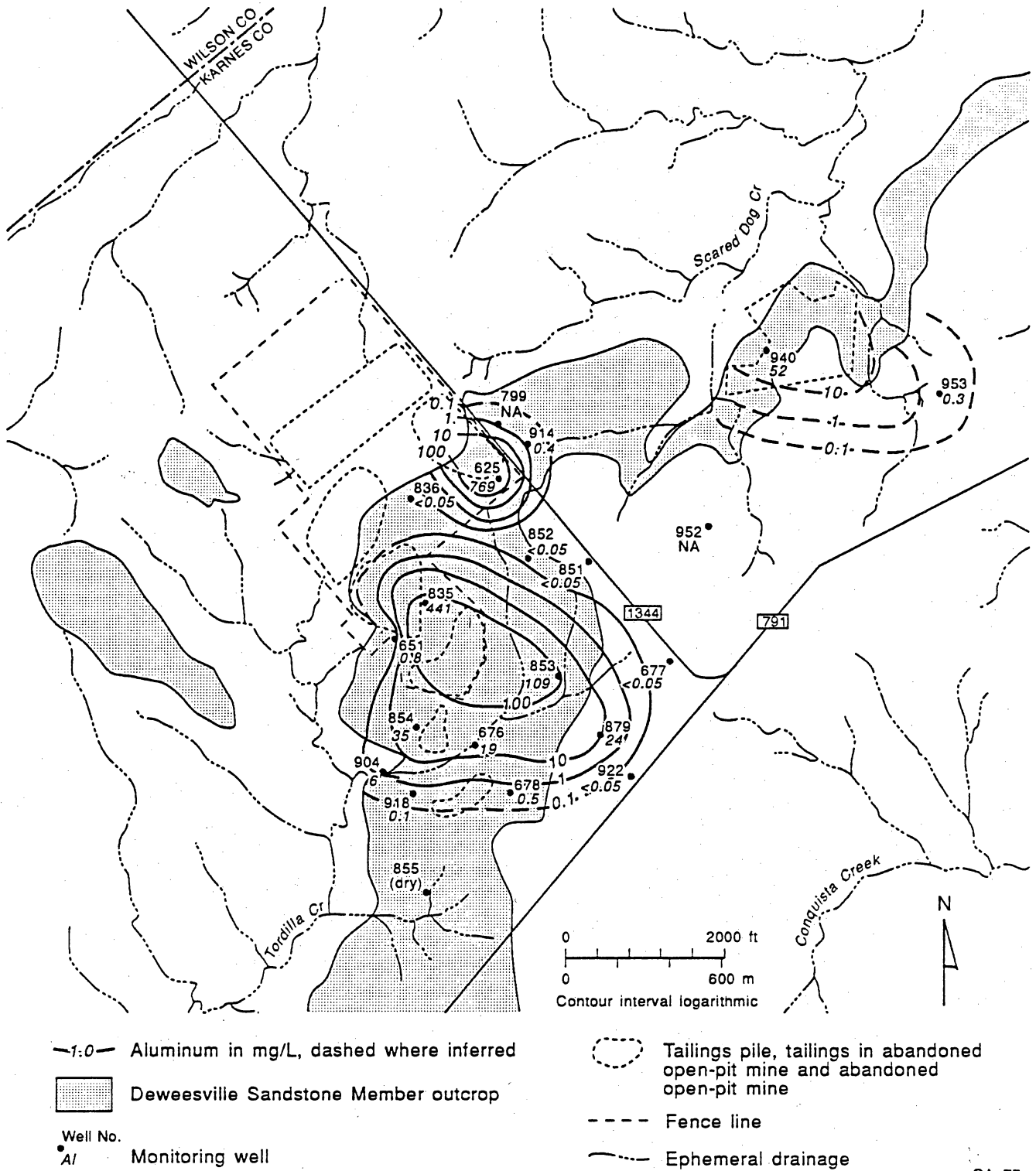
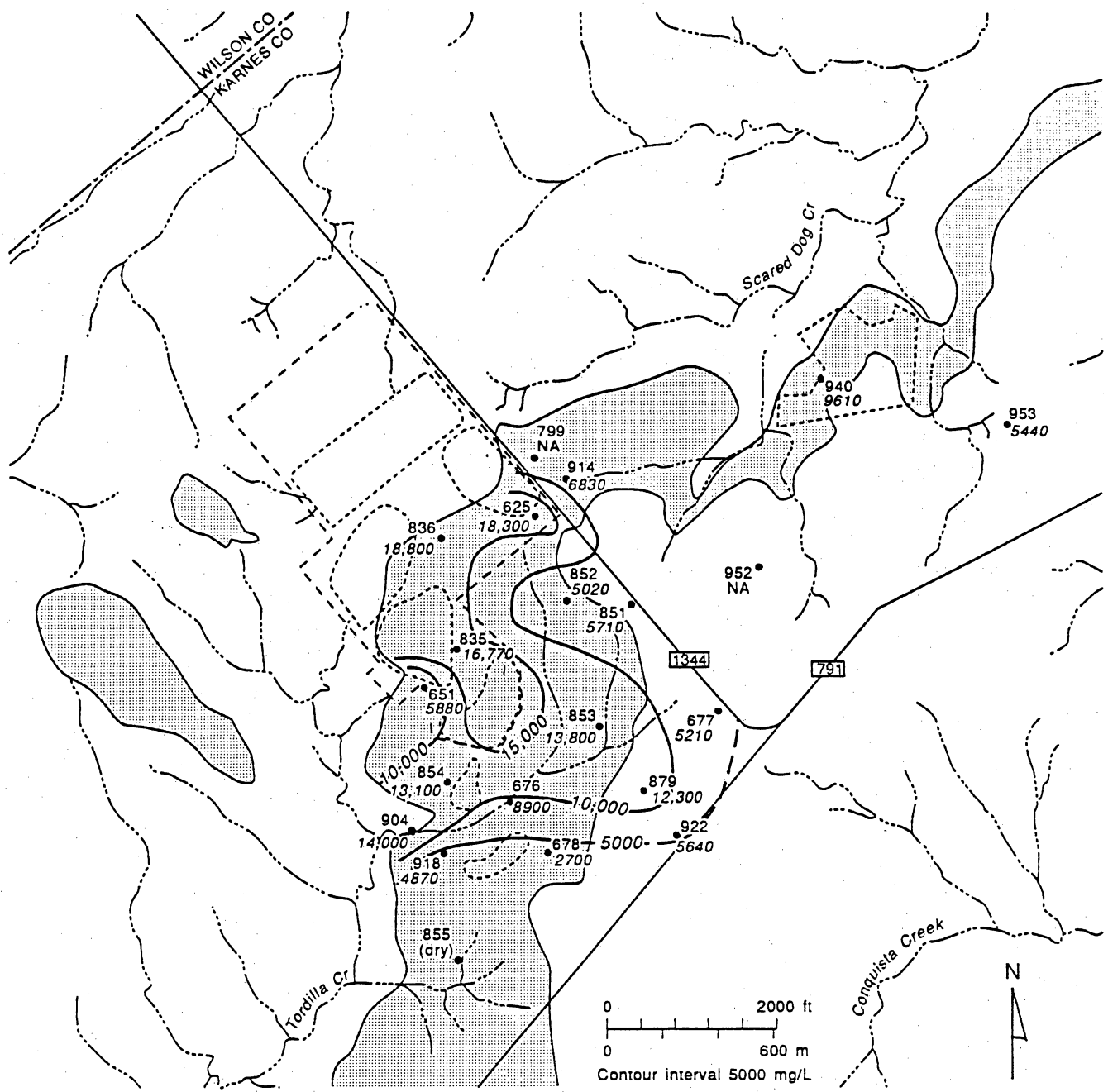


Figure 4.13. Aluminum in Deweesville ground waters.



-4000- Total dissolved solids in mg/L, dashed where inferred

Deweesville Sandstone Member outcrop

Well No.
• TDS Monitoring well

Tailings pile, tailings in abandoned open-pit mine and abandoned open-pit mine

--- Fence line

Ephemeral drainage

0 2000 ft
0 600 m
Contour interval 5000 mg/L

QAa76c

Figure 4.14. Total dissolved solids (mg/L) in Deweesville ground waters.

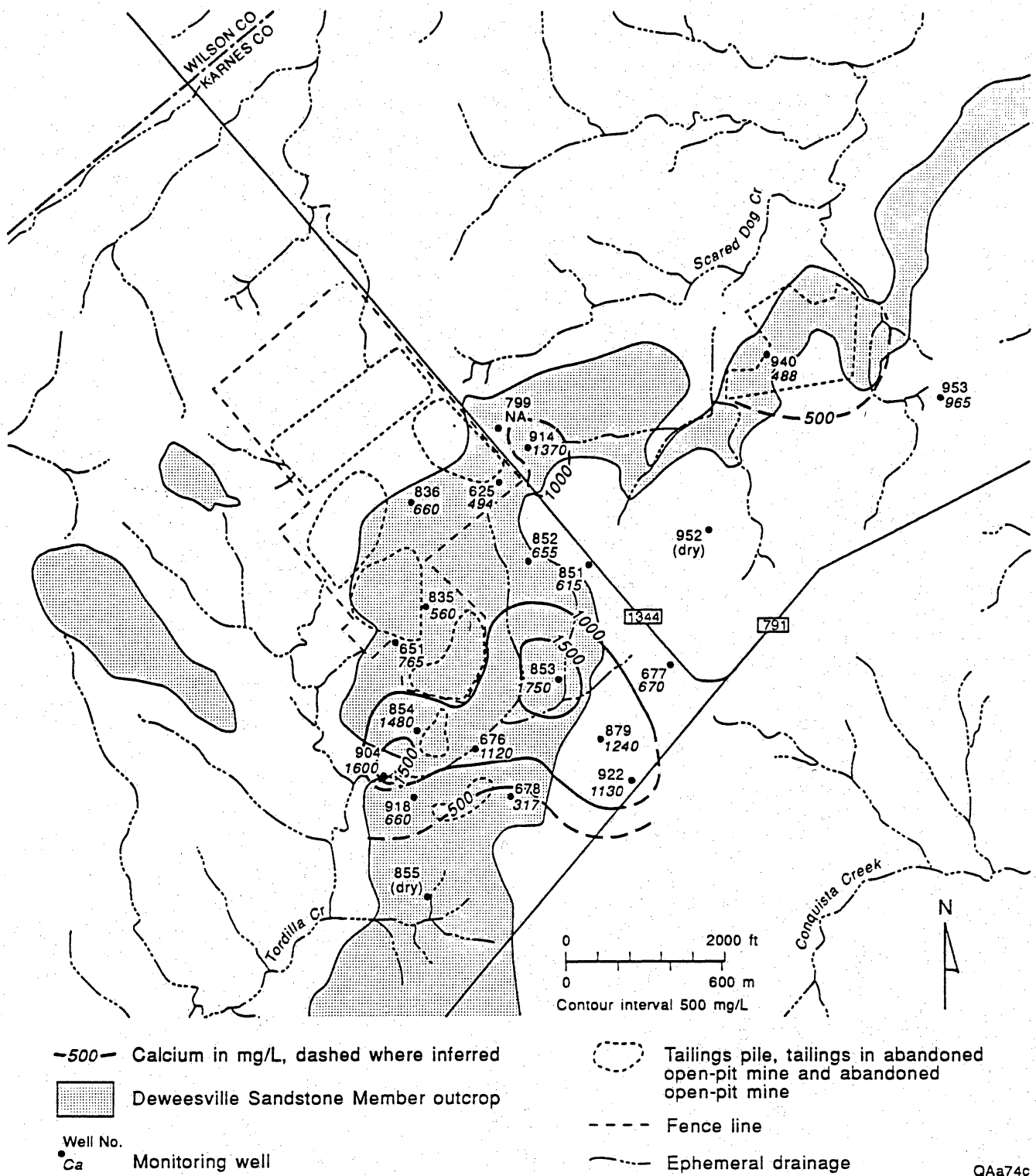
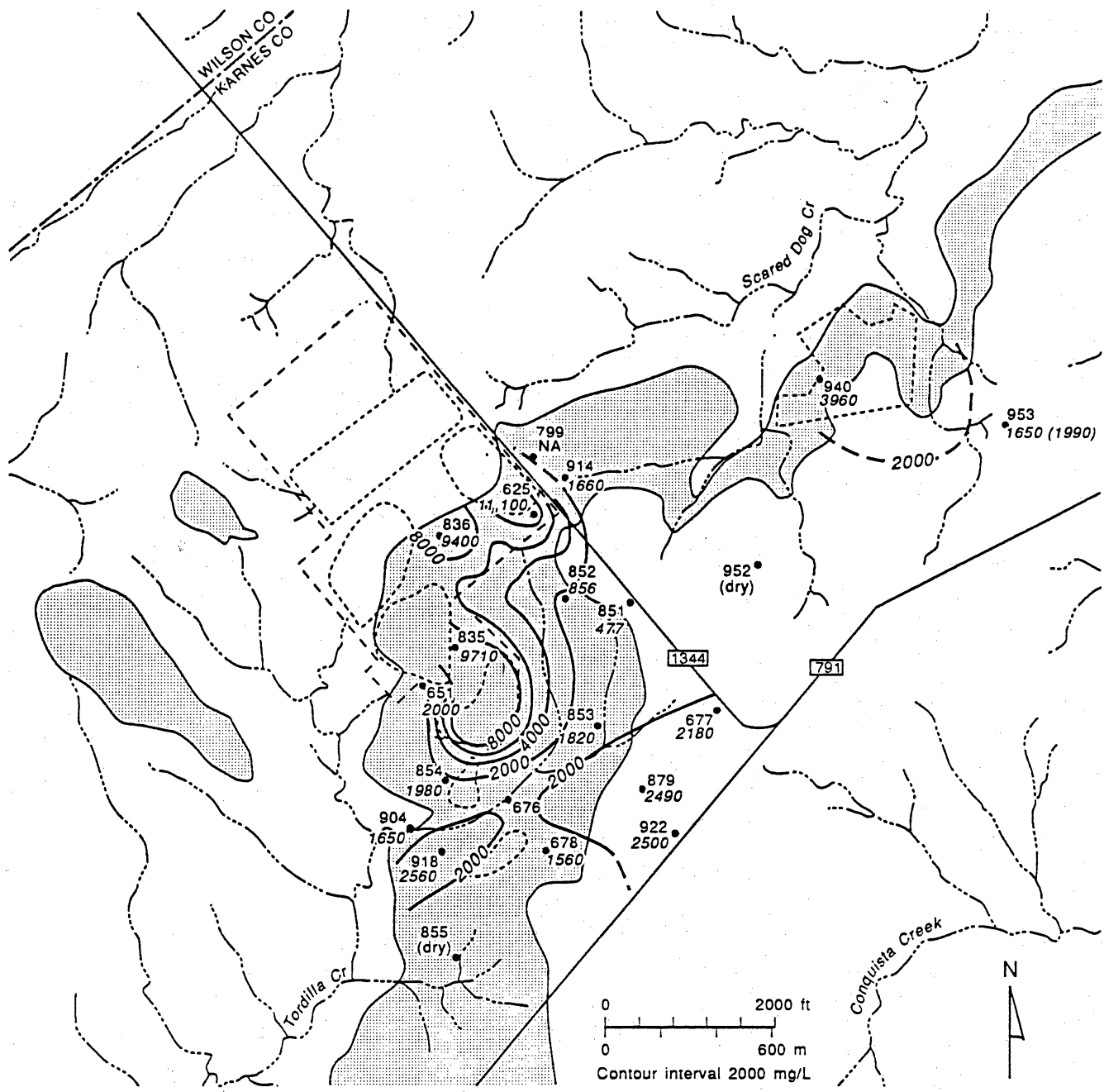


Figure 4.15. Calcium (mg/L) in Deweesville ground waters.



-2000- Sulfate in mg/L, dashed where inferred
 [Shaded Box] Deweesville Sandstone Member outcrop

Well No.
 •SO₄ Monitoring well

[Dashed Circle] Tailings pile, tailings in abandoned open-pit mine and abandoned open-pit mine
 - - - Fence line
 [Dashed Line] Ephemeral drainage

QAa73c

Figure 4.16. Sulfate (mg/L) in Deweesville ground waters.

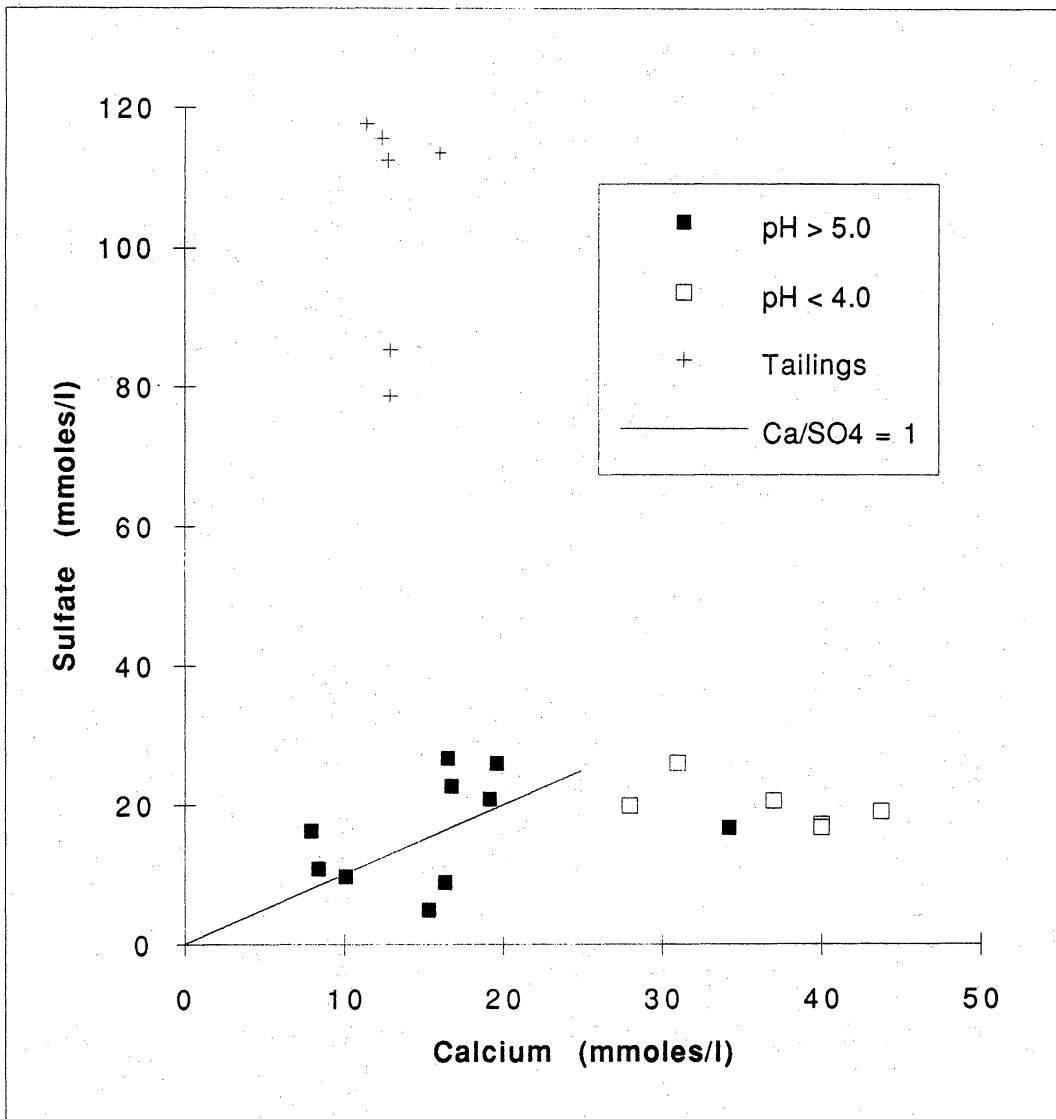
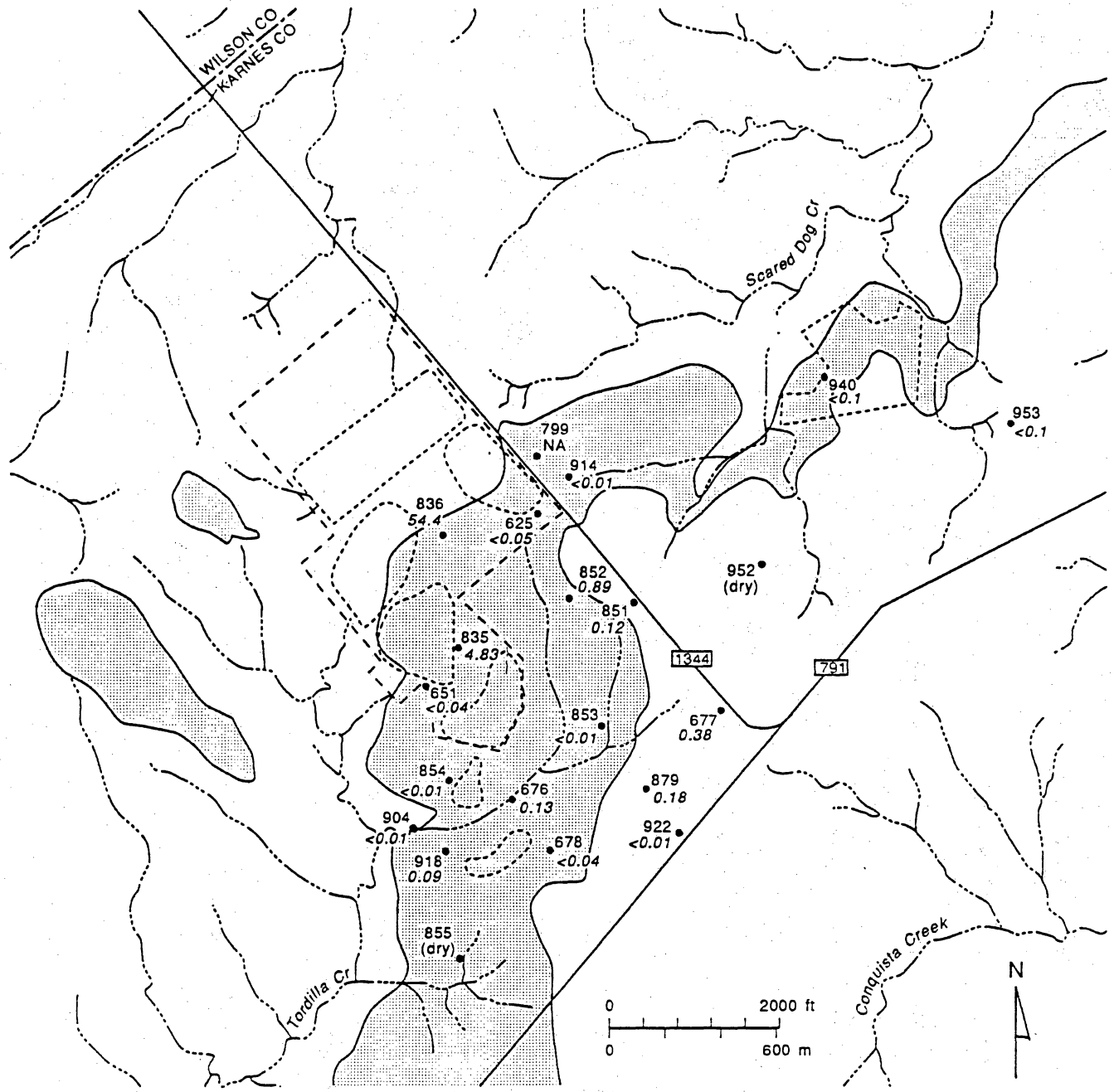


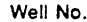





Figure 4.17. Sulfate versus calcium in Deweesville ground waters. Also shown are values of tailings solution in piles 4 and 5.



-  Deweesville Sandstone Member outcrop
-  Fence line
-  Well No.
-  Mo Monitoring well, Molybdenum (Mo) values in mg/L
-  Tailings pile, tailings in abandoned open-pit mine and abandoned open-pit mine
-  Ephemeral drainage

QAa71c

Figure 4.18. Molybdenum (mg/L) in Deweesville ground waters.

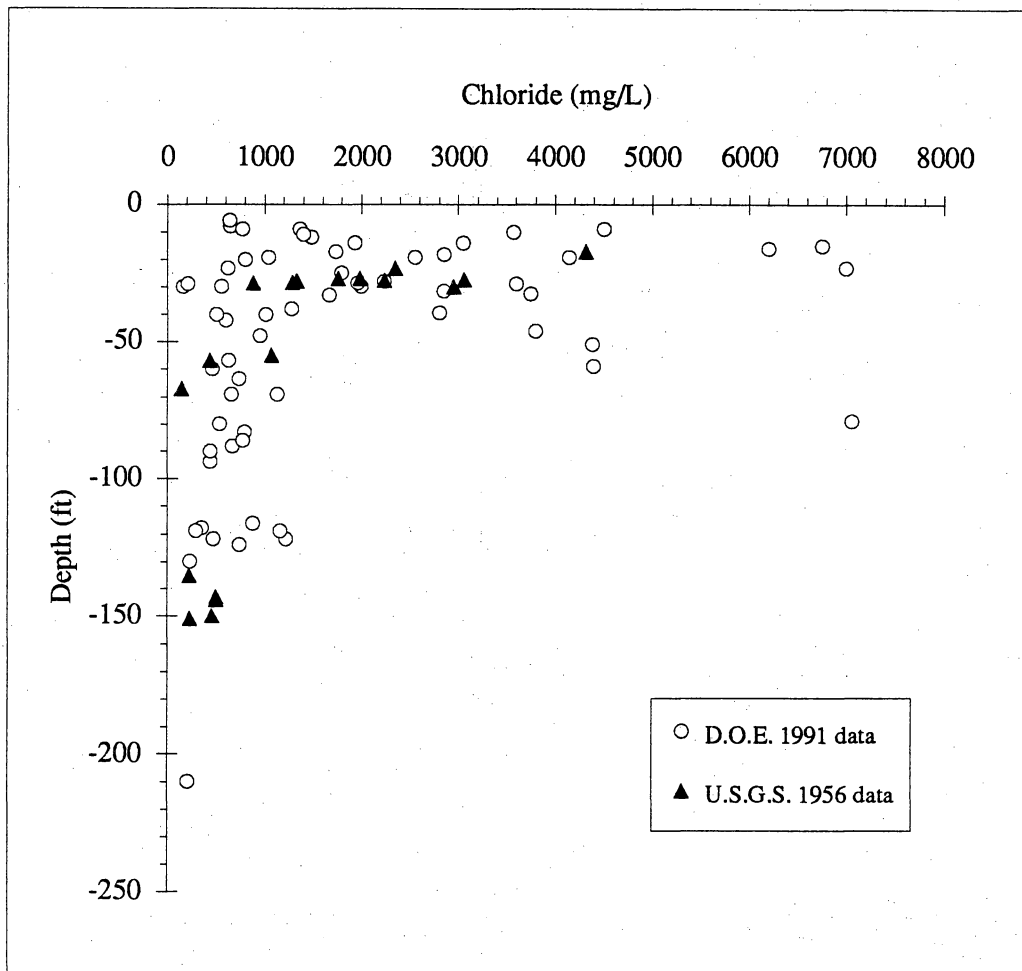


Figure 4.19. Chloride concentration in ground waters versus depth. Above the normal ground-water table (~30 ft) chloride concentrations are in excess of 1,000 mg/L for both the 1956 (pre-milling) and 1991 (post-milling) data. (Data for 1956 are from U.S. Geological Survey, 1958).

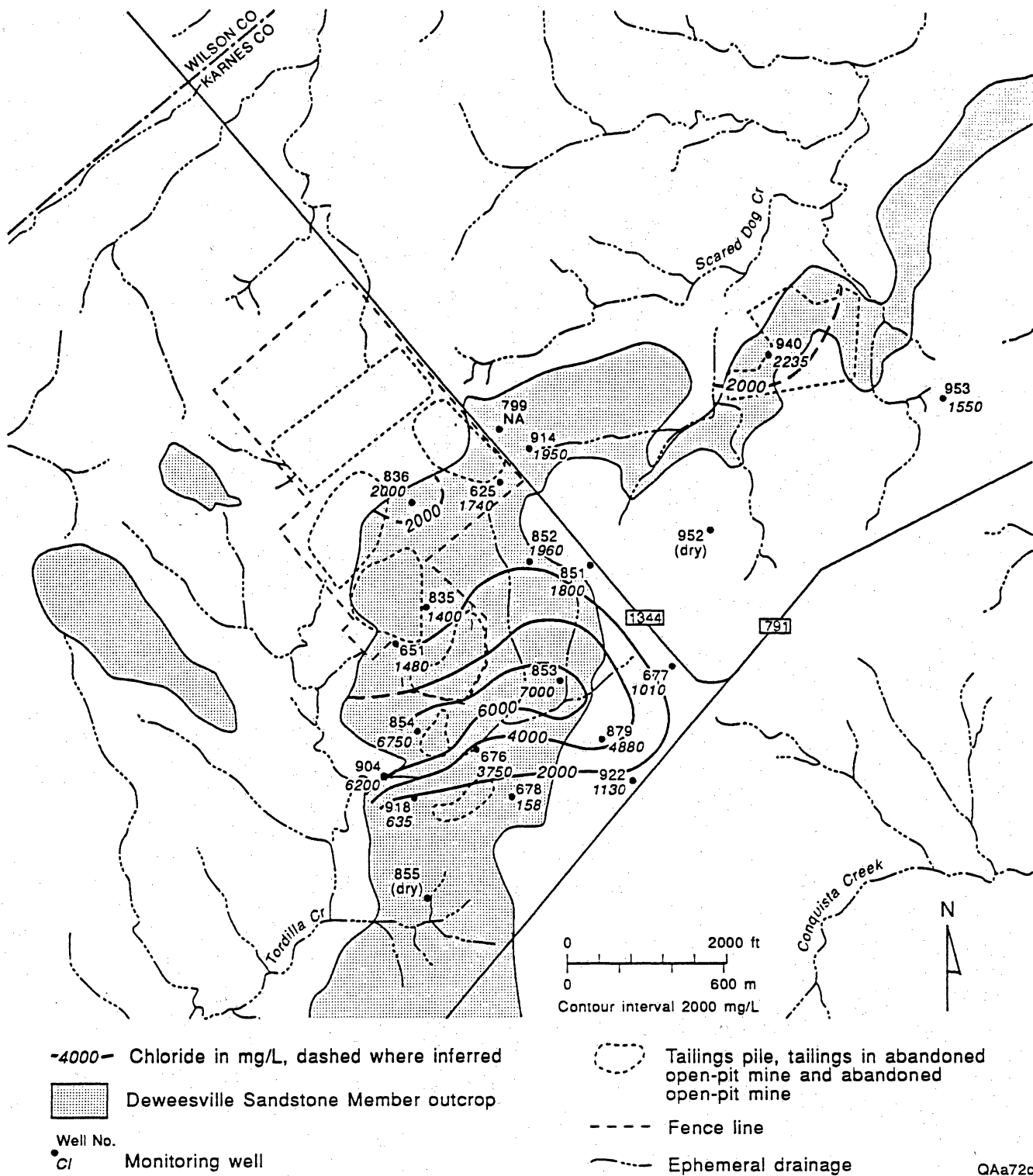


Figure 4.20. Chloride (mg/L) in Deweesville ground waters.

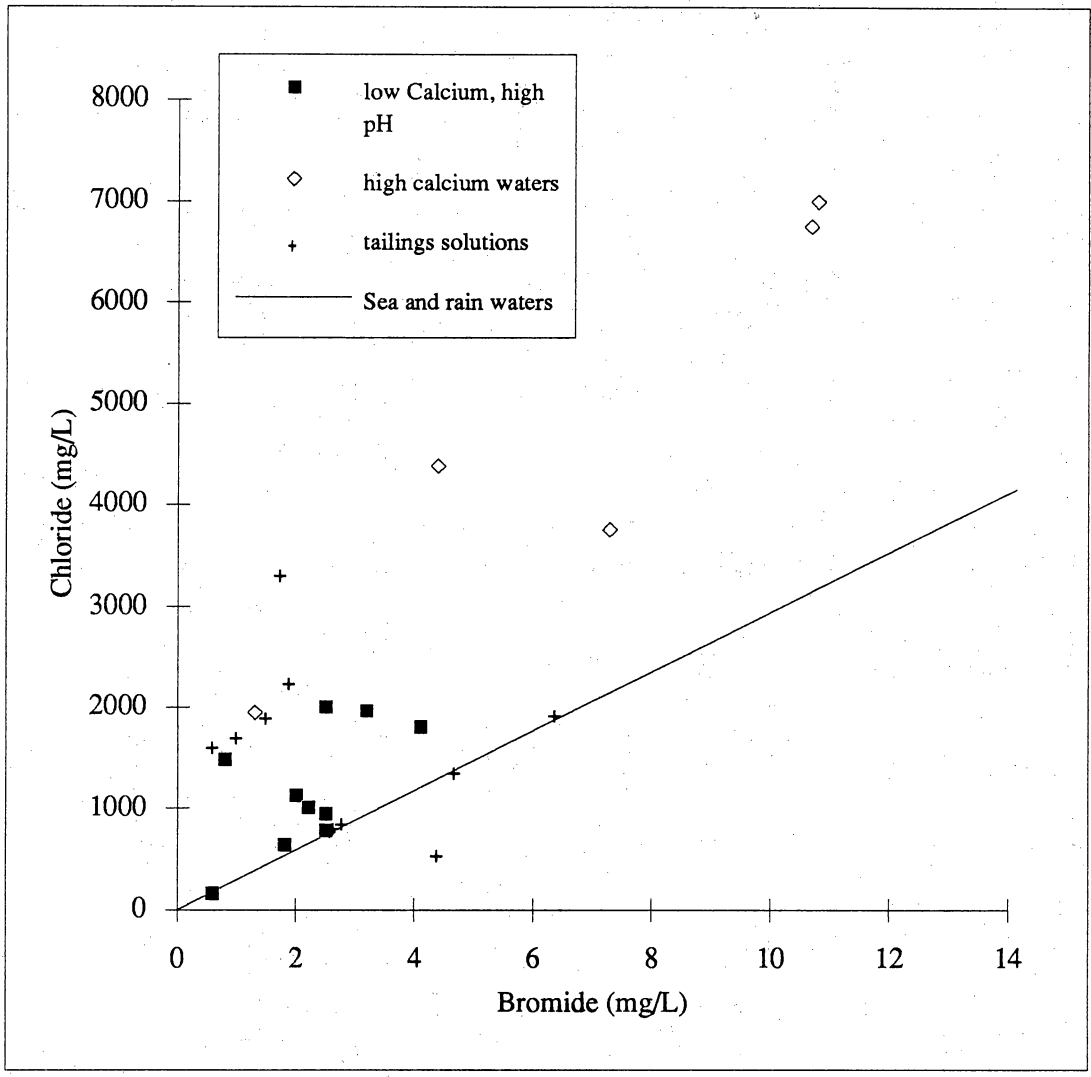
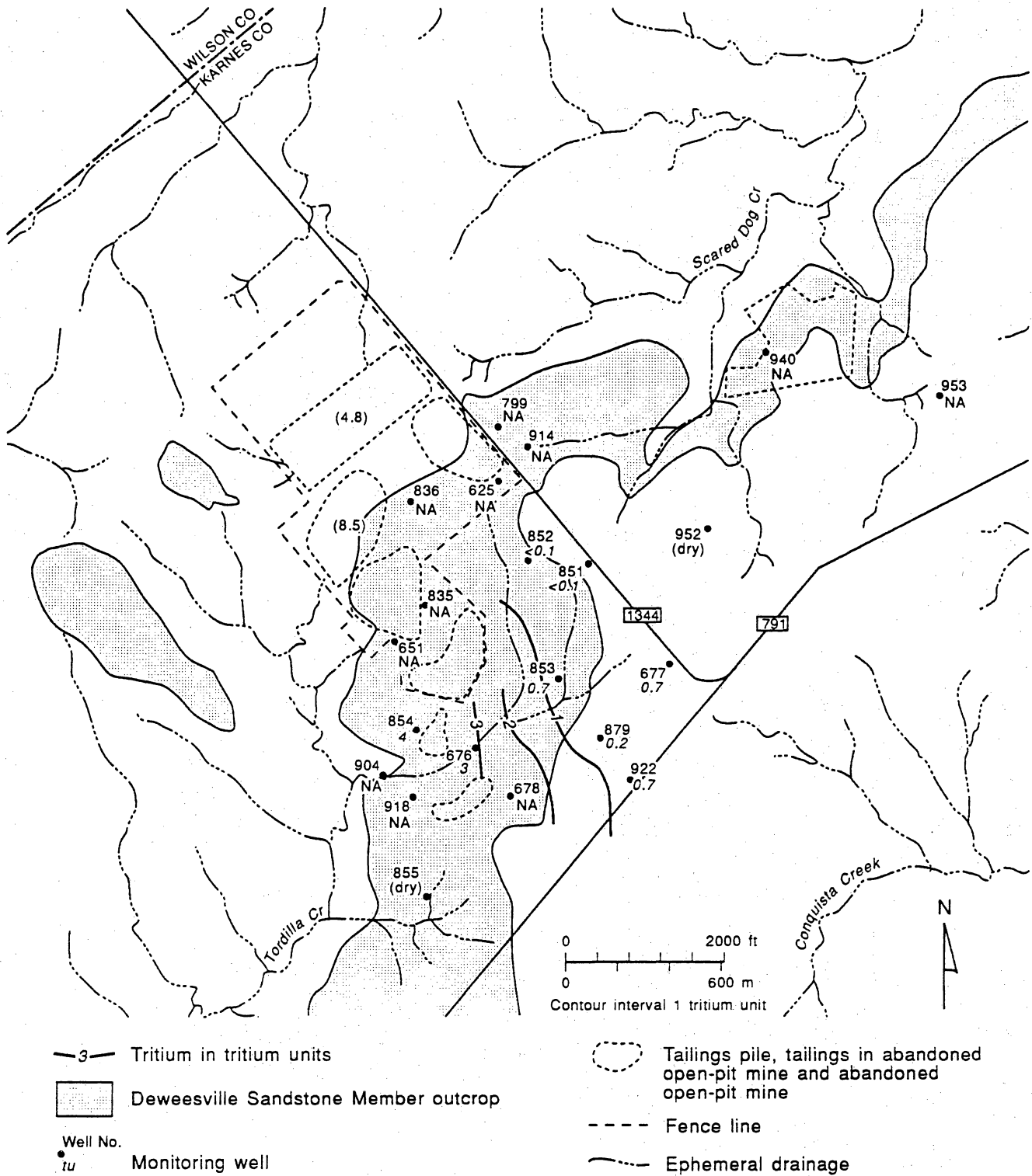


Figure 4.21. Chloride versus bromide in Deweesville ground waters and tailings solutions.



QAa175c

Figure 4.22. Tritium in Deweesville ground waters.

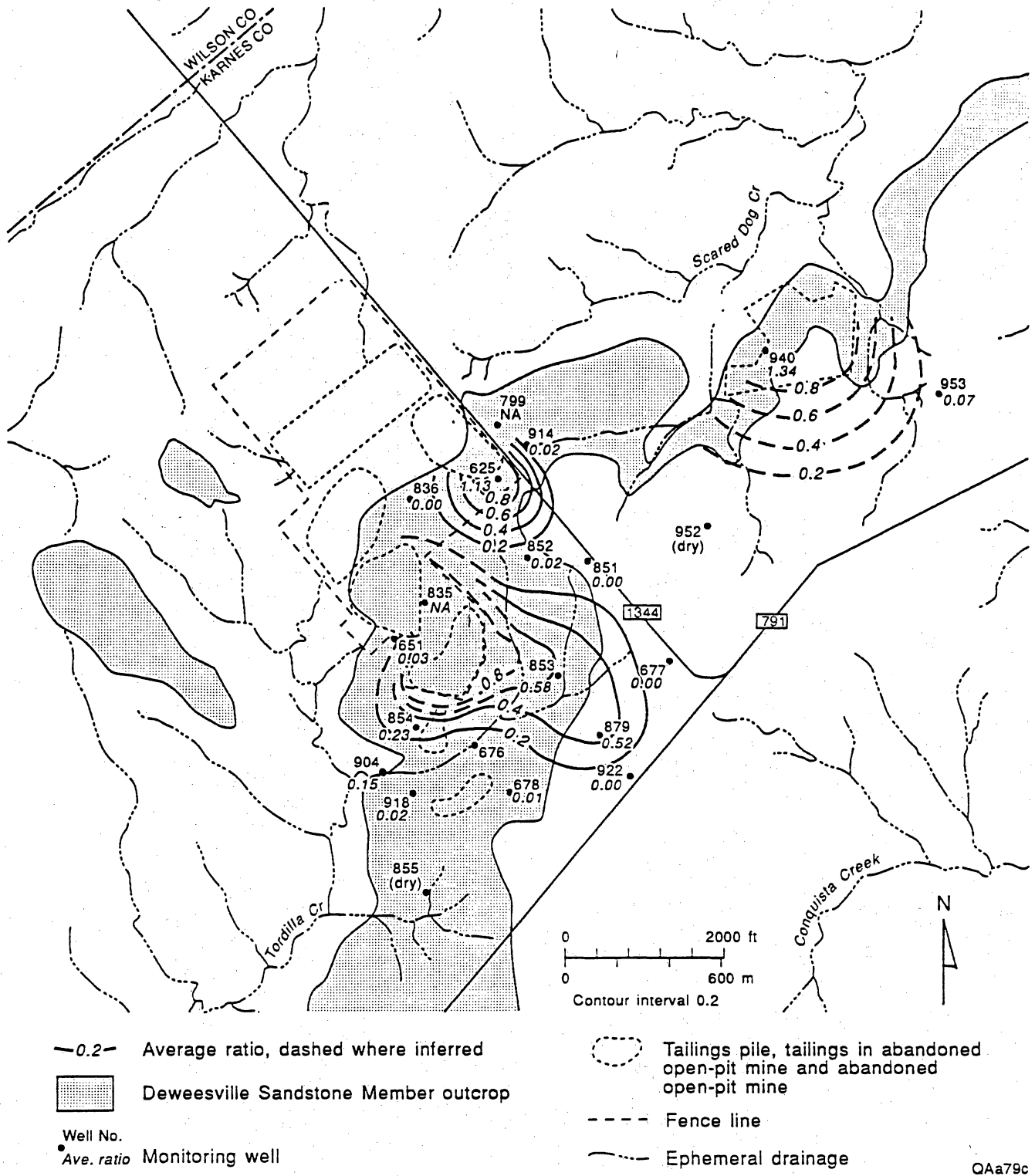


Figure 4.23. Average normalized cation trace metals in Deweesville ground waters.

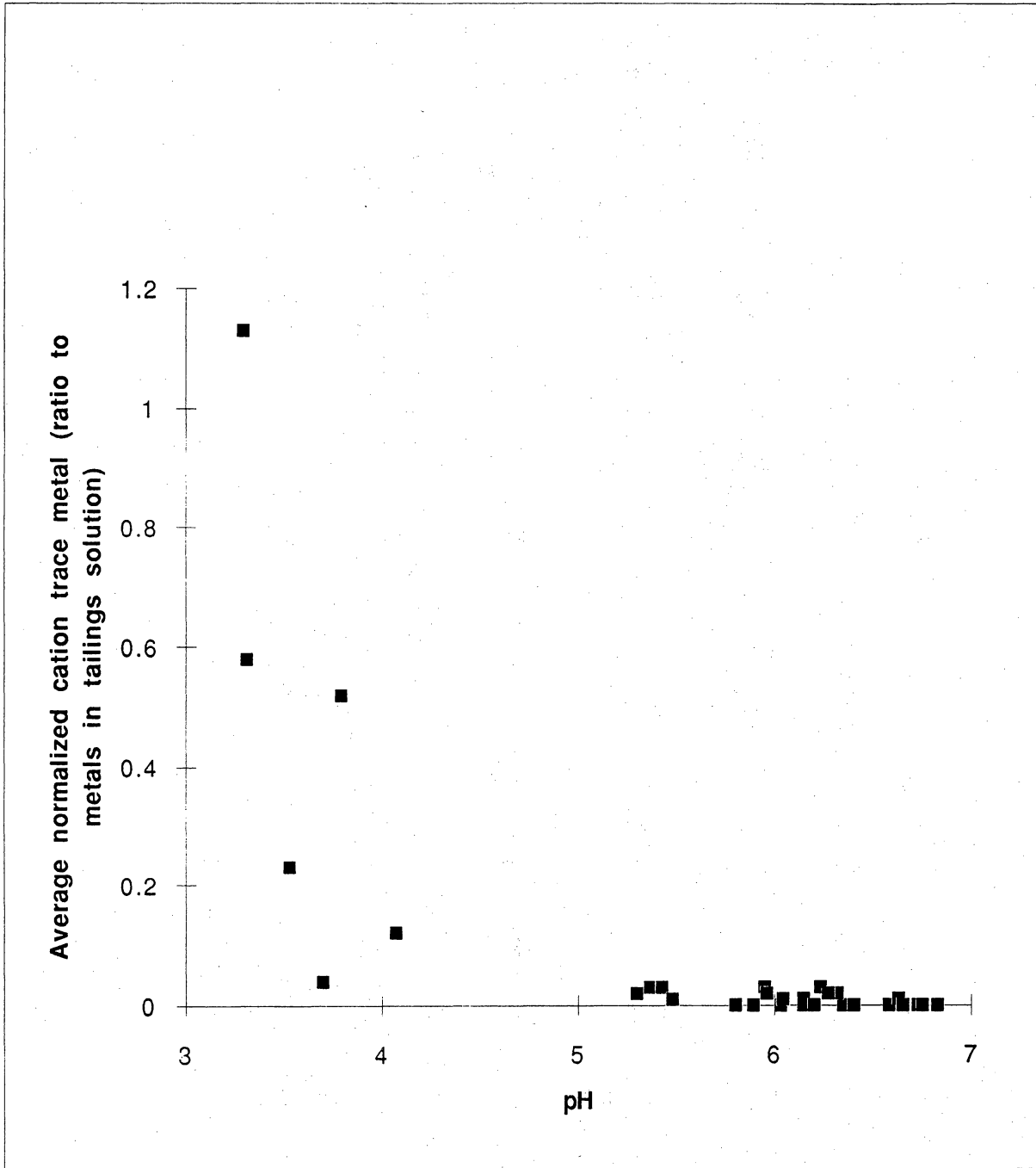
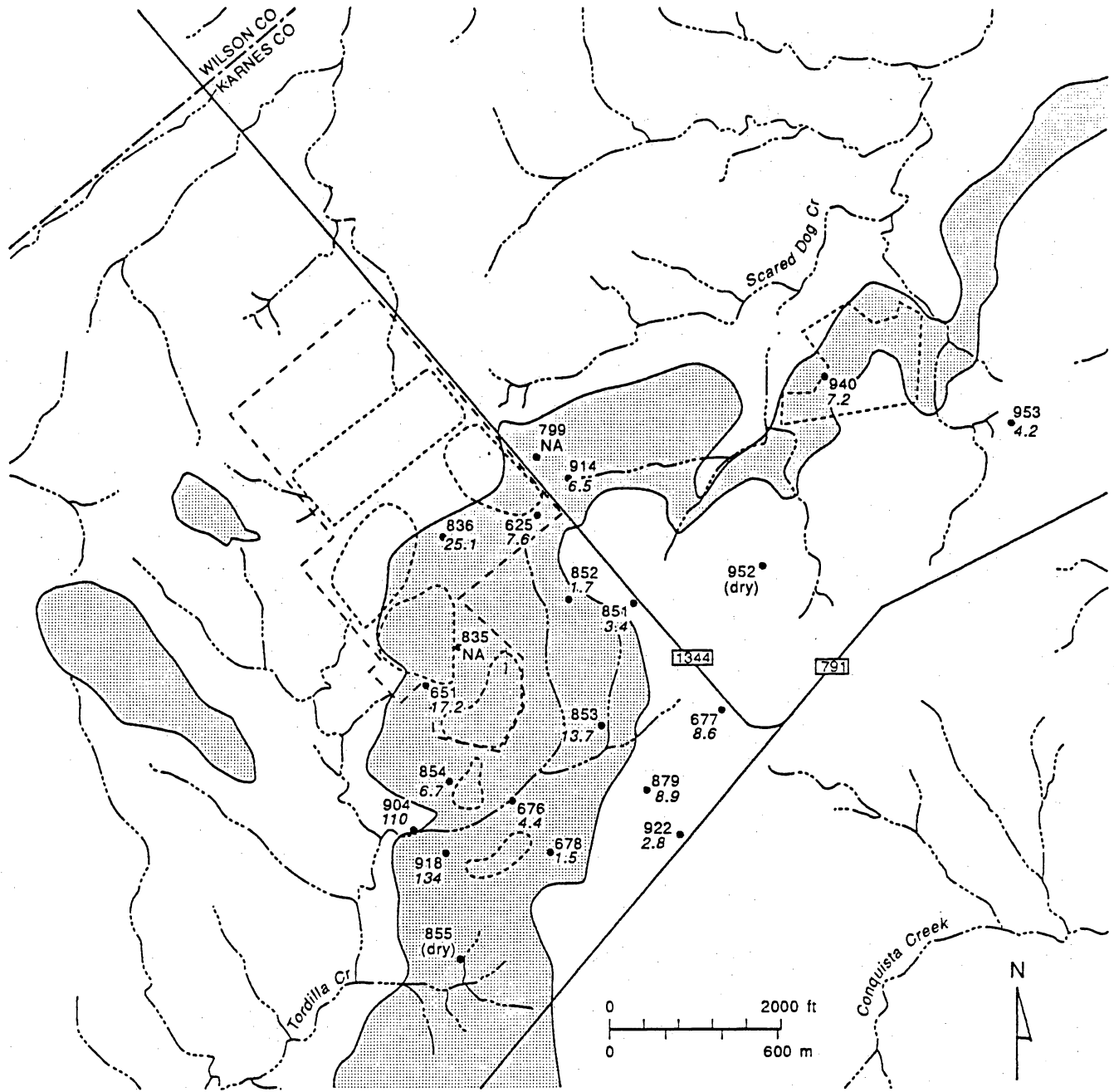
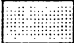






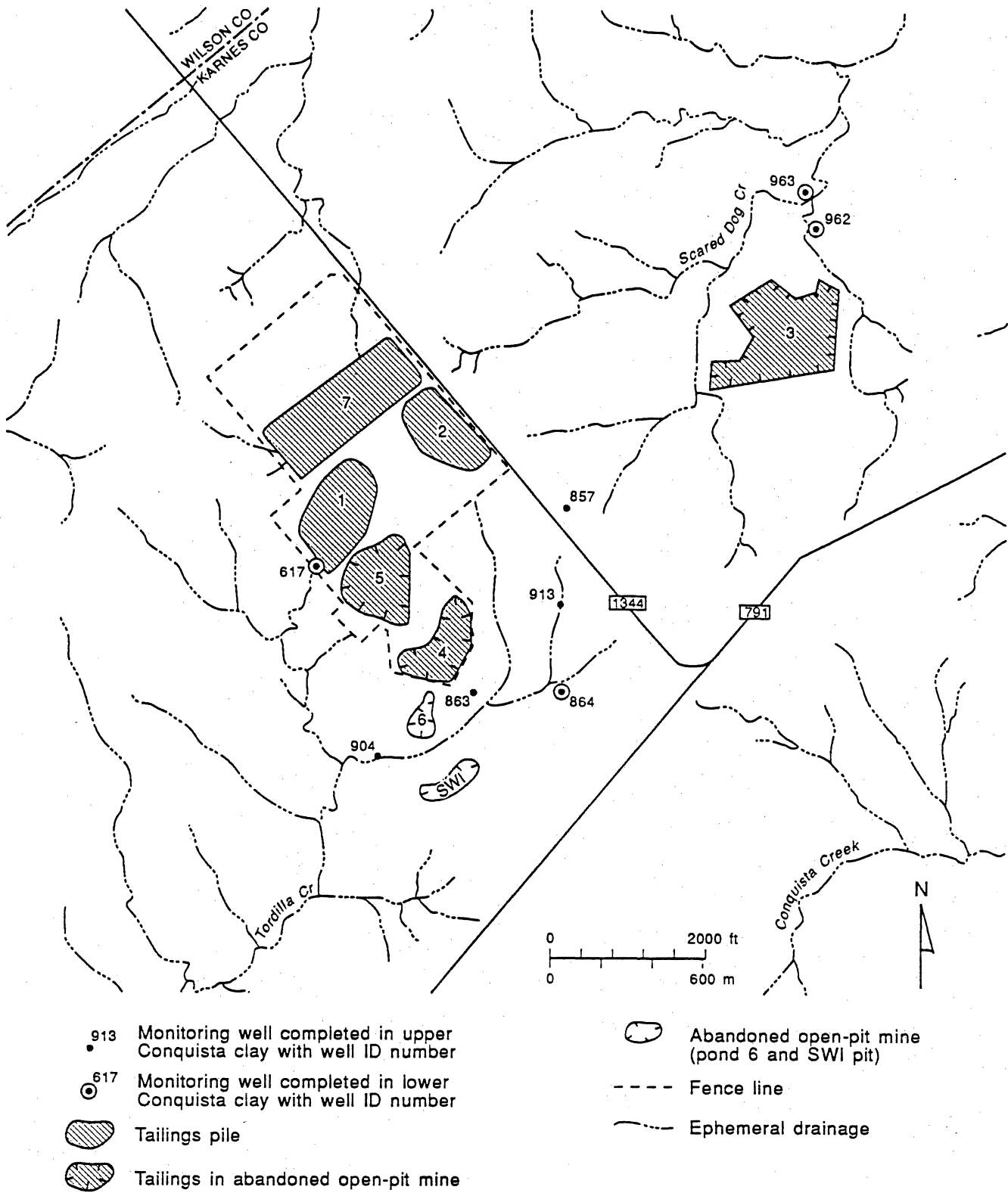
Figure 4.24. Effect of pH on cation trace metal species. Each point is the average cation trace metals in a sample to the same trace metal in the average tailings solution. Samples are from the Deweesville and Conquista sands.



-  Deweesville Sandstone Member outcrop
-  Fence line
-  Ephemeral drainage
- Well No.
-  Ra-226 Monitoring well, Radium-226 (Ra-226) in pCi/L
-  Tailings pile, tailings in abandoned open-pit mine and abandoned open-pit mine

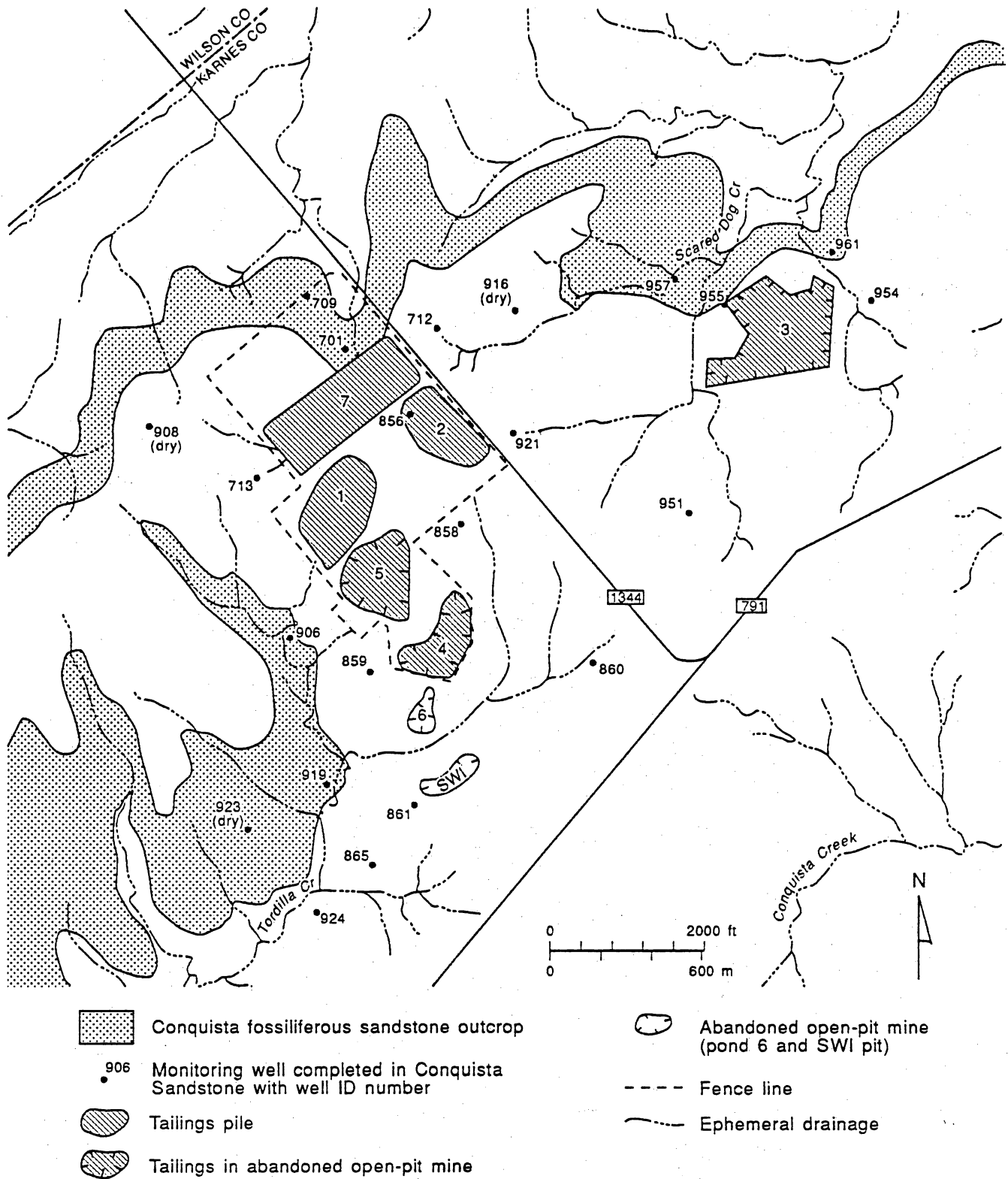
QAa75c

Figure 4.25. Radium (pCi/L) in Deweesville ground waters.



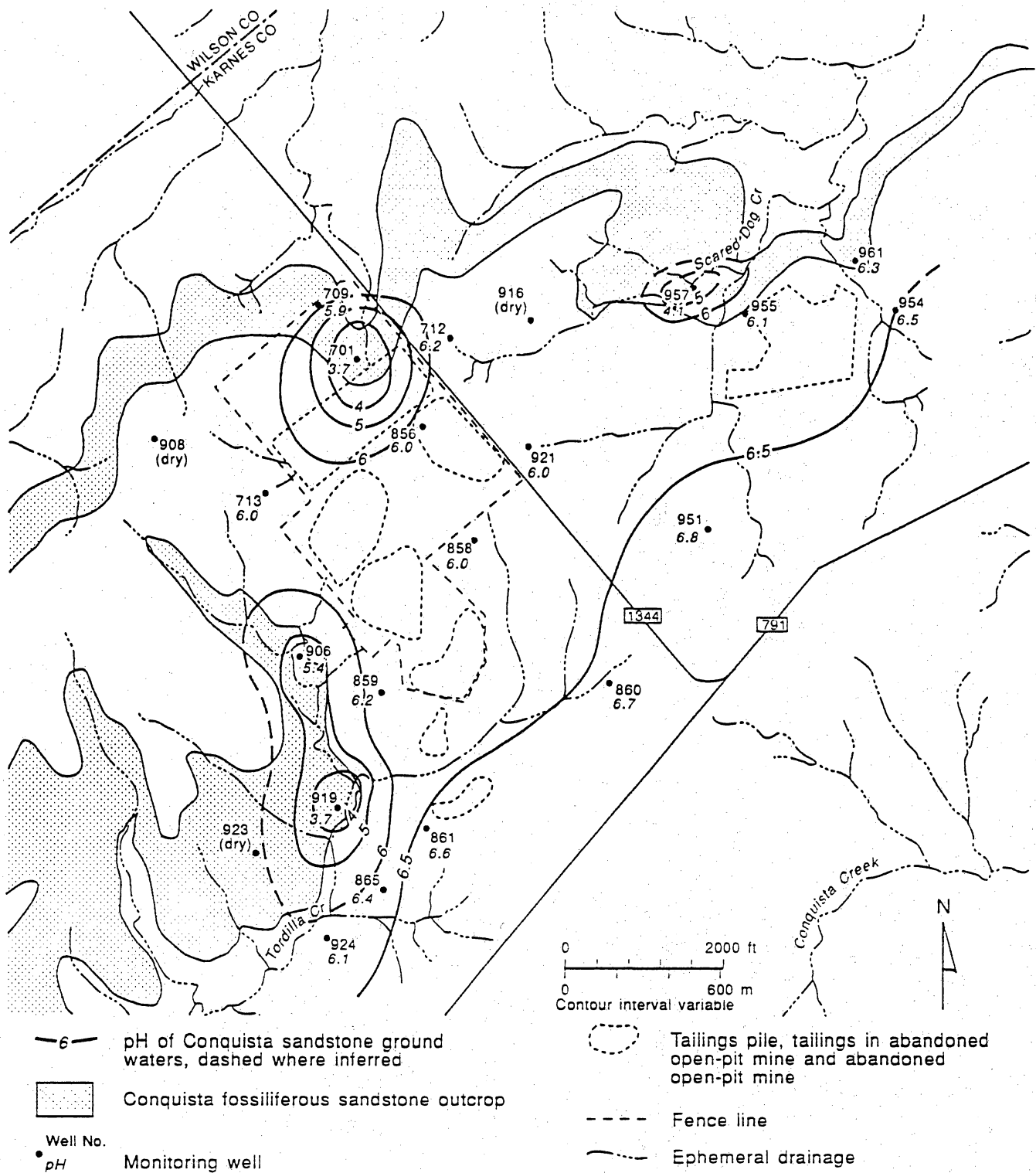
QA20374c

Figure 4.26. Locations of upper and lower Conquista clay monitoring wells.



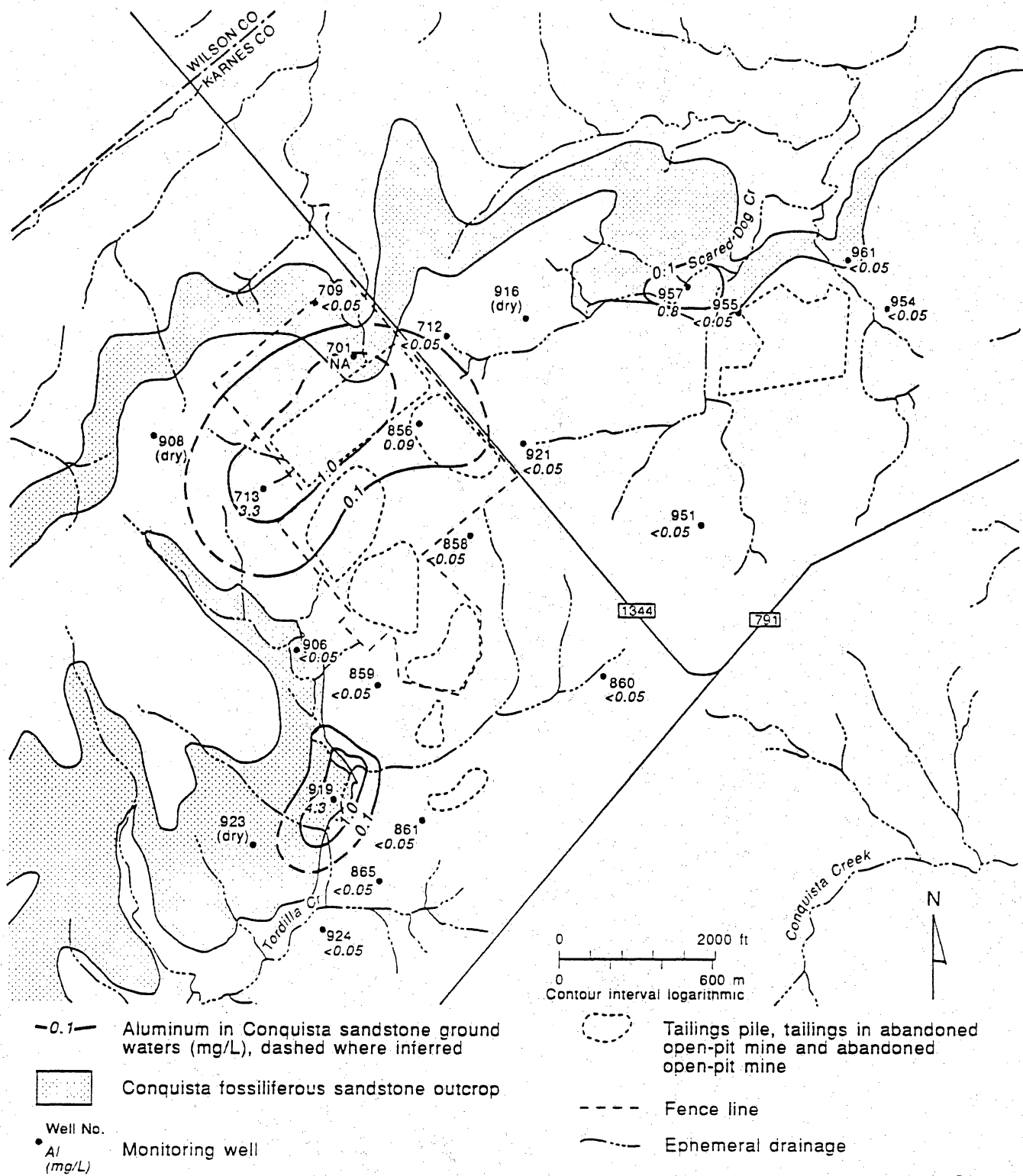
QA20375c

Figure 4.27. Locations of Conquista fossiliferous sandstone monitoring wells.



QAa178c

Figure 4.28. pH in Conquista fossiliferous sandstone ground waters.



QAa181c

Figure 4.29. Aluminum (mg/L) in Conquista fossiliferous sandstone ground waters.

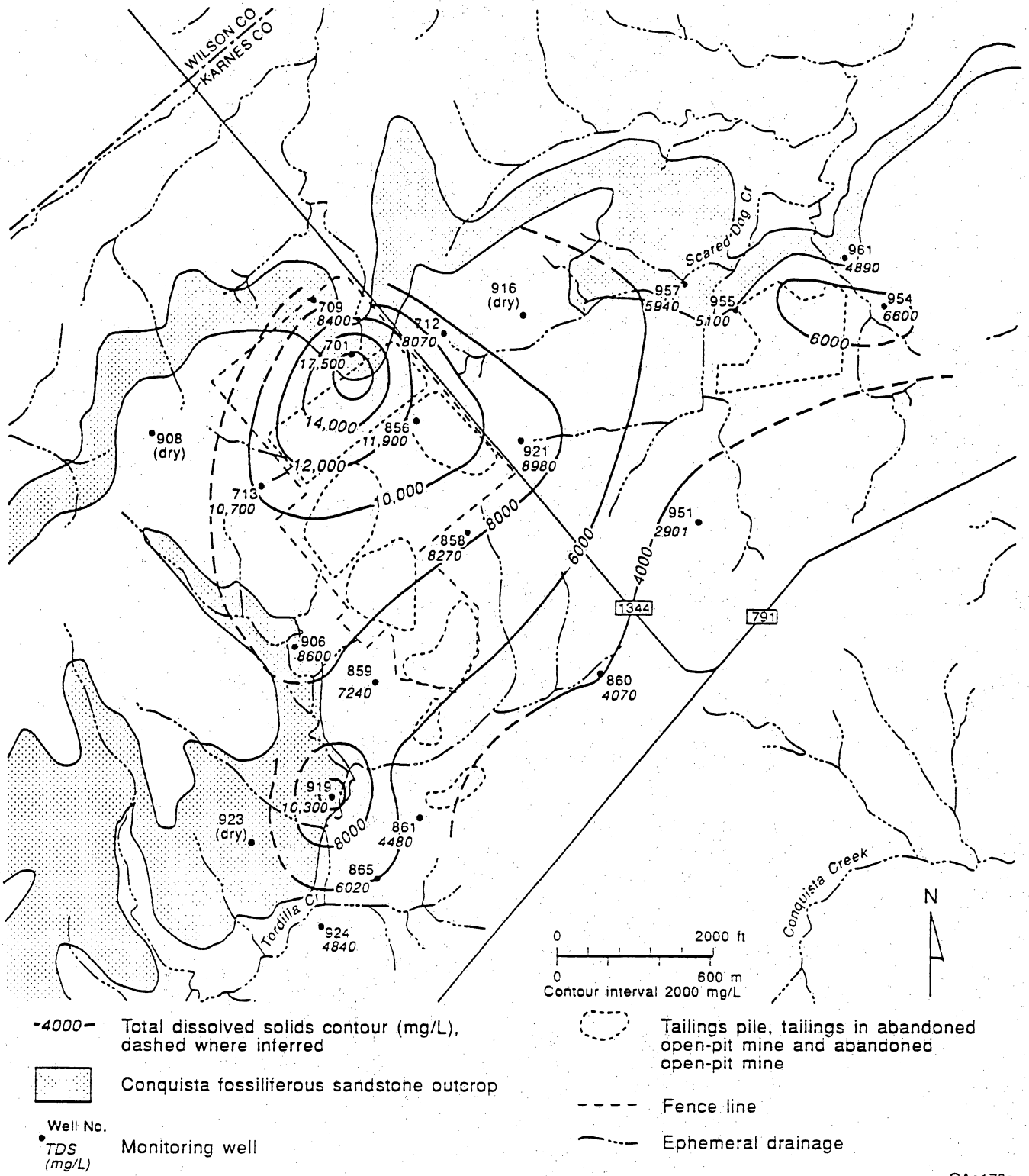
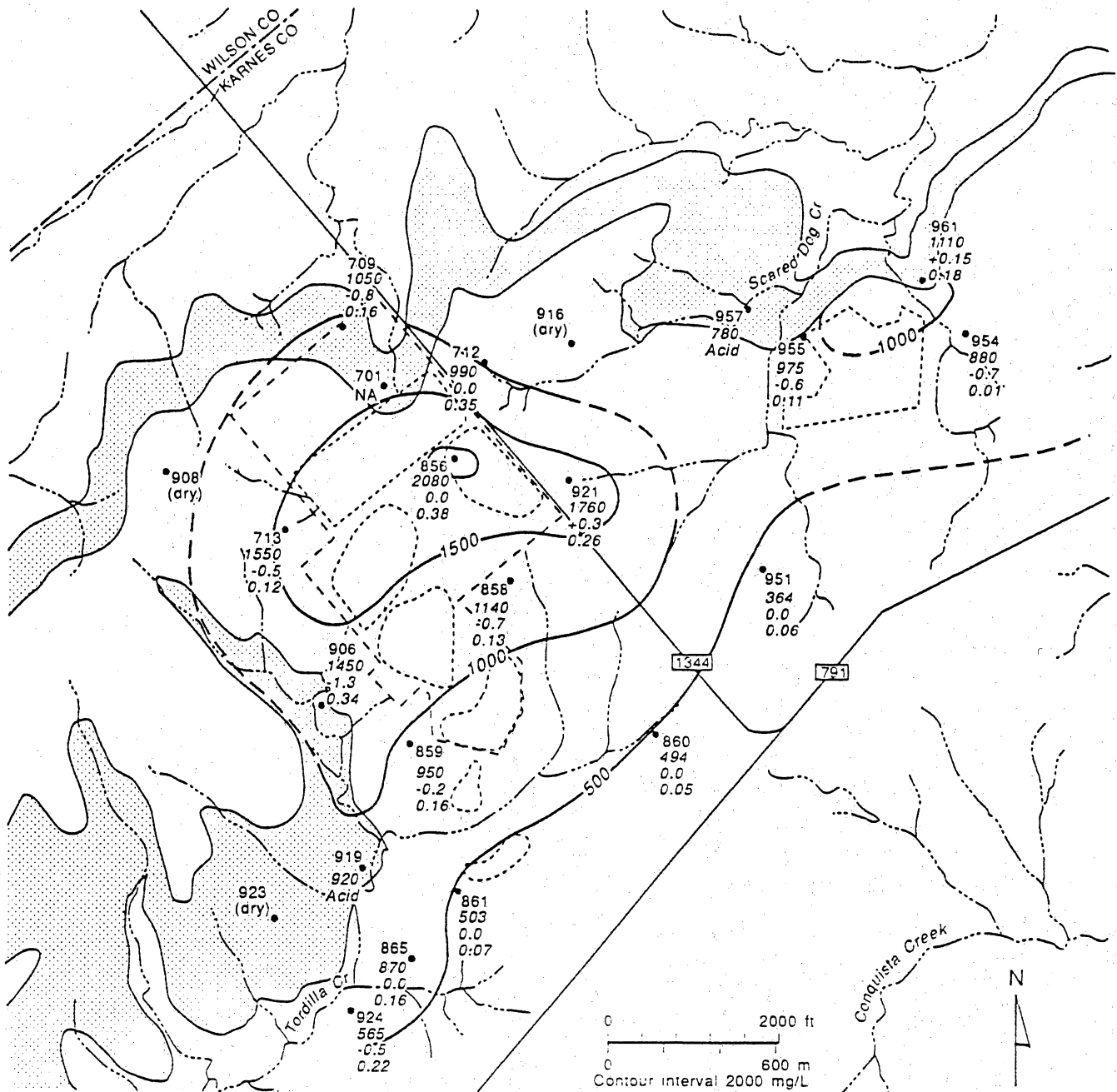


Figure 4.30. Total dissolved solids (mg/L) in Conquista fossiliferous sandstone ground waters.



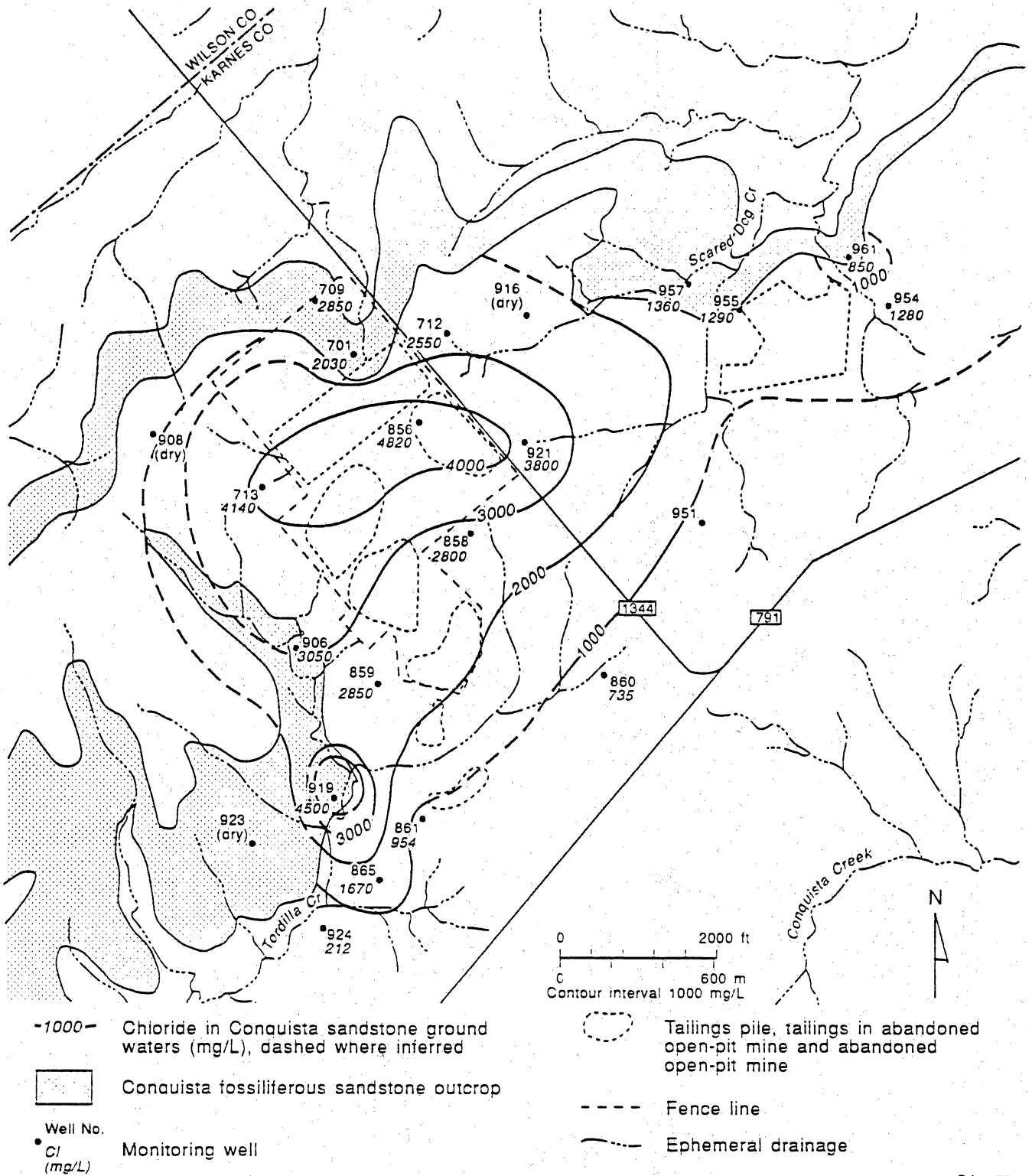
-500- Calcium (mg/L), dashed where inferred
 [Stippled Area] Conquista fossiliferous sandstone outcrop
 • Well No. Monitoring well
 • 364 Calcium (mg/L)
 c.i. Calcite saturation index
 c.06 CO₂ (atmospheres)

0 2000 ft
 0 600 m
 Contour interval 2000 mg/L

[Dashed Line] Tailings pile, tailings in abandoned open-pit mine and abandoned open-pit mine
 [Dashed Line] Fence line
 [Dotted Line] Ephemeral drainage

QAa180c

Figure 4.31. Calcium, calcite saturation, and carbon dioxide partial pressure in Conquista fossiliferous sandstone ground waters.



QAa177c

Figure 4.32. Chloride (mg/L) in Conquista fossiliferous sandstone ground waters.

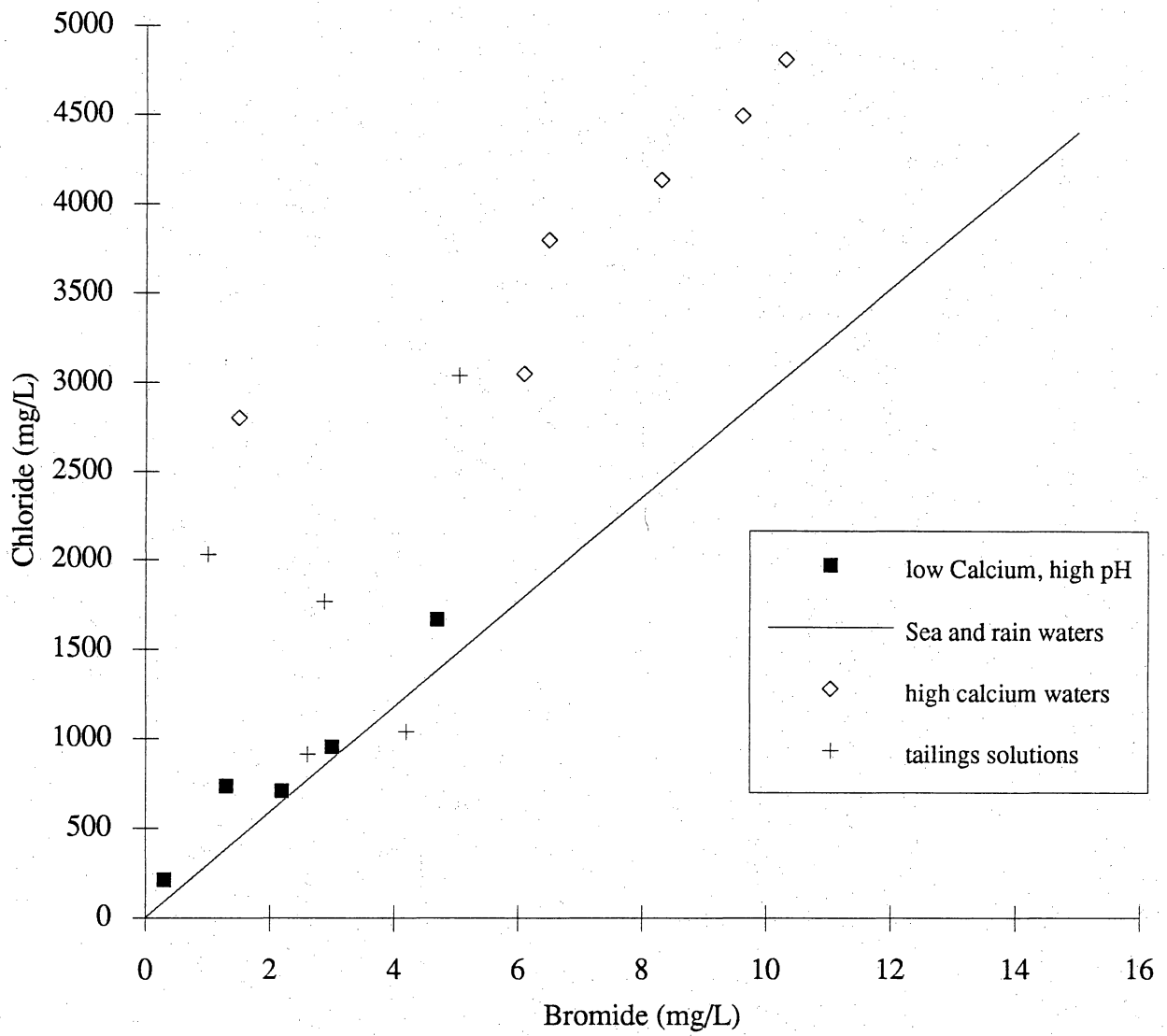
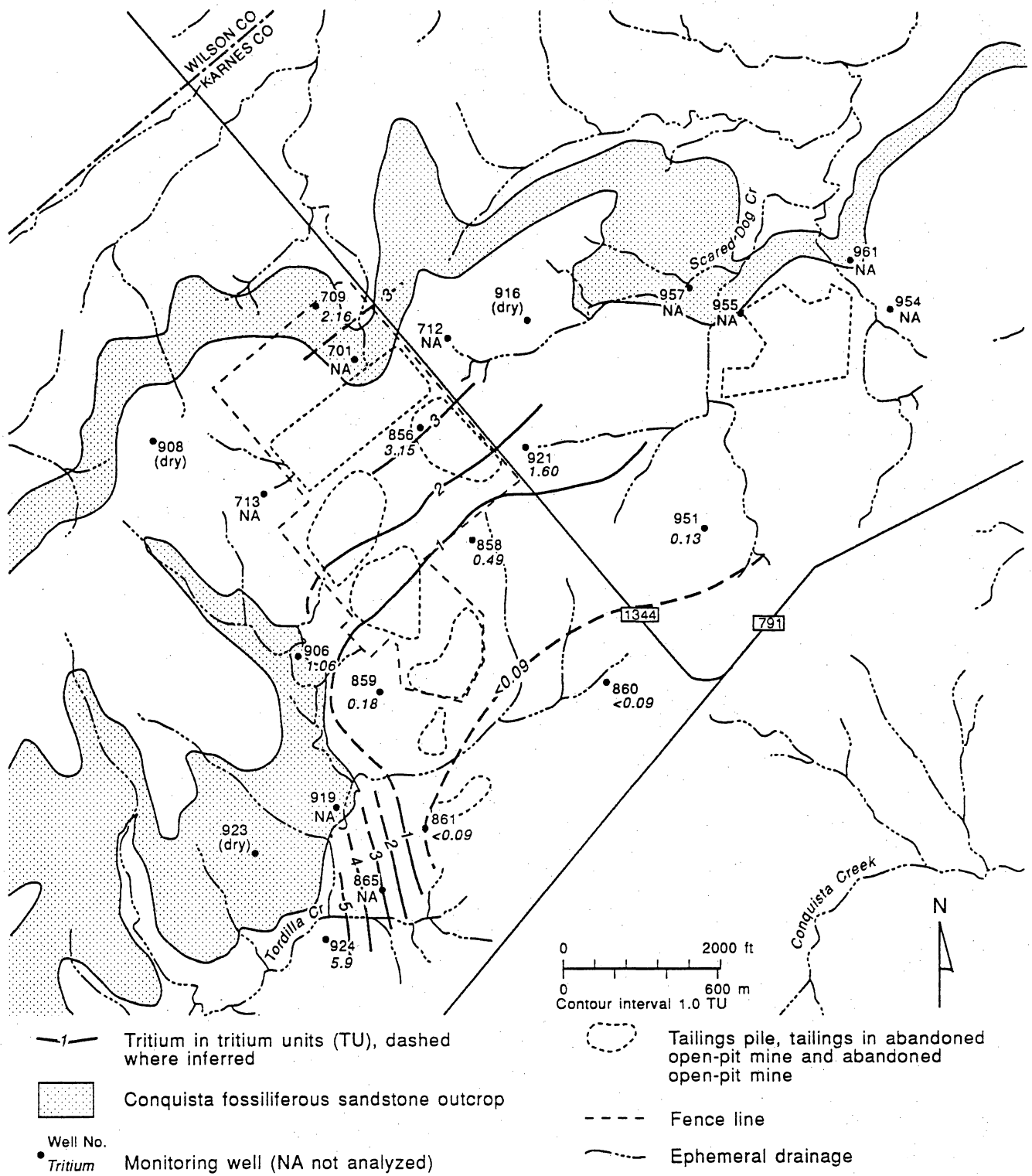
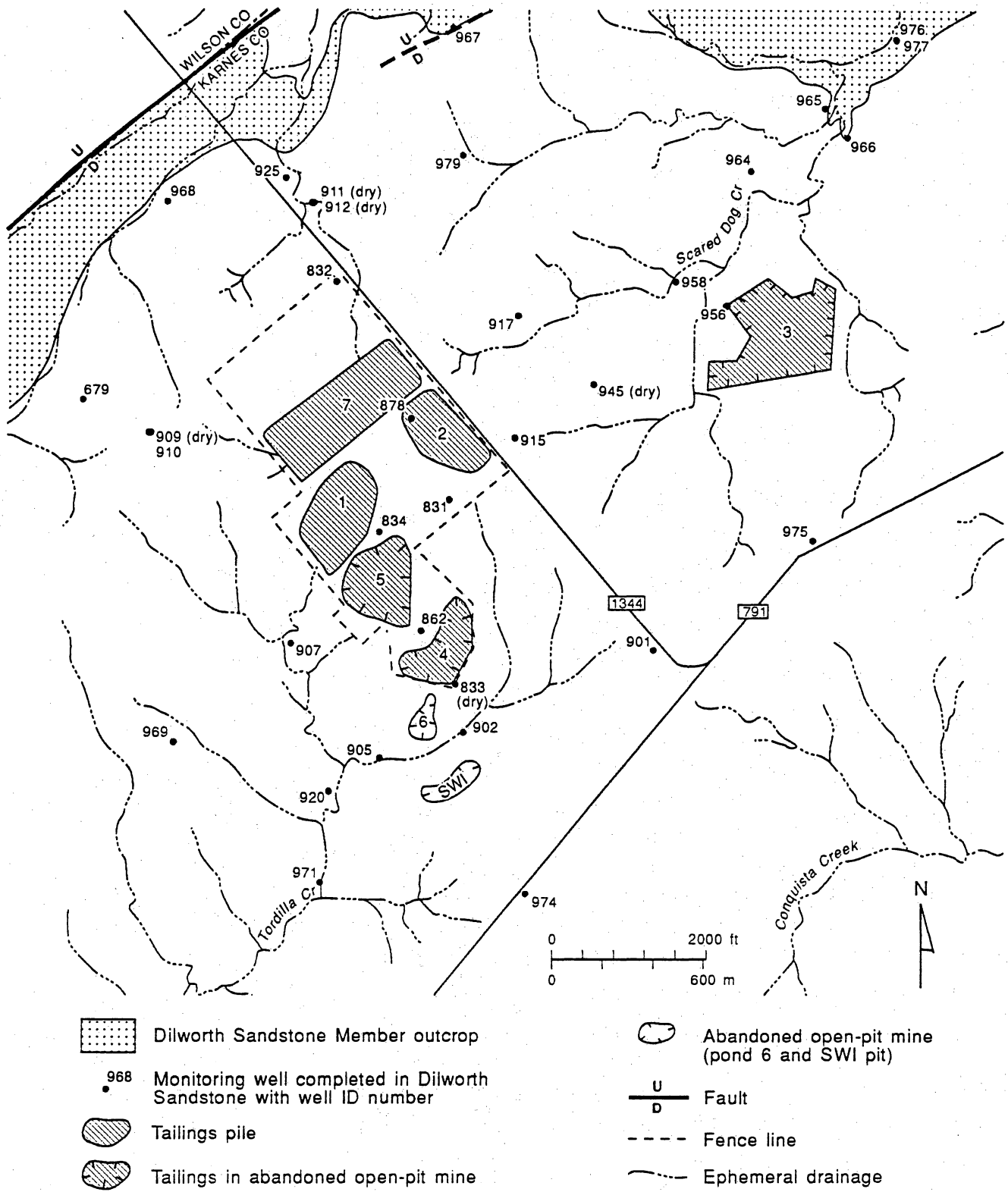


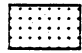
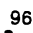



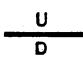
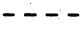
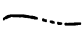
Figure 4.33. Chloride versus bromide in Conquista fossiliferous sandstone ground waters and tailings solutions in pile 7.



QAa203c

Figure 4.34. Tritium in Conquista fossiliferous sandstone ground waters.



-  Dilworth Sandstone Member outcrop
-  968 Monitoring well completed in Dilworth Sandstone with well ID number
-  Tailings pile
-  Tailings in abandoned open-pit mine
-  Abandoned open-pit mine (pond 6 and SWI pit)
-  Fault
-  Fence line
-  Ephemeral drainage

QA20376c

Figure 4.35. Locations of Dilworth Sandstone Member monitoring wells.

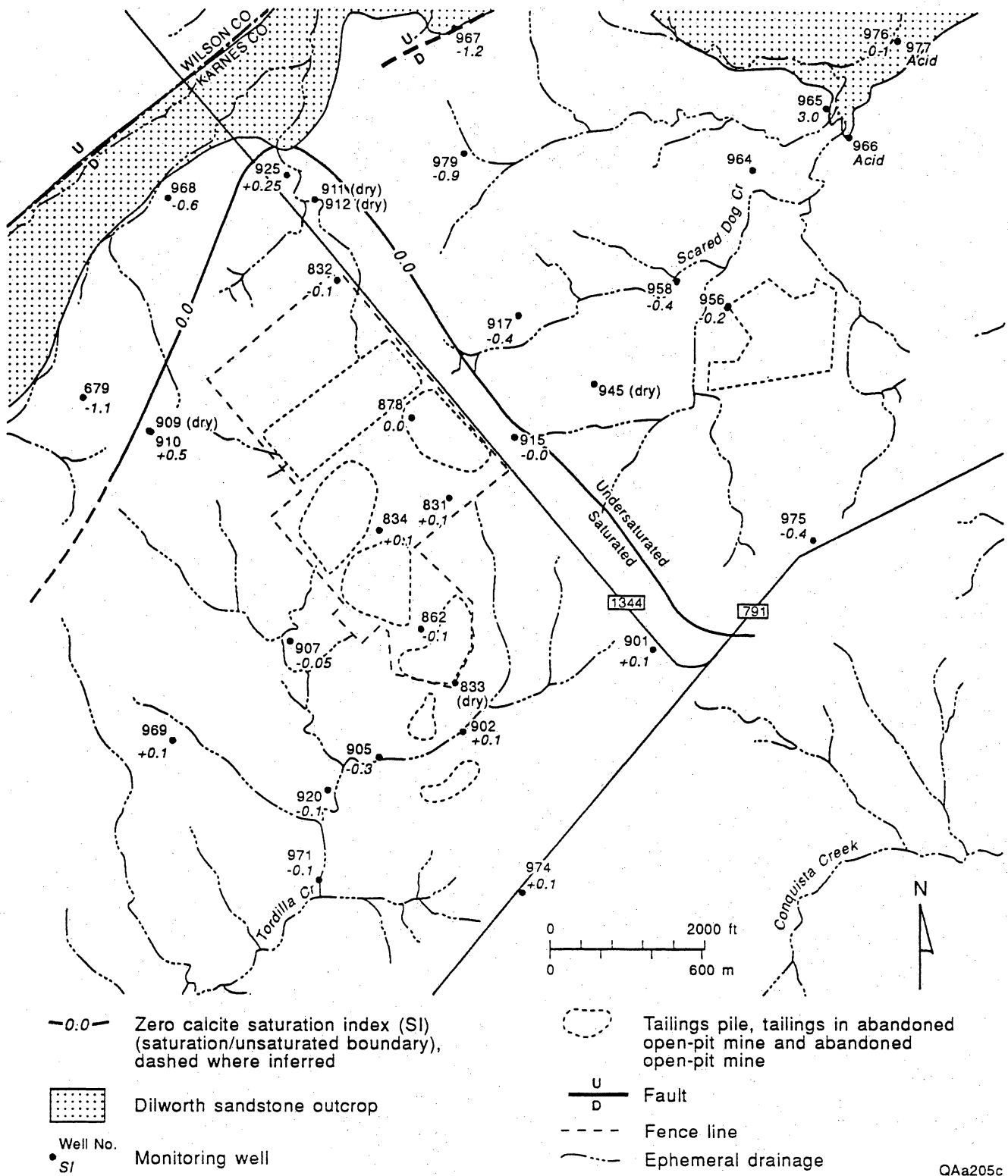


Figure 4.36. Calcite saturation of Dilworth sandstone ground waters.

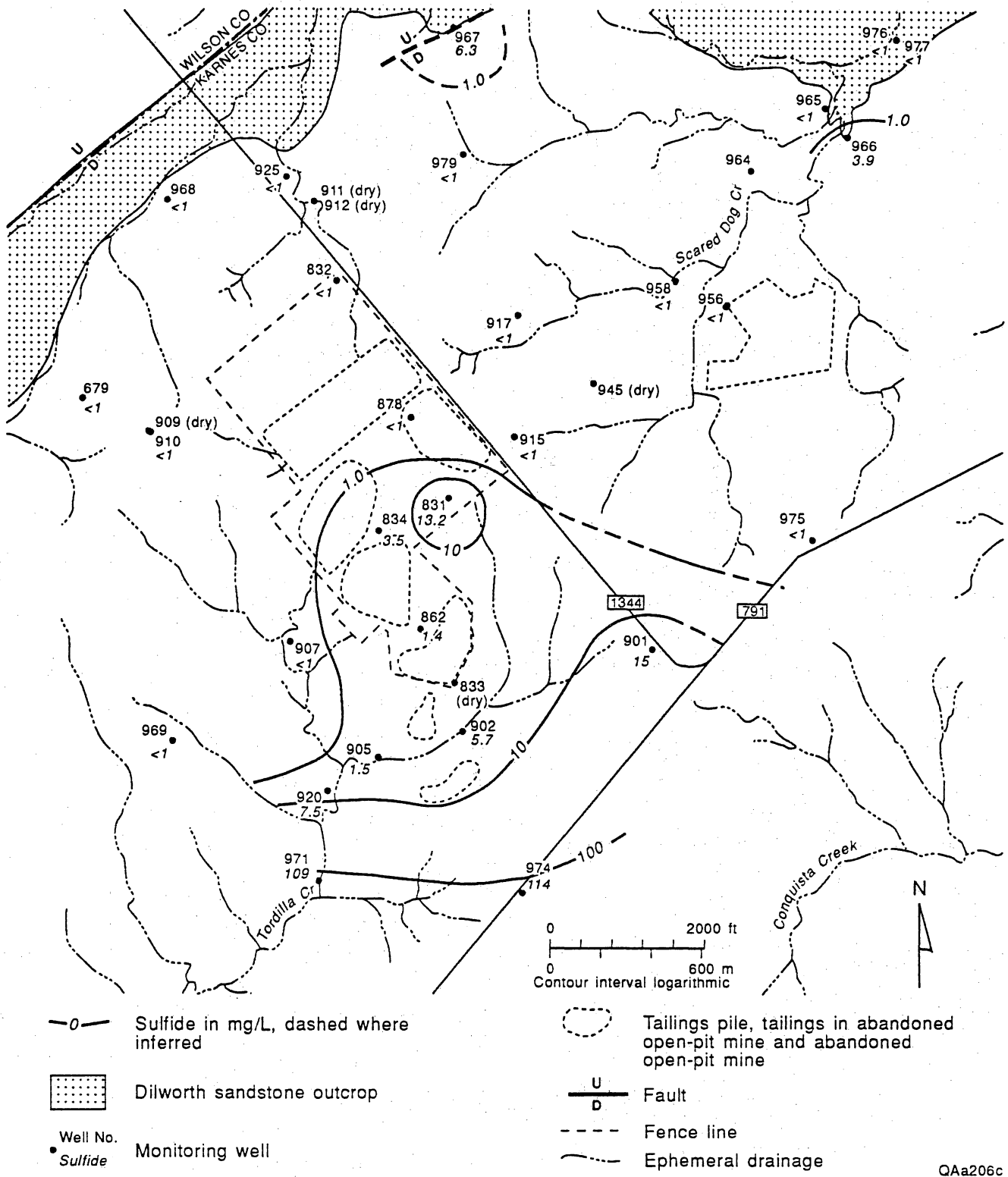
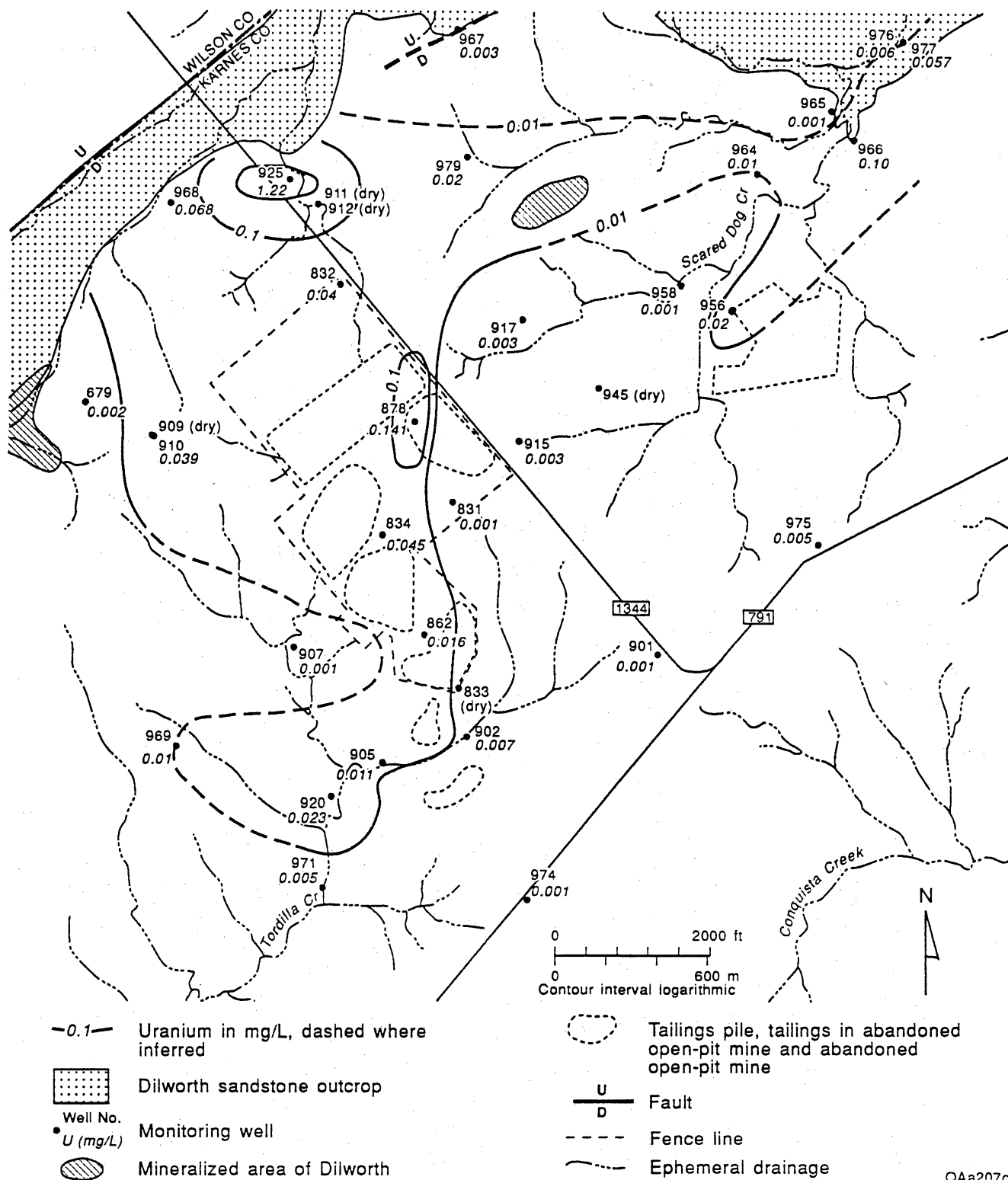
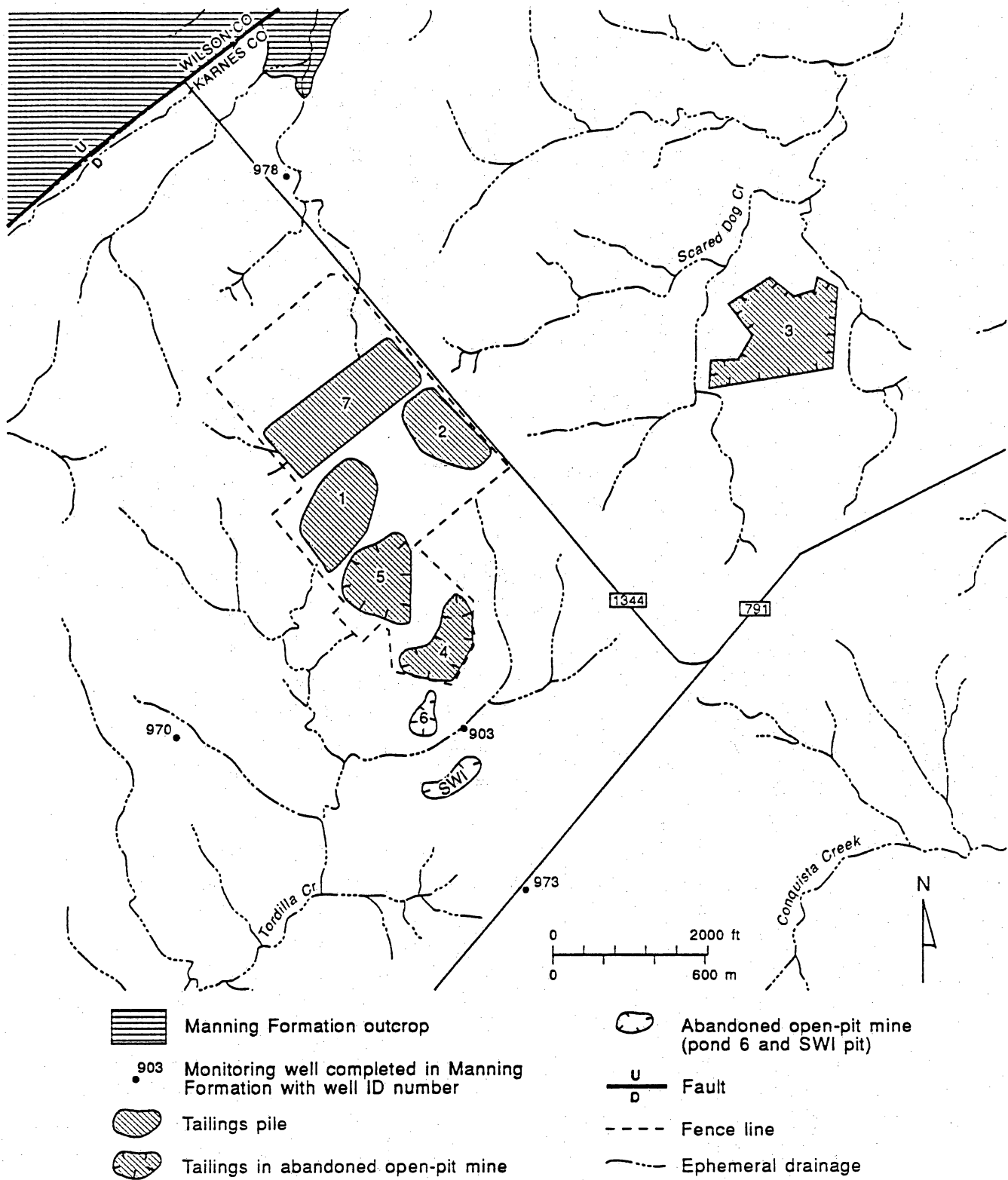


Figure 4.37. Sulfide (mg/L) in Dilworth sandstone ground waters.



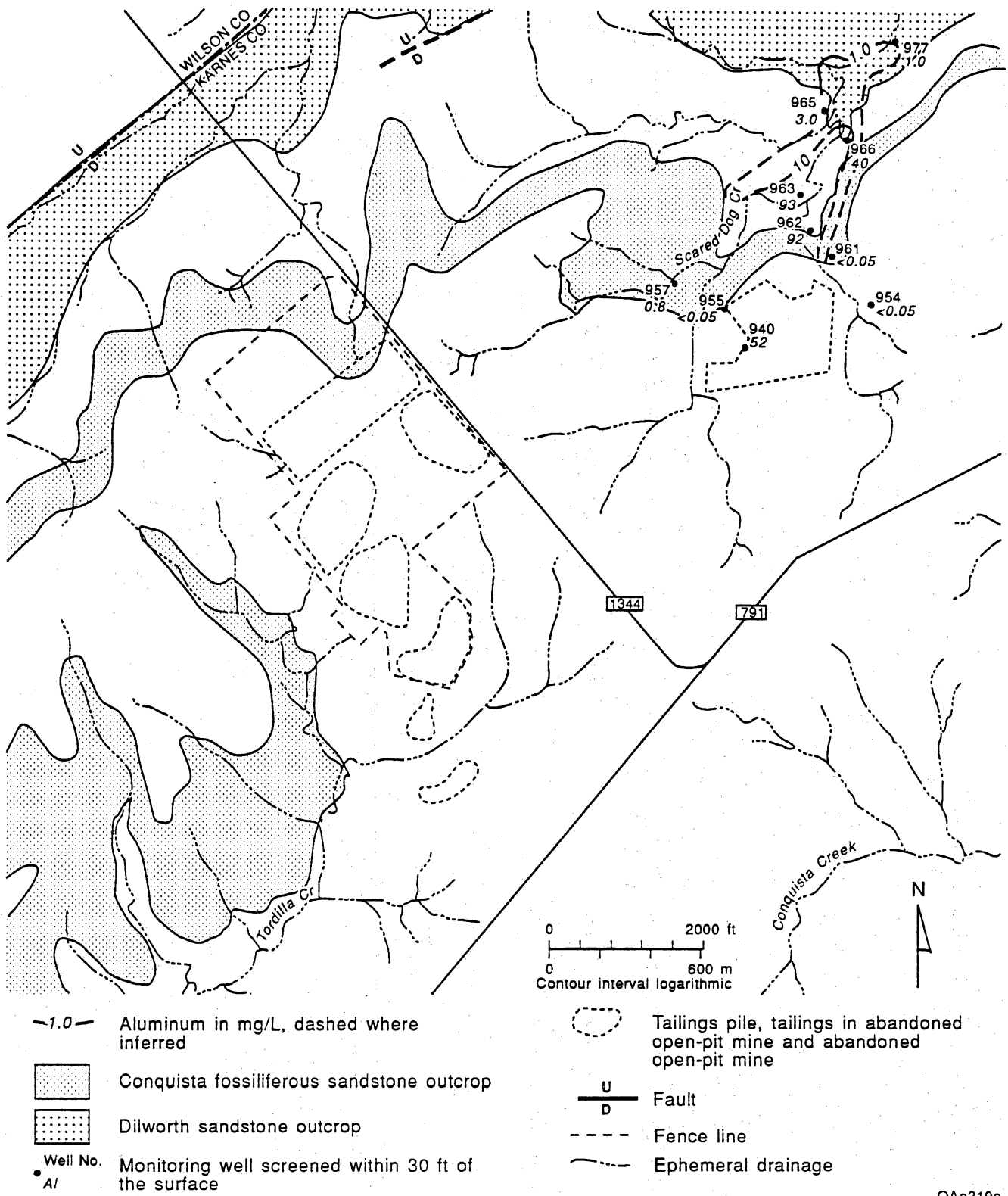
QAa207c

Figure 4.38. Uranium (mg/L) in Dilworth sandstone ground waters.



QA20377c

Figure 4.39. Locations of monitoring wells in Manning Formation.



QAa210c

Figure 4.40. Dilute acidic aluminum sulfate plume along Scared Dog Creek.

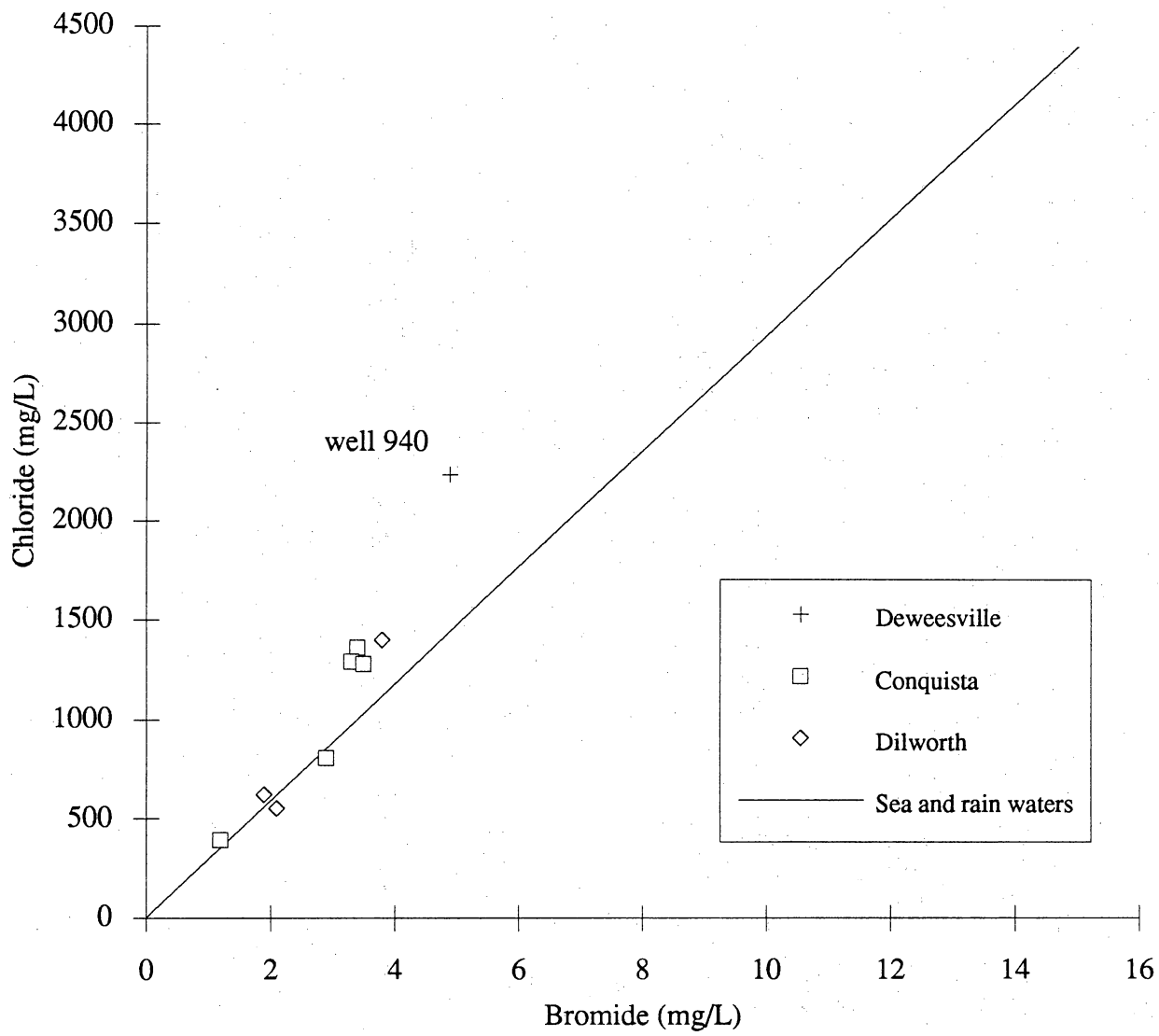


Figure 4.41. Chloride versus bromide in ground waters near tailings pile 3 (eastern area).

Table 4.1. Tailings water chemistry—lysimeter and well data.

Well ID Lith/unit		211 pile 1	212 pile 1	213 pile 1	601 pile 1	221 pile 2	222 pile 2	223 pile 2
Temperature	° C	18.2	18.9	17.5	23.4	18.5	18	-
Conductivity	µmhos/cm	7000	6400	10500	12040	9500	14900	-
pH	-	3.89	4.12	2.96	2.82	3.15	3.1	-
Eh	mvolts	482.1	476.8	486.4		477.2	476	-
TDS	mg/L	8630	7880	14500	16800	12800	22700	5130
Alkalinity	mg/L	-	-	-	-	-	-	-
Al	mg/L	267	238	872	980	640	1390	58
NH4	mg/L	165	70	193	43	587	327	142
Ba	mg/L	0.02	0.04	0	0.01	0.02	0.03	0.04
B	mg/L	2.4	1.95	1.45	2.3	2.25	1.95	2
Br	mg/L	3	3.5	3.1	0.3	2.6	1.9	4.4
Ca	mg/L	470	535	500	383	515	530	550
Cl	mg/L	811	592	2940	641	810	2280	570
F	mg/L	15.6	9.2	29.5	32	24	50.4	7.8
Fe	mg/L	190	422	466	736	362	765	86
Mg	mg/L	132	175	290	257	270	495	110
Mn	mg/L	5.74	16.5	30	25	31	51	35
NO3	mg/L	0	36.2	142	26	0	2.9	0
PO4	mg/L	2.6	0.9	1.2	1.3	3.5	29	4.1
K	mg/L	74	105	80	36	290	420	101
SiO2	mg/L	106	47	117	96.1	119	119	68
Na	mg/L	1020	990	1310	1260	960	1800	525
SO4	mg/L	5450	4950	9420	11200	8230	13900	3030
Sr	mg/L	7.89	5.3	9.1	5.53	12.4	21.8	5.7
Sulfide	mg/L	<0.4	<0.4	<0.4	1.8	<0.4	<0.4	<0.4
Sb	mg/L	<0.05	<0.05	<0.05	0.03	<0.05	<0.05	<0.003
As	mg/L	0.22	<0.12	<0.12	0.01	<0.12	6.5	0.7
Be	mg/L	0.047	0.095	0.227	0.26	0.109	0.232	0.048
Cd	mg/L	0.039	0.072	0.284	0.11	0.231	0.456	0.044
Cr	mg/L	<0.01	<0.05	<0.02	0.01	0.06	0.13	<0.01
Co	mg/L	0.24	0.5	0.9	0.8	0.6	0.95	0.25
Cu	mg/L	0.15	<0.05	0.15	0.1	0.04	0.04	0.11
Cn	mg/L	<0.01	<0.01	0.01	0.01	<0.01	<0.01	<0.04
Pb	mg/L	<0.1	<0.1	<0.1	0.03	<0.1	<0.1	<0.1
Hg	mg/L	<0.0002	<0.0002	<0.0002	0.001	<0.0002	<0.0002	<0.0002
Mo	mg/L	1.8	0.1	0.05	0.05	0.14	0.5	0.3
Ni	mg/L	0.26	0.5	1.1	0.78	0.75	1.25	0.19
Se	mg/L	<0.05	0.125	<0.12	0.235	<0.12	<0.25	<0.05
Ag	mg/L	<0.01	<0.05	<0.05	0.05	<0.05	<0.05	<0.01
Tl	mg/L	0.1	<0.1	<0.2	0.1	<0.2	<0.2	<0.1
Sn	mg/L	<0.05	<0.05	<0.1	0.3	<0.1	<0.1	<0.05
U	mg/L	5.34	11.4	29.7	24.7	1.95	3.99	7
V	mg/L	0.6	0.5	2.6	2.6	1.05	3.3	0.18
Zn	mg/L	1.57	2.4	5.35	3.55	3.8	4.89	0.749
TKN	mg/L	-	-	136	41	433	-	-
TOC	mg/L	28	18	33	14	61	54	-
Gross alpha	pCi/L	677	6600	17900	14251	3160	4900	-
Gross beta	pCi/L	4800	5100	12600	10425	1980	5440	-
Ra-226	pCi/L	252	49.5	170	55.4	268	906	-
Ra-228	pCi/L	-	-	-	0	-	-	-
Tritium	t.u.	-	-	-	8.51	-	-	-
Gypsum SI	-	0.00	0.01	0.01	-0.06	0.04	0.05	-

Table 4.1 (cont.)

602 Well ID pile 2 Lith/unit		241 pile 4	242 pile 4	251 pile 5	252 pile 5	253 pile 5	261 pile 6
23.3 Temperature	° C	18	17	18	-	-	17
16700 Conductivity	µmhos/cm	11100	11100	11100	-	-	9200
3.01 pH	-	3.05	3.78	3.85		3.73	3.55
540.4 Eh	mvolts	567.2	484.6				
23600 TDS	mg/L	2810	12100	15600	6230	8560	5990
- Alkalinity	mg/L	-	-	-	-	-	-
1450 Al	mg/L	630	664	886	0.21	616	58
529 NH4	mg/L	572	464	605	0		10
0.03 Ba	mg/L	0.04	0.03	0.02	0.03	0.03	0.02
2.8 B	mg/L	2.85	2.8	1.3	2.92	2.65	1.75
1.5 Br	mg/L	4.7	6.4	2.8	0.6	4.9	7.4
492 Ca	mg/L	515	515	510	640	455	960
1930 Cl	mg/L	1390	1960	887	1640	844	3340
50 F	mg/L	28.1	30.8	32.2	1.2	40.8	9.8
970 Fe	mg/L	382	528	962	48.4	910	0.56
427 Mg	mg/L	270	270	280	140	290	250
53.3 Mn	mg/L	17	17.2	31	13	37	15
2.7 NO3	mg/L	0	0	71			0
15.1 PO4	mg/L	8.4	4.7	7.8		9.3	5.5
429 K	mg/L	295	125	165	29	190	74
116 SiO2	mg/L	136	70	108	63.1	110	87
1320 Na	mg/L	820	910	720	1110	750	1600
14600 SO4	mg/L	8190	7550	10800	1090	11300	2420
14.9 Sr	mg/L	15.3	12	12.7	6.08	-	12.1
<1 Sulfide	mg/L	<0.4	<0.4	<0.8	-	-	-
<0.03 Sb	mg/L	<0.05	<0.05	<0.05	<0.003	<0.003	<0.050
0.49 As	mg/L	2.1	4.2	4	<0.050	4	<0.120
0.37 Be	mg/L	0.145	0.139	0.144	<0.005	0.112	0.15
0.25 Cd	mg/L	0.176	0.151	0.344	<0.001	0.332	0.067
<0.05 Cr	mg/L	0.13	0.08	0.04	<0.010	0.11	<0.100
1.2 Co	mg/L	0.6	0.85	1.35	0.18	0.85	0.3
<0.05 Cu	mg/L	<0.05	<0.05	<0.05	0.01	0.2	0.02
<0.01 Cn	mg/L	<0.04	<0.04	0.06	-	-	-
<0.05 Pb	mg/L	<0.1	<0.1	<0.1	<0.005	<0.1	<0.100
<0.0002 Hg	mg/L	<0.0002	<0.0002	-	-	-	-
<0.05 Mo	mg/L	0.3	0.2	11.4	3.14	2.25	<0.05
1.3 Ni	mg/L	0.8	1.1	1.7	0.08	1.65	0.32
0.006 Se	mg/L	<0.12	<0.05	<0.12	<0.030	<0.05	0.255
<0.05 Ag	mg/L	<0.05	<0.02	<0.05	<0.010	<0.05	<0.05
<0.1 Tl	mg/L	<0.2	0.4	0.2	<0.050	0.2	<0.2
0.3 Sn	mg/L	<0.1	<0.1	<0.1	<0.010	<0.10	<0.1
0.005 U	mg/L	5.26	16.1	9.33	5.73	6.57	30.5
3.9 V	mg/L	1.15	0.7	3.9	<0.010	1.3	<0.100
5.65 Zn	mg/L	3.45	3.36	6.7	0.087	8.3	0.94
410 TKN	mg/L	-	362	-	-	-	7
7 TOC	mg/L	74	63	105	-	-	7
3000 Gross alpha	pCi/L	3930	10400	8040	-	-	14400
2060 Gross beta	pCi/L	4270	6950	5280	-	-	9240
147 Ra-226	pCi/L	-	116	537	-	-	856
50 Ra-228	pCi/L	-	-	-	-	-	-
- Tritium	t.u.	-	-	-	-	-	-
0.03 Gypsum SI	-	0.04	0.00	0.07	-	-	0.01

Table 4.1 (cont.)

Well ID		271	272	273	607
Lith/unit		pile 7	pile 7	pile 7	pile 7
Temperature	° C	-	18.5	19.5	24.2
Conductivity	µmhos/cm	-	10000	16100	11530
pH	-	4	2.86	3.44	2.93
Eh	mvolts	-	-	-	540.1
TDS	mg/L	12700	23100	18300	11900
Alkalinity	mg/L	-	-	-	-
Al	mg/L	56	1500	460	725
NH4	mg/L	263	1020	992	435
Ba	mg/L	0.02	0.04	0.02	0.03
B	mg/L	2.6	2.88	5.05	4.2
Br	mg/L	0.5	0.3	5	1
Ca	mg/L	420	490	505	510
Cl	mg/L	912	1770	3040	1040
F	mg/L	10.9	58.3	36.6	27.02
Fe	mg/L	84	680	1480	544
Mg	mg/L	88	390	445	214
Mn	mg/L	18.5	40	71	22.6
NO3	mg/L	5	1	0	1
PO4	mg/L	2.1	26.6	4.1	12.7
K	mg/L	58	220	175	238
SiO2	mg/L	60	128	102	133
Na	mg/L	540	1040	2130	832
SO4	mg/L	3420	15700	10700	7390
Sr	mg/L	6.82	17.2	14.9	13.7
Sulfide	mg/L	<0.8	<0.8	<0.8	4.3
Sb	mg/L	<0.050	<0.050	<0.050	<0.030
As	mg/L	0.8	5.2	1.8	5.7
Be	mg/L	0.022	0.195	0.175	0.09
Cd	mg/L	0.052	0.492	0.116	0.42
Cr	mg/L	0.01	0.18	<0.020	0.1
Co	mg/L	0.3	0.95	1.25	0.6
Cu	mg/L	0.2	0.1	0.1	0.05
Cn	mg/L	<0.050	<0.040	<0.040	<0.010
Pb	mg/L	<0.100	<0.100	<0.100	<0.006
Hg	mg/L	-	-	-	<0.0002
Mo	mg/L	0.32	1.1	0.2	1.22
Ni	mg/L	0.22	1.3	1.1	1.06
Se	mg/L	<0.050	<0.120	<0.050	<0.005
Ag	mg/L	<0.020	<0.050	<0.050	<0.050
Tl	mg/L	<0.200	0.4	0.6	0.1
Sn	mg/L	<0.050	<0.100	<0.100	0.3
U	mg/L	0.081	4.66	1.53	0.001
V	mg/L	0.07	3	1	1.8
Zn	mg/L	0.704	6.05	8.6	3
TKN	mg/L	-	22200	-	120
TOC	mg/L	-	130	141	6
Gross alpha	pCi/L	388	2960	610	2830
Gross beta	pCi/L	291	3240	935	1610
Ra-226	pCi/L	-	279	34.2	281
Ra-228	pCi/L	-	-	-	2.5
Tritium	t.u.	-	-	4.78	-
Gypsum SI	-	-0.06	0.07	0.02	-0.02

Table 4.2. Major constituents of tailings solutions expressed as neutral salts. Data are in chemical equivalent percent, not weight percent. Each column is an average of data from table 4.1.

	Pile 1	Pile 2	Pile 4	Pile 5	Pile 7	overall
Al ₂ SO ₄	30	33	34	39	28	31
(NH ₄) ₂ SO ₄	4	9	13	13	15	11
FeSO ₄	11	9	10	17	12	11
CaSO ₄	14	15	12	10	12	13
MgSO ₄	9	11	10	9	9	10
K ₂ SO ₄	1	3	3	2	2	2
NaSO ₄	13	7	0	2	1	5
NaCl	14	16	18	10	20	17
Total	96%	103%	100%	102%	99%	100%

Table 4.3. Comparison of an average tailings solution to an average shale. Enrichment/ depletion factor computed as the ratio of the element to aluminum in the solution, divided by the ratio of the element to aluminum in the shale. Average shale value from Krauskopf (1967).

	Average shale (ppm)	Average tailings solution (mg/L)	Enrichment / Depletion Factor		
			less than shale	approx. equal to shale	greater than shale
Al	80000	715		1.000	
Ba	580	0.026	0.005		
B	100	2.6		2.9	
Br	6	2.9			54
Ca	25000	493		2.2	
Cl	160	1401			980
F	500	30		6.8	
Fe	47000	598		1.4	
Mg	13400	275		2.3	
Mn	850	31		4.1	
PO4	2604	8		0.4	
K	23000	188		0.9	
SiO2	171000	102	0.07		
Na	13400	1058		8.8	
SO4	660	9114			1546
Sr	450	12		2.9	
Sb	1.5	<0.03		<2.2	
As	6.6	2.23			38
Be	3	0.15		5.6	
Cd	0.3	0.22			82
Cr	100	<0.06	<0.07		
Co	20	0.76		4.3	
Cu	57	0.08	0.16		
Pb	20	<0.01	<0.06		
Hg	0.4	<0.0002	<0.10		
Mo	2	1.25			70
Ni	95	0.94		1.1	
Se	0.6	<0.02		<3.7	
Ag	0.1	<0.01			<11
Tl	1	<0.14			<16
Sn	6	<0.06		<1.1	
U	3.2	7.98			279
V	130	1.73		1.5	
Zn	80	4.26		6.0	
Ra-226	2.6 pCi/kg	304.000 pCi/L			13092

Table 4.4. Tailings solution saturation indices for selected solids. Positive values indicate oversaturated solutions, zero values are at saturation, and negative values are undersaturated. Indices computed using SOLMINEQ.88.

Monitoring We	211	212	213	221	222	241	242	251	261	271	272	273	601	602	607	Average
AgCl	-0.1	-0.2	-	-	-	-1.1	-	-	-	0.0	-	-0.9	-0.2	-0.6	-0.4	-0.4
albite	-3.8	-0.3	-3.9	-2.9	-2.5	-3.2	-1.1	-0.3	-2.0	-2.1	-3.8	-1.6	-4.1	-2.9	-3.4	-2.5
alunite	8.1	10.2	3.8	5.2	5.9	4.6	8.6	9.4	4.6	7.1	4.1	6.7	3.5	5.9	4.7	6.2
amorph. silica	0.0	-0.4	0.1	0.1	0.1	0.1	-0.2	0.0	-0.1	-0.3	0.1	0.0	-0.1	0.0	0.7	0.0
barite	0.5	0.7	-	0.5	0.7	0.8	0.7	0.6	0.1	0.4	0.9	0.4	0.2	0.6	0.6	0.6
Fe(OH)3 amorp	-1.5	-0.2	-3.9	-3.5	-3.5	-2.3	-1.4	-	-	-	-	-	-3.8	-2.2	-10.1	-3.2
FePO4	1.8	1.9	0.5	1.3	2.4	2.9	2.0	-	-	-	-	-	0.6	3.2	-4.6	1.2
goethite	2.9	4.1	0.5	0.9	0.9	2.1	3.0	-	-	-	-	-	0.5	2.1	-5.8	1.1
gypsum	0.0	0.0	0.0	0.0	0.1	0.0	0.0	0.1	0.0	-0.1	0.1	0.0	-0.1	0.0	0.0	0.0
K-clinoptilolite	6.3	4.6	0.5	2.6	3.6	2.4	4.9	7.5	1.6	2.8	0.8	3.2	-2.7	2.0	1.3	2.8
K-feldspar	1.5	1.6	-1.6	-0.5	-0.1	-0.7	1.1	2.0	-0.5	0.4	-1.5	0.1	-2.8	-0.6	-1.1	-0.2
PbSO4	-2.4	-2.2	-	-2.4	-	-2.1	-	-	-	-2.7	-	-2.8	-2.0	-1.8	-	-2.3
smectites	3.0	3.9	-2.5	-1.4	-1.0	-2.0	2.3	3.5	-0.8	1.8	-3.0	0.4	-3.0	-1.4	-1.9	-0.1
SrSO4	-0.3	-0.5	-0.3	-0.1	0.2	0.0	-0.1	0.0	-0.4	-0.3	0.1	0.0	-0.4	0.0	-0.1	-0.1
ZnSO4	-11.1	-10.7	-11.0	-10.7	-10.6	-10.8	-10.9	-10.0	-11.0	-11.6	-10.0	-10.7	-10.4	-10.3	-10.6	-10.7

Table 4.5. Computer-simulated neutralization of an aluminum sulfate solution by calcium carbonate (calcite). System is closed to carbon dioxide loss.

	Units	Initial solution	Boehmite (Al(OH) ₃) saturated	Calcite dissolution to gypsum saturation	Further calcite dissolution	Calcite saturated
pH	-	3.8	3.25	3.34	3.84	5.89
TDS	mg/L	4504	4497	5335	4130	5013
Al	mg/L	714	706	455	9.24	0.0001
SO ₄	mg/L	3808	3805	3806	1658	1367
Ca	mg/L	0	0	558	670	872
TIC	mg/L	0	0	167	470	569
HCO ₃	mg/L	0	0	1.073	9.66	915
H ₂ CO ₃	mg/L	0	0	862	2418	2007
PCO ₂	atmospheres	0	0	0.416	1.1517	0.959
Saturation Indices; oversaturated (+), saturated (0), undersaturated (-).						
boehmite	-	1.67	0.00	0.05	0.00	0.01
gypsum	-	under	under	0.04	0.05	0.03
calcite	-	under	under	-5.78	-4.18	-0.06
Net precipitation (-) of dissolution (+).						
boehmite	mg/L	-	-25	-745	-2035	-2009
gypsum	mg/L	-	0	0	-3854	-3854
calcite	mg/L	-	0	1390	3910	3103

Table 4.6. Computer-simulated neutralization of an aluminum sulfate solution by a bicarbonate solution. System is closed to carbon dioxide loss.

		Aluminum sulfate solution 1	Sodium bicarbonate solution 2	Mixes of solutions 1 and 2.		
				10 % soln. 1	5 % soln. 1	1 % soln. 1
pH	-	3.29	6.2	3.71	4.67	6.04
TDS	mg/L	6179	3493	3958	3811	3713
Na	mg/L	0	375	337	356	371
Al	mg/L	703	0	31.9	0.045	0.00004
SO4	mg/L	4983	2180	2461	2320	2208
Ca	mg/L	492	670	651	659	669
TIC	mg/L	0	109	104	103	108
HCO3	mg/L	0	268	1.6	14.2	234
H2CO3	mg/L	0	268	536	517	318
PCO2	atmos.	0.00	0.14	0.26	0.25	0.15
Saturation indices; oversaturated (+), saturated (0), undersaturated (-).						
boehmite	-	0.02	under	0.01	0.02	0.02
gypsum	-	-0.03	0.08	0.10	0.10	0.09
calcite	-	under	-0.44	-5.17	-3.26	-0.77

Table 4.7. Water chemistry for the Deweesville sandstone aquifer (May 1991 data).

Well ID unit		625 Dew/ Conq	835 1986 data	853 Dew	854 Dew	879 Dew	676 Dew/ Conq	651 Dew/ Conq	678 Dew/ Conq
Temperature	°C	26.4	-	23.9	24.2	24.2	23.8	24.7	23.6
Conductivity	µmhos/cm	15540	-	16900	16710	14340	12370	7460	3320
pH	-	3.29	3.23	3.31	3.53	3.79	4.07	5.43	5.48
Eh	mvolts	546.4	-	492	449.9	453.9	477.1	468.5	346.2
TDS	mg/L	18300	16770	13800	13100	12300	8900	5880	2700
alkalinity	mg/L	-	-	-	-	-	-	132	37
Al	mg/L	796	441	109	34.6	24.3	18.6	0.79	0.48
NH4	mg/L	185	500	0.2	0.2	1.5	0.2	2.3	0.2
Ba	mg/L	0.02	-	0.03	0.03	0.04	0.02	0.02	0.01
B	mg/L	1.8	-	1.78	2.23	2.37	1.3	1.29	0.73
Br	mg/L	1	-	10.8	10.7	4.4	7.3	0.8	0.6
Ca	mg/L	494	499	1750	1480	1240	1120	765	317
Cl	mg/L	1740	1400	7000	6750	4380	3750	1480	158
F	mg/L	10.5	-	7.2	4.3	11.2	6	0.7	0.9
Fe	mg/L	458	1170	0.24	0.26	42.5	0.57	0.46	1.38
Mg	mg/L	498	295	270	334	560	128	101	57
Mn	mg/L	73.3	45.4	18	15.5	41.6	3.28	3.88	2.89
NO3	mg/L	1.3	0	8.9	17.7	1.3	30.1	1.3	5.8
PO4	mg/L	13.6	-	0.1	0.1	0.5	0.1	0.1	0.7
K	mg/L	203	243	76	107	136	49	66	44
SiO2	mg/L	169	-	102	98.5	102	88.8	55.1	78.4
Na	mg/L	2270	1000	2070	2210	1520	1640	837	355
Sr	mg/L	11.5	-	11.3	19.1	15.7	8.16	7.33	2.53
SO4	mg/L	11100	9710	1820	1980	2490	1900	2000	1560
Sulfide	mg/L	<1	<1	<1	<1	10.7	<1	<1	2.1
Sb	mg/L	0.03	-	0.03	0.03	0.03	0.03	<0.003	<0.003
As	mg/L	0.16	<0.01	<0.01	<0.01	0.29	<0.01	<0.01	0.25
Be	mg/L	0.38	-	0.145	0.077	0.19	0.046	<0.005	0.014
Cd	mg/L	0.25	0	0.14	0.04	0.01	0.02	0.03	<0.001
Cr	mg/L	0.1	-	<0.01	<0.01	<0.01	0.05	<0.01	<0.01
Co	mg/L	0.4	-	0.59	0.19	0.49	0.1	0.04	<0.03
Cu	mg/L	0.1	-	0.03	0.02	<0.01	0.02	<0.01	<0.01
Cn	mg/L	0.01	-	<0.01	<0.01	<0.01	<0.01	<0.01	<0.01
Pb	mg/L	0.03	-	<0.005	0.03	<0.005	<0.005	<0.005	<0.005
Hg	mg/L	0.001	-	<0.0002	<0.0002	<0.0002	<0.0002	<0.0002	<0.0002
Mo	mg/L	0.05	4.83	<0.01	<0.01	0.18	0.13	<0.01	0.82
Ni	mg/L	0.79	-	0.52	0.23	0.81	0.11	<0.04	0.04
Se	mg/L	0.033	0.005	0.144	0.45	0.005	0.199	0.005	0.005
Ag	mg/L	0.1	-	<0.01	<0.01	<0.01	<0.01	<0.01	<0.01
Tl	mg/L	0.1	-	<0.01	<0.01	<0.01	0.1	<0.01	<0.01
Sn	mg/L	0.3	-	<0.05	<0.05	<0.05	<0.05	<0.05	<0.05
U	mg/L	0.009	15.1	5.7	0.875	0.012	25.9	<0.001	<0.001
V	mg/L	3	3	0.1	<0.01	<0.01	0.2	<0.01	<0.01
Zn	mg/L	3.1	-	1.86	0.845	1.83	0.272	0.208	0.11
TKN	mg/L	128	-	1	1	2	1	2	1
TOC	mg/L	6	-	3	2	5	2	2	2
NOX	mg/L	0.31	-	2.07	3.99	1.31	6.81	0.3	1.28
Gross alpha	pCi/L	4880	-	3030	576	30.3	11115	516	14.2
Gross beta	pCi/L	3050	-	2550	408	107	7265	358	60.3
Ra-226	pCi/L	33.5	-	40.7	30	69.5	82	14	8.1
Ra-228	pCi/L	7.6	-	13.7	6.7	8.9	4.4	17.2	1.5
Tritium	t.u.	-	-	0.67	4.02	0.17	3.09	-	-
Gypsum SI	-	0.02	-	-0.01	-0.03	0.03	-0.01	-0.01	-0.28
Calcite SI	-	-	-	-	-	-	-	-1.40	-2.22
PCO2	bars	-	-	-	-	-	-	0.46	0.12

Table 4.7 (cont.)

Well ID		914	918	922	677	836	852	851	668	667
unit		1990	Dew/ Conq	Dew	Dew/ Conq	Dew/ Conq	Dew	Dew	Dew CONOCO	Dew CONOCO
Temperature	°C	25	26.5	25.3	25.2	27.2	24.6	23.5	27.8	27.6
Conductivity	µmhos/cm	8500	5520	680	6450	16190	6920	5710	4760	4520
pH	-	6.32	5.3	5.8	6.2	6.83	6.27	6.4	6.63	6.65
Eh	mvolts	-	421.4	482.1	434.5	453	428.6	438.3	340.6	313.7
TDS	mg/L	6830	4870	5640	5210	18800	5020	4540	3310	3120
alkalinity	mg/L	1061	42	81	268	1036	78	379	250	252
Al	mg/L	0.4	0.14	<0.05	<0.05	<0.05	<0.05	<0.05	<0.05	<0.05
NH4	mg/L	0.2	0.2	0.4	0.6	1.9	0.1	0.1	0.1	0.3
Ba	mg/L	0.05	0.02	0.02	0.02	0.02	0.08	0.04	0.03	0.06
B	mg/L	1.58	0.88	1.63	1.14	2.53	0.45	0.51	0.56	1
Br	mg/L	1.3	1.8	2	2.2	2.5	3.2	4.1	2.5	2.5
Ca	mg/L	1370	660	785	670	660	655	615	405	335
Cl	mg/L	1950	635	1130	1010	2000	1960	1800	944	785
F	mg/L	0.4	0.7	0.2	1.1	2	0.3	0.8	0.6	0.6
Fe	mg/L	0.87	0.11	0.27	0.08	0.03	0.03	0.03	0.19	0.45
Mg	mg/L	120	96.1	159	85.1	93.3	81.6	60	45.1	31.8
Mn	mg/L	0.4	1.5	6.8	4.56	1.82	0.03	0.01	0.78	0.21
NO3	mg/L	<1	2.2	3.1	1.8	4.4	50.5	9.3	3.5	4.9
PO4	mg/L	0.4	0.1	0.3	0.1	2.6	0.3	0.4	0.1	0.1
K	mg/L	19	51	102	50	39	43	45	29	43
SiO2	mg/L	118	79.3	50.2	39.4	54.3	73	66.7	49	58.4
Na	mg/L	730	879	775	657	5320	591	670	583	678
Sr	mg/L	9.16	6.8	9.2	5.29	7.06	4.99	4.17	2.82	2.54
SO4	mg/L	1660	2560	2500	2180	9400	856	477	930	1043
Sulfide	mg/L	0.3	3.1	<1	<1	<1	<1	<1	1.4	<1
Sb	mg/L	<0.05	0.03	<0.003	<0.003	0.03	0.006	<0.003	<0.003	<0.003
As	mg/L	0.05	0.01	<0.01	<0.01	1.73	0.06	0.07	<0.01	0.02
Be	mg/L	0.006	0.009	<0.005	<0.005	<0.005	<0.005	<0.005	<0.005	<0.005
Cd	mg/L	0.022	0.01	<0.001	<0.001	0.002	<0.001	<0.001	<0.001	<0.001
Cr	mg/L	<0.05	0.05	<0.01	<0.01	0.05	<0.01	<0.01	<0.01	<0.01
Co	mg/L	<0.03	<0.03	<0.03	<0.03	<0.03	<0.03	<0.03	<0.03	<0.03
Cu	mg/L	<0.01	<0.01	<0.01	<0.01	<0.01	0.02	<0.01	<0.01	0.01
Cn	mg/L	<0.01	<0.01	<0.01	<0.01	<0.01	<0.01	<0.01	<0.01	<0.01
Pb	mg/L	<0.1	0.005	0.005	0.03	0.03	0.005	0.005	<0.005	<0.005
Hg	mg/L	<0.0002	<0.0002	<0.0002	<0.0002	<0.0002	<0.0002	<0.0002	<0.0002	<0.0002
Mo	mg/L	<0.01	0.09	<0.01	0.38	54.4	0.89	0.12	<0.01	<0.01
Ni	mg/L	<0.04	0.05	<0.04	<0.04	<0.04	<0.04	<0.04	<0.04	<0.04
Se	mg/L	<0.005	0.024	0.005	0.005	0.035	0.278	0.086	<0.005	<0.005
Ag	mg/L	<0.05	<0.01	<0.01	<0.01	<0.01	<0.01	<0.01	<0.01	<0.01
Tl	mg/L	<0.1	<0.01	<0.01	<0.01	0.1	<0.01	<0.01	<0.01	<0.01
Sn	mg/L	<0.05	<0.05	<0.05	<0.05	0.3	<0.05	<0.05	<0.05	<0.05
U	mg/L	25.4	9.3	<0.001	<0.001	0.005	0.265	1.8	0.017	0.015
V	mg/L	<0.1	0.05	<0.01	<0.01	0.21	0.02	0.02	<0.01	<0.01
Zn	mg/L	<0.005	0.103	0.006	0.041	0.013	0.006	0.006	0.301	<0.005
TKN	mg/L	<1	1	1	1	3	<1	<1	<1	<1
TOC	mg/L	40	4	2	3	16	<1	<1	2	<1
NOX	mg/L	0.07	0.48	0.67	0.46	0.98	11.4	2.08	0.83	1.16
Gross alpha	pCi/L	11800	5550	0	0	3200	111	1290	0	12.3
Gross beta	pCi/L	10500	2530	69.1	45.3	1760	110	633	47.7	64.3
Ra-226	pCi/L	15.1	134	2.8	8.6	25.1	1.7	3.4	2.2	2.5
Ra-228	pCi/L	6.5	4.9	0	6.2	6.2	2.4	0.4	1.1	0
Tritium	t.u.	-	-	0.66	0.72	-	<0.09	<0.09	<0.09	<0.09
Gypsum SI	-	-	0.04	0.07	0.00	-	-0.46	-0.59	-0.41	-0.44
Calcite SI	-	-	-2.12	-1.24	-0.37	-	-1.33	0.03	-0.04	-0.10
PCO2	bars	-	0.19	0.12	0.16	-	0.04	0.14	0.06	0.06

Table 4.7 (cont.)

952 dry	855 dry	799 dry?
------------	------------	-------------

Table 4.8. Normalized metals in Deweesville ground waters.

DEWEESVILLE SANDSTONE			625	835	853	854	879	676	651	678	914	918	922	677	836	852	851	668	667
Well ID	AVE. TAIL	LLD	RATIOS TO AVERAGE TAILINGS SOLUTION METALS																
pH			3.29	3.23	3.31	3.53	3.79	4.07	5.43	5.48	6.32	5.30	5.80	6.20	6.83	6.27	6.40	6.63	6.65
MAJOR METAL RATIOS																			
Al	714	0.05	1.11	0.62	0.15	0.05	0.03	0.03	0.00	0.00	0.00	0.00	0.00	0.00	0.00	0.00	0.00	0.00	0.00
Fe	598	0.01	0.64	1.64	0.00	0.00	0.06	0.00	0.00	0.00	0.00	0.00	0.00	0.00	0.00	0.00	0.00	0.00	0.00
Mn	31	0.01	0.10	0.06	0.03	0.02	0.06	0.00	0.01	0.00	0.00	0.00	0.01	0.01	0.00	0.00	0.00	0.00	0.00
CATION TRACE METAL RATIOS																			
Be	0.15	0.005	2.50	-	0.93	0.48	1.23	0.27	0.00	0.06	0.01	0.03	0.00	0.00	0.00	0.00	0.00	0.00	0.00
Cd	0.22	0.001	1.13	-	0.63	0.18	0.04	0.09	0.13	0.00	0.10	0.04	0.00	0.00	0.00	0.00	0.00	0.00	0.00
Co	0.76	0.03	0.49	-	0.74	0.21	0.61	0.09	0.01	0.00	0.00	0.00	0.00	0.00	0.00	0.00	0.00	0.00	0.00
Cu	0.08	0.01	1.13	-	0.25	0.13	0.00	0.13	0.00	0.00	0.00	0.00	0.00	0.00	0.00	0.13	0.00	0.00	0.00
Ni	0.94	0.04	0.80	-	0.51	0.20	0.82	0.07	0.00	0.00	0.00	0.01	0.00	0.00	0.00	0.00	0.00	0.00	0.00
Zn	4.26	0.005	0.73	-	0.44	0.20	0.43	0.06	0.05	0.02	0.00	0.02	0.00	0.01	0.00	0.00	0.00	0.07	0.00
AVERAGE			1.13	-	0.58	0.23	0.52	0.12	0.03	0.01	0.02	0.02	0.00	0.00	0.00	0.02	0.00	0.01	0.00
ANION TRACE METAL RATIOS																			
As	2.23	0.01	0.07	0.00	0.00	0.00	0.13	0.00	0.00	0.11	0.02	0.00	0.00	0.00	0.77	0.02	0.03	0.00	0.00
Cr	0.06	0.01	1.50	-	0.00	0.00	0.00	0.67	0.00	0.00	0.00	0.67	0.00	0.00	0.67	0.00	0.00	0.00	0.00
Mo	1.25	0.01	0.03	3.86	0.00	0.00	0.14	0.10	0.00	0.65	0.00	0.06	0.00	0.30	43.51	0.70	0.09	0.00	0.00
V	1.73	0.01	1.73	1.73	0.05	0.00	0.00	0.11	0.00	0.00	0.00	0.02	0.00	0.00	0.12	0.01	0.01	0.00	0.00
Se	0.02	0.005	1.40	0.00	6.95	22.25	0.00	9.70	0.00	0.00	0.00	0.95	0.00	0.00	1.50	13.65	4.05	0.00	0.00
AVERAGE			0.95	1.40	1.40	4.45	0.05	2.11	0.00	0.15	0.00	0.34	0.00	0.06	9.31	2.88	0.83	0.00	0.00
U	8	0.001	0.00	1.89	0.71	0.11	0.00	3.24	0.00	0.00	3.17	1.16	0.00	0.00	0.00	0.03	0.22	0.00	0.00
Ra-226	304	1	0.11	-	0.13	0.10	0.23	0.27	0.04	0.02	0.05	0.44	0.01	0.03	0.08	0.00	0.01	0.00	0.00

Table 4.9. Trace metals in waters associated with uranium mines.

	Sickenius #5	Galea #3	Butler #6	Butler #3	Units
pH	7.7	7.5	7.6	7.5	-
Total solids	2452	1685	1975	3033	mg/L
Suspended solids	10	6	5	29	mg/L
Nitrate	0.5	0.5	0.5	0.5	mg/L
Bicarbonate	84.7	89.1	82.6	84.4	mg/L
Chloride	309	181	163	178	mg/L
Sulfate	1230	867	1101	1842	mg/L
Arsenic	.63	.14	<0.01	0.01	mg/L
Barium	0.044	0.049	0.064	0.046	mg/L
Boron	1.5	0.96	0.76	0.64	mg/L
Cadmium	0.012	0.01	0.01	0.011	mg/L
Copper	0.011	0.009	0.007	0.007	mg/L
Chromium	0.007	0.007	0.006	0.007	mg/L
Lead	0.044	0.041	0.026	0.033	mg/L
Manganese	0.143	0.322	0.134	0.126	mg/L
Mercury	<0.0002	<0.0002	<0.0002	<0.0002	mg/L
Molybdenum	23.7	2.6	1.1	0.48	mg/L
Nickel	0.086	0.072	0.077	0.075	mg/L
Selenium	0.007	0.057	0.053	0.013	mg/L
Silver	0.005	0.006	0.006	0.006	mg/L
Zinc	0.028	0.028	0.032	0.014	mg/L

Table 4.10. Water chemistry for upper Conquista clay (May 1991 data).

Well ID		863	913	904	857
Lith/unit		upper	upper top	Qal/upper	upper
Temperature	° C	25.5	25.1	23.4	24.9
Conductivity	µmhos/cm	12250	10940	18780	3080
pH	-	3.94	3.57	3.78	6.7
Eh	mvolts	433	417.3	509.3	458.3
TDS	mg/L	2410	8770	14000	1840
Alkalinity	mg/L	-	-	-	440
Al	mg/L	30	16.8	6.06	<0.05
NH4	mg/L	0.8	0.2	0.1	0.1
Ba	mg/L	0.03	0.02	0.03	0.03
B	mg/L	2.19	1.38	1.74	0.47
Br	mg/L	8.4	7.7	12.6	1
Ca	mg/L	905	1600	1600	180
Cl	mg/L	3750	3600	6200	600
F	mg/L	8.5	3	2.1	1.6
Fe	mg/L	2.16	0.09	0.03	0.03
Mg	mg/L	214	164	344	23.6
Mn	mg/L	10.8	6.24	8.82	0.11
NO3	mg/L	17.7	58.9	4	11.1
PO4	mg/L	0.1	0.1	0.1	0.1
K	mg/L	112	106	98	28
SiO2	mg/L	63.7	82.5	89.4	60.1
Na	mg/L	1540	1450	2120	450
SO4	mg/L	2150	1600	1650	235
Sr	mg/L	9.65	11.6	22.1	1.41
Sulfide	mg/L	<1	19.2	<1	4.6
Sb	mg/L	<0.03	<0.03	<0.03	<0.03
As	mg/L	<0.01	<0.01	<0.01	0.03
Be	mg/L	0.14	0.045	0.039	0.005
Cd	mg/L	0.04	0.056	0.05	<0.001
Cr	mg/L	<0.05	<0.05	<0.05	<0.01
Co	mg/L	0.21	0.15	0.11	<0.03
Cu	mg/L	0.03	0.02	0.02	<0.01
Cn	mg/L	<0.01	<0.01	<0.01	<0.01
Pb	mg/L	0.009	0.005	0.05	<0.005
Hg	mg/L	0	0	0	0
Mo	mg/L	<0.01	<0.01	<0.01	0.03
Ni	mg/L	0.24	0.14	0.15	0.04
Se	mg/L	0.076	0.63	0.116	0.024
Ag	mg/L	<0.01	<0.01	<0.01	<0.01
Tl	mg/L	<0.01	<0.01	0.1	<0.01
Sn	mg/L	<0.05	<0.05	<0.05	<0.05
U	mg/L	0.265	2.8	0.36	0.517
V	mg/L	<0.01	<0.01	0.05	0.08
Zn	mg/L	1.14	0.588	0.377	0.007
TKN	mg/L	1	1	1	1
TOC	mg/L	5	2	1	1
NOX	mg/L	4	13.3	0.9	2.53
Gross alpha	pCi/L	871	1710	2912	328
Gross beta	pCi/L	771	844	1862	172
Ra-226	pCi/L	16	116	110	0.9
Ra-228	pCi/L	11.8	24.2	7	5.1
Tritium	t.u.	<0.09	-	-	<0.09
Gypsum SI	-	-0.05	0.02	-0.05	-1.16
Calcite SI	-	-	-	-	0.01
Pco2	bars	-	-	-	0.09

Table 4.11. Normalized metals in ground waters of Conquista clays.

CONQUISTA CLAYS - RATIOS TO AVERAGE TAILINGS SOLUTION METALS									
Well ID	AVE.	LLD	upper Conquista clay				lower Conquista clay		
			863	913	904	857	617	864	663
pH	TAIL		3.94	3.57	3.78	6.70	6.16	6.49	7.06
MAJOR METAL RATIOS									
Al	714	0.05	-	0.02	0.01	0.00	0.00	0.00	0.00
Fe	598	0.01	-	0.00	0.00	0.00	0.00	0.00	0.00
Mn	31	0.01	-	0.20	0.28	0.00	0.04	0.07	0.00
TRACE CATION METAL RATIOS									
Be	0.15	0.005	-	0.27	0.23	0.00	0.00	0.00	0.00
Cd	0.22	0.001	-	0.25	0.22	0.00	0.04	0.04	0.00
Co	0.76	0.03	-	0.16	0.11	0.00	0.00	0.00	0.00
Cu	0.08	0.01	-	0.13	0.13	0.00	0.00	0.25	0.00
Ni	0.94	0.04	-	0.11	0.12	0.00	0.00	0.00	0.00
Zn	4.26	0.005	-	0.14	0.09	0.00	0.01	0.27	0.00
AVERAGE			-	0.17	0.15	0.00	0.01	0.09	0.00
ANION TRACE METAL RATIOS									
As	2.23	0.01	-	0.00	0.00	0.01	0.00	0.00	0.00
Cr	0.06	0.01	-	0.67	0.02	0.00	1.50	0.00	0.00
Mo	1.25	0.01	-	0.00	0.00	0.02	0.00	0.00	0.01
V	1.73	0.005	-	0.00	0.03	0.04	0.05	0.00	0.00
Se	0.02	0.01	-	31.00	5.30	0.70	0.00	0.00	0.00
AVERAGE			-	6.33	1.07	0.15	0.31	0.00	0.00
U	8	0.001	0.03	0.35	0.04	0.06	3.75	-	0.00
Ra-226	304	0.1	0.05	0.38	0.36	0.00	0.05	-	0.00

Table 4.12. Water chemistry for Conquista fossiliferous sandstone (May 1991 data).

Well ID		701	919	713	856	921	906	858
Lith/unit		ss	ss	ss	ss	ss	ss-lwr outcrop	ss
Temperature	°C	24.6	24.2	26.1	23.8	24.3	25	24.3
Conductivity	µmhos/cm	16110	13960	13600	15080	11040	10500	10060
pH	-	3.82	3.7	6.03	5.95	6.04	5.37	5.96
Eh	mvolts	455.8	396.9	478.7	426.1	424.8	449.3	438.8
TDS	mg/L	17500	10300	10700	11900	8980	8600	8270
Alkalinity	mg/L	-	-	160	432	359	93	141
Al	mg/L	-	4.33	3.32	0.09	0.05	0.05	0.05
NH4	mg/L	0.5	0.2	0.1	0.2	0.1	0.1	0.7
Ba	mg/L	-	0.02	0.04	0.03	0.03	0.06	0.03
B	mg/L	2.18	0.96	3.02	1.64	1.42	1.44	2.49
Br	mg/L	1	9.6	8.3	10.3	6.5	6.1	1.5
Ca	mg/L	-	920	1550	2080	1760	1450	1140
Cl	mg/L	2030	4500	4140	4820	3800	3050	2800
F	mg/L	89.5	0.6	0.4	0.2	0.1	0.2	1
Fe	mg/L	-	1.33	1.38	0.03	0.03	0.03	0.03
Mg	mg/L	-	182	105	112	224	104	204
Mn	mg/L	-	4.37	0.03	0.03	0.44	0.9	4.36
NO3	mg/L	1	2.9	3.6	80.1	28.3	2.2	72
PO4	mg/L	0.2	0.2	0.2	0.2	1.2	0.3	0.2
K	mg/L	-	84	32	40	102	58	90
SiO2	mg/L	101	83.6	86.6	53.5	54.5	67.6	45
Na	mg/L	-	1600	1900	1610	1190	873	1350
SO4	mg/L	9390	1860	1740	1460	1490	1110	2020
Sr	mg/L	-	10.2	8.93	11.7	19.6	10.4	9.6
Sulfide	mg/L	-	<1	2.6	<1	<1	1.74	<1
Sb	mg/L	-	0.03	<0.003	0.03	0.03	<0.003	0.03
As	mg/L	-	<0.01	<0.01	<0.01	<0.01	<0.01	<0.01
Be	mg/L	-	0.01	<0.005	<0.005	<0.005	<0.005	<0.005
Cd	mg/L	-	0.02	0.005	0.01	0.01	0.01	0.02
Cr	mg/L	-	<0.01	<0.01	0.05	<0.01	<0.01	0.01
Co	mg/L	-	0.05	<0.03	<0.03	<0.03	<0.03	0.03
Cu	mg/L	-	<0.01	<0.01	0.02	<0.01	0.02	0.01
Cn	mg/L	<0.01	<0.01	<0.01	<0.01	<0.01	<0.01	0.01
Pb	mg/L	-	0.03	<0.005	<0.005	<0.005	0.03	0.005
Hg	mg/L	-	0	0	0	0	0	0
Mo	mg/L	-	0.01	0.02	0.02	0.04	<0.01	<0.01
Ni	mg/L	-	0.05	<0.04	<0.04	<0.04	<0.04	0.05
Se	mg/L	-	0.038	0.067	0.043	0.169	0.011	0.033
Ag	mg/L	-	<0.01	<0.01	<0.01	<0.01	<0.01	<0.01
Tl	mg/L	-	<0.01	0.1	<0.01	<0.01	<0.01	0.1
Sn	mg/L	-	<0.05	<0.05	0.3	<0.05	<0.05	<0.05
U	mg/L	0.036	0.289	0.002	9.8	0.657	<0.001	0.06
V	mg/L	-	<0.01	<0.01	0.05	<0.01	<0.01	<0.01
Zn	mg/L	-	0.339	0.018	0.008	0.037	0.032	0.046
TKN	mg/L	1	1	1	1	1	1	1
TOC	mg/L	4	3	1	4	3	3	4
NOX	mg/L	0.26	0.56	0.85	18.3	6.4	0.5	16.8
Gross alpha	pCi/L	16900	163	901	4570	176	36.6	43.3
Gross beta	pCi/L	11500	244	735	2390	172	67.9	91.9
Ra-226	pCi/L	4	7.2	1.8	2.1	4.3	4.4	4.6
Ra-228	pCi/L	2.7	7.3	4	6.8	4	2.3	9.2
Tritium	t.u.	-	-	-	3.15	1.6	1.06	0.49
Gypsum SI	-	-	-0.1	0.04	0.04	0.02	-0.09	0.03
Calcite SI	-	-	-	-0.48	-0.04	-0.06	-1.34	-0.71
Pco2	bars	-	-	0.12	0.38	0.26	0.34	0.13

Table 4.12 (cont.)

Well ID		709	712	859	865	924	861	860	951
Lith/unit		ss	ss	ss	ss	ss	ss	ss	up/ss?
Temperature	°C	25.1	24	24.9	24.6	24.9	24.8	24.7	26.7
Conductivity	µmhos/cm	-	10120	8980	7780	5320	5860	5230	4150
pH	-	5.89	6.15	6.23	6.35	6.15	6.58	6.73	6.75
Eh	mvolts	498.2	417	413.3	393.6	444.7	415.5	422.5	451.3
TDS	mg/L	8400	8070	7240	6020	4840	4480	4070	2901
Alkalinity	mg/L	135	551	308	384	313	283	249	307
Al	mg/L	0.05	0.05	0.05	0.05	0.05	0.05	0.05	0.05
NH4	mg/L	0.1	0.1	0.4	0.3	0.1	0.4	0.6	0.3
Ba	mg/L	0.01	0.02	0.02	0.04	0.01	0.02	0.02	0.02
B	mg/L	0.97	4.43	1.29	1.24	0.75	1.01	1.22	0.91
Br	mg/L	5.4	3.2	4.6	4.7	0.3	3	1.3	2.2
Ca	mg/L	1050	990	950	870	565	503	494	364
Cl	mg/L	2850	2550	2850	1670	212	954	735	708
F	mg/L	0.7	1	0.1	0.1	0.5	0.2	0.2	0.8
Fe	mg/L	0.03	0.03	0.03	0.49	0.03	0.18	0.06	0.03
Mg	mg/L	86.8	91	135	117	97.6	89.8	58	28.7
Mn	mg/L	0.01	0.01	1.95	2.55	0.07	2.71	2.34	0.21
NO3	mg/L	42.5	19	4.4	4	4	4	3.5	4
PO4	mg/L	0.2	0.2	0.1	0.1	0.4	0.1	0.1	0.1
K	mg/L	36	74	80	72	57	68	60	45
SiO2	mg/L	66.3	63	44.4	35.6	57.5	42	45	49.2
Na	mg/L	945	1390	1340	1140	811	839	773	652
SO4	mg/L	1630	1930	1990	1880	2890	1680	1790	856
Sr	mg/L	5.89	9.56	9.25	7.7	5.84	4.65	4.11	2.85
Sulfide	mg/L	<1	<1	<1	3.1	<1	<1	<1	9.2
Sb	mg/L	<0.003	<0.003	0.03	0.03	<0.003	0.03	<0.003	0.03
As	mg/L	<0.01	<0.01	0.02	<0.01	<0.01	<0.01	<0.01	<0.01
Be	mg/L	<0.005	<0.005	<0.005	<0.005	<0.005	<0.005	<0.005	<0.005
Cd	mg/L	0.005	0.01	0.01	<0.001	<0.001	<0.001	<0.001	<0.001
Cr	mg/L	<0.01	0.05	<0.01	<0.01	<0.01	<0.01	<0.01	<0.01
Co	mg/L	<0.03	<0.03	<0.03	<0.03	<0.03	<0.03	<0.03	<0.03
Cu	mg/L	<0.01	<0.01	0.02	<0.01	<0.01	<0.01	<0.01	<0.01
Cn	mg/L	<0.01	<0.01	<0.01	<0.01	<0.01	<0.01	<0.01	<0.01
Pb	mg/L	<0.005	<0.005	<0.005	<0.005	<0.005	<0.005	0.03	<0.005
Hg	mg/L	<0.0002	<0.0002	<0.0002	<0.0002	<0.0002	<0.0002	<0.0002	<0.0002
Mo	mg/L	0.02	<0.01	<0.01	<0.01	<0.01	0.03	<0.01	<0.01
Ni	mg/L	<0.04	<0.04	<0.04	<0.04	<0.04	<0.04	<0.04	<0.04
Se	mg/L	0.049	<0.005	<0.005	<0.005	<0.005	<0.005	<0.005	<0.005
Ag	mg/L	<0.01	<0.01	<0.01	<0.01	<0.01	<0.01	<0.01	<0.01
Tl	mg/L	<0.01	<0.01	0.1	<0.01	<0.01	<0.01	<0.01	<0.01
Sn	mg/L	<0.05	<0.05	<0.05	<0.05	<0.05	<0.05	<0.05	<0.05
U	mg/L	<0.001	5.5	0.003	0.003	0.091	0.02	0.022	0.008
V	mg/L	<0.01	0.05	<0.01	<0.01	<0.01	<0.01	<0.01	<0.01
Zn	mg/L	0.008	0.017	0.008	0.025	<0.005	0.007	0.02	<0.005
TKN	mg/L	1	1	1	1	1	1	1	1
TOC	mg/L	2	1	2	2	3	2	1	1
NOX	mg/L	9.6	4.35	1.05	0.96	0.92	0.92	0.8	0.92
Gross alpha	pCi/L	139	2366	0	0	26.8	0	0	0
Gross beta	pCi/L	212	1293	0	84.6	46.3	55.4	0	37.9
Ra-226	pCi/L	5.6	4.4	0.3	1.3	0.7	2.4	1.1	1.3
Ra-228	pCi/L	4.4	3.7	0	0	2.5	2	0.7	3.1
Tritium	t.u.	2.16	-	0.18	-	5.9	<0.09	<0.09	0.13
Gypsum SI	-	-0.02	-0.01	-0.02	-0.03	0.02	-0.19	-0.15	-0.47
Calcite SI	-	-0.79	0.01	-0.17	0.03	-0.47	-0.06	0.02	0.12
Pco2	bars	0.16	0.35	0.16	0.16	0.22	0.07	0.05	0.06

Table 4.13. Normalized metals in ground waters of Conquista fossiliferous sandstone.

CONQUISTA SANDSTONE			701	919	713	856	921	906	858	709	712	859	865	924	861	860	951
Well ID																	
	AVE. TAIL	LLD	RATIOS TO AVERAGE TAILINGS SOLUTION METALS														
pH			3.82	3.70	6.03	5.95	6.04	5.37	5.96	5.89	6.15	6.23	6.35	6.15	6.58	6.73	6.75
MAJOR METAL RATIOS																	
Al	714	0.05	-	0.01	0.00	0.00	0.00	0.00	0.00	0.00	0.00	0.00	0.00	0.00	0.00	0.00	0.00
Fe	598	0.01	-	0.00	0.00	0.00	0.00	0.00	0.00	0.00	0.00	0.00	0.00	0.00	0.00	0.00	0.00
Mn	31	0.01	-	0.14	0.00	0.00	0.01	0.00	0.14	0.00	0.00	0.06	0.08	0.00	0.09	0.08	0.01
TRACE CATION METAL RATIOS																	
Be	0.15	0.005	-	0.03	0.00	0.00	0.00	0.00	0.00	0.00	0.00	0.00	0.00	0.00	0.00	0.00	0.00
Cd	0.22	0.001	-	0.09	0.02	0.04	0.04	0.04	0.09	0.02	0.04	0.04	0.00	0.00	0.00	0.00	0.00
Co	0.76	0.03	-	0.03	0.00	0.00	0.00	0.00	0.00	0.00	0.00	0.00	0.00	0.00	0.00	0.00	0.00
Cu	0.08	0.01	-	0.00	0.00	0.13	0.00	0.13	0.00	0.00	0.00	0.13	0.00	0.00	0.00	0.00	0.00
Ni	0.94	0.04	-	0.01	0.00	0.00	0.00	0.00	0.01	0.00	0.00	0.00	0.00	0.00	0.00	0.00	0.00
Zn	4.26	0.005	-	0.08	0.00	0.00	0.01	0.01	0.01	0.00	0.00	0.00	0.00	0.00	0.00	0.00	0.00
AVERAGE			-	0.04	0.00	0.03	0.01	0.03	0.02	0.00	0.01	0.03	0.00	0.00	0.00	0.00	0.00
ANION TRACE METAL RATIOS																	
As	2.23	0.01	-	0.00	0.00	0.00	0.00	0.00	0.00	0.00	0.00	0.00	0.00	0.00	0.00	0.00	0.00
Cr	0.06	0.01	-	0.00		0.67	0.00	0.00	0.00	0.00	0.67	0.00	0.00	0.00	0.00	0.00	0.00
Mo	1.25	0.01	-	0.00	0.01	0.01	0.02	0.00	0.00	0.01	0.00	0.00	0.00	0.00	0.02	0.00	0.00
V	1.73	0.01	-	0.00	0.00	0.02	0.00	0.00	0.00	0.00	0.02	0.00	0.00	0.00	0.00	0.00	0.00
Se	0.02	0.005	-	1.65	3.10	1.90	8.20	0.30	1.40	2.20	0.00	0.00	0.00	0.05	0.00	0.00	0.00
AVERAGE			-	0.33	0.78	0.52	1.64	0.06	0.28	0.44	0.14	0.00	0.00	0.01	0.00	0.00	0.00
U	8	0.001	0.00	0.04	0.00	1.22	0.08	0.00	0.01	0.00	0.69	0.00	0.00	0.01	0.00	0.00	0.00
Ra-226	304	1	0.01	0.02	0.00	0.00	0.01	0.01	0.01	0.01	0.02	0.01	0.00	0.00	0.00	0.00	0.00

Table 4.14. Water chemistry of lower Conquista clay (May 1991 data).

Well ID		617	864	663
Lith/unit		lwr	lwr	lwr
Temperature	° C	24.6	25.3	25.8
Conductivity	µmhos/cm	9070	8770	6660
pH	-	6.16	6.49	7.06
Eh	mvolts	389.7	421.1	-
TDS	mg/L	6970	-	4880
Alkalinity	mg/L	560	183	-
Al	mg/L	0.27	0.07	<0.05
NH4	mg/L	0.3	1	-
Ba	mg/L	0.01	0.04	0.01
B	mg/L	1.41	1.23	1.01
Br	mg/L	4.4	-	3.7
Ca	mg/L	914	935	575
Cl	mg/L	1550	-	1230
F	mg/L	0.4	-	0.2
Fe	mg/L	0.03	0.03	0.03
Mg	mg/L	72.5	88.5	46.3
Mn	mg/L	1.31	2.04	0.12
NO3	mg/L	23	20.8	-
PO4	mg/L	0.8	-	1.3
K	mg/L	34	65	65
SiO2	mg/L	55.5	-	44.8
Na	mg/L	1320	1330	875
SO4	mg/L	1900	-	1710
Sr	mg/L	4.77	6.01	3.74
Sulfide	mg/L	<1	<1	-
Sb	mg/L	<0.003	<0.003	<0.003
As	mg/L	0.02	<0.01	<0.01
Be	mg/L	<0.005	<0.005	<0.005
Cd	mg/L	0.01	0.01	<0.001
Cr	mg/L	0.1	<0.01	<0.01
Co	mg/L	<0.03	<0.03	<0.03
Cu	mg/L	<0.01	<0.01	<0.01
Cn	mg/L	<0.01	0.01	-
Pb	mg/L	<0.005	<0.005	<0.005
Hg	mg/L	<0.0002	<0.0002	<0.0002
Mo	mg/L	<0.02	0.68	0.03
Ni	mg/L	<0.04	<0.04	<0.04
Se	mg/L	<0.005	0.055	<0.005
Ag	mg/L	<0.01	<0.01	<0.01
Tl	mg/L	<0.01	0.1	<0.01
Sn	mg/L	<0.05	<0.05	<0.05
U	mg/L	30	-	0.013
V	mg/L	0.1	<0.01	<0.01
Zn	mg/L	0.068	1.15	0.005
TKN	mg/L	1	1	-
TOC	mg/L	4	5	-
NOX	mg/L	5.26	4.82	-
Gross alpha	pCi/L	17400	-	0
Gross beta	pCi/L	8680	-	35.8
Ra-226	pCi/L	14.3	-	0.2
Ra-228	pCi/L	2.9	-	-
Tritium	t.u.	-	-	-
Gypsum SI	-	0.02	-	-0.13
Calcite SI	-	-0.05	-	N.A.
Pco2	bars	0.29	-	N.A.

Table 4.15. Water chemistry of Dilworth sandstone (May 1991 data).

Well ID unit		878 Dil	905 Dil	831 Dil/ lwr c	907 Dil	956 Dil	969 Dil	832 Dil	917 Dil
Temperature	° C	26.7	26.4	24.4	26.3	24.9	24.9	25	24.9
Conductivity	µmhos/cm	5840	13470	5800	4570	5410	4820	5180	4580
pH	-	6.42	6.53	6.5	6.48	6.47	6.7	6.49	6.39
Eh	mvolts	435.3	452.4	351.7	458.5	447.3	372.3	419.3	434.3
TDS	mg/L	4780	9940	4500	2590	4110	3650	3750	3160
alkalinity	mg/L	298	145	415	318	276	291	284	245
Al	mg/L	0.05	0.05	0.05	0.05	0.05	0.05	0.05	0.05
NH4	mg/L	0.7	1.2	0.6	0.6	0.5	0.6	0.1	0.4
Ba	mg/L	0.03	0.05	0.01	0.01	0.01	0.04	0.05	0.02
B	mg/L	1.19	0.62	0.83	0.69	0.55	0.53	0.97	0.81
Br	mg/L	3	8.4	2.8	2.1	2.4	2.6	3.4	1.4
Ca	mg/L	745	655	640	504	495	495	487	397
Cl	mg/L	878	4400	912	630	855	779	1220	660
F	mg/L	0.2	0.2	0.2	0.2	0.2	0.3	0.5	0.1
Fe	mg/L	0.09	0.18	0.04	0.05	0.09	0.87	0.03	0.13
Mg	mg/L	67.8	129	66.7	50.8	55.1	60.5	53.8	40.7
Mn	mg/L	3.89	1.07	0.38	1.35	1.68	2.94	0.99	1.31
NO3	mg/L	3.1	3.7	3.1	1.8	2.7	1.3	9.7	6.1
PO4	mg/L	0.1	0.1	0.1	0.1	0.1	0.5	0.4	0.1
K	mg/L	53	83	46	42	46	43	40	40
SiO2	mg/L	43.1	65.5	47.1	51	68.1	70.4	55.7	48.6
Na	mg/L	928	960	772	594	614	550	613	558
Sr	mg/L	2020	1160	1690	1390	1620	1290	850	1230
SO4	mg/L	5.75	6.65	3.5	3.15	2.91	3.24	3.91	3.08
Sulfide	mg/L	<1	1.53	13.2	<1	<1	<1	<1	<1
Sb	mg/L	<0.003	0.04	<0.003	0.03	<0.003	<0.003	<0.003	<0.003
As	mg/L	<0.01	<0.01	0.02	<0.01	<0.01	0.22	<0.01	<0.01
Be	mg/L	<0.005	<0.005	<0.005	<0.005	<0.005	<0.005	<0.005	<0.005
Cd	mg/L	<0.001	<0.001	<0.001	<0.001	<0.001	<0.001	<0.001	<0.001
Cr	mg/L	<0.01	<0.01	<0.01	<0.01	<0.01	<0.01	<0.01	<0.01
Co	mg/L	<0.03	<0.03	<0.03	<0.03	<0.03	<0.03	<0.03	<0.03
Cu	mg/L	<0.01	<0.01	<0.01	<0.01	<0.01	<0.01	<0.01	<0.01
Cn	mg/L	<0.01	<0.01	<0.01	<0.01	<0.01	<0.01	<0.01	<0.01
Pb	mg/L	<0.005	0.03	<0.005	<0.005	0.03	<0.005	<0.005	<0.005
Hg	mg/L	<0.0002	<0.0002	<0.0002	<0.0002	<0.0002	<0.0002	<0.0002	<0.0002
Mo	mg/L	0.03	<0.01	<0.01	<0.01	<0.01	0.02	<0.01	<0.01
Ni	mg/L	<0.04	<0.04	<0.04	<0.04	<0.04	<0.04	<0.04	<0.04
Se	mg/L	<0.005	<0.005	<0.005	<0.005	<0.005	<0.005	0.01	<0.005
Ag	mg/L	<0.01	<0.01	<0.01	<0.01	<0.01	<0.01	<0.01	<0.01
Tl	mg/L	<0.01	<0.01	<0.01	<0.01	<0.01	<0.01	<0.01	<0.01
Sn	mg/L	<0.05	<0.05	<0.05	<0.05	<0.05	<0.05	<0.05	<0.05
U	mg/L	0.141	0.011	0.001	0.001	0.02	0.01	0.043	0.003
V	mg/L	<0.01	<0.01	<0.01	<0.01	<0.01	<0.01	<0.01	<0.01
Zn	mg/L	0.02	<0.005	<0.005	<0.005	<0.005	<0.005	<0.005	<0.005
TKN	mg/L	1	1	1	1	1	1	1	1
TOC	mg/L	2	1	1	2	2	4	1	2
NOX	mg/L	0.69	0.84	0.76	0.37	0.6	0.32	2.21	1.27
Gross alpha	pCi/L	0	0	112	0	0	7.3	45.5	0
Gross beta	pCi/L	59.5	107	37.6	15.6	21.6	47.1	34	0
Ra-226	pCi/L	2.1	3.3	1.6	0.1	0.7	2.8	0.9	0.4
Ra-228	pCi/L	1.7	5.9	0.4	0	0	5.9	0	0
Tritium	t.u.	0.19	-	<0.09	-	-	<0.06	-	-
Gypsum SI	-	0.00	-0.33	-0.10	-0.21	-0.17	-0.24	-0.41	-0.31
Calcite SI	-	-0.03	-0.29	0.12	-0.05	-0.18	0.11	-0.09	-0.36
Pco2	bars	0.11	0.04	0.13	0.11	0.09	0.06	0.09	0.10

Table 4.15 (cont.)

Well ID unit		964 Dil/Man	975 Dec 90 data	915 Dil	834 Dil	958 Dil	920 Dil/l c	967 Dil	979 Man?
Temperature	° C	24.3	25.3	25.4	27.4	25	25	25.4	25.1
Conductivity	µmhos/cm	4600	3540	3820	3800	4020	4960	4030	3230
pH	-	6.09	6.42	6.6	6.73	6.45	6.7	5.98	6.08
Eh	mvolts	453.8	259	430	425.9	440.3	211.3	423	469.3
TDS	mg/L	3480	3750	2910	2750	3100	3980	2750	2210
alkalinity	mg/L	163	271	365	356	257	349	116	193
Al	mg/L	0.05	0.05	0.05	0.05	0.05	0.05	0.05	0.05
NH4	mg/L	0.3	0.4	0.4	0.4	0.5		0.1	0.1
Ba	mg/L	0.02	0.03	0.02	0.01	0.02	0.01	0.01	0.02
B	mg/L	0.68	0.89	0.74	0.69	0.71	0.43	1.1	0.67
Br	mg/L	2.2	1	0.8	1.6	1.5	1.3	2.2	2.1
Ca	mg/L	374	364	345	342	335	292	278	258
Cl	mg/L	670	393	448	472	456	500	793	672
F	mg/L	0.4	0.3	0.1	0.1	0.3	0.2	0.3	0.4
Fe	mg/L	0.38	0.67	0.03	0.05	0.28	0.03	0.03	0.03
Mg	mg/L	46.3	32.9	28.4	25.6	30.9	27	30.5	28.3
Mn	mg/L	0.99	0.89	0.52	0.48	1.33	0.37	0.02	0.07
NO3	mg/L	2.7	1.4	6.2	4.4	2.7		10.2	4.4
PO4	mg/L	1.3	0.54	0.1	0.1	0.4	0.1	0.9	0.3
K	mg/L	45	41	37	41	37	67	30	36
SiO2	mg/L	93	54.6	48.2	47.7	64.7	40.4	70.3	84.3
Na	mg/L	671	681	528	502	518	471	675	531
Sr	mg/L	1420	1900	1240	1060	1360	1870	817	569
SO4	mg/L	2.73	2.78	2.28	2.15	2.87	1.73	2.56	2.25
Sulfide	mg/L	<1	<0.1	<1	3.5	<1	7.5	6.3	<1
Sb	mg/L	0.03	<0.02	0.03	<0.003	<0.003	<0.003	<0.003	<0.003
As	mg/L	0.04	<0.05	<0.01	<0.01	<0.01	0.02	0.02	0.02
Be	mg/L	<0.005	<0.005	<0.005	<0.005	<0.005	<0.005	<0.005	<0.005
Cd	mg/L	<0.001	<0.0005	<0.001	<0.001	<0.001	<0.001	<0.001	<0.001
Cr	mg/L	<0.01	<0.01	<0.01	<0.01	<0.01	<0.01	<0.01	<0.01
Co	mg/L	<0.03	<0.03	<0.03	<0.03	<0.03	<0.03	<0.03	<0.03
Cu	mg/L	<0.01	<0.01	<0.01	<0.01	<0.01	<0.01	<0.01	<0.01
Cn	mg/L	<0.01	<0.01	<0.01	<0.01	<0.01	<0.01	<0.01	<0.01
Pb	mg/L	<0.005	<0.05	0.03	<0.005	<0.005	0.03	<0.005	<0.005
Hg	mg/L	<0.0002	<0.0002	<0.0002	<0.0002	<0.0002	<0.0002	<0.0002	<0.0002
Mo	mg/L	<0.01	0.05	<0.01	<0.01	<0.01	<0.01	<0.01	<0.01
Ni	mg/L	<0.04	<0.04	<0.04	<0.04	<0.04	<0.04	<0.04	<0.04
Se	mg/L	<0.005	<0.03	<0.005	<0.005	<0.005	<0.005	0.02	0.006
Ag	mg/L	<0.01	<0.01	<0.01	<0.01	<0.01	<0.01	<0.01	<0.01
Tl	mg/L	<0.01	<0.05	<0.01	<0.01	<0.01	<0.01	<0.01	<0.01
Sn	mg/L	<0.05	<0.05	<0.05	<0.05	<0.05	<0.05	<0.05	<0.05
U	mg/L	0.01	0.005	0.003	0.015	0.001	0.023	0.003	0.025
V	mg/L	<0.01	<0.01	<0.01	<0.01	<0.01	<0.01	<0.01	<0.01
Zn	mg/L	<0.005	0.017	<0.005	0.008	<0.005	<0.005	<0.005	<0.005
TKN	mg/L	1	1	1	1	1		1	1
TOC	mg/L	5	4	2	4	1		1	1
NOX	mg/L	0.62	0.39	1.4	0.99	0.6		2.28	1.02
Gross alpha	pCi/L	0	25.4	0	1.6	0	28.6	0	0
Gross beta	pCi/L	41.1	172	52.3	26.3	14.3	78.7	28.4	36.7
Ra-226	pCi/L	1.2	19.9	0.9	0.5	0.1	0.1	1	0.9
Ra-228	pCi/L	5.3	59.2	1.2	1.3	1.6	25.8	3.5	0
Tritium	t.u.	-	-	-	<0.06	-	-	<0.07	<0.08
Gypsum SI	-	-0.30	-0.22	-0.35	-0.39	-0.32	-0.29	-0.57	-0.70
Calcite SI	-	-0.88	-0.38	-0.03	0.14	-0.36	-0.09	-1.19	-0.86
Pco2	bars	0.13	0.10	0.09	0.07	0.09	0.07	0.12	0.17

Table 4.15 (cont.)

Well ID		901	925	862	976	971	902	679	968	974
unit		Dil/ lwr c	Dil/ man	Dil	Dil	Dec 90 data	Dil		Dil	Dil
Temperature	° C	26.4	24.6	25.5	24.5	24	26.3	26.2	24.9	25.4
Conductivity	µmhos/cm	4550	3120	3250	4210	2810	2910	1410	859	3000
pH	-	6.85	6.8	6.69	6.79	6.87	6.97	6.14	6.58	7.06
Eh	mvolts	358.4	426.6	435	425.6	-34	294.5	363.5	449.3	-113
TDS	mg/L	3100	2070	2220	3010	1990	1980	910	624	1900
alkalinity	mg/L	328	497	348	341	360	343	200	226	542
Al	mg/L	0.05	0.05	0.05	0.05	0.05	0.05	0.05	0.05	0.05
NH4	mg/L	0.9	0.2	0.5	1.1	0.7	0.6	0.4	0.1	1
Ba	mg/L	0.02	0.02	0.02	0.01	0.04	0.02	0.03	0.02	0.02
B	mg/L	1.19	0.41	0.64	1.62	0.61	0.6	0.67	0.53	0.78
Br	mg/L	2.1	1.6	0.6	1.8	0.8	1.1	0.9	0.5	1.2
Ca	mg/L	245	243	233	200	167	165	120	89.9	85.7
Cl	mg/L	743	448	354	541	280	299	239	338	418
F	mg/L	0.3	0.5	0.1	0.2	0.2	0.2	0.1	0.2	0.2
Fe	mg/L	0.03	0.03	0.04	0.03	0.03	0.03	1.41	0.03	0.03
Mg	mg/L	13.9	23.6	14.5	13.3	17.5	8	8.4	8.1	4
Mn	mg/L	0.36	0.01	0.3	1.11	0.05	0.22	0.74	0.01	0.03
NO3	mg/L	1.8	6.9	3.5	2.7	<1.0	1.3	3.5	12.4	2.2
PO4	mg/L	0.3	0.2	0.2	0.1	0.37	0.2	2	0.4	0.2
K	mg/L	44	45	36	39	30	32	24	18	28
SiO2	mg/L	77.3	70.6	47.6	66.1	81.6	58	93.6	99.7	45.5
Na	mg/L	755	378	462	669	479	431	158	121	459
Sr	mg/L	1010	473	876	1090	684	750	903	156	457
SO4	mg/L	1.65	1.69	1.5	1.02	1.34	1.05	0.57	0.74	0.62
Sulfide	mg/L	14.7	<1	1.4	<1	109	5.7	<1	<1	114.3
Sb	mg/L	<0.003	0.005	<0.003	<0.003	<0.02	<0.003	<0.003	<0.003	0.03
As	mg/L	0.02	<0.01	<0.01	<0.01	<0.05	<0.01	<0.01	0.03	<0.01
Be	mg/L	<0.005	<0.005	<0.005	<0.005	<0.005	<0.005	<0.005	<0.005	<0.005
Cd	mg/L	<0.001	<0.001	<0.001	<0.001	<0.001	<0.001	<0.001	<0.001	<0.001
Cr	mg/L	<0.01	<0.01	<0.01	<0.01	<0.01	<0.01	<0.01	<0.01	<0.01
Co	mg/L	<0.03	<0.03	<0.03	<0.03	<0.03	<0.03	<0.03	<0.03	<0.03
Cu	mg/L	<0.01	<0.01	<0.01	<0.01	<0.01	<0.01	<0.01	<0.01	<0.01
Cn	mg/L	<0.01	<0.01	<0.01	<0.01	<0.01	<0.01	<0.01	<0.01	<0.01
Pb	mg/L	0.03	<0.005	<0.005	0.03	<0.05	<0.005	<0.005	<0.005	<0.005
Hg	mg/L	<0.0002	<0.0002	<0.0002	<0.0002	<0.0002	<0.0002	0.0002	<0.0002	<0.0002
Mo	mg/L	0.02	0.03	<0.01	0.01	<0.01	<0.01	<0.01	0.06	<0.01
Ni	mg/L	<0.04	<0.04	<0.04	0.04	<0.04	<0.04	<0.04	<0.04	<0.04
Se	mg/L	<0.005	0.01	<0.005	<0.005	<0.005	<0.005	<0.005	<0.005	<0.005
Ag	mg/L	<0.01	0.01	<0.01	<0.01	<0.01	<0.01	<0.01	<0.01	<0.01
Tl	mg/L	<0.01	0.01	<0.01	<0.01	<0.01	<0.01	<0.01	<0.01	<0.01
Sn	mg/L	<0.05	<0.05	<0.05	<0.05	<0.05	<0.05	<0.05	<0.05	<0.05
U	mg/L	0.001	1.22	0.016	0.006	0.005	0.007	0.002	0.068	0.001
V	mg/L	<0.01	0.02	<0.01	<0.01	<0.01	<0.01	<0.01	0.02	<0.01
Zn	mg/L	<0.005	<0.005	<0.005	<0.005	<0.005	<0.005	0.007	<0.005	<0.005
TKN	mg/L	1	1	2	1	1	1	1	1	1
TOC	mg/L	2	3	3	2	<1	1	3	2	2
NOX	mg/L	0.41	1.55	0.81	0.66	0.22	0.3	0.77	2.77	0.52
Gross alpha	pCi/L	0	606	0	0	23.8	0	0	37.6	0
Gross beta	pCi/L	0	276	27.1	44	104	45.9	19.4	27.6	30.2
Ra-226	pCi/L	2.8	0.7	0.2	0.4	4.1	0.5	0.9	0.8	1.1
Ra-228	pCi/L	2.7	0.7	0.1	0.2	2.3	3.4	1.5	5.1	2.4
Tritium	t.u.	-	8.51	-	<0.09	-	-	<0.06	-	-
Gypsum SI	-	-0.56	-0.77	-0.57	-0.60	-0.77	-0.60	-0.74	-1.42	-1.17
Calcite SI	-	0.06	0.25	-0.07	-0.10	-0.10	0.14	-1.13	-0.60	0.12
Pco2	bars	0.05	0.08	0.07	0.06	0.04	0.03	0.16	0.07	0.05

Table 4.15 (cont.)

Well ID unit	833 Dil dry	909 Dil dry	910 Dil dry	911 Dil dry	912 Dil dry
Temperature					
Conductivity					
pH					
Eh					
TDS					
alkalinity					
Al					
NH4					
Ba					
B					
Br					
Ca					
Cl					
F					
Fe					
Mg					
Mn					
NO3					
PO4					
K					
SiO2					
Na					
Sr					
SO4					
Sulfide					
Sb					
As					
Be					
Cd					
Cr					
Co					
Cu					
Cn					
Pb					
Hg					
Mo					
Ni					
Se					
Ag					
Tl					
Sn					
U					
V					
Zn					
TKN					
TOC					
NOX					
Gross alpha					
Gross beta					
Ra-226					
Ra-228					
Tritium					
Gypsum SI					
Calcite SI					
Pco2					

Table 4.16. Water chemistry of Manning Formation (May 1991 data).

Well ID		903	978	973	970
Lith/unit		clay and lignite	sandy clay	fossiliferous clay	not analyzed
Temperature	° C	27	25	27	
Conductivity	µmhos/cm	2150	2840	2750	
pH	-	10	7	7	
Eh	mvolts	357	425	-20	
TDS	mg/L	1460	3640	1810	
Alkalinity	mg/L	85	529	339	
Al	mg/L	<0.05	<0.05	<0.05	
NH4	mg/L	1	0	1	
Ba	mg/L	0	0	0	
B	mg/L	1	0	1	
Br	mg/L	0	3	1	
Ca	mg/L	41	369	75	
Cl	mg/L	216	1160	291	
F	mg/L	0	0	0	
Fe	mg/L	0	0	0	
Mg	mg/L	1	34	3	
Mn	mg/L	0	0	0	
NO3	mg/L	4	4	4	
PO4	mg/L	0	0	1	
K	mg/L	23	42	23	
SiO2	mg/L	93	43	48	
Na	mg/L	418	405	536	
SO4	mg/L	623	702	763	
Sr	mg/L	1	3	0	
Sulfide	mg/L	1	1	79	
Sb	mg/L	<0.003	<0.003	<0.003	
As	mg/L	<0.01	<0.01	<0.01	
Be	mg/L	<0.005	<0.005	<0.005	
Cd	mg/L	<0.001	<0.001	<0.001	
Cr	mg/L	<0.01	<0.01	<0.01	
Co	mg/L	<0.03	<0.03	<0.03	
Cu	mg/L	<0.01	<0.01	<0.01	
Cn	mg/L	<0.01	<0.01	<0.01	
Pb	mg/L	<0.005	<0.005	<0.005	
Hg	mg/L	<0.0002	<0.0002	<0.0002	
Mo	mg/L	0	<0.01	<0.01	
Ni	mg/L	<0.04	<0.04	<0.04	

Table 4.16 (cont.)

Se	mg/L	<0.005	0	<0.005
Ag	mg/L	<0.01	<0.01	<0.01
Tl	mg/L	<0.01	<0.01	<0.01
Sn	mg/L	<0.05	<0.05	<0.05
U	mg/L	<0.001	1	0
V	mg/L	<0.01	<0.01	<0.01
Zn	mg/L	<0.005	<0.005	<0.005
TKN	mg/L	1	1	1
TOC	mg/L	2	2	2
NOX	mg/L	1	1	1
Gross alpha	pCi/L	0	645	23
Gross beta	pCi/L	22	309	11
Ra-226	pCi/L	1	1	1
Ra-228	pCi/L	0	1	4
Tritium	t.u.	-	-	-
Gypsum SI	-	-1	-1	-1
Calcite SI	-	1	0	0
Pco2	bars	2.80E-06	0	0

Table 4.17. Water chemistries in eastern area around tailings pile 3.

Well ID		963	962	940	966	965	977	957
Lith/unit			lwr Conq	pile 3/ Dew	Dil	Dil	Dil	Conq ss/ lwr Conq
Temperature	°C	23.7	23.7	24.8	24.8	23.7	24.2	24.1
Conductivity	µmhos/cm	6550	470	10750	6780	7700	3890	6630
pH	-	3.31	4.31	3.19	3.37	3.67	4.23	4.07
Eh	mvolts	485.2	434	431.4	455.4	501.2	446.9	425
TDS	mg/L	6400	4380	9610	6250	6400	3430	5440
Alkalinity	mg/L	-	-	-	-	-	-	-
Al	mg/L	92.5	92	52.5	40.2	3.02	1.02	0.82
NH4	mg/L	2.8	0.5	0.5	0.7	0.1	0.2	0.2
Ba	mg/L	0.02	0.02	0.01	0.01	0.01	0.01	0.01
B	mg/L	2.04	1.01	1.28	1.72	1.28	0.8	1.18
Br	mg/L	2.6	1.2	4.9	1.9	3.8	2.1	3.4
Ca	mg/L	503	580	488	560	560	282	780
Cl	mg/L	769	393	2235	621	1400	553	1360
F	mg/L	1.8	3.9	39.9	1.8	1.3	0.2	0.2
Fe	mg/L	119	51.2	26.7	67.5	2.43	1.43	0.03
Mg	mg/L	100	71.1	350	117	113	32.9	84.7
Mn	mg/L	5.21	4.12	31.7	4.77	5.34	2.37	1.9
NO3	mg/L	1.3	1.9	3.1	1.3	2.7	1.8	15.9
PO4	mg/L	0.2	0.59	0.1	0.1	1.1	0.1	0.1
K	mg/L	52	50	45	71	78	37	62
SiO2	mg/L	150	97.2	76.2	136	91.5	95.7	92.5
Na	mg/L	897	532	1260	1060	1030	520	775
SO4	mg/L	8.23	2550	3960	3420	2740	1580	1880
Sr	mg/L	3420	5.4	8.6	7.75	8.74	2.62	6.8
Sulfide	mg/L	3	<0.1	5.4	3.9	<1	<1	<1
Sb	mg/L	<0.003	0.02	0.03	0.03	0.03	<0.003	<0.003
As	mg/L	0.04	0.05	<0.01	<0.01	<0.01	<0.01	<0.01
Be	mg/L	0.049	0.045	0.285	0.052	0.037	<0.005	<0.005
Cd	mg/L	0.01	0.015	0.166	0.02	<0.001	0.02	0.005
Cr	mg/L	<0.01	<0.01	0.05	<0.01	<0.01	<0.01	<0.01
Co	mg/L	0.14	0.08	0.64	0.13	<0.03	0.09	<0.03
Cu	mg/L	<0.01	<0.01	0.25	<0.01	<0.01	<0.01	<0.01
Cn	mg/L	<0.01	<0.01	<0.01	<0.01	<0.01	<0.01	<0.01
Pb	mg/L	0.03	0.05	<0.03	<0.03	<0.005	<0.005	<0.03
Hg	mg/L	<0.0002	<0.0002	<0.001	<0.0002	<0.0002	<0.0002	<0.0002
Mo	mg/L	<0.01	<0.01	<0.01	<0.01	<0.01	<0.01	<0.01
Ni	mg/L	0.13	0.12	0.61	0.16	<0.04	0.1	<0.04
Se	mg/L	<0.005	<0.03	0.408	<0.005	<0.005	<0.005	0.221
Ag	mg/L	<0.01	<0.01	<0.01	<0.01	<0.01	<0.01	<0.01
Tl	mg/L	<0.01	<0.05	<0.01	<0.01	<0.01	<0.01	<0.01
Sn	mg/L	<0.05	<0.05	<0.05	<0.05	<0.05	<0.05	<0.05
U	mg/L	<0.001	0.228	27.4	0.1	0.001	0.054	0.107
V	mg/L	<0.01	<0.01	0.05	<0.01	<0.01	<0.01	<0.01
Zn	mg/L	1.09	0.49	1.48	0.789	0.208	0.206	0.102
TKN	mg/L	3	3	1	1	1	1	1
TOC	mg/L	46	9	3	35	7	4	3
NOX	mg/L	0.3	-	0.71	0.3	0.65	0.37	3.6
Gross alpha	pCi/L	206	381	12803	34.6	0	0	27.3
Gross beta	pCi/L	67.6	463	9647	90.1	119	58.4	45
Ra-226	pCi/L	10.5	24.8	7.2	2.2	0	0.7	5.1
Ra-228	pCi/L	1.8	0.9	1.3	2.3	0	5.7	11.7
Tritium	t.u.	-	-	-	-	-	-	-
Gypsum SI	-	0.02	-0.02	-0.01	0.02	-0.03	-0.34	-0.01
Calcite SI	-	-	-	-	-	-	-	-
Pco2	bars	-	-	-	-	-	-	-

Table 4.17 (cont.)

Well ID		953	961	955	954	964
Lith/unit		Dew/Dub	Conq ss/ lwr	Conq ss	Conq ss/ up/bkg	
Temperature	°C	25.6	23.1	24.4	24.4	24.3
Conductivity	µmhos/cm	6950	4690	6380	6660	4600
pH	-	4.56	6.31	6.09	6.49	6.09
Eh	mvolts	440	484.5	454.7	454.7	453.8
TDS	mg/L		4150	5100	5500	3480
Alkalinity	mg/L	21	411	151	47	163
Al	mg/L	0.34	<0.05	<0.05	<0.05	<0.05
NH4	mg/L	0.1	0.5	0.1	0.5	0.3
Ba	mg/L	0.04	0.03	0.02	0.02	0.02
B	mg/L	0.6	0.72	1.11	0.88	0.68
Br	mg/L		2.9	3.3	3.5	2.2
Ca	mg/L	965	1110	975	880	374
Cl	mg/L		805	1290	1280	670
F	mg/L		1	0.3	0.1	0.4
Fe	mg/L	0.03	0.24	0.03	0.06	0.38
Mg	mg/L	82.8	15.9	72.3	85.4	46.3
Mn	mg/L	2.02	15.6	0.01	1.96	0.99
NO3	mg/L	10.2	1.8	7.1	2.7	2.7
PO4	mg/L		0.7	0.2	0.1	1.3
K	mg/L	69	24	47	64	45
SiO2	mg/L	120	59.5	88.6	47.6	93
Na	mg/L	720	276	731	895	671
SO4	mg/L	6.5	1430	1720	2020	2.73
Sr	mg/L		3.48	5.9	7.4	1420
Sulfide	mg/L		<1	<1	<1	<1
Sb	mg/L	<0.003	<0.003	<0.003	0.004	0.03
As	mg/L	<0.01	0.44	<0.01	<0.01	0.04
Be	mg/L	<0.005	<0.005	<0.005	<0.005	<0.005
Cd	mg/L	0.02	0.005	<0.001	<0.001	<0.001
Cr	mg/L	<0.01	<0.01	0.05	<0.01	<0.01
Co	mg/L	0.11	<0.03	<0.03	<0.03	<0.03
Cu	mg/L	0.02	<0.01	<0.01	<0.01	<0.01
Cn	mg/L	<0.01	<0.01	<0.01	<0.01	<0.01
Pb	mg/L	<0.005	<0.03	<0.005	<0.005	<0.005
Hg	mg/L	<0.0002	<0.0002	<0.0002	<0.0002	<0.0002
Mo	mg/L	<0.01	0.08	<0.01	<0.01	<0.01
Ni	mg/L	0.06	<0.04	<0.04	<0.04	<0.04
Se	mg/L	0.136	<0.005	0.226	<0.005	<0.005
Ag	mg/L	<0.01	<0.01	<0.01	<0.01	<0.01
Tl	mg/L	<0.01	<0.01	<0.01	<0.01	<0.01
Sn	mg/L	<0.05	<0.05	<0.05	<0.05	<0.05
U	mg/L	0.225	0.289	<0.001	0.025	0.01
V	mg/L	0.03	<0.01	<0.01	<0.01	<0.01
Zn	mg/L	0.224	<0.005	<0.005	<0.005	<0.005
TKN	mg/L	1	1	1	1	1
TOC	mg/L		5	1	4	5
NOX	mg/L	2.36	0.4	1.63	0.62	0.62
Gross alpha	pCi/L	0	67.8	105	0	0
Gross beta	pCi/L	46.5	72.4	73.9	92.2	41.1
Ra-226	pCi/L	4.2	2.9	1.2	1	1.2
Ra-228	pCi/L	2.4	2.6	2	2.2	5.3
Tritium	t.u.	-	-	-	-	-
Gypsum SI	-	-	0.06	0.03	0.05	
Calcite SI	-	-	0.15	-0.56	-0.73	
Pco2	bars	-	0.18	0.11	0.01	

COMPUTER MODEL OF EXCHANGE AND NEUTRALIZATION REACTIONS

(SECTION 5)

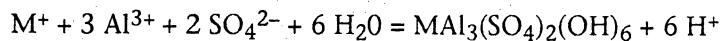
The areal changes in chemical parameters away from the tailings piles suggest that acid tailings solutions are reacting with the sediments as the solutions migrate through those sediments. Comparison of two sets of data from monitoring wells 625 and 914 provides an example of these hypothesized reactions. Both wells are completed in the Deweesville sandstone adjacent to tailings pile 2 (fig. 4.11). Monitoring well 625 is located about 100 ft southeast of tailings pile 2, and the chemistry of samples from that well indicates that the ground water is essentially a tailings solution with a major element composition similar to that in monitoring well 602 and lysimeter 222 (table 4.1). Monitoring well 914 is located about 500 ft east of tailings pile 2 and 500 ft northeast of monitoring well 625. Water from well 914 has only slightly greater chloride content than that in 625, which simplifies comparison of the two wells. Bromide is similar in the two wells and the chloride-to-bromide ratios are high (1,333 to 1), about the same as those in the high-chloride tailings solutions in pile 2. Thus, the chloride-to-bromide ratio of monitoring well 914 is consistent with a tailings pile source for this ground water, and its major element chemistry is thought to be due to reaction of a tailings solution with the Deweesville sandstone.

Comparison of the changes in major element chemistry of waters from 625 to 914 (table 5.1) indicates very substantial decreases in aluminum, sulfate, iron, ammonium, sodium, potassium, and magnesium; and substantial increases in calcium and bicarbonate. Both waters are saturated with gypsum, but sample 625, which has a pH value of 3.3, is undersaturated with calcite, while sample 914, with a pH value of 6.3, is oversaturated with respect to calcite. Further, both the partial pressure of carbon dioxide (P_{CO_2}) and the bicarbonate concentration of sample 914 are anomalously high for a ground water (0.44 atmosphere and 1,000 mg/L, respectively) and indicative of acid solutions reacting

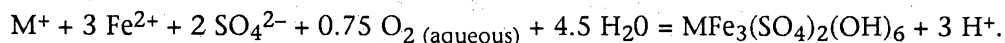
with calcite. Thus, these two wells were chosen to ascertain the reactions that take place between the sediments at the site and tailings solution plumes.

Reactions that neutralize aluminum and iron sulfate solutions were discussed in a previous section in which boehmite was used to compute the amount of calcite required to neutralize the tailings solutions. However, the relation between pH and pAl indicates that alunite rather than boehmite probably controls aluminum concentrations in the tailings and ground waters. In the following model, aluminum is precipitated as alunite rather than as boehmite, although this choice of aluminum precipitate is not critical to the modeled results.

The precipitation of alunite produces hydrogen ions and results in a decrease in sulfate and other cations besides aluminum. The reaction is



where M may be potassium, ammonium, or sodium and jarosite is the iron analog of alunite. However, the tailings solutions contain primarily ferrous iron and thus, precipitation of jarosite requires oxidation of the iron. Assuming that dissolved oxygen is sufficient to oxidize the iron, the reaction is



In this reaction model, iron is assumed to precipitate as jarosite by the above reaction (and thus iron is treated as aluminum precipitating as alunite; steps 1 and 2, table 5.1).

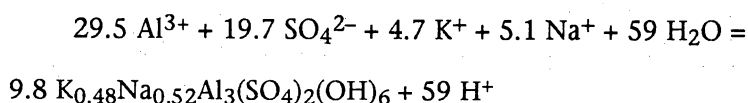
Comparison of the aluminum and iron in samples 625 and 914 indicates that precipitation of alunite and jarosite cannot explain more than about 5 percent of the combined decrease in ammonium, potassium, and sodium or the observed decrease in magnesium. There must be another reaction to account for these decreases.

Precipitation of sodium- and magnesium-aluminum silicates (for example, albite, sodium smectite, and magnesium smectite) likewise cannot explain the decreases relative to aluminum. A probable explanation of the decreases in magnesium, sodium, and ammonium—beyond that required for alunite and jarosite precipitation—is cation

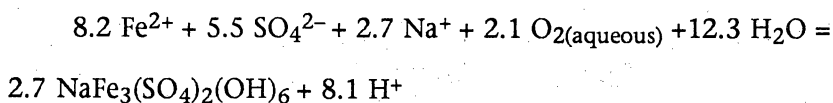
exchange for calcium. This reasonable inference is supported by the strong activity relations between Ca, Mg, and Na (discussed in an earlier section).

Assuming that cation exchange and precipitation of alunite and jarosite have taken place, then mass balance computations give the following net changes in chemistry (in mmole/L) during a reaction of sample 625 with the Deweesville sandstone to form sample 914.

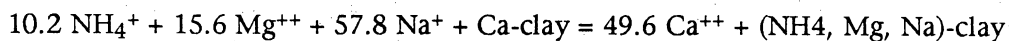
Potassium-sodium alunite precipitation:



Sodium-jarosite precipitation:



Cation exchange for calcium:



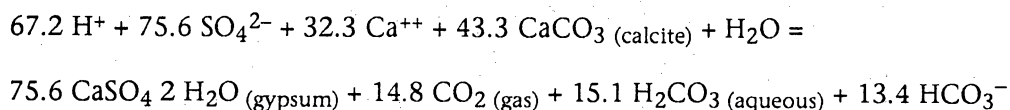
These presumed reactions account for the observed differences (between samples 625 and 914) in the aluminum, iron, potassium, magnesium, sodium, and ammonium. They are *a priori* assumptions to the model.

To model the reaction of sample 625 with calcite, using the SOLMINEQ.88 computer code, the solution resulting from the above reactions (step 3, table 5.1) is allowed to equilibrate with calcite and gypsum in a system closed to CO₂ loss (step 4, table 5.1). At step 4 (table 5.1) the computer program solves for the pH, Pco₂, and concentrations of calcium, sulfate, bicarbonate, and carbonic acid.

The modeled equilibrated solution at step 4 is very similar to sample 914 (table 5.1). The major difference is that the Pco₂ is higher in the modeled solution than in sample 914 (Pco₂ of 0.9 versus 0.44 atmosphere). Also, the chloride concentration of sample 914 is 1.12 times that in 625. Sample 914 is from a shallow well producing from near the ground-water table at a depth of 12 ft. Degassing of CO₂ and evapotranspirative concentration are reasonable explanations for these differences in Pco₂ and chloride,

and inputting these two processes into the computer model gives an almost exact fit to the observed and modeled water chemistries (step 6, table 5.1).

The net reaction of calcite and gypsum with the acid solution formed by cation exchange precipitation of alunite and jarosite is the following (in mg/L prior to evaporation):



The reactant acid is from alunite and jarosite precipitation, and the reactant calcium from cation exchange and calcite. Note that about 42 percent of the sulfate decrease is due to gypsum precipitation resulting from cation exchange of sodium, ammonium, and so on, for calcium, whereas 52 percent of the decrease is due to neutralization reactions.

Computed volumes of precipitates and dissolved calcite relative to a sediment with 33 percent porosity are as follows: The net reaction will result in about 0.05 volume percent calcite dissolution, 0.063 percent alunite and jarosite precipitation, and 0.22 percent gypsum precipitation, for a net change of 0.23 volume percent precipitation. These values are within a factor of 4 or less of those computed using the much simpler computations of aluminum neutralization presented earlier (and those types of computations, based simply on aluminum concentrations, provide a good estimate of the calcite required to neutralize a tailings solution).

The purpose of detailed modeling of the neutralization reactions is to demonstrate that reaction of the low-calcium/high-sulfate tailings solutions with calcite and cation exchangers will produce high-calcium, low-sulfate ground waters, providing additional evidence that the high-calcium waters at the site are reacted tailings solutions. These high-calcium waters (with calcium concentrations >1,000 mg/L) may be acid or nonacid, depending on the degree of neutralization of aluminum, which in turn depends upon the amount of calcium carbonate present along the ground-water flow path.

Within the Deweesville sandstone, the amount of carbonate must be very small (<0.05 volume percent). An acid plume extends about 2,000 ft south of tailings pile 4 (fig. 4.12). Geologic and geochemical profiles through this plume, from tailings piles 4 and 5 to monitoring well 922, can now be interpreted in light of the proposed reaction path model. In and immediately adjacent to the tailings piles, the solutions and ground waters are essentially solutions of aluminum, ammonium, sodium, calcium, iron, magnesium sulfate, and sodium chloride. As these solutions migrate into the Deweesville, the aluminum, sodium, ammonium, potassium, magnesium, and sulfate concentrations decrease, and calcium concentrations increase. There is a slight increase in pH, but the solution remains acid (<4.0) as long as the aluminum concentration remains above 1 mg/L. Between monitoring wells 879 and 922, the aluminum concentration decreases to less than 0.05 mg/L, pH values rise to 5.8, and Ca concentrations decrease to below 1,000 mg/L. At this point, the relatively low concentrations of calcium in a high-pH water indicate that the monitoring well is beyond the influence of the tailings solution plume, although time-dependent trends in monitoring well 922 (decreasing pH and increasing Ca) suggest that the plume is beginning to influence ground waters in the area of monitoring well 922.

In contrast to the Deweesville, the Conquista sand appears to have significant calcite, a conclusion supported by the logged occurrences of calcite in core and the predominance of calcite-saturated ground waters. Tailings solutions entering the Conquista at pile 7, and perhaps pile 2, are neutralized, except in areas immediately adjacent to pile 7 (monitoring well 701). The highest calcium content of any water at the site, 2,050 mg/L, is found in monitoring well 856, screened in the Conquista sand below pile 2. As with monitoring well 914 in the Deweesville, monitoring well 856 has a high P_{CO_2} (0.4 atmosphere), is in equilibrium with both calcite and gypsum, and contains low ammonium, magnesium, potassium, and sodium concentrations and low trace metal concentrations relative to the tailings solutions. The exceptions are uranium and

selenium, which are equal to their concentrations in the tailings solutions. Calcium concentrations decrease with distance from pile 7, reaching background levels (<950 mg/L) about 3,000 ft from pile 7. This decrease may reflect mixing of background waters with the neutralized tailings solutions, or it may represent variation in tailings solutions chemistry over time.

Table 5.1. Model of a reaction in which waters having the composition of sample 625 react to become waters having the composition of sample 914.

		Reaction model of sample 625 to form sample 914.							
		Monitoring well 625	Step 1	Step 2	Step 3	Step 4	Step 5	Step 6	Monitoring well 914
			NH ₄ , Mg, Na exchanged for K. Fe expressed as Al	Precipitation of Al (and Fe) as alunite (and jarosite)	K exchanged for Ca	Calcite dissolution at gypsum and alunite saturation	Evaporation	De-gas Carbon Dioxide (final step)	
pH	-	3.3	3.3	1.2	1.5	5.9	5.8	6.2	6.3
TDS	mg/L	18300	18300	15900	13975	8078	9053	7046	6830
PCO ₂	atmospheres	-	-	-	-	0.9	1	0.4	0.44
H ₂ CO ₃	mg/L	0	0	0	0	1768	2046	914	
HCO ₃	mg/L	0	0	0	0	905	953	953	1061
Al	mg/L	796	943.6	0	0	0	0	0	0.4
NH ₄	mg/L	185	0	0	0	0	0	0	0.2
Ca	mg/L	494	494	494	2522	1234	1384	1384	1370
Cl	mg/L	1740	1740	1740	1740	1750	1963	1963	1950
Fe	mg/L	458	0	0	0	0	0	0	0.9
Mg	mg/L	498	120	120	120	120	137	138	120
K	mg/L	203	4428.5	3974.1	44	44	49.3	49	19
Na	mg/L	2270	730	730	730	744	835	835	730
SO ₄	mg/L	11000	11000	8763.3	8763	1539	1724.7	1724	1660
Saturation indices: undersaturated (-), saturated (0), oversaturated (+).									
gypsum	-	0	0	0	0.6	0	0.1	0.1	0.1
calcite	-	undersat.	undersat.	undersat.	undersat.	0	0	0.3	0.6
alunite	-	6.8	8.9	-8.3	-10.7	0.1	0.1	0.3	8.2
boehmite	-	-0.2	0.1	-7.3	-7.5	0.8	0.7	0.2	4
Net precipitation (-) or dissolution (+)									
gypsum	moles/L		0	0	0	-75.6	-84.8	-84.8	-
alunite	moles/L		0	-11.7	-11.7	-11.7	-13.1	-13.1	-
calcite	moles/L		0	0	0	43.3	48.5	48.5	-
Net cation exchange (meq/L)			108	108	101	101	113	113	-

BATCH LEACH EXPERIMENTS (CORE 869) (SECTION 6)

Methods

Samples were selected from core 869 for batch leach experiments. This core came from pile 7 (fig. 3.2) and intersects tailings and the underlying Conquista clay Member. Samples from core were subjected to both a deionized water leach and an acid leach.

For the deionized water leach, 25 g of each sample were placed in plastic 250 ml centrifuge bottles. Deionized water (100 ml) was added to each sample. The sample bottles were then sealed, placed upon a shaker table, and intermittently shaken for approximately 24 hr. The samples were removed from the table and centrifuged, and the solutions were tested for Eh, pH, and conductivity. Splits of the remaining solution were taken for cation and anion analysis. The cation splits were diluted 1:1 with 2.0 percent HNO₃ (nitric acid) prior to analysis. Results are provided in table 6.1. Note that the ammonium and bicarbonate were not analyzed. Electrical imbalance of the analyzed solutions coupled with a knowledge of the tailings solutions and ground-water chemistries suggested that ammonium was present in the low-pH leachates, whereas, bicarbonate was present in the high-pH leachates. The concentrations of these two ions were thus estimated from the electrical imbalance (tables 6.1 and 6.2).

For the acid leach, 25 g of samples were placed in 250 ml centrifuge bottles and 75 ml of dilute HNO₃ solution (pH = 1.9) was added to each sample and allowed to equilibrate overnight. The pH was monitored and the appropriate amount of dilute HNO₃ was added to each sample to bring the sample solution to a pH of 2.0. Some carbonate-buffered samples required several more additions of dilute HNO₃ to reach a pH of 2.0. After all the samples reached a pH of between 1.9 and 2.1, they were brought to a total volume of 200 ml with a dilute (pH = 2.0) HNO₃ solution. The solutions were allowed to equilibrate for 2 days. After 2 days the samples were

centrifuged and tested for pH and aliquots were taken for cation analysis. The final pH of all samples ranged from 1.96 to 2.17. Results are provided in table 6.2.

Core Description

The core intersected about 17 ft of fill above the top of tailings. The fill consists of black, clayey, calcite- and gypsum-bearing soil layers, white bentonitic clay, and gray sandy clay (table 6.1). The tailings, from 17 to 36.5 ft, consist of pale-yellow to gray sands interlayered with dark-brown sandy clays. The upper 3 ft is marked by iron hydroxide stains and jarosite. Dark gray, saturated sands occur from 20 to 36.5 ft. After sampling, oxidation of the saturated solutions, drained from the tailings, produced jarosite.

The tailings rest on the upper Conquista clay, which is an iron-hydroxide-stained, friable sandy, silty clay, containing abundant gypsum as nodules and along fractures. At 45 ft, a sandy clay contains small (1/2-inch) nodules of gypsum and calcite (identified by X-ray diffraction). The powdery, finely crystalline gypsum in these nodules may be a product of relatively rapid reactions of tailings contaminants with calcite nodules in a zone immediately above the Conquista sand.

At 47 ft, the sandy clay grades into an indurated, limonite-stained, vuggy sandstone, the Conquista fossiliferous sandstone. The vugs are molds of fossil pelecypods. Thin sections of the sandstone reveal that some pelecypod shell material is replaced by iron hydroxides and some of the molds are sites of gypsum crystallization. The vugs, iron hydroxides, and gypsum are probably products of natural reactions between natural acid-sulfate ground waters and calcium-carbonate shell material. Reasons for considering these as natural are (1) the volume of the vugs is large and total dissolution of shell material would require unrealistically large volumes of tailings solutions, (2) similar vugs and geochemical textures were observed in outcrops of Conquista fossiliferous

sandstone, outcrops beyond the influence of tailings contamination, (3) in thin section, gypsum occurs as large, clear crystals within vugs rather than the disseminated crystallites found in the nodules at 45 ft, and (4) iron hydroxides, which replace shell material, preserve the original internal microstructure of the shell, suggesting slow replacement rather than rapid reactions.

The indurated sand grades into unconsolidated sand at 55 ft and then into light tan, iron-hydroxide-stained clay at 59 ft (the top of the lower Conquista clay). This clay contains abundant gypsum and iron hydroxides along fracture planes. The last diagenetic iron-hydroxide- and gypsum-filled fracture occurs at 68.6 ft, where a color change indicates the top of the reduced zone at 68.8 ft. Below the color change, the clay is dark-gray, silty, and carbonaceous, although a zone of partially oxidized (medium gray) clay occurs at 78 ft. The reduced clays contain pyrite, identified by X-ray diffraction.

Batch Leach Results

There were few differences between the results of the deionized water and acid leach experiments. Unless noted otherwise, the following discussion refers to the results of the deionized water leach.

The uppermost, carbonate-bearing fill material and the upper 2 ft of the tailings contains no leachable aluminum or iron (fig. 6.1). Below what appears to be a 2-ft-thick leached zone at the top of the tailings, the tailings contain large amounts of soluble aluminum (about 1,000 mg/kg solids) and iron (up to 400 mg/kg) that are associated with large amounts of calcium and sulfate. Aluminum, iron, and sulfate have infiltrated at least 8 ft into the Conquista clay beneath the tailings, but are below detection at 45 ft, just above the top of the Conquista sand. The low aluminum, iron, and sulfate are accompanied by an increase in calcium at 45 ft that may indicate neutralization

of tailings contaminants by calcite in the sandy clay. X-ray diffraction confirmed that both calcite and gypsum are present as small white nodules at this depth.

The Conquista sand contains almost as much soluble aluminum, iron, calcium and sulfate as the tailings, indicating that at this location the Conquista sand is contaminated by undiluted, unreacted tailings solutions. Some of this solution has infiltrated into the upper 1 ft or more of the lower Conquista clay. At 65 ft, 7 ft below the sandstone base, the clay is uncontaminated with low concentrations of soluble aluminum, iron, calcium, and sulfate (but with a relatively high chloride concentration). Below the oxidation-reduction front (69 ft) the iron, calcium, and sulfate concentrations increase, and chloride decreases. This is probably due to oxidation of pyrite in the clays just below the oxidation-reduction front.

Note that the fill material contains more soluble sodium and chloride than the tailings. Also, chloride peaks at three points in the core: at surface, at the buried top of the tailings, and just above the oxidation-reduction front (fig. 6.1). These chloride peaks are probably the result of evaporative concentration above saturated sediments, and the peak just below the oxidation-reduction front may be related to a pretailings groundwater table at the oxidation-reduction front that would have been about 28 below the pretailings surface.

The pH tracks the soluble aluminum and/or iron concentrations, but pH alone provides no information as to the cause of acidity (aluminum or iron sulfates) or the amount of acidity. Trace metals that form anionic complexes—vanadate, molybdate, and chromate—are soluble in the tailings but insoluble in the fill above the tailings and in the sediments below the tailings (tables 6.1 and 6.2; fig. 6.2). In contrast, the cationic trace metals, including cobalt, nickel, zinc, beryllium, and cadmium, are soluble both in the tailings and in the acid leachates beneath the tailings, but insoluble in leachates having pH values greater than 6 (tables 6.1 and 6.2; fig. 6.2).

Discussion

The source of the trace metals and major metals (aluminum and iron) in tailings solutions is certainly due to dissolution of the tailings by sulfuric acid. However, the source of the metals in the sediments below is less certain. There are two basic possible mechanisms. The most direct is the migration of a metals bearing tailings solutions into the sediments, which is referred to here as the allochemical model, meaning that the metals have been introduced to the sediments by migrating solutions. The second mechanism involves migration of an initial sulfuric acid tailings solution into the sediments, which, over time, react with both the tailings and sediment matrix, releasing metals in situ. This second model is referred to here as the intrachemical model. The intrachemical model can further be divided into a dissolution process or a desorption process. In the dissolution process, the aluminum, iron, manganese, and trace metals are released by dissolution of the sediment matrix. In the desorption process, the trace metals are released by desorption from surface sites in the sediments rather than dissolution of the matrix.

The intrachemical desorption process is not supported by the batch leach data. The process cannot explain aluminum or iron concentrations because their concentrations are far greater than that expected on surface sites. And, if desorption of trace metals is due to adding acid solutions to high-pH sediments, then the more basic sediments subjected to an acid leach should release cation trace metals. This is not the case. Comparison of water leachates of sediments having neutral soil pH values (samples 2, 4, 13, and 17) to acid leachates of the same sediments demonstrates that, in three of four cases, there is no significant increase metals concentrations with acid treatment (tables 6.1 and 6.2). Although this is a small sample, the lack of change suggests that most of the sediments do not have trace metals on sorption sites available for release by acid solutions. There was an increase in metals during acid treatment of one sample, sample

13. This is the sample at 45 ft, and the increase in metals with acid treatment is best explained as desorption of metals sorbed during tailings solution neutralization by calcite. Thus metals sorbed during neutralization of tailings solutions can be remobilized by the addition of acid.

Intrachemical release of metals by dissolution of the sediment matrix is dependent on whether the contaminant solutions were sulfuric acid solutions, which reacted with the sediment aluminosilicate and iron hydroxide matrix, or iron and aluminum sulfate solutions which were pre-equilibrated with aluminosilicates and iron hydroxides and are thus unable to dissolve those minerals and release aluminum, iron, or trace metals. At present, nearly all acid solutions at the site are aluminum-sulfate-type solutions, but available analyses of tailings pile solutions during operations recorded pH values of 1, indicative of sulfuric acid in the ponds rather than aluminum sulfate. It is possible that the initial contaminant plumes were sulfuric acid solutions that reacted, probably over a very short period, with aluminosilicates and iron oxides in both the tailings and sediments. At present, however, there are no sulfuric acid solutions and the cation trace metals are migrating as constituents of contaminant plumes that are equilibrated with the aluminosilicates and the oxides of iron and probably, manganese. Thus, further migration of unreacted tailings solutions will not result in increased cation trace metal concentrations, and neutralization processes that result in a decrease in aluminum and/or iron concentrations may also result in decreasing cation trace metals.

The relation of cation trace metal concentrations to pH is clearly shown in plots of cadmium, cobalt, nickel, and zinc versus pH (fig. 6.3). Each metal displays a decrease in concentration over the pH range of 3 to 4.5, the pH range buffered by the aluminum sulfate in the leachates. Results of the experiments indicate that both pH and leachable metals are controlled by the amount of aluminum (or iron) sulfate in the solutions, and thus, pH and metals are covariant. Note the difference in maximum concentrations, ranging from 0.4 mg/kg cadmium to 10 mg/kg zinc (fig. 6.3). These maximums tend to

reflect the abundance of the metals in both an average rock and the tailings solutions (table 4.3).

Pyrite Oxidation

There may be one exception to the conclusion that the trace metals in the contaminant plumes are allochemical. This exception is related to the fact that the tailings solutions are not equilibrated to sulfides, and in particular, pyrite. Pyrite exists in the reduced sediments that are located downdip of the mined areas and within the low-permeability shales between the major sandstone units. At present, most of the contaminant plumes are located within the oxidized portions of the sandstones but are approaching the reduced portions. If contaminants enter the reduced shales between the oxidized sandstones, reactions with pyrite may be of importance. One such situation may occur in the lower Conquista shale in core 869. This core displays a transition from oxidized to reduced shale at a depth of about 68 ft, between samples 17 and 20 (table 4.18). Over this depth range, the leachate pH shows a zone of acid, iron-rich waters (samples 18 and 19), associated with large concentrations of cobalt, nickel, and zinc and moderate concentrations of aluminum. X-ray diffraction indicates the presence of pyrite in the reduced gray and black shales, and it seems likely that pyrite oxidation is responsible for this zone of acid iron-rich solutions. The question is whether natural oxidation or oxidation by contaminant solutions are responsible for these acid leachates. Considering that (1) the acid zone is separated from the Conquista sand by a near-neutral clay sample, (2) the acid zone is at the top of a natural redox boundary, and (3) the iron-to-aluminum ratio in the acid zone is far greater than that in the overlying acid leachate, it seems likely that the acid leachate is a product of natural pyrite oxidation. The possibility that natural redox interfaces are associated with acid leachates

containing high metals concentrations can neither be proved nor disproved at this point, but other evidence, presented next, suggests that this is quite likely.

Leachate pH Profiles

Acid leachates are produced by hydrolysis of aluminum or iron sulfate salts. At Falls City, leachates derived from the tailings tend to be dominated by aluminum sulfates. Preliminary data suggest that there are also naturally acidic sediments associated with iron sulfates at the site. These iron-sulfate-bearing sediments appear to produce an acidity titration curve different from that produced by aluminum sulfate (fig. 4.2).

It was originally thought that leachate pH of sediment cuttings and core would delineate acid plumes at the Falls City site. However, this is impossible because of the presence of naturally acidic sediments. Naturally acidic sediments with leachate-pH values of 3.5 to 5.0 were reported by the USGS prior to mining (within the Deweesville sandstone and upper Conquista clay from 16 to 38 ft below the surface; U.S. Geological Survey, 1958). Batch leach pH data from our study also indicate a number of acid sediments in the Dubose, Deweesville, Conquista, and Dilworth Members (fig. 6.4), and those in the Dubose Clay Member are certainly naturally acidic soils. The Dubose is stratigraphically and topographically higher than sources of tailings contamination; thus, contamination of the Dubose is impossible. However, leachates of Dubose cuttings had pH values in the range of 4 to 6 (fig. 6.4), the lowest pH (4.0) being associated with a redox boundary just above or at the ground-water table (fig. 6.4, boring 879). Also, note that below this acid zone is a calcareous zone (pH of 7.3, at 36 ft, boring 879; fig. 6.4). In other units, acidic pH values of as low as 3.5 were associated with redox boundaries,

oxidized sediments, and reduced sediments (fig. 6.4). In some cases, these acidic zones are associated with contaminants, but in others they are not. Values of pH alone cannot differentiate contaminated from uncontaminated sediments. Further work might demonstrate that acidity titrations can make this discrimination (as in fig. 4.2).

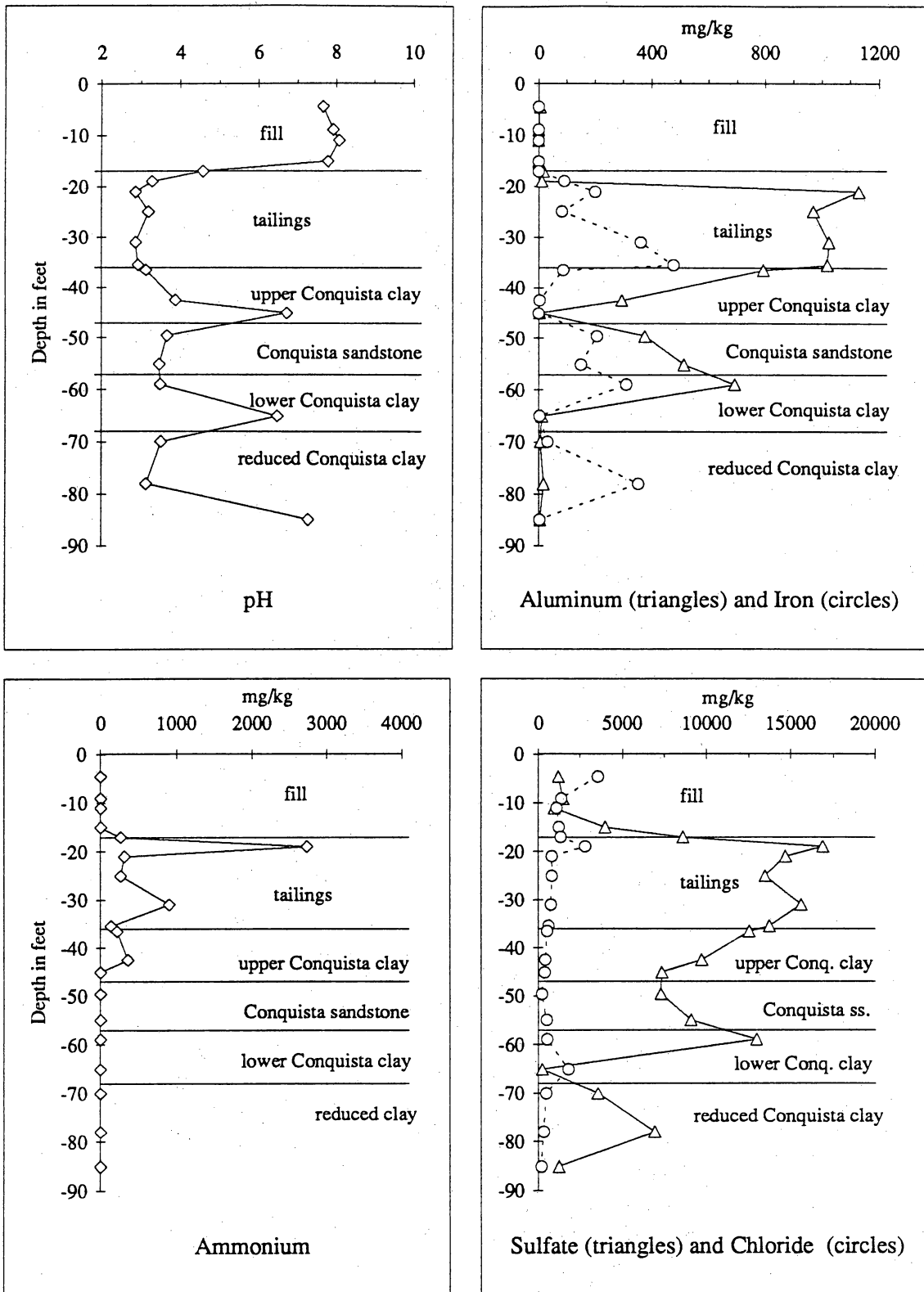


Figure 6.1. pH and water-soluble major elements, core 869.

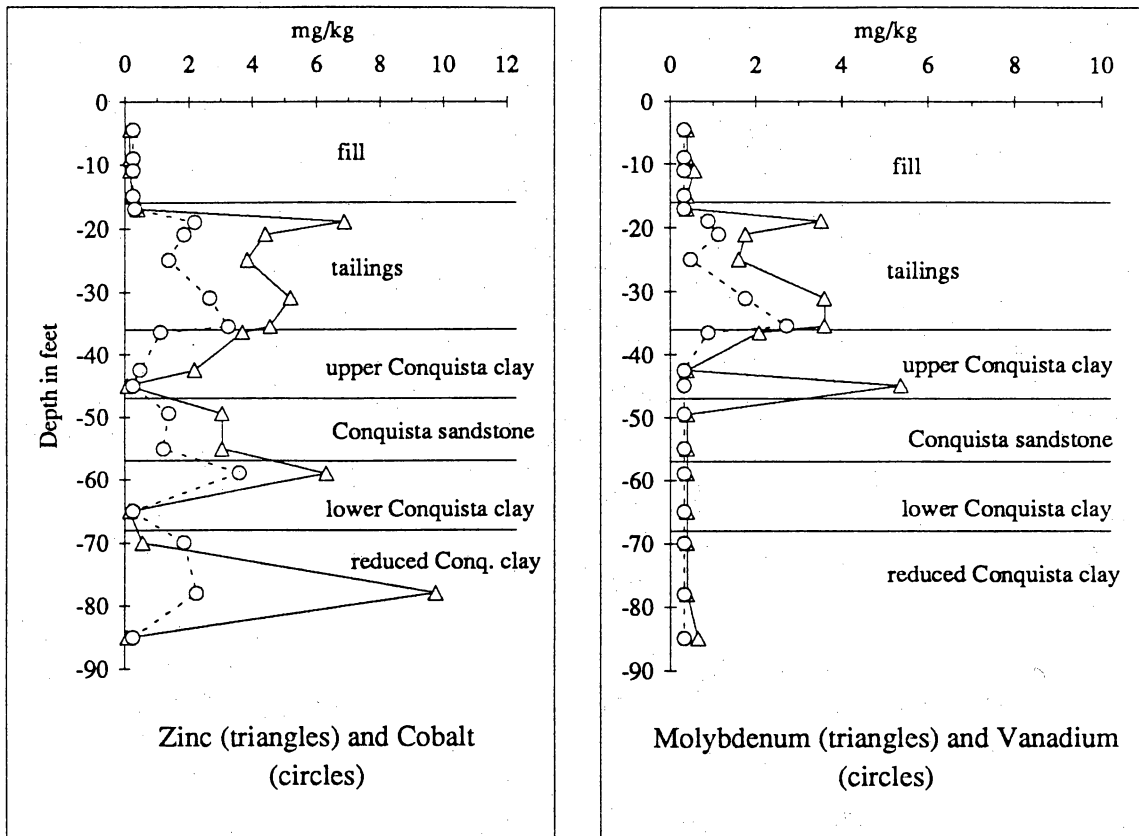


Figure 6.2. Water-soluble trace elements, core 869.

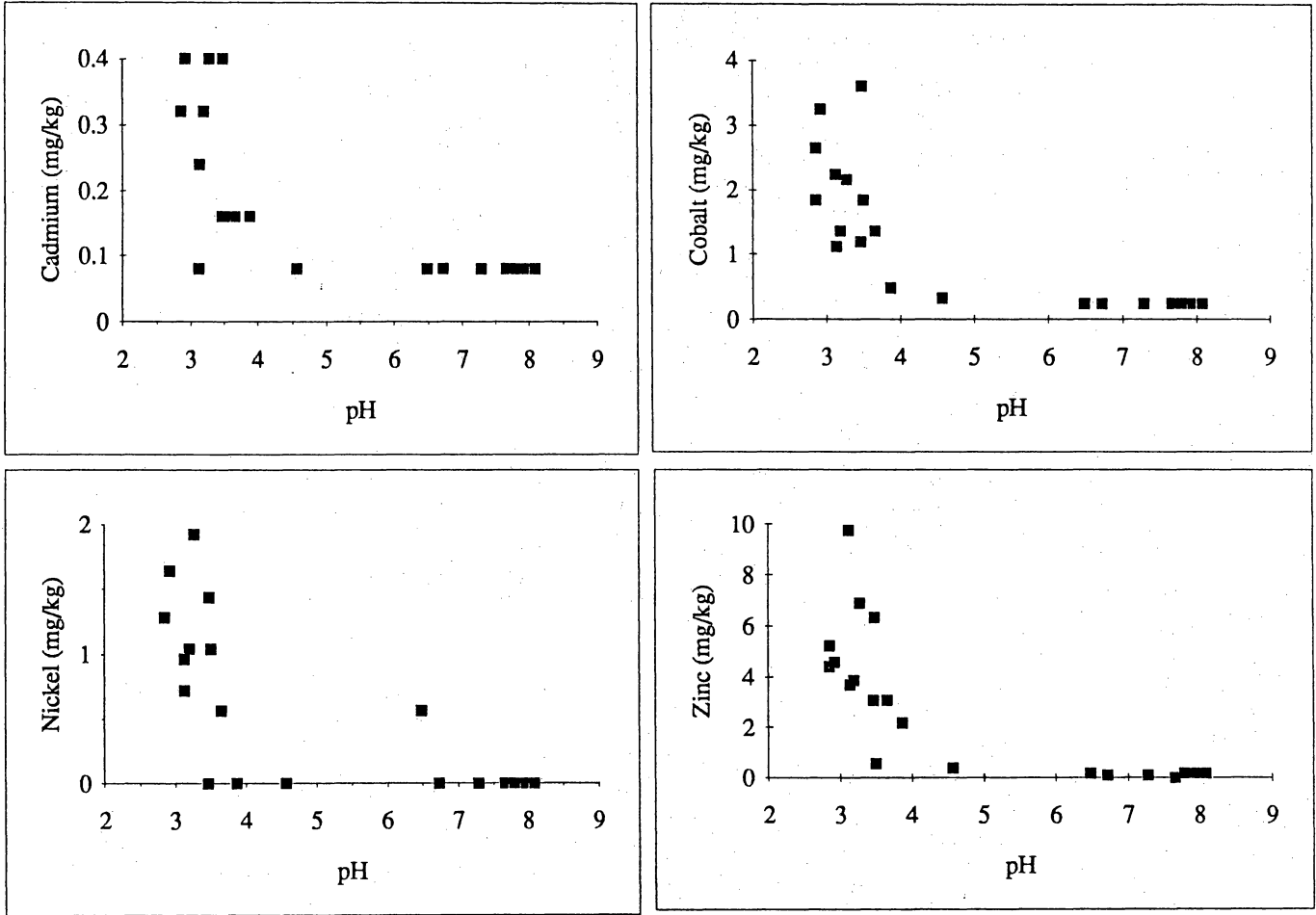


Figure 6.3. Relation of trace metals to pH.

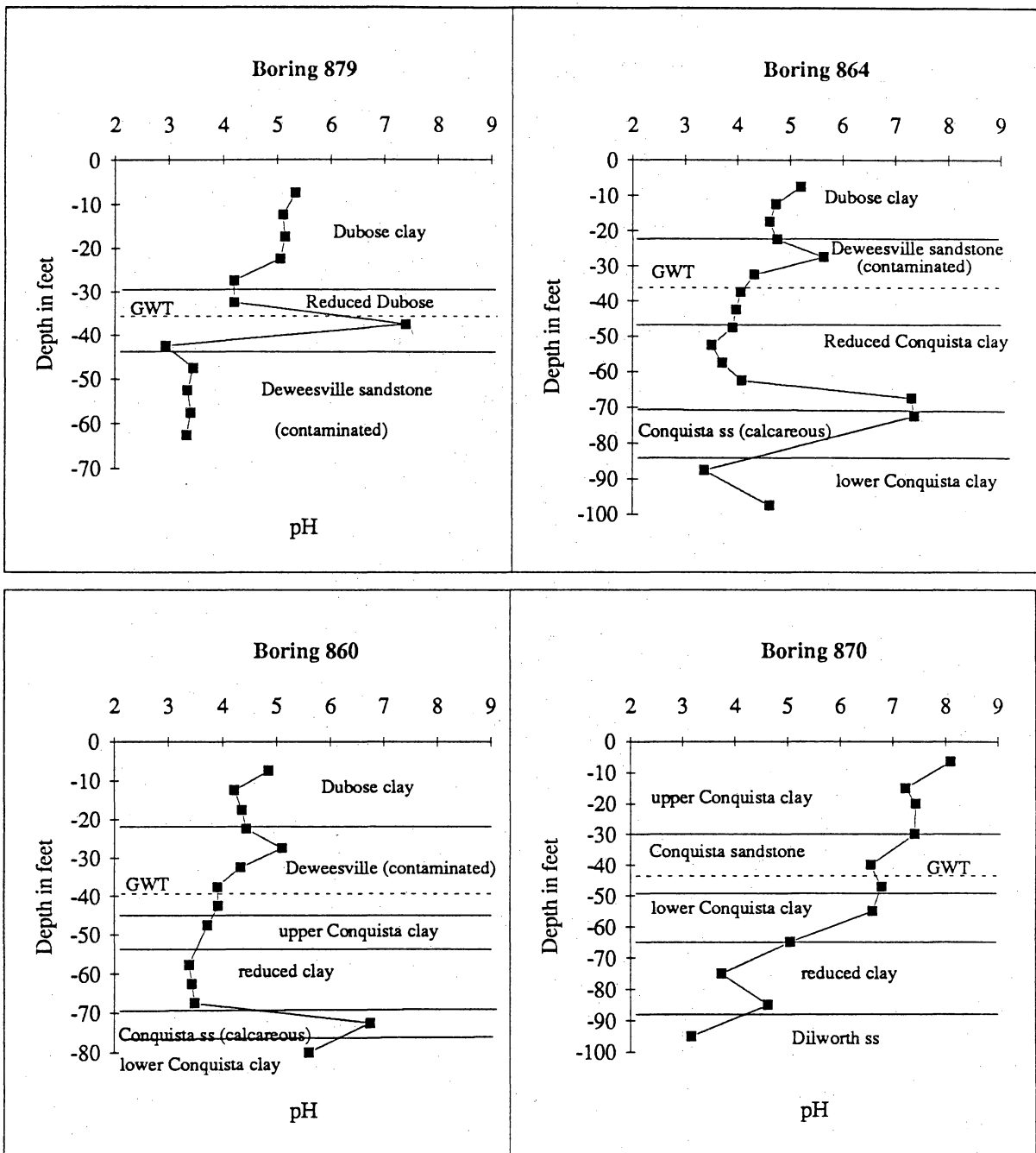


Figure 6.4. pH of leachates from sediments treated with water.

Table 6.1. Results of water leach, core 869.

Sample		1	2	3	4	5	6	7
	units							
Depth	feet	4.5	9	11	15	17	19	21
Type		Fill sand	Fill sand	Fill clay	Fill clay	Tailings sand	Tailings clay	Tailings sand
pH	-	7.66	7.93	8.08	7.79	4.57	3.27	2.85
Eh	millivolts	209	209	202	203	282	551	586
HCO3*	mg/kg	641	626	674	772	-	-	-
Al	mg/kg	4	0	0	0	16.4	10.8	1128
NH3*	mg/kg	-	-	-	-	265	2733	313
Ba	mg/kg	0.16	0.08	0.24	0.08	0.16	0.24	0.24
B	mg/kg	4.4	4.1	5.3	4.4	3.7	5.5	0.3
Ca	mg/kg	816	298	186	1152	2312	2320	2344
Cl	mg/kg	3576	1368	1116	1244	1332	2800	796
Fe	mg/kg	1.04	0.16	0.4	0.16	0.16	91.2	197.6
K	mg/kg	26.8	16.8	14	26	145.6	460	237.2
Mg	mg/kg	40.8	16.8	12	72.4	191.2	548	273.6
Mn	mg/kg	0.08	0.08	0.08	0.08	39.52	86.4	33.6
P	mg/kg	na	na	na	na	na	na	na
Na	mg/kg	2064	1416	1144	1504	1408	2000	684
Si	mg/kg	92	83.2	70	70.8	57.2	328	282.4
Sr	mg/kg	6.96	2.48	1.6	8	21.04	28.88	19.04
SO4	mg/kg	1204	1472	932	4000	8600	16880	14680
e-balance	meq/kg	11	10	11	13	-16	-161	-18
As	mg/kg	na	na	na	na	na	na	na
Cr	mg/kg	<0.24	<0.24	<0.24	<0.24	<0.24	<0.24	0.4
Mo	mg/kg	<0.4	<0.4	<0.4	<0.4	<0.4	3.52	1.76
V	mg/kg	<0.32	<0.32	<0.32	<0.32	<0.32	0.88	1.12
Cd	mg/kg	<0.08	<0.08	<0.08	<0.08	<0.08	0.4	0.32
Co	mg/kg	<0.24	<0.24	<0.24	<0.24	0.32	2.16	1.84
Cu	mg/kg	<0.24	<0.24	<0.24	<0.24	<0.24	0.4	0.64
La	mg/kg	<0.4	<0.4	<0.4	<0.4	<0.4	2.16	1.68
Li	mg/kg	<0.32	<0.32	<0.32	<0.32	<0.32	0.96	0.32
Ni	mg/kg	<0.56	<0.56	<0.56	<0.56	<0.56	1.92	1.28
Zn	mg/kg	<0.16	<0.16	<0.16	<0.16	0.4	6.88	4.4

* Bicarbonate or ammonia estimated from electrical imbalance of the analyses.

Table 6.1 (cont.)

Sample		8	9	10	11	12	13	14
Depth	feet	25	31	35.5	36.5	42.5	45	49.5
Type		Tailings sand	Tailings sand	Tailings sand	Conquista upper clay	Conquista upper clay	Conquista upper clay	Conquista sandstone
pH	-	3.19	2.85	2.92	3.13	3.87	6.72	3.65
Eh	millivolts	556	587	569	587	473	202	502
HCO3*	mg/kg	-	-	-	-	-	258	795
Al	mg/kg	968	1024	1016	792	294.4	1.92	375.2
NH3*	mg/kg	268	902	140	214	361	-	-
Ba	mg/kg	0.24	0.24	0.24	0.16	0.08	0.08	0.16
B	mg/kg	1.2	0.3	0.3	0.9	0.8	0.4	0.3
Ca	mg/kg	2312	2288	2300	2240	2336	2560	1520
Cl	mg/kg	828	740	616	512	436	398	192
Fe	mg/kg	82.4	361.6	476	86.4	2.4	0.16	204
K	mg/kg	216.8	213.6	240.8	376.8	127.6	208	10.8
Mg	mg/kg	279.2	235.2	224.8	251.2	196.8	148.8	182.4
Mn	mg/kg	37.92	26	2.52	21.2	33.92	25.6	19.12
P	mg/kg	na	na	na	na	na	4.96	na
Na	mg/kg	724	596	564	628	524	500	656
Si	mg/kg	108	296.8	279.6	108	33.2	3.44	58
Sr	mg/kg	18.8	22.16	20.68	34.16	5.76	4.08	18.88
SO4	mg/kg	13480	15640	13720	12520	9720	7360	7280
e-balance	meq/kg	-16	-53	-8	-13	-21	4	13
As	mg/kg	na	na	na	na	na	2.4	na
Cr	mg/kg	<0.24	0.88	0.44	<0.24	<0.24	<0.24	0.24
Mo	mg/kg	1.6	3.6	3.6	2.08	<0.4	5.36	0.4
V	mg/kg	0.48	1.76	2.72	0.88	<0.32	<0.32	0.32
Cd	mg/kg	0.32	0.32	0.4	0.24	0.16	<0.08	0.16
Co	mg/kg	1.36	2.64	3.24	1.12	0.48	<0.24	1.36
Cu	mg/kg	0.32	0.4	0.24	0.24	<0.24	<0.24	0.32
La	mg/kg	1.6	1.36	1.4	1.52	<0.4	<0.4	0.64
Li	mg/kg	0.48	0.4	0.36	0.4	<0.32	<0.32	0.32
Ni	mg/kg	1.04	1.28	1.64	0.72	<0.56	<0.56	0.56
Zn	mg/kg	3.84	5.2	4.56	3.68	2.16	<0.08	3.04

* Bicarbonate or ammonia estimated from electrical imbalance of the analyses.

Table 6.1 (cont.)

Sample		15	16	17	18	19	20
Depth	feet	55	59	65	70	78	85
Type		Conquista sandstone	Conquista lower clay	Conquista lower clay oxidized	Conquista lower clay oxi/red	Conquista lower clay oxi/red	Conquista lower clay reduced
pH	-	3.46	3.48	6.48	3.5	3.12	7.28
Eh	millivolts	485	526	261	536	579	189
HCO3*	mg/kg	139	1431	243	400	778	355
Al	mg/kg	512	692	9.84	5.6	17.44	3.12
NH3*	mg/kg	-	-	-	-	-	-
Ba	mg/kg	0.24	0.16	0.08	0.08	0.08	0.08
B	mg/kg	0.5	0.6	2.6	1.8	0.3	1.1
Ca	mg/kg	1976	2248	126	740	1680	129
Cl	mg/kg	504	508	1820	448	325	180
Fe	mg/kg	148.8	310.4	2.24	30.8	354.4	1.08
K	mg/kg	39.6	38.8	15.6	74	130.8	46.4
Mg	mg/kg	212	584	15.28	95.2	196.8	15.4
Mn	mg/kg	27.76	140	0.04	5.6	24.64	0.4
P	mg/kg	na	na	4.96	na	4.96	4.96
Na	mg/kg	564	1208	1152	1008	1088	624
Si	mg/kg	25.2	90.4	113.6	90.4	158.4	54.4
Sr	mg/kg	16.96	15.6	1.2	7.28	15.76	1.12
SO4	mg/kg	9080	12960	222.4	3552	6960	1244
e-balance	meq/kg	2	23	4	7	13	6
As	mg/kg	na	na	2.4	na	2.4	2.4
Cr	mg/kg	<0.24	<0.24	<0.24	<0.24	<0.24	<0.24
Mo	mg/kg	<0.4	<0.4	<0.4	<0.4	<0.4	0.64
V	mg/kg	<0.32	<0.32	<0.32	<0.32	<0.32	<0.32
Cd	mg/kg	0.16	0.4	<0.08	0.16	<0.08	<0.08
Co	mg/kg	1.2	3.6	<0.24	1.84	2.24	<0.24
Cu	mg/kg	0.32	0.32	<0.24	<0.24	<0.24	<0.24
La	mg/kg	0.56	0.88	<0.4	<0.4	<0.4	<0.4
Li	mg/kg	<0.32	0.56	<0.32	<0.32	0.4	<0.32
Ni	mg/kg	<0.56	1.44	0.56	1.04	0.96	<0.56
Zn	mg/kg	3.04	6.32	<0.16	0.56	9.76	<0.08

* Bicarbonate or ammonia estimated from electrical imbalance of the analyses.

Table 6.2. Results of acid leach, core 869.

Sample		2	4	6	8	10	12	13	17	18
	units									
Depth	feet	9	15	19	25	35.5	42.5	45	65	70
Type		Fill	Fill	Tailings	Tailings	Tailings	Conq. up. clay	Conq. up. clay	Conq. lwr. clay	Conq. lwr. clay
pH		-	-	-	-	-	-	-	-	-
Eh	millivolts	-	-	-	-	-	-	-	-	-
HCO3*	mg/kg	-	-	-	-	-	-	-	-	-
Al	mg/kg	69.6	287.2	1552	920	928	864	1096	44.56	37.04
NH3*	mg/kg	-	-	-	-	-	-	-	-	-
Ba	mg/kg	1.84	1.36	0.56	0.4	0.56	0.08	0.48	2.4	0.56
B	mg/kg	7.0	7.2	4.6	0.9	0.3	0.4	0.3	1.4	0.9
Ca	mg/kg	4504	11120	7208	5296	5040	4968	2344	2504	2192
Cl	mg/kg	-	-	-	-	-	-	-	-	-
Fe	mg/kg	6.72	9.28	736	402.4	759.2	152	391.2	11.12	266.4
K	mg/kg	69.2	92.8	640.8	278.4	331.2	226.4	46.4	252.8	243.2
Mg	mg/kg	205.6	406.4	583.2	252.8	202.4	261.6	221.6	277.6	275.2
Mn	mg/kg	19.84	50.64	93.6	33.36	21.84	46.16	24.72	2.72	11.92
P	mg/kg	43.04	18.56	61.44	22.16	35.28	15.6	23.12	7.04	13.84
Na	mg/kg	2208	2040	2056	720	584	552	1448	1424	1480
Si	mg/kg	872	968	1328	444.8	412	572.8	434.4	848	628
Sr	mg/kg	30.56	42.4	56.24	33.76	36.88	15.52	35.44	24	23.36
SO4	mg/kg	-	-	-	-	-	-	-	-	-
e-balance	meq/kg	-	-	-	-	-	-	-	-	-
As	mg/kg	<2.4	<2.4	22.8	7.44	9.92	<2.4	<2.4	<2.4	<2.4
Cr	mg/kg	<0.24	0.24	0.48	0.4	0.48	0.72	<0.24	<0.24	<0.24
Mo	mg/kg	<0.4	0.4	24.16	16.08	16	<0.4	<0.4	<0.4	<0.4
V	mg/kg	0.8	<0.32	5.92	1.76	6.4	2.96	2.96	<0.32	<0.32
Cd	mg/kg	<0.08	<0.08	0.4	0.24	0.32	0.16	0.16	<0.08	1.76
Co	mg/kg	0.4	0.8	4.72	2.8	4.8	1.2	2.4	<0.24	6.08
Cu	mg/kg	<0.24	<0.24	1.2	0.64	0.24	0.24	0.48	<0.24	<0.24
La	mg/kg	<0.4	1.76	4.72	2.32	2	0.48	4.64	<0.4	0.48
Li	mg/kg	<0.4	0.64	0.88	0.32	0.32	0.32	0.48	0.48	0.32
Ni	mg/kg	<0.56	<0.56	2.16	0.96	1.6	0.8	<0.56	<0.56	2.56
Zn	mg/kg	<0.16	0.4	7.84	3.76	4	3.52	4.72	0.96	2.48

Cd	Co	Cu	La	Li	Ni	pH	Al	As	Cr	Mo	V	Zn
0.08	0.24	<0.24	<0.4	<0.32	<0.56	7.66	4	na	<0.24	<0.4	<0.32	<0.16
0.08	0.24	<0.24	<0.4	<0.32	<0.56	7.93	0	na	<0.24	<0.4	<0.32	0.16
0.08	0.24	<0.24	<0.4	<0.32	<0.56	8.08	0	na	<0.24	<0.4	<0.32	0.16
0.08	0.24	<0.24	<0.4	<0.32	<0.56	7.79	0	na	<0.24	<0.4	<0.32	0.16
0.08	0.32	<0.24	<0.4	<0.32	<0.56	4.57	16.4	na	<0.24	<0.4	<0.32	0.4
0.4	2.16	0.4	2.16	0.96	1.92	3.27	10.8	na	<0.24	3.52	0.88	6.88
0.32	1.84	0.64	1.68	0.32	1.28	2.85	1128	na	0.4	1.76	1.12	4.4
0.32	1.36	0.32	1.6	0.48	1.04	3.19	968	na	<0.24	1.6	0.48	3.84
0	3	0	1	0	1	3	1024	na	1	4	2	5
0.4	3.24	0.24	1.4	0.36	1.64	2.92	1016	na	0.44	3.6	2.72	4.56
0.24	1.12	0.24	1.52	0.4	0.72	3.13	792	na	<0.24	2.08	0.88	3.68
0.16	0.48	<0.24	<0.4	<0.32	<0.56	3.87	294.4	na	<0.24	<0.4	<0.32	2.16
0.1	0.2	<0.24	<0.4	<0.32	<0.56	6.7	1.9	2.4	<0.24	5.4	<0.32	0.1
0	1	0	1	0	1	4	375	na	0	0	0	3
0.16	1.2	0.32	0.56	<0.32	<0.56	3.46	512	na	<0.24	<0.4	<0.32	3.04
0.4	3.6	0.32	0.88	0.56	1.44	3.48	692	na	<0.24	<0.4	<0.32	6.32
0.08	0.24	<0.24	<0.4	<0.32	0.56	6.48	9.84	2.4	<0.24	<0.4	<0.32	0.16
0.16	1.84	<0.24	<0.4	<0.32	1.04	3.5	5.6	na	<0.24	<0.4	<0.32	0.56
0.08	2.24	<0.24	<0.4	0.4	0.96	3.12	17.44	2.4	<0.24	<0.4	<0.32	9.76
0.08	0.24	<0.24	<0.4	<0.32	<0.56	7.28	3.12	2.4	<0.24	0.64	<0.32	0.08
0.08	0.4	<0.24	<0.4	<0.4	<0.56			<2.4	<0.24	<0.4	0.8	0.16
0	1	<0.24	2	1	<0.56			<2.4	0	0	<0.32	0
0.4	4.72	1.2	4.72	0.88	2.16			22.8	0.48	24.16	5.92	7.84
0.24	2.8	0.64	2.32	0.32	0.96			7.44	0.4	16.08	1.76	3.76
0.32	4.8	0.24	2	0.32	1.6			9.92	0.48	16	6.4	4
0.16	1.2	0.24	0.48	0.32	0.8			<2.4	0.72	<0.4	2.96	3.52
0.16	2.4	0.48	4.64	0.48	<0.56			<2.4	<0.24	<0.4	2.96	4.72
<0.08	<0.24	<0.24	<0.4	0.48	<0.56			<2.4	<0.24	<0.4	<0.32	0.96
1.76	6.08	<0.24	0.48	0.32	2.56			<2.4	<0.24	<0.4	<0.32	2.48

STRATAMODEL (SECTION 7)

Methods

StrataModel (copyright Silicon Graphics, Inc.) is a computer program for creating three-dimensional displays of stratigraphic units and parameters within those units. Stratigraphic surfaces, hydrologic data, and hydrochemical data for the Falls City UMTRA site were entered into the program to see if (1) contaminant distribution could be effectively mapped, (2) volumes of contaminated sediments could be computed, and (3) movement could be monitored in three dimensions. Time constraints limited us to mapping contaminant distribution.

StrataModel is a powerful tool for visualizing contaminant plumes in three dimensions. Once a model is created, the display can be viewed from any angle, cross sections and maps can be drawn, and volumes of selected features can be computed. However, the process of creating the model is time consuming. For the model to be realistic and to avoid errors in stratigraphy, traditional methods of mapping must be done first so that the scientist has a thorough understanding of what the model should look like.

The first step in creating a model is to build the stratigraphic framework. This requires a large number of control points to create a model with good resolution. Core logs, cuttings logs, and geophysical logs from 168 borings were used to create the model of the Falls City site. Each of these logs was carefully reviewed and tops of stratigraphic units recorded. The stratigraphic data are provided in table 6 of the appendix. Once the stratigraphic tops of units at the site were picked, topographic maps of land surface and stratigraphic surfaces (unit tops) were plotted (using a digitizing program—CPS) and then contoured, either by the CPS program or by hand if the results of the computer contouring were unrealistic. Each of the contour maps were then digitized creating a file of x, y, and z coordinates for a network of grid points. This grid has hundreds of data

points surrounding each borehole. As our understanding of the stratigraphy evolved, some stratigraphic picks were changed. Whenever a stratigraphic pick was changed, the entire set of maps had to be recontoured and redigitized, a time-consuming task.

To use StrataModel each contour data file is merged into a single computer file, which is transported to StrataModel. StrataModel builds a stratigraphic model from that file, consisting of stratigraphic layers referenced to an absolute elevation datum and divided into a three-dimensional grid. Locations of monitoring wells are then digitized, and that file transported to an electronic spreadsheet program, where additional data, such as chemical data, are added to the file. For each monitoring well, a depth grid is established and each cell of the grid must have a parameter value assigned to it, even if it is a null value. This spreadsheet is then transported to StrataModel, where the parameter values are assigned to the three-dimensional grid. StrataModel allows the operator to view the distribution of parameter values (assigned colors) within the stratigraphic or topographic framework.

Three-Dimensional Views of Contaminant Plumes

The surface geology and topography of the Falls City UMTRA site is shown in figure 7.1. There are some minor errors in this map (for example the green topographic "spike" at the far northeast corner), but the general geology and topography are accurate. Note that the Dubose (yellow) crops out at higher elevations along the southeast edge of the site. Deweesville outcrops (light green) extend beneath the tailings (red). Conquista outcrops (green and lighter blue) also extend under tailings and crop out along the lower reaches of the Tordilla Creek drainage at the south end of the site and along the Scared Dog Creek drainage extending from the tailings in the center of the figure toward the northeast (fig. 7.1). Dilworth outcrops (dark blue) are located along the north edge of the site and do not intersect tailings.

The distribution of aluminum in the Deweesville sandstone is shown in figure 7.2. The aluminum values (as colors) are mapped on the top of the Deweesville sandstone. This top combines both surface topography at the outcrop with structural topography in the subsurface. Data from tailings piles are not included. Only data from within the Deweesville are displayed. Structural dip is toward the southeast. The roughly north-south trough in the top of the Deweesville is a portion of the Tordilla Creek drainage running across the Deweesville outcrop toward tailings pile 2. The trough is not a structural feature. Two acid, aluminum-bearing, contaminant plumes are mapped, one associated with tailings pile 2 (pink, red, and yellow area, indicating aluminum greater than 10 mg/L), and a second plume to the south (yellow only; fig. 7.2) probably associated with tailings piles 4 and 5. The migration of the southern plume toward the southeast (downdip) and southwest (down the Tordilla Creek drainage) is readily seen.

Figures 7.3 and 7.4 show the distribution of aluminum and calcium in the Conquista sand. Again, the data are within only the Conquista sand and are plotted on the top of the sandstone. Structural dip is to the southeast. The north-south ridge on the top of the Conquista is caused by an error in geologic mapping, where sandy alluvium and upper Conquista clay at outcrop were misidentified as Conquista sand. The distribution of aluminum indicates three plumes, one in the northeast (red) associated with tailings pile 3, a second (yellow) in the northwest under tailings piles 7 and 1, and a third (yellow) in the southeast at the outcrop of the Conquista sand along Tordilla Creek. The latter is a continuation of the southern plume migrating down Tordilla Creek within the Deweesville (compare figs. 7.2 and 7.3). Note that the amount of aluminum in the two western area plumes (yellow areas) is small (<5 mg/L) and thus these plumes have low acidity. Calcium concentrations in the Conquista sand delineate a large area where high-acidity contaminants have reacted with calcite beneath and surrounding tailings pile 7 (red and yellow areas, fig. 7.4). The results of chemical mapping using StrataModel are in good agreement with the hand-drawn maps provided in section 4.

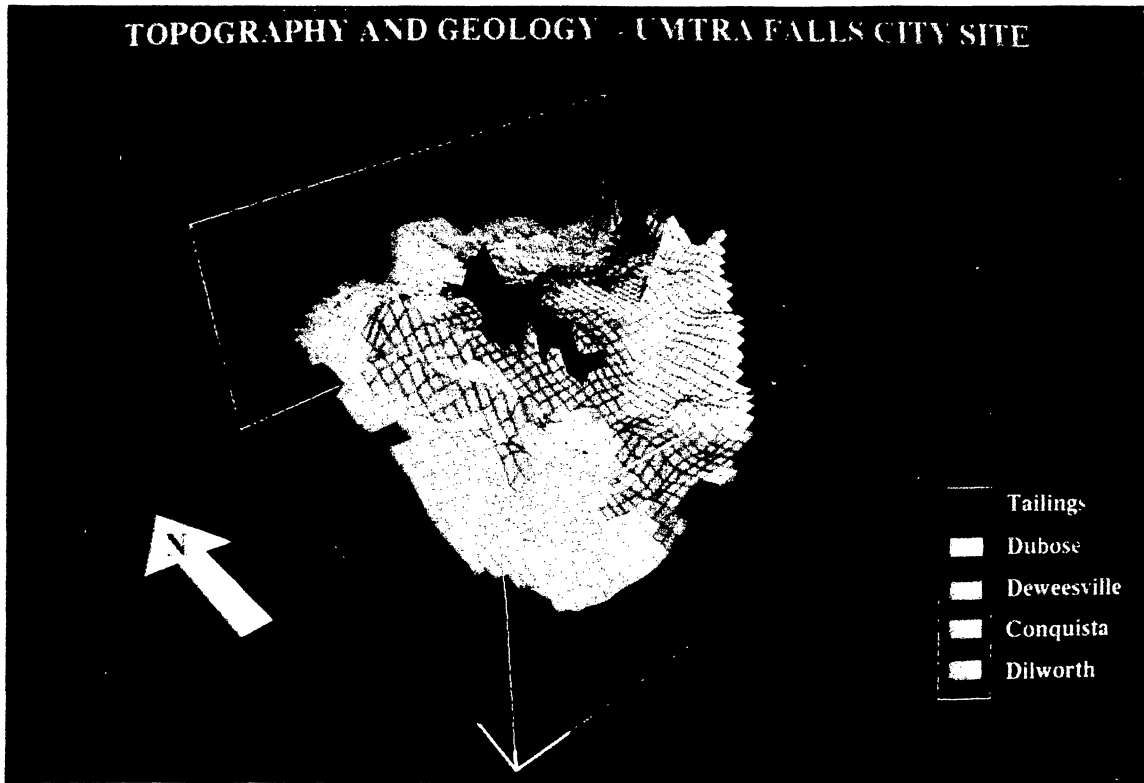


Figure 7.1. Geology and topography of Falls City UMTRA site (StrataModel).

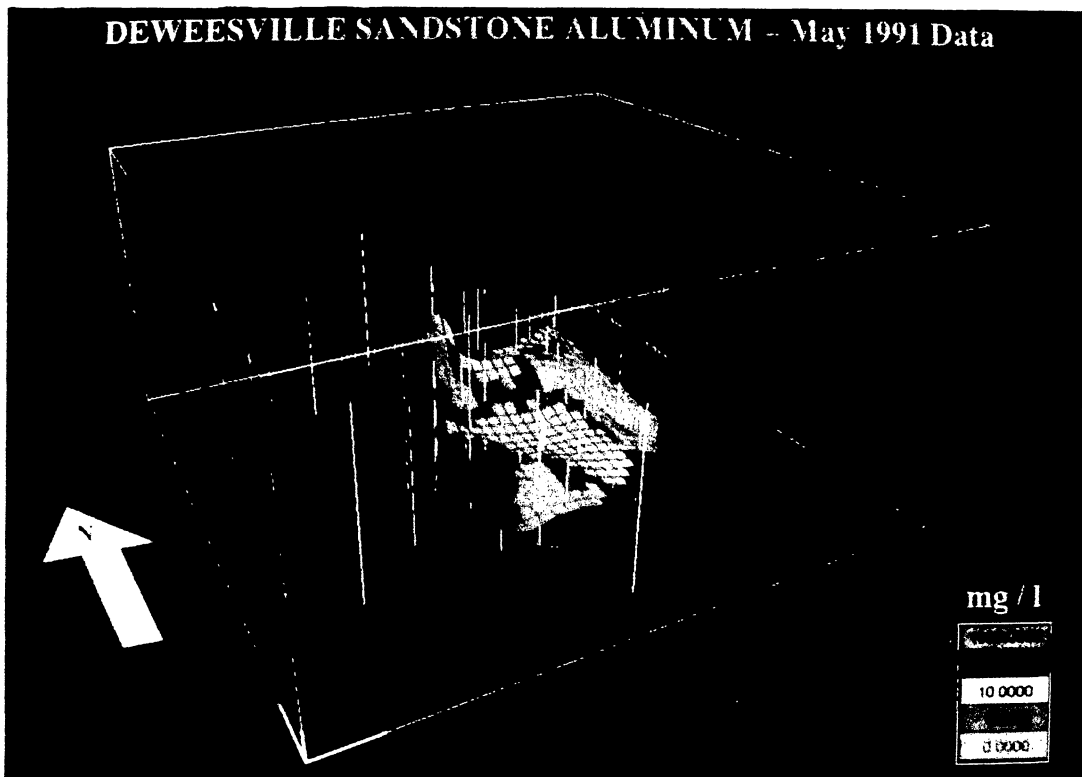


Figure 7.2. Aluminum concentration in Deweesville sandstone aquifer (StrataModel).

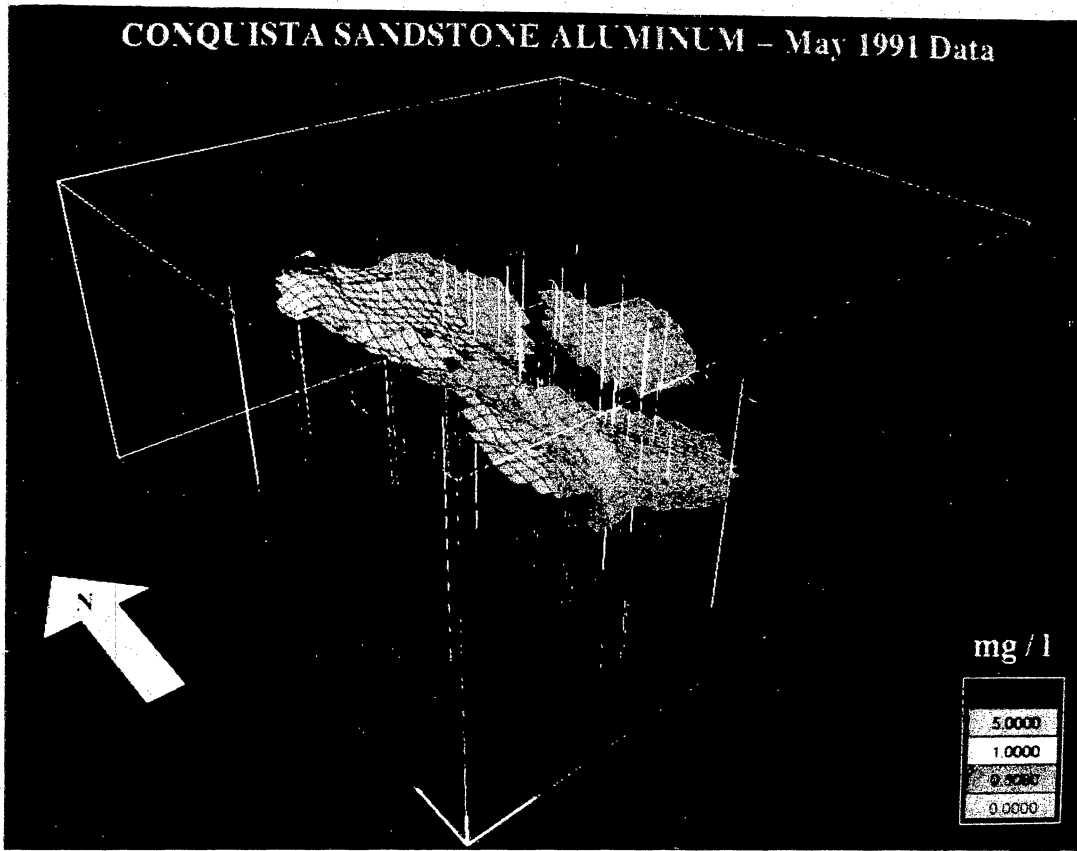


Figure 7.3. Calcium in Conquista fossiliferous sandstone aquifer (StrataModel).

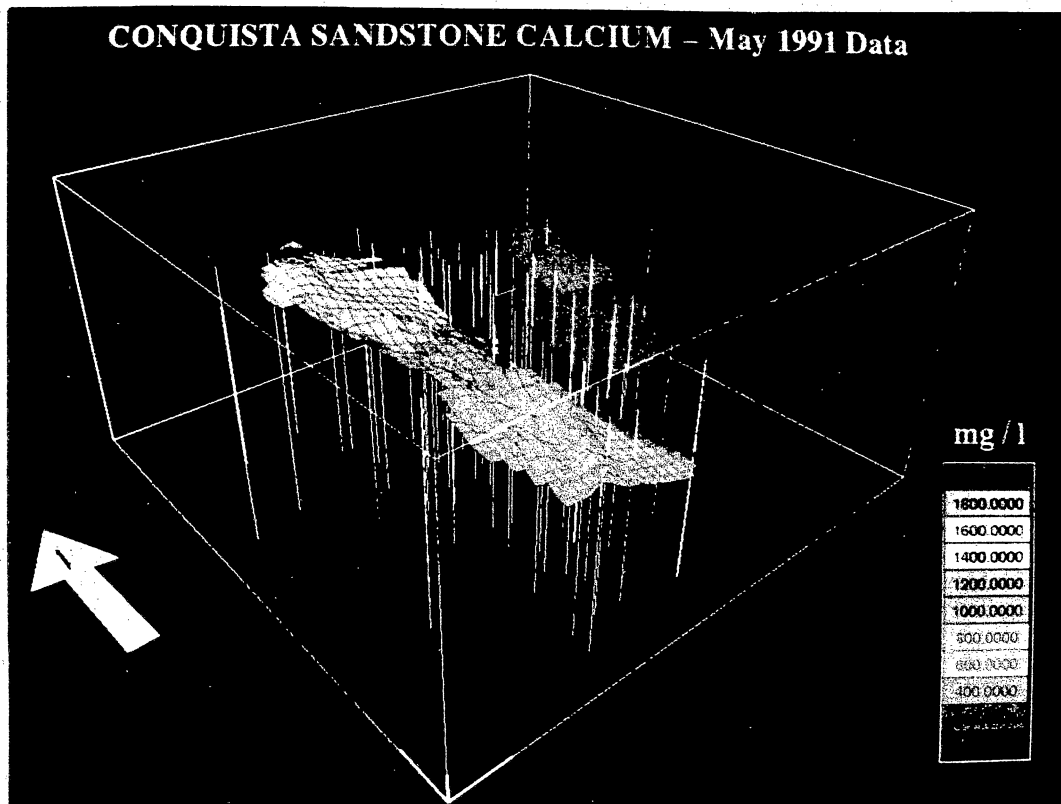


Figure 7.4. Aluminum in Conquista fossilifersou sandstone aquifer (StrataModel).

CONCLUSIONS (SECTION 8)

Geologic Framework

Tailings piles were placed on and within sandstone and claystone units of the Whitsett Formation. These units dip toward the south-southeast, and erosion has produced a series of cuestas. The tailings piles are located on the dip slope of one of these cuestas.

The principal units in direct contact with tailings are the Deweesville Sandstone Member and Conquista clay Member of the Whitsett Formation. The Conquista is further divided into an upper clay unit, middle sandstone unit, and a lower clay unit. Previous hydrologic and hydrochemical studies combined the Conquista and Deweesville members as the Deweesville/Conquista aquifer. These data were mapped together as part of the "uppermost aquifer" (as defined by the Code of Federal Regulations, 40CFR192). The present study treats each lithologic unit (Deweesville sandstone, upper Conquista clay, Conquista sand, and lower Conquista clay) as a separate aquifer and geochemical unit. As a result, maps of potentiometric surfaces and ground-water contamination display good resolution, and geochemical processes, especially neutralization by calcite, are apparent.

Beneath and adjacent to the tailings piles is a third member of the Whitsett Formation, the Dilworth sandstone. The Dilworth is not in direct contact with tailings, and thus contaminants must pass through other geologic units before reaching the Dilworth. The Dilworth is a fine-grained quartz sandstone with interbedded silt, clay, and lignite. It ranges from 20 to 43 ft in thickness. It is underlain by the Manning Formation and overlain by 30 to 44 ft of lower Conquista clay (except in areas of outcrop located north of the tailings area). Above the lower Conquista clay is the Conquista fossiliferous sandstone. The Conquista sand thickness is 20 to 25 ft near outcrop but thins to 5 ft of clayey sandstone south of the tailings area. Tailings pile 7 is

located on its outcrop. The Conquista sand is fine to medium grained, silty and bentonitic, and shell intervals are common, although in the oxidized, updip areas, shell material has been leached by natural processes leaving only shell molds, in some cases filled with gypsum and iron hydroxides.

The Conquista sand is overlain by the upper Conquista clay, a silty, bentonitic clay with numerous gypsum and iron hydroxide filled fractures in the oxidized, updip areas near the tailings. Layers of large carbonate concretions are found in both the upper and lower Conquista clays, and this carbonate, as well as shell debris and perhaps some caliche, has generally neutralized the acidic effluent migrating through the Conquista from pile 7.

The uppermost unit in contact with the tailings is the Deweesville Sandstone Member. The Deweesville was mined for uranium at the mill site, and tailings were placed into open-pits within the Deweesville. The sandstone ranges in thickness from 46 ft to an erosional feather edge. It is a tuffaceous fine- to coarse-grained sandstone that contains lignite, clay, volcanic ash, and bentonite. Gypsum-filled fractures are prevalent, and silica- and carbonate-cemented zones occur locally.

A clay-filled channel in the Deweesville on the site is described in reports of the USGS. The clay was thought to have influenced the uranium ore deposition, and would have influenced ground-water and contaminant movement in the sandstone. However, the clay channel has not been identified in this study. It may have been removed by mining operations and is no longer a factor in ground-water or contaminant movement at the site.

Tailings Leakage

The tailings piles are leaking acidic solutions into the Deweesville and Conquista Members of the Whitsett Formation. This leakage probably began during milling operations in the 1960's and early 1970's and, by 1976, water-level data had

documented a ground-water mound beneath the piles. Water levels increased further during in situ leach operations (within the tailings piles) during the late 1970's and early 1980's. Hydrologic connection between the tailings pile solutions and the ground water is indicated by good correlations between water-level changes in pile 2 and water-level changes in surrounding monitoring wells during the period of in situ leach operations.

Prior to tailings disposal, the upper Conquista, Conquista sand, and the Deweesville were probably dry near outcrop. Thus, shallow ground waters at the Falls City UMTRA site are actually tailings solutions that have saturated the sediment. The chemical composition of these solutions has changed because of reactions with the sediment.

Tailings Hydrochemistry

Tailings solutions are composed of dissolved neutral salts of aluminum and ammonium sulfate with lesser amounts of iron, calcium, magnesium and potassium sulfate, and sodium chloride. These salts were created by reaction of sulfuric acid with aluminosilicates and oxides in the ores. Those reactions also produced soluble salts of trace metals including the cation species beryllium, cadmium, cobalt, copper, nickel, zinc, and radium, and the anion species arsenate, chromate, molybdate, selenite, uranyl, and vanadate. Trace metals that form relatively insoluble oxidized chloride or sulfate salts (barium, silver, mercury, and lead) are generally in concentrations that are below detection in the tailings.

Hydrolysis of aluminum sulfate produces the acid pH (pH 3 to 4) of the tailings solution. Aluminum sulfate is a strong pH buffer and controls the acidity of the solutions. This buffer explains the cluster of tailings and ground waters in the range of pH 3 to pH 4. A second cluster in the range of pH 6 to pH 7 is due to buffering by carbonate.

Cation trace metals are held in solution as long as the pH remains in the range of 3 to 4. Buffering of the pH by aluminum is thus the primary control on cation trace metal

concentrations in the tailings solutions and ground water. These metals include beryllium, cadmium, cobalt, nickel, and zinc. Precipitation of aluminum and iron hydroxides has little effect on these cation trace metal concentrations. Only the neutralization, by calcium carbonate, of aluminum- and iron-depleted solutions results in a substantial decrease in cation trace metal concentrations. These reactions do not have a significant effect on selenite, an anionic species.

The bromide concentrations of the tailings solutions are variable, but those with higher chloride concentrations are relatively depleted in bromide when compared to natural ground waters. Thus, a high chloride-to-bromide ratio, probably related to the addition of chloride reagents during processing, serves as a tracer for tailings solutions in the aquifers.

Reactions of Tailings Solutions with Sediments

The tailings solutions and acid ground waters are equilibrated with the common aluminosilicates and will not significantly react with those minerals. However, two types of reactions do modify the composition of the tailings solutions as they migrate through the sediments: cation exchange and neutralization by calcium carbonate (calcite).

Ground waters at the site are in equilibrium with cation exchangers, predominantly calcium smectite. Exchange reactions between those smectites and migrating tailings solutions probably result in near-total removal of ammonium and considerable decreases in sodium, strontium, magnesium, and potassium. These ions are exchanged for calcium, which then precipitates as gypsum, resulting in a decrease in sulfate concentrations. Geochemical modeling suggests that about 40 percent of the sulfate decrease in migrating tailings solutions is due to cation exchange and gypsum precipitation. The postulated exchange reactions could be proved with further study of available core. One possibly important effect of precipitation of gypsum could be the coprecipitation of

²²⁶Ra. Radium concentrations in acidic ground waters adjacent to tailings piles are 10 to 20 percent of those in the tailings piles, and either cation exchange or coprecipitation with gypsum as a result of cation exchange may contribute to this decrease.

Neutralization of the tailings solutions is predominantly a reaction of aluminum sulfate with calcite to produce a basic aluminum salt. A mere 0.05 volume percent of calcite will neutralize an average tailings solution migrating through sediment. These reactions will have only a negligible effect on porosity and permeability. Neutralization by calcite also results in further precipitation of gypsum. Geochemical modeling suggests that about 60 percent of the sulfate decrease in migrating tailings solutions is due to neutralization reactions.

In contrast, neutralization of a tailings solution by mixing with a typical alkaline bicarbonate water requires a large volume of alkaline water (>90 percent) due to the buffering capacity of aluminum sulfate. Conversely, mixing less than 10 percent of tailings solutions with an alkaline water will produce acid (pH <4) ground waters. Thus, pH is a sensitive indicator of small amounts of contamination, and aluminum is a direct indicator of the remaining acidity of the contaminant.

Both cation exchange and neutralization by calcite result in decreased sulfate and increased calcium concentrations due to reaction of tailings solutions with sediments. Acidic, partially neutralized contaminants are distinguishable from acidic tailings solutions by high calcium concentrations (>900 mg/L). Completely neutralized tailings solutions (pH >6) are distinguishable from natural ground waters (pH >6) by high calcium concentrations as well (>900 mg/L).

No single parameter identifies contaminants in the aquifers. Only an understanding of the chemistry of the contaminants and chemical processes affecting the contaminants provides a clear delineation of the plume geometries.

Delineation of the Contaminant Plumes

Three hydrogeologic units are important in understanding the setting of contaminant migration from the tailings disposal. These are the Deweesville, Conquista, and Dilworth aquifers. Within two of these units, the Deweesville and Conquista, hydrologic and geochemical mapping has defined at least four contaminant plumes in the western area of the site, associated with tailings piles 1, 2, 4, 5, and 7, and perhaps three more plumes in the eastern area, near pile 3, although data are too limited to accurately map the contamination. A map of all seven plumes is provided in figure 8.1. The boundaries of these plumes, as defined by more than 1 part per million (ppm) aluminum in acid plumes, or more than 1,000 ppm calcium in neutralized plumes, probably represent the limits of detectable contamination at the site.

Deweesville

The Deweesville sandstone crops out across the Falls City UMTRA site where tailings piles 2, 4, and 5 are located and also crops out further to the east (in the area of pile 3). Most of the tailings piles are located on the Deweesville because it was the host formation for the uranium mining, and disposal of tailings, subsequent to initial mining, occurred in the abandoned pits. Ground water is recharged at higher elevations by leakage from the tailings piles. It flows down hydraulic gradient and discharges to the eastern tributary of Tordilla Creek or continues to flow downdip into the subsurface. The disposal of tailings into the old pits and onto the outcrop of the Deweesville has resulted in a ground-water mound in the Deweesville. Water levels have risen to as much as 16 ft beneath the piles and 12 ft downdip in the aquifer. In the outcrop of the Deweesville, there was very little ground water prior to mining and milling operations. The mound has developed from the long-term tailings disposal and has been relatively stable since 1976. It is not solely the result of SEI's in situ leach operations. Correlation

of changes in water levels in pond 2 and ground-water levels in the Deweesville proximal to pond 2 during SEI's in situ leach operations confirms that there has been leakage from the piles into the underlying aquifers.

Analysis of the distribution of pH, aluminum, and TDS indicates two sources, tailings pile 2 and tailings piles 4 and 5, for two acid plumes in the Deweesville in the western area of the site (shown as two aluminum plumes in fig. 8.1). Decreases in aluminum concentrations and increases in calcium concentrations away from both these sources indicate partial to complete neutralization of the plumes. Concurrent increases in chloride suggest evaporative concentration along the flow paths. Low chloride concentrations suggest a local fresh-water recharge point associated with the water-filled SWI pit.

There is good agreement between (1) the extent of the geochemical plumes and the extent of the ground-water mound in the Deweesville, and (2) the hydrologic potential for flow and observed areal trends in contaminants. Notably, both hydrologic flow potentials and geochemical trends indicate (1) eastward and southeastward migration of contaminants from the tailings pile 2 toward Scared Dog Creek and its tributaries, (2) south and southeastern migration from piles 4 and 5 toward Conquista Creek, and (3) southwestward migration from piles 4 and 5 into the Tordilla Creek drainage. Data in the area of pile 3 are too few to map, but pH, aluminum, TDS, and calcium concentrations suggest that an acid plume may extend about 1,000 ft southeast from the tailings pile (the southern aluminum plume shown in fig. 8.1).

Total dissolved solids, sodium, sulfate, bicarbonate, and molybdenum indicate a small, nonacid, sodium-sulfate-sodium bicarbonate contaminant with high molybdenum content located in the vicinity of monitoring well 836 (fig. 8.1), just north of the old mill site. The source is probably sludge pits located north of monitoring well 836, between tailings piles 1, 2, and 7. Water chemistry indicates that solutions dumped in this pit included those from the uranium precipitation stage of processing.

Color changes in the sediments logged from core by BEG and by McCulloh and Roberts (1981) indicate that each sandstone (Deweeseville, Conquista, and Dilworth) has a downdip zone in which oxidized sediments grade into reduced sediments. Figure 8.2 is a map of these oxidation-reduction (redox) boundaries. Contaminant plumes in the Deweesville are generally located in the oxidized section of the Deweesville (north of the Deweesville redox boundary), although the southern margins of the plumes are at or slightly within the reduced zones. Potential effects of reduction of contaminants by sulfides associated with the reduced sediments have not been addressed in this report.

Conquista

The Conquista aquifer is composed of three units: an oxidized and fractured upper Conquista silty clay, a Conquista sandstone, and a relatively impermeable lower Conquista clay. These rock units are nearshore marine in origin and contain numerous shell fragments. The Conquista sand is a relatively thick nearshore-marine sandstone in outcrop. It thins and becomes clayey and silty downdip. This sandstone pinchout provides a downdip hydrologic barrier to ground-water flow. The Conquista sand extends downdip into the subsurface, but thins significantly and becomes more silty and laminated.

Ground-water flow in the overall Conquista aquifer is under water-table conditions and follows topography. The Conquista sand generally is confined. Recharge is considered to occur both where the Conquista sand crops out and through the fractured, oxidized upper Conquista. Ground water flows in a strike direction toward Tordilla Creek (to the south) and Scared Dog Creek (to the east and southeast). Discharge is considered to be dominated by evapotranspiration in the region of the creeks.

Emplacement of the tailings piles has resulted in an elevated potentiometric surface in the Conquista. Water levels beneath pile 7 may be as much as 40 ft over

background hydrologic conditions. The size of the contaminant mound permits ground-water flow and therefore contaminants from the tailings piles to migrate (1) north and west toward the outcrop of the Conquista sand, (2) east and southeast toward Scared Dog Creek and its tributaries, and (3) south and southwest toward Tordilla Creek and its tributaries (fig. 8.1). The predominant direction of flow appears to be southwest toward Tordilla Creek. The pinch-out of the sands in the Conquista sand downdip (south) probably forces the ground water to flow toward Tordilla Creek rather than down the structural gradient into the deeper subsurface (fig. 8.1).

The updip section of the Conquista sand and upper Conquista clays probably were unsaturated and similar to the unsaturated outcrops of the Deweesville and Dilworth. Most water in the updip section of the Conquista, therefore, is tailings fluid and not natural ground waters.

Data on TDS, pH, and chloride concentrations indicate at least two sources of ground-water contamination of the Conquista sand by tailings solutions, one located along the north edge of tailings pile 7 (near monitoring well 701), and the other located at the confluence of the north and east tributaries of Tordilla Creek (near monitoring well 919).

The map of the potentiometric surface indicates a large ground-water mound centering on tailings pile 7. Geochemical mapping also delineates a large calcium-rich plume associated with tailings pile 7 comprised of tailings solutions neutralized by calcite (the western calcium plume shown in fig. 8.1). This interpretation is strongly supported by the spatial distributions of TDS, pH, aluminum, calcium, chloride, selenium, carbon dioxide partial pressures, calcite saturation indices, and gypsum saturation indices. In addition to the increase in calcium and decrease in sulfate associated with the neutralization reaction, there are major decreases in other chemical parameters, especially ammonium but also in sodium, potassium, and magnesium. Cation trace metals

also decrease to near-background levels, as do radium, molybdenum, vanadium, chrome, arsenic, and uranium. Selenium, however, remains in solution.

A second source of contamination to the Conquista sand is discharge from the southwest-trending plume in the Deweesville. This acid plume is part of the large acidic plume in the Deweesville that migrates from the Deweesville, into the sandy alluvium and upper Conquista shale subcrop beneath Tordilla Creek, down the creek as underflow, and into the Conquista sandstone subcrop beneath the alluvium (fig. 8.1). This interpretation is based upon consistent trends in pH, aluminum, TDS, calcium, and chloride along this proposed flow path. There is also evidence for a neutralized plume in the Conquista sand beneath tailings pile 3 (the northeast calcium plume shown in fig. 8.1).

Dilworth

The Dilworth aquifer is beneath the Deweesville and Conquista units. The potentiometric surface is far below water levels in the Deweesville and Conquista, thus providing a potential for downward leakage of ground water from the overlying aquifers. Exploration drilling by SWI provided numerous pathways for this leakage. Fortuitously, SWI drilling was, in general, not in the region of the tailings piles.

There are several discrete ground-water mounds in the Dilworth, but only two show slight evidence of ground-water contamination. In other mounds, leakage from the Deweesville and Conquista into the underlying Dilworth is in areas where contaminated ground waters are absent.

Both hydrologic and geochemical data indicate localized vertical leakage of tailings solutions into the Dilworth near monitoring wells 878 and 905. In both wells, the solutions have been neutralized by calcite. Except in monitoring well 905, chloride-to-bromide ratios in the Dilworth are generally the same as those expected for natural

waters rather than contaminants. Some waters with natural chloride-to-bromide ratios are high in uranium or radium, and these uranium or radium anomalies appear to be natural.

The Dilworth is also contaminated at its outcrop along Scared Dog Creek. Analysis of the geochemical and geologic data indicated a zone of shallow, acidic ground-water contamination extending along Scared Dog Creek north and northeast of tailings pile 3 (the northeastern aluminum plume shown in fig. 8.1). This zone horizontally crosses lithologic boundaries, indicating that it is either a ground-water plume migrating as underflow beneath Scared Dog Creek, surface recharge from contaminated surface waters flowing within the creek, or leachates of tailings deposited in the sediments along Scared Dog Creek.

Aluminum concentrations (92 mg/L) are greatest in the Scared Dog Creek drainage immediately downstream from the northeast corner of tailings pile 3, within alluvium and the lower Conquista clay, and seepage, drainage, or windblown tailings from tailings pile 3 are possible sources of the contamination. The acidity of the contaminant plume decreases downstream, and at the monitoring well farthest downstream (monitoring well 977, completed within the Dilworth Sandstone Member) the pH buffering capacity of the aluminum sulfate is nearly exhausted. Therefore, this probably represents the edge of the contaminant plume. The decrease in acidity is due to dilution of contaminants by background waters rather than neutralization by calcite.

Identification of Background Ground Waters

Maps of pH, TDS, aluminum, and calcium concentrations strongly support the geochemical model of aluminum sulfate solutions migrating and reacting with calcite in the Deweesville and Conquista aquifers. These maps provide clear delineation of the contaminant plumes and therefore, clear delineation of uncontaminated ground waters.

These delineations are also supported by the mapping of ground-water mounds in the Deweesville and Conquista aquifers.

Locations of wells in the Deweesville and Conquista sandstones that are probably not contaminated are provided in figure 8.3. Total dissolved solids, aluminum, pH, calcium, and tritium data indicate that three monitoring wells in the Deweesville are not contaminated by tailings solutions. These are monitoring wells 852, 851, and 677. The earliest (1989) data for monitoring well 922 could also be used as a background, but more recent changes (1991) in pH and calcium data provide evidence of recent contaminant influx.

Monitoring wells in the Conquista sand that are probably not contaminated by tailings solutions are all located downslope and downdip of the outcrop, generally within the reduced portion of the Conquista sand (monitoring wells 860, 861, 865, 924, and 951; fig. 8.3).

Most monitoring wells in the Dilworth do not show evidence of contamination. The contaminated exceptions are wells 905 and 878 in the western area and monitoring wells 977 and 966 at the Dilworth outcrop along Scared Dog Creek. The remaining Dilworth wells are thought to be uncontaminated by tailings solutions, although some are associated with localized ground-water mounds indicating vertical leakage of natural ground waters from overlying units, probably through uranium exploration borings.

Nearly all of the monitoring wells tentatively identified as containing natural ground waters are located downdip of the tailings area and downdip of the area of outcrop for each unit. These wells are located within what was probably the saturated (phreatic) zone of each aquifer prior to mining and milling operations. Leakage of tailings solutions from the tailings piles at the outcrops of each aquifer resulted in saturation of the unsaturated zones (vadose) in the updip portions of these aquifers. Thus, monitoring wells located along outcrop but lateral to these artificially saturated ground-water mounds, are within the uncontaminated vadose zone. These are the dry

monitoring wells, as denoted in figure 8.3. One of the problems in determining background within the areas of the uranium deposits is that they are within this unsaturated zone. Thus, a monitoring well will not produce water for sampling. Lysimeters are required to sample water from the unsaturated zone. Geologic evidence suggests that the both uranium deposits and pore waters in the vadose zone are associated with acid sulfate sediments. Those unsaturated-zone pore waters may be of different chemistry than those located in a naturally saturated zone.

Natural Acid-Sulfate Sediments

The occurrence of naturally acid sediments at the Falls City UMTRA site is related to natural oxidation of pyrite, which produces acid-sulfate salts and solutions. In addition to the direct measurement of sediment pH, other geologic evidence supports the existence of natural acid-sulfate sediments within the Whitsett Formation at and around the site. The evidence includes (1) the great abundance of iron oxide, manganese oxide and gypsum-filled fractures, which are products of neutralization of acid-sulfate ground waters, (2) the occurrence of the mineral alunite, also a product of neutralization of acid-sulfate ground waters, surrounding carbonate nodules in the lower Conquista clay, (3) an abundance of silcrete- and calcrete-like concretions, which are reported to form in association with acid-sulfate sediments, and (4) the association and replacement of fossils with iron hydroxides and gypsum, indicative of neutralization of acid sulfate waters by calcite.

At present, acid-sulfate sediments and ground waters generated by pyrite oxidation are particularly widespread in coastal plains in the tropics (van Breemen, 1973). Ground waters associated with acid-sulfate sediments contain moderate concentrations of iron and aluminum (on the order of 1 mg/L for both; van Breemen, 1973). Basic sulfate salts, including alunite and jarosite, are indicators of acid-sulfate sediments and ground waters

(van Breemen, 1973; Goldbery, 1978; McArthur and others, 1991; Rye and others, 1992) although processes (ferrolysis) other than pyrite oxidation may produce acid sediments and ground waters containing about 100 mg/L dissolved aluminum and iron (McArthur and others, 1991). Alums (neutral aluminum sulfate salts) that produce acid-sulfate solutions are also fairly common as salts in unsaturated, weathered, oxidized, carbonate-free clays and shales (Ladoo and Myers, 1951). In the Jackson Group itself, acid-sulfate, gypsum-equilibrated ground water with a pH of 4.0, 28 mg/L dissolved aluminum, and 0.9 mg/L iron has been reported from Arkansas (Hem, 1985). Thus, naturally occurring acid ground water could exist in the Whitsett Formation of the Jackson Group near the Falls City UMTRA site.

Despite the potential for naturally-occurring acid-sulfate ground waters at the site, the presence of ground-water mounds and the areal distribution of pH, aluminum, sulfate, TDS, and calcium is best explained as contamination by tailings solutions. No clearly natural acid-sulfate waters have been identified, although one possibility is that natural acid-sulfate salts (alums) are concentrated above the ground-water table. One test of this hypothesis would be to install lysimeters in some of the dry monitoring wells located beyond the influence of the ground-water mounds. Another test would be to perform batch leach experiments on sediments from the numerous uranium open-pit mines in the area (slated to be reclaimed in the next few years) and from core now available at the BEG. These data might provide further support for natural occurrences of ground waters with relatively high concentrations of uranium, selenium, and molybdenum.

Further Study

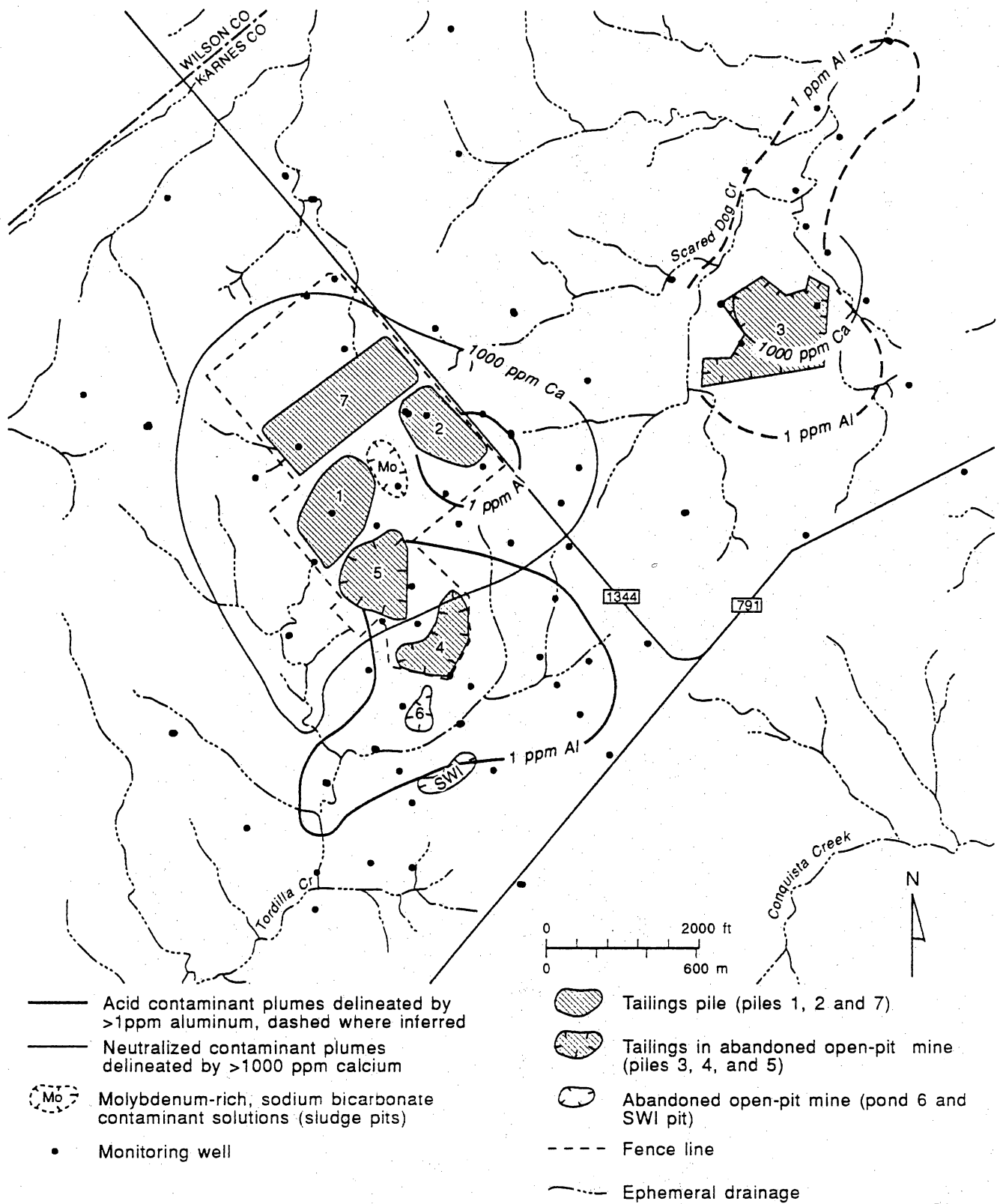
Both ammonium and radium appear to be exchanged, sorbed, or precipitated from the contaminant solutions only a short distance from the tailings piles, even under acid

conditions. Radium concentrations in acid ground waters adjacent to tailings piles are 10 to 20 percent of those in the tailings piles, and either cation exchange or coprecipitation with gypsum as a result of cation exchange of ammonium for calcium may be significant factors in this decrease. Further study of available core and of sediments exposed during the removal and consolidation of tailings would identify (1) the presence of a zone of radium ammonium and metals in the sediments surrounding the tailings piles, (2) the processes that sequestered ammonium, radium, and metals within this possible zone, and (3) processes that could remobilize ammonium, radium, and metals left in the sediments after the tailings have been removed.

There are similarities between the tailings and natural acid-sulfate sediments, and between tailings solutions and natural acid-sulfate ground waters. These similarities make it difficult to distinguish between natural and contaminant effects on both ground water and sediments at the site, though the areal distribution of pH and major elements is clearly related to contamination by tailings solutions. In one sense, the major contaminant at the site is water, and part of the problem in determining background water chemistry at the site is that (1) the contaminated water has generally saturated shallow sediments in what was the unsaturated zone and (2) shallow monitoring wells located beyond the influence of the contamination are, therefore, within the remaining unsaturated zone and will not produce water. Batch leach data and geologic evidence suggest that natural acid-sulfate salts exist in this unsaturated zone, and geologic evidence indicates that the uranium deposits are also within this zone. Further study of leachates and waters produced (using lysimeters) from these naturally acidic sediments would help to (1) better define the background water chemistry of the unsaturated zone, especially in the areas of uranium mineralization and (2) further understand the chemical interactions between the contaminants and sediments in the unsaturated zone. The latter objective could also be applied to problems of uranium

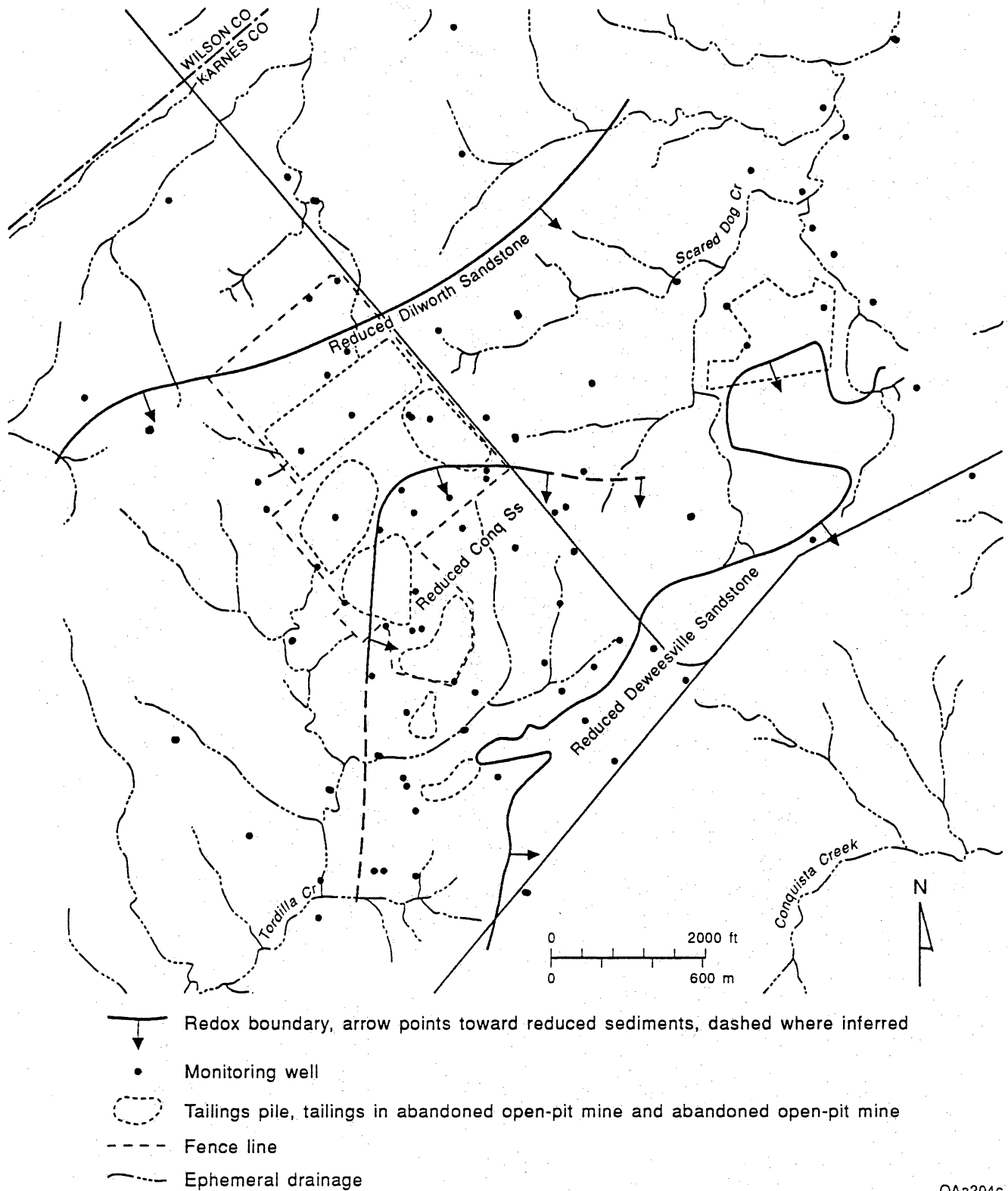
mine reclamation, which commonly results in artificial ponds overlying or adjacent to unsaturated, uranium-bearing sediments. Artificial recharge from those ponds might leach radioactive and nonradioactive metals from the unsaturated zone. In addition, large amounts of ground water data collected from uranium mines during operations remain to be analyzed. Those data, available from the Railroad Commission of Texas could be used to support the existence of baseline metals (uranium, molybdenum, selenium, arsenic, lead, zinc, and so on) in the shallow ground waters and unsaturated zone waters near the Falls City site.

More work on the natural acid-sulfate sediments at the site is warranted. Over the long term, naturally occurring acid-sulfate ground waters or acid-sulfate waters produced by reclamation activities may be mistaken for ground-water contamination from tailings piles. Certain parameters, such as aluminum versus iron concentrations, respective differences in acidity titration curves, and chloride-to-bromide ratios may serve to delineate the natural acid waters (that may contain soluble salts of uranium, radium, and other metals) from tailings contamination.



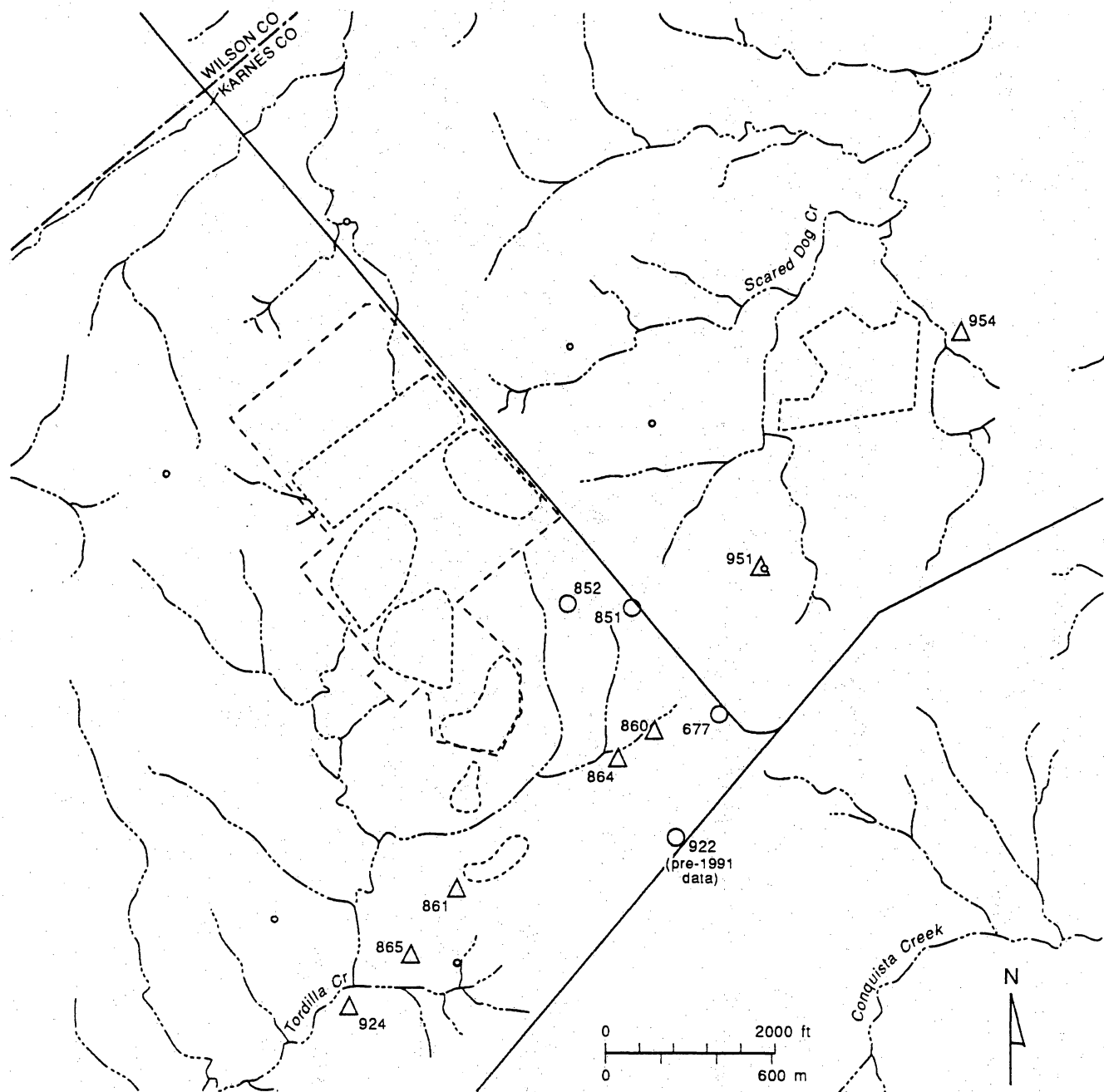
QAa209c

Figure 8.1. Identified contaminant plumes, Falls City UMTRA site.



QAa204c

Figure 8.2. Oxidation-reduction fronts in the Dilworth, Conquista, and Deweesville sandstones.



- ⁶⁷⁷ Deweesville monitoring wells with well number, possibly background
- △⁸⁶¹ Conquista monitoring wells with well number, possibly background
- Dry monitoring wells in Conquista, Deweesville, and Dilworth sandstones
- Tailings pile, tailings in abandoned open-pit mine and abandoned open-pit mine
- - - Fence line
- Ephemeral drainage

QAa208c

Figure 8.3. Monitoring wells for ascertaining probable background concentrations.

ACKNOWLEDGMENTS

Funding for this research was provided by the U.S. Department of Energy under Cooperative Agreement No. IAC (92-93)-0389. Many individuals and organizations have provided data and assistance in the course of this investigation; we appreciate their support and interest in the study:

U.S. Department of Energy (DOE), UMTRA Project Office: Denise Bierley, Paul Mann.

Jacobs Engineering Group: Eric Storms, Bill Downs.

Bureau of Radiation Control, Texas Department of Health: Gary Gartzke, Bill Price, Steve Etter.

Rio Grande Resources (formerly Chevron Resources Co.): Ed Griffin.

Surface Mining and Reclamation Division laboratory, Railroad Commission of Texas.

Tritium Laboratory, University of Miami.

Carol A. Edwards, U. S. Geological Survey Field Records Library.

Louisiana Geological Survey: R. P. McCulloh

Staff of the Bureau of Economic Geology, The University of Texas at Austin, have contributed materially to the project. We thank Raul Herrera and Steve Tweedy for laboratory analyses; Stu Goldsmith and Bernd Richter for drill sample and water sample collection; Joseph Yeh and Robin Domisse for assistance with StrataModel; Arten Avakian, Rick Edson, and Diane Spinney for computer counsel; Jay Raney for technical review of the manuscript; Tari Weaver and Eve Davis for drafting the figures; Lucille Harrell, Randy Hill, and Susan Lloyd for word processing and data entry; Amanda R. Masterson and Kitty Challstrom for copyediting; and Margaret L. Evans for report assembly.

REFERENCES

- American Public Health Association, 1985, Standard methods for the examination of water and wastewater (16th ed.): Washington, D.C., American Public Health Association, 1268 p.
- Barnes, V. E., 1976, project director, Geologic Atlas of Texas, Crystal City–Eagle Pass sheet: The University of Texas at Austin, Bureau of Economic Geology, Geologic Atlas, scale 1:250,000.
- Blount, J. G., and Kreitler, C. W., 1990, Alternate site selection process for the Falls City, Texas, UMTRA project: The University of Texas at Austin, Bureau of Economic Geology, final report for U.S. Department of Energy, contract DE-FC04-87AL20532, 27 p.
- Bryson, H. C., 1987, Ground-water contamination at the Falls City, Texas, uranium mill tailings site: University of Virginia, Department of Environmental Sciences, Master's thesis, 131 p.
- Bunker, C. M., and MacKallor, J. A., 1973, Geology of the oxidized uranium ore deposits of the Tordilla Hill-Deweeseville area, Karnes County, Texas: a study of a district before mining: U.S. Geological Survey Professional Paper 765, 36 p.
- Drever, J. I., 1982, The geochemistry of natural waters: Englewood Cliffs, N. J., Prentice-Hall, Inc., 388 p.
- Eargle, D. H., Dickinson, K. A., and Davis, B. O., 1975, South Texas uranium deposits: American Association of Petroleum Geologists Bulletin, v. 59, p. 766–779.

- Eargle, D. H., Hinds, G. W., and Weeks, A. M. D., 1971, Uranium geology and mines, South Texas: The University of Texas at Austin, Bureau of Economic Geology Guidebook 12, 59 p.
- Eargle, D. H., Pinkley, G. R., and de Vergie, P. C., 1958, Eocene-Miocene, oil and uranium: South Texas Geological Society, 1958 fall field trip guidebook, 67 p.
- Eargle, D. H., and Snider, J. L., 1957, A preliminary report on the stratigraphy of the uranium-bearing rocks of the Karnes County area, south-central Texas: The University of Texas at Austin, Bureau of Economic Geology Report of Investigations No. 30, 30 p.
- Eargle, D. H., and Weeks, A. M. D., 1973, Geologic relations among uranium deposits, South Texas coastal plain region, U.S.A., *in* Amstutz, G. C., and Bernard, A. J., eds., Ores in Sediments: International Union of Geological Scientists, p. 101-113.
- Espey, Huston & Associates, Inc., 1980, Environmental report: radioactive material license renewal for the Conquista Project Uranium Mill, Karnes County, Texas: Prepared for Conquista Project / Conoco Inc., Falls City, Texas, variously paginated.
- Etco Engineers and Associates, 1961, Subsurface exploration and analysis, tailings pond, Falls City, Texas: report prepared for Susquehanna-Western, Inc., 3 p.
- _____ 1963a, Final report, subsurface exploration and analysis, S.W.I. tailings pond #3, Falls City, Texas: report prepared for Susquehanna-Western, Inc. 3 p.
- _____ 1963b, Subsurface investigation and analysis, tailings pond: report prepared for Susquehanna-Western, Inc., 3 p.
- _____ 1966a, Subsurface exploration and analysis, new tailings dam, Falls City, Texas: report prepared for Susquehanna-Western, Inc., 4 p.

- _____ 1966b, Subsurface investigation and analysis, Lyssy mine nos. 1 and 2, for use as tailings pond, Falls City, Texas: report prepared for Susquehanna-Western, Inc., 4 p.
- Farrah, H., Hatton, D., and Pickering, W. F., 1980, The affinity of metal ions for clay surfaces: *Chemical Geology*, v. 28, p. 55-68.
- Farrah, H., and Pickering, W. F., 1979, pH effects in the adsorption of heavy metal ions by clays: *Chemical Geology*, v. 25, p. 317-326.
- Fisher, W. L., Proctor, C. V., Jr., Galloway, W. E., and Nagle, J. S., 1970, Depositional systems in the Jackson Group of Texas—their relationship to oil, gas, and uranium: The University of Texas at Austin, Bureau of Economic Geology Geological Circular 70-4, 27 p.
- Folk, R. L., Hayes, M. O., Brown, T. E., Eargle, D. H., Weeks, A. D., Barnes, V. E., and Clabaugh, S. E., 1961, Field excursion—Central Texas: bentonites, uranium-bearing rocks, vermiculites: University of Texas, Austin, Bureau of Economic Geology Guidebook 3, 53 p.
- Ford, Bacon & Davis Utah, Inc., 1978, Geologic and hydrologic conditions at the inactive uranium millsites at Falls City and Ray Point, Texas: Salt Lake City, Utah: prepared for the U.S. DOE, ERDA Contract No. E(05-1)-1658, variously paginated.
- _____ 1981, Engineering assessment of inactive uranium mill tailings, Falls City site: Salt Lake City, Utah, prepared for U.S. Department of Energy, Contract No. DE-AC04-76GJ01658, 139 p.
- Galloway, W. E., 1979, Jackson and Catahoula systems of the Texas Gulf Coastal Plain, *in* Galloway, W. E., Kreitler, C. W., and McGowen, J. H., eds., *Depositional and*

ground-water flow systems in the exploration for uranium: The University of Texas at Austin, Bureau of Economic Geology, proceedings of research colloquium, p. 181-196.

Galloway, W. E., Finley, R. J., and Henry, C. D., 1979, South Texas uranium province—geologic perspective: The University of Texas at Austin, Bureau of Economic Geology Guidebook 18, 81 p.

Galloway, W. E., Henry, C. D., and Smith, G. E., 1982, Depositional framework, hydrostratigraphy, and uranium mineralization of the Oakville Sandstone (Miocene), Texas Coastal Plain: The University of Texas at Austin, Bureau of Economic Geology Report of Investigations No. 113, 51 p.

Goldbery, Ron, 1978, Early diagenetic, nonhydrothermal Na-alunite in Jurassic flint clays, Makhtesh Ramon, Israel: Geological Society of America Bulletin, v. 89, p. 687-698.

Hem, J. D., 1977, Reactions of metal ions at surfaces of hydrous iron oxide: *Geochimica et Cosmochimica Acta*, v. 41, p. 527-538.

_____ 1985, Study and interpretation of the chemical characteristics of natural water: U.S. Geological Survey Water-Supply Paper 1473, 363 p.

Henry, C. D., and Kapadia, R. R., 1980, Trace elements in soils of the South Texas uranium district: concentrations, origin, and environmental significance: The University of Texas at Austin, Bureau of Economic Geology Report of Investigations No. 101, 52 p.

Henry, C. D., Galloway, W. E., Smith, G. E., Ho, C. L., Morton, J. P., and Gluck, J. K., 1982, Geochemistry of ground water in the Miocene Oakville Sandstone, a major

- aquifer and uranium host of the Texas Coastal Plain: The University of Texas at Austin, Bureau of Economic Geology Report of Investigations No. 118, 63 p.
- Kharaka, Y. K., and Barnes, I., 1973, SOLMINEQ: U.S. Geological Survey, Computer Contributions, National Technical Information Service No. PB 215 899, 81 p.
- Kharaka, Y. K., Gunter, W. D., Agarwal, P. K., Perkins, E. H., and DeBraal, J. D., 1988, SOLMINEQ.88: A computer program for modeling of water-rock interactions: U.S. Geological Survey, Water Resources Investigations Report 88-4227, 420 p.
- Krauskopf, K. B., 1967, Introduction to geochemistry: New York, McGraw-Hill, 720 p.
- Ladoo, R. B., and Myers, W. M., 1951, Nonmetallic minerals: New York, McGraw-Hill, 603 p.
- Longmire, P. L., Douglas, G. B., and Thomson, B. M., 1990, Hydrogeochemical interactions and evolution of acidic solutions in soil, *in* Melchior, D. C., and Bassett, R. L., eds., Chemical modeling of aqueous systems II: Washington, D.C., American Chemical Society, 556 p.
- MacKallor, J. A., Moxham, R. M., Tolozko, L. R., and Popenoe, P., 1962, Radioactivity and geologic map of the Tordilla Hill-Deweeseville area, Karnes County, Texas: U.S. Geological Survey Map GP-199.
- Manger, G. E., 1958, A comparison of the physical properties of uranium-bearing rocks in the Colorado Plateau and Gulf Coast of Texas (abs.): *Economic Geology*, v. 53, no. 7, p. 922-923.
- Manger, G. E., and Eargle, D. H., 1967, Physical and associated properties of uranium-bearing rock in five drill holes in Karnes County, Texas: U.S. Geological Survey, Open-File Report 67-153, 19 p. and log cross sections.

- Markos, G., and Bush, K. J., 1982, Geochemical processes in uranium mill tailings and their relationship to contamination, *in* Management of Wastes from Uranium Mining and Milling: Vienna, Austria, International Atomic Energy Agency, p. 231–246.
- _____ 1983, Data for the geochemical investigation of UMTRAP-designated site at Falls City, Texas: Prepared by GECR, Inc., for the U.S. Department of Energy, variously paginated.
- McArthur, J. M., Turner, J. V., Lyons, W. B., Osborn, A. O., and Thirlwall, M. F., 1991, Hydrochemistry on Yilgarn Block, Western Australia: ferrolysis and mineralisation in acidic brines: *Geochimica et Cosmochimica Acta*, v. 55, p. 1273–1288.
- McCulloh, R. P., and Roberts, C., 1981, Geology of the Nuhn uranium ore body, Jackson Group, south Texas uranium district: *South Texas Geological Society Bulletin*, v. 24, p. 23–46.
- Merritt, R. C., 1971, The extractive metallurgy of uranium: Golden, Colorado, Colorado School of Mines Research Institute, 576 p.
- Morrison, S. J., and Lorie, S. C., 1991, Mineralogical residence of alpha-emitting contamination and implications for mobilization from uranium mill tailings: *Journal of Contaminant Hydrology*, v. 8, p. 1–18.
- Perkins, E. H., Kharaka, Y. K., Gunter, W. D., and DeBraal, J. D., 1990, Geochemical modeling of water-rock interactions using SOLMINEQ.88, *in* Melchior, D. C., and Bassett, R. L., eds., *Chemical modeling of aqueous systems II*: Washington, D.C., American Chemical Society, 556 p.

- Price, W., 1991, Surface resistivity survey at Falls City, Texas, UMTRA site: Bureau of Radiation Control, unpublished memorandum, 10 p.
- Pyrh and Associates, 1986, Geochemical properties of soil and sediment samples from uranium tailings disposal site at Falls City, Texas (FCT03): Prepared for Jacobs Engineering Group under Subcontract No. ASD-34-6703-S-86-0018, variously paginated.
- Rye, R. O., Bethke, P. M., and Wasserman, M. D., 1992, The stable isotope geochemistry of acid sulfate alteration: *Economic Geology*, v. 87, p. 225-262.
- Shuman, L. M., 1977, Adsorption of Zn by Fe and Al hydrous oxides as influenced by aging and pH: *Soil Science Society of America Journal*, v. 41, p. 703-706.
- Solution Engineering, Inc., 1976, Application for in-situ mining permit: Texas Water Quality Board, Application No. 4102, variously paginated.
- Texas Department of Health, Bureau of Radiation Control, 1984, Report on trip to Solution Engineering, Inc., License #9-2169: Interoffice memorandum in license file 9-2169, 14 p.
- Turk, Kehle, and Associates (TKA), 1976, Reconnaissance hydrogeology of uranium mill tailings, Falls City, Texas: Prepared for Ford, Bacon & Davis Utah, Salt Lake City, Utah, variously paginated.
- U.S. Department of Energy (DOE), 1990, UMTRA Project—Remedial action planning and disposal cell design: UMTRA Project Office, Albuquerque, New Mexico, UMTRA-DOE/AL 400503/0000, variously paginated.
- U.S. Geological Survey, 1957-58, Field notes: Some published as U.S.G.S. TEI-690, 1957; TEI-740, 1958; TEI-750, 1958, various field geologists' notes.

_____ 1958, Geologic investigations of radioactive deposits, semiannual progress reports: Trace Elements Investigations Report 740 and other unnumbered excerpts, December 1, 1957, to May 31, 1958, various authors.

van Breemen, N., 1973, Dissolved aluminum in acid sulfate soils and in acid mine waters: Soil Science Society of America Proceedings, v. 37, p. 694-697.

Watzlaf, G. R., 1988, Chemical stability of manganese and other metals in acid mine drainage sludge, *in* Mine drainage and surface mine reclamation, volume I: mine water and mine waste: U.S. Bureau of Mines Information Circular 9183, p. 83-90.

Appendices

Table 1. BEG water well data, Falls City, Texas, UMTRA Site.

Well ID (DOE)	Well ID (BEG)	Well Identification and Location			Geology	
		y	x	Land-surface elevation (ft)	Surface geology	Formation screened
851	0006	59877.7	67424.6	432	Dubose	Deweeseville
852	0003	59902.0	66684.6	438	Deweeseville	Deweeseville
853	0011	58402.9	67051.2	415	Dubose	Deweeseville
854	0014	57716.3	65230.6	410	Deweeseville	Deweeseville
855	0004	55580.2	65392.1	412	Deweeseville	Deweeseville
856	0008	61631.1	65281.8	458	Upper Conquista	Conquista Sand
857	0007	60451.4	67319.2	442	Dubose	Upper Conquista
858	0010	60184.4	65945.2	442	Deweeseville	Conquista Sand
859	0015	58209.3	64798.2	426	Deweeseville	Conquista Sand
860	0012	58361.8	67690.2	420	Dubose	Conquista Sand clay
861	0013	56466.9	65333.3	415	Dubose	Conquista Sand clay
862	0009	58816.9	65415.5	437	Deweeseville	Dilworth
863	0001	57986.4	66138.6	416	Deweeseville	Conquista Sand
864	0002	58028.6	67276.2	416	Dubose	Lower Conquista
865	0005	55659.6	64803.2	415	Deweeseville	Conquista Sand clay
878	0016	61659.6	65240.8	458	Upper Conquista	Dilworth
879	0017	57625.5	67600.5	412	Dubose	Deweeseville

Table 1 (cont.)

Well Characteristics

Well ID (DOE)	Depth to screen (ft)	Top screen elevation (ft)	Screen length (ft)	Base screen elevation (ft)	TD of well (ft)	Bottom well elevation (ft)	TD of hole (ft)	Bottom hole elevation (ft)
851	25	407	10	397	42.00	390	50	382
852	28.5	409.5	10	399.5	45.50	392.5	47	391
853	23	392	10	382	40.00	375	40	375
854	15	395	10	385	32.00	378	33	377
855	9	403	10	393	36.00	376	35	377
856	38.5	419.5	10	409.5	50.00	408	80	378
857	42	400	10	390	59.00	383	73	369
858	39.6	402.4	10	392.4	56.60	385.4	80	362
859	31.5	394.5	10	384.5	43.50	382.5	79	347
860	63.5	356.5	10	346.5	80.50	339.5	83	337
861	48	367	10	357	65.00	350	70	345
862	118	319	10	309	135.00	302	141	296
863	32.5	383.5	10	373.5	44.50	371.5	45	371
864	88.5	327.5	10	317.5	105.50	310.5	106	310
865	33	382	10	372	50.00	365	60	355
878	116	342	10	332	122.00	336	123	335
879	51	361	10	351	63.00	349	64.5	347.5

Comments: Total depth of hole may be deeper than total depth of well because many of the holes were backfilled and screened to shallower depths.

Table 1 (cont.)

Well ID (DOE)	Water Elevation		Measurement date	Geophysical Logs			
	Depth to water (ft)	Water elevation (ft)		Gamma	Neutron	Caliper	Den/Res
851	26	406	4/25/91	x	x	x	x
852	23	415	4/19/18	x	x	x	x
853	15.9	399.1	4/22/91	x	x	x	x
854	12	398	4/23/91	x	x	x	x
855	dry			x	x	x	x
856	31.5	426.5	4/23/91	x	x	x	x
857	33.7	408.3	4/24/91	x	x	x	x
858	18.5	423.5	4/24/91	x	x	x	x
859	26	400	4/23/91	x	x	x	x
860	39	381	4/24/91	x	x	x	x
861	24.7	390.3	4/24/91	x	x	x	x
862	116	321	4/24/91	x	x	x	x
863	13.5	402.5	4/24/91	x	x	x	x
864	91	325	4/24/91	x	x	x	x
865	34.7	380.3	4/25/91	x	x	x	x
878	107.6	350.4	6/7/91				
879	35.1	376.9	6/7/91				

Table 1 (cont.)

Chemical Field Measurements

Well ID (DOE)	Measurement date	Alkalinity (mg/L)	pH	Eh (mv)	Salinity (ppm)	Conductivity (Mmhos)
851	4/25/91	444	6.6	310	1400	2500
852	4/25/91	95	6.2	330	1800	3000
853	4/22/91		3.6	300	8000	13000
854	4/23/91		3.7	280		
855						
856	4/23/91	530	6.1	310	6100	10000
857	4/27/91	539	7.1	310	1000	2000
858	4/28/91	95	5.3	380	1800	3000
859	4/26/91	348	6.6	330	2700	4200
860	4/29/91	305	6.8	140	1300	2500
861	4/28/91	402	6.7	330	1800	3000
862	4/25/91	417	7	200	1000	2000
863	4/25/91		3.8	320	4900	8000
864	4/29/91		n.d.	n.d.	n.d.	n.d.
865	4/30/91	472	6.6	n.d.	5000	8000
878	6/7/91	380	6.6	n.d.	n.d.	n.d.
879	6/7/91		4.1		9800	15000

Comments: n.d. = no data.

Table 1 (cont.)

Well ID (DOE)	Redox Depth and Formation			Base of Major Gamma Anomaly	
	Redox depth (ft)	Redox Elevation (ft)	Fm (Redox)	Depth base gamma (ft)	Elevation base gamma (ft)
851	40	392	Upper Conquista	28	404
852	39	399	Top Conquista Sand	40	398
853	40	375	not encountered	36	379
854	28	382	Upper Conquista	20	390
855	24	388	Upper Conquista	12	400
856	58	400	Base Conquista Sand	36	422
857	41	401	Upper Conquista	22	420
858	34	408	Upper Conquista	35	407
859	27	399	Upper Conquista	32	394
860	52	368	Upper Conquista	50	370
861	26	389	Upper Conquista	30	385
862	38	399	Upper Conquista	40	397
863	36	380	Upper Conquista	34	382
864	45	371	Upper Conquista	48	368
865	28	387	Upper Conquista	28	387
878	66	392	Top Lower Conquista	no log	
879	29	383	Dubose	no log	

Comments: Redox depth is based on color changes observed in well cuttings.
Depth base of gamma is depth of major gamma anomaly from gamma log.

Table 2. Lithologic descriptions of cuttings described by Jon Blount (JGB), Pat Dickerson (PWD), and Stu Goldsmith (SRG) and collected during the drilling of 16 monitoring wells from February 1, 1991, to April 25, 1991, at the Falls City, Texas, UMTRA site. Drilling was under the supervision of Jacobs Engineering Group. General information on monitoring wells is presented in table 1. Location of BEG monitoring wells is shown in the location map.

Borehole ID 851 (#6)

Field Sample Log (Cuttings)

Date 3/29/91

TD 50'

Drilling Foreman: Bill Wood

Date	Initials	Interval	Mineralogy	Grain size	Color	Comments/description
3/29/91	JGB	0-5'	Clay minerals	Clay	Variable	Black clayey soil 0-4; encountered <u>Dubose</u> at 4.0' (dark gray clay); contains a few chips of light olive to whitish bentonitic clay; could be from a discrete layer or they are remnants.
		5-10'	Qtz., clay minerals	Clay, silt, f.g. sand	Variable	5-7' steel gray to black clay; from 7.0-10' light olive brown sand, silty clay to clayey sand, gyp, limonitic staining common; probable contact w / <u>Deweeseville</u> at 8.0' although gradational.
		10-15'	Qtz., clay minerals	F.g. sand	Lt. olive, brown/tan	Clayey sand; sand increases w/depth.
		15-20'	Qtz., clay minerals	F.g. sand, clay	Lt. olive gray	Clayey f.g. sand; light limonite staining, slightly damp; relatively clean sand from 19-20'.
		20-25'	Qtz., clay minerals	F.g. sand, silty clay	Lt. olive gray/red brown	Same as above to 23' from 23-25', reddish brown lignitic clay and silty clay.
		25-30'	Qtz., clay minerals	F.g. sand, silt, clay	Lt. olive gray/white	Back into clayey f.g. sand, silty.
		30-35'	Qtz., clay minerals	F.g. sand, silt, clay	Lt. olive	Same as above.
		35-40'	Qtz., clay minerals	F.g. sand, clay	Lt. olive gray	Clayey sand, sandy clay; estimated contact w/ <u>Conquista</u> at 37'. Est. redox boundary 40'.
		40-45'	Clay minerals	Silt, clay	Dk. olive gray	Silty clay w/some lighter, more oxidized fragments.
		45-50'	Qtz., clay minerals	F.g. sand, silt, clay	Dk. olive gray	Clay; some sand and silt, which is oxidized and probably interbedded.

Table 2 (cont.)

Borehole ID 852 (#3)

Field Sample Log (Cuttings)

Date 3/29/91

TD 47'

Drilling Foreman: Richard Papusch

Date	Initials	Interval	Mineralogy	Grain size	Color	Comments/description
2/17/91	RGP	0-5'	Clay minerals, quartz	Clay, silt	Dk. gray	Topsoil—dark gray clayey silt, damp
		5-10'	Clay minerals, quartz	Clay, silt, fine sand	Dk. gray	As above, grading downward to clayey sand
		10-15'	Quartz	Fine sand	Lt. yellow, lt. tan, buff	Top of <u>Deweeseville</u> at 10'; light yellow to light tan to buff sandstone; fine grained, subangular; loose to moderately indurated
		15-20'	Quartz	Fine sand to silty sand	Lt. tan to buff	As above, moderately hard; becomes silty at 17'.
		20-25'	Quartz	Fine sand to silt	Yellow-green	Silty sand, well sorted sand fraction, subangular, slightly moist.
		25-30'	Quartz	Fine sand to silt	Yellow-green	As above; damp.
		30-35'	Quartz	Fine sand to silt	Yellow-green	As above; water table at 32'.
		35-40'	Quartz; clay minerals	Fine sand to silt	Yellow-green, then dark gray with some ochre stain	As above to 37'; top of <u>upper Conquista Clay</u> at 37'. Massive, soft, dark gray clay; limonite staining from 37' to 39'.
		40-45'	Clay minerals	Clay	Dark gray	Conquista clay as above. No limonite staining below 37'.
		45-47'	Clay minerals	Clay	Dark gray	As above.

Table 2 (cont.)
 Borehole ID 853 (#11)
 Field Sample Log (Cuttings)

Date 2/26/91

TD 40'

Drilling Foreman: Richard Papusch

Date	Initials	Interval	Mineralogy	Grain size	Color	Comments/description
2-26-91	RSG	0-3'	Clay minerals	Clay	Black	Topsoil.
		3-5'	Quartz	Fine sand/ clay	Black	Sandier topsoil.
		5-10'	Qtz., fspar	Fine sand	White/lt. tan	Possibly tuffaceous, but not well indurated sandstone: <u>Deweeseville</u> .
		10-15'	Qtz., fspar	Fine sand	Tan	Sand, not well consolidated.
		15-20'	Qtz., fspar	V. fine sand	Tan/lt. gray	Sandstone, some silicified.
		20-25'	Qtz., clay minerals	V. fine sand, silt/clay	Lt. brown	Sand, silt, and clay.
		25-30'	Qtz., clay minerals	V. fine sand, silt/clay	Lt. brown	Wet, silty sand, some limonite; hit water ~26'.
		30-35'	Qtz., clay minerals	V. fine sand, silt/clay	Lt. brown	Sandy silt, clay contact in this interval, ~33' <u>upper Conquista</u> .
		35-40'	Clay minerals	Silt, clay	Lt.-dark brown	Silt and clay

Table 2 (cont.)

Borehole ID 854 (#14)

Field Sample Log (Cuttings)

Date 2/26/91

TD 33'

Drilling Foreman: Richard Papusch

Date	Initials	Interval	Mineralogy	Grain size	Color	Comments/description
2-26-91	RSG	0-5'	Quartz	V. f. sd/silt	Lt. tan	Topsoil, sand and silt, possibly silicified sandstone chips.
		5-10'	Quartz	V. f. sd/silt	Lt. tan	Silty sand.
		10-15'	Quartz	V.f. sd, silt, clay	Lt. brown	Silty sand and clay.
		15-20'	Quartz	V.f. sd, silt, clay	Lt. brown	Sand, silt, clay, somewhat less sand.
		20-25'	Quartz	V.f. sd, silt, clay	Lt. brown	Wet, sandy clay; poss. contact with <u>upper Conquista</u> @23'.
		25-30'	Clay minerals	Clay	Lt.-dark brown	Clay, soft, cohesive; redox boundary ~28'.
		30-33'	Clay minerals	Clay	Dk. gray	Clay, soft, cohesive.

Table 2 (cont.)
 Borehole ID 855 (#4)
 Field Sample Log (Cuttings)

Date 4/1/91

Drilling Foreman: Bill Wood

TD 35'

Date	Initials	Interval	Mineralogy	Grain size	Color	Comments/description
4/1/91	RSG	0-5'	Clay/qtz.	Clay/fine	Tan	Black clay topsoil; hard clay and sandstone; <u>Deweeseville</u> sandstone.
		5-10'	Qtz., clay	Clay/v. fine	Tan	Sandy siltstone, some clay, gypsum flakes.
		10-15'	Qtz., clay min.	Clay/v. fine	Lt. brown	Sandy siltstone; more clay and more gypsum than prev. interval.
		15-20'	Qtz., clay min.	Clay/v. fine	Lt. brown	Less sand than prev. interval; gypsiferous, slightly damp. <u>Conquista</u> contact ~19'.
		20-25'	Clay min.	Silt/clay	Reddish brown	Some dark gray clay (<10%); slightly damp.
		25-30'	Clay min.	Silt/clay	Dark gray	Siltstone and claystone.
		30-35'	Clay min.	Clay/silt	Dark gray	Silty claystone.

Table 2 (cont.)
Borehole ID 856 (#8)
Field Sample Log (Cuttings)

Dates 2/27/91 and 2/28/91

Drilling Foreman: Richard Papusch

TD 80'

Date	Initials	Interval	Mineralogy	Grain size	Color	Comments/description
2-27-91	RSG	0-5'	Qtz., feldspar	Fine sand, silt	Lt. brown	Silty sand, some unconsolidated, some chips more indurated. (<u>Deweeseville</u>)
		5-10'	Quartz	Fine	Lt. brown	Sand, silt, clay; clay starts ~7'. (<u>upper Conquista</u> contact)
		10-15'	Clay minerals	Silt/clay	Lt. brown	Silt and clay (switch to mud drilling fluid). Synthetic mud.
2-28-91	RSG	15-20'	Clay minerals	Clay	Lt. brown	Clay soft but cohesive, some FeOOH.
		20-25'	Clay minerals	Clay	Lt. brown	Same clay as above, more limonite.
		25-30'	Quartz	Clay/silt	Brown/lt. gray	Soft cohesive clay; also some silt and a very little sand.
		30-35'	Quartz	Clay/silt	Brown	Clay, slightly more silty, sandy.
		35-40'	Quartz	Fine sand, silt, clay	Brown	Sand, silt clay, limonite, some carbonaceous material. <u>Conquista</u> sand contact ~36'
		40-45'	Qtz., feldspar	V. fine	Lt. brown	Unconsolidated sand.
		45-50'	Qtz., feldspar	V. fine	Lt. brown	Unconsolidated sand.
		50-55'	Qtz., feldspar	V. fine	Lt. brown	Unconsolidated sand.
		55-60'	Qtz., feldspar	V. fine clay	Brown, gray	Driller possibly hit clay bed ~58'; clay soft, but cohesive. Redox at 58'.
		60-65'	Quartz	Fn. sand	Brown	Sand, some silicified, darker brown; some clay but not much; still <u>Conquista</u> sand.
		65-70'	Clay minerals	Silt, clay	Dk. brown	Dark claystone in chips, some sand; hard drilling (lower <u>Conquista</u> contact?); contact @66'
		70-75'	Clay minerals	Clay	Chocolate brown	Chocolate-colored clay, some limonite; hard drilling.
		75-80'	Clay minerals	Clay	Chocolate brown	Same as above.

Table 2 (cont.)
 Borehole ID 857 (#7)
 Field Sample Log (Cuttings)

Dates 3/13/91 and 3/14/91

Drilling Foreman Bill Wood

TD 73'

Date	Initials	Interval	Mineralogy	Grain size	Color	Comments/description
3-13-91	JGB	0-5'	Qtz, clay	F.g. sand, clay		0-2' black clayey soil; 2-4.5' gray to brown sandy clayey soil; 4.5-5.0'; hit indurated <u>Deweeseville</u> .
		5-10'	Qtz, clay	F.g. sand, clay	Lt. olive gray	Relatively soft friable <u>Deweeseville</u> sand w/some clay.
		10-15'	Qtz, fspar, clay	F.g. sand, clay	Lt. olive gray	Light olive gray clayey soft <u>Deweeseville</u> ss., f. g.; some feldspar weathered reddish ore present.
		15-20'	Qtz, clay, bentonite	F.g. sand, clay	Lt. olive gray	Relatively soft sand from 15-18'; fairly hard sandstone from 18-19'; hit clay bed from ~19-20'; bentonitic clay.
		20-25'	Qtz, clay	F.g. sand, clay	Brown/lit. olive green	From 20' to ~20.5' encountered brown coated clay, clay chips ore, lt. olive green on inside but brown on outside. Hit <u>very</u> hard sandstone at 23', relatively soft sand from 20.5'-23'; lost U joint drilling in very hard sand at ~23.5'.
3-14-91	JGB	20-25' (cont.)	Qtz, clay	F.g. sand, clay		Resumed drilling next day at ~23.5'; very hard sand to 24'; from 24-25' drilled soft clayey sand.
		25-30'	Qtz, clay	F.g. sand, clay	Lt. olive gray	Grades from a clayey sand to a sandy clay at ~28'.
		30-35'	Clay	Silt, clay	Lt. olive gray	Silty clay-damp.
		35-40'		Silt, clay	Lt. olive gray	Wet silty clay (oxidized <u>Conquista</u>); hit hard waxy bentonite at 39'.
		40-45'	Clay, bentonite	Clay	Lt. olive gray	Mostly hard, waxy bentonite, but some softer clay.
		45-50'	Clay, bentonite, limonite	Clay		As above to 46'; at 46' hit dark grayish brown clay; 46-50' dark grayish brown clay w/some clots of more oxidized grayish green clay intermixed, some limonite; Redox at 49'.
		50-55'	Clay	Clay	Variable	Very dark olive green to greenish and brownish black clay; significant number of clumps of lighter green clay.
		55-60'	Clay, qtz	Clay		Dark greenish gray clay; fewer oxidized clumps and less brownish color clay, slightly silty.

Table 2 (cont.)

Borehole ID 857 (#7)

Field Sample Log (Cuttings) (cont.)

		60-65'	Clay, qtz	Clay, silt		Same as above.
		65-70'	Clay, qtz	Clay, silt	Dk. green-gray	Fossiliferous clay, slightly silty.
		70-73'	Clay, qtz	Clay, silt	Dk. green-gray	Same as above, some shell fragments ~1/2-inch long.

Table 2 (cont.)
 Borehole ID 858 (#10)
 Field Sample Log (Cuttings)

Date 3/1/91

TD 80'

Drilling Foreman: Richard Papusch

Date	Initials	Interval	Mineralogy	Grain size	Color	Comments/description
3-1-91	RSG	0-5'	Qtz., fspar., mafic minerals	Fine sand	White	Tuffaceous sandstone, indurated, some limonite staining.
		5-10'	Quartz, clay minerals	Fine sand, silty clay	White/ brown	Sandstone is white; sandy siltstone and bentonitic clay are lt. brown.
		10-15'	Qtz., fspar	Fine sand, silt	Lt. brown	Silty sandstone, poorly consolidated, more limonite; casing set @ 15'.
		15-20'	Qtz., fspar	Fine sand	Lt. brown	Wet, poorly consolidated sand, carbonaceous.
		20-25'	Qtz., fspar	Fine sand	Brown	Wet unconsolidated sand.
		25-30'	Qtz., clay minerals	V. fine, silt, clay	Brown	Sandy siltstone and clay; siltstone and clay dominate; hit water table ~29'; <u>upper Conquista</u> contact ~27'.
		30-35'	Qtz., clay minerals	V. f. sand, silt, clay	Brown/ gray	Sandy siltstone and clay; sand-gray, brown; siltstone-reddish brown; clay-gray; Redox contact ~34'.
		35-40'	Qtz., clay minerals	V. f. sand, silt, clay	Dark gray	Sand, siltstone, and clay - mostly siltstone and clay.
		40-45'	Qtz., clay minerals	V. fine silt, clay	Dk. green	Sandstone - lt. brown siltstone and dk. green clay; siltstone and clay dominate.
		45-50'	Qtz., clay minerals	V. fine sand, silt, clay	Dk. green	Sandstone, siltstone, and clay.
		50-55'	Qtz., clay minerals	V. fine sand, silt clay	Dk. green	Siltstone, clay, sand; more clay, less sand; <u>lower Conquista</u> contact @ 55'.
		55-60'	Clay minerals	V. fine sand, silt, clay	Dk. brn/ black	Mostly clay, some siltstone.
		60-65'	Clay minerals	Silt, clay	Dk. gray, green/red	Siltstone and claystone chips, indurated, particularly siltstone, which is reddish brown.
		65-70'	Clay minerals	Silt, clay	Dk. gray/ red	Reddish brown indurated siltstone and dark gray clay - more clay than previous interval.

Table 2 (cont.)

Borehole ID 858 (#10)

Field Sample Log (Cuttings) (cont.)

		70-75'	Quartz	V. fine sand, silt, clay	Dk. gray, red	Siltstone chips - red, indurated; clay and claystone chips; sand and sandstone; mostly siltstone and clay.
		75-80'	Quartz	V. fine sand, silt, clay	Dk. gray, red	Siltstone chips - red indurated; clay and claystone; sand and sandstone; mostly siltstone and clay.

Table 2 (cont.)

Borehole ID 859 (#15)

Field Sample Log (Cuttings)

Dates 3/3/91 and 3/4/91

TD 79'

Drilling Foremen: Boyle - T. Robertson; Jacobs - R. Papusch

Date	Initials	Interval	Mineralogy	Grain size	Color	Comments/description
3-3-91	PWD	0-5'	Quartz, biotite(?), sulfides, waxy yellow mineral	Silt, F-M SD	Off-white to light beige	<u>Deweesville</u> . 1' Dk. brn. soil, gummy; 4-5' qtz. ss to slts; minor ?biotite, sulfide grains, waxy yellow xline mineral (autunite?)
		5-10'	Qtz., clay sulfides			5-8' as above but finer - f. sd. to slt; occas. fragments of tough tan clay; 8' friable fine sd; 8-10' clay increases downward.
		10-15'	Qtz., clay, hematite, limonite		Darker tan; greyish tan	10-15' Darker tan f. ss. to sltst; more oxidized - hematite and limonite; more clay - more indurated claystone chips, grayish tan, silty, fissile.
		15-20'	Clay, qtz., gypsum	Silt, clay	Dk. tan, reddish tan	15-20' silty clay; darker tan to reddish tan; abund. coarse xline clear gypsum (prob. from void fillings); abund. hematite, limonite.
		20-25'	Qtz., clay, gypsum, pyrite	Silt, clay		20-25' Tan clayey qtz. silt; unindurated, oxidized; abund. coarsely xline gypsum, pyrite grains.
		25-30'	Qtz., clay, gypsum, pyrite	Silt-f. sd., clay; silt, clay	Med.-dk. gray	25-27' clayey slt/f. sd.. as above; redox boundary ?; 27' top <u>upper Conquista</u> ; 27-30' dk. gray clayey slt to silty clay; abund. gyp., fine pyrite xls.
		30-35'	Clay, qtz. slt. sulfides	Clay, silt	Med.-dk. gray	30-35' med.-dk. gray silty clay to claystone; fissile, but not hard; v. fine sulfide grains; 36' drilling rate increased; 37' damp clay.
		35-40'	Clay, gyp., qtz., silt	Clay, silt, minor	Dk. gray	35-40'; 35' top of <u>Conquista Sand</u> . Dk. gray silty, sl. sdy. clayst. to clayey sltst; very abund. clear xline gyp., oxidized patches, limonitic ox.
		40-45'	Gypsum, clay, qtz., silt, pyrite		Med.-dk. gray	40-43' as above, but more moist; gypsum, pyrite abundant; 43' top of <u>lower Conquista</u> ; 43-45' med.-dk. gray, sl. indurated chippy slty clayst.; less silt, very little gypsum.
		45-50'	Clay, qtz., silt, pyrite	Clay, silt	Dk. gray	45-50' dk. gray silty clay; weathered and unweathered sulfides; v. minor gypsum; less indurated, less chippy than 43-45'.

Table 2 (cont.)

Borehole ID 859 (#15)

Field Sample Log (Cuttings) (cont.)

		50-55'	Clay, qtz., silt, limonite, hematite	Clay, silt	Dk. gray	50-55' as above, minor silt; more gypsum (now white, amorphous); occas. limonite, hematite patches.
		55-60'	Yellow-grn. grains	Clay, silt	Dk. gray	55-60' as above, sl. more silt, crumbly; occas. yellow-green mineral grains.
		60-65'	Clay, pyrite	Clay	Med. gray	60-65' med. gray claystone, slightly chippy, slightly indurated; v. fine fresh sulfide grains.
		65-70'	Clay, trace gypsum	Clay	Dk. gray-black	65-70' v. dk. gray to black gummy clay, minor gyp.
		70-75'	Clay, trace gypsum	Clay	Dk. gray-black/ chocolate brown	70-73' as above; sl. indurated; 73' chocolate-brown lignite; dry, fibrous, slightly indurated.
		75-80'	Lignite, quartz	SS-F-GR	Lt. gray, dk. brown	75-77' Chocolate brown lignite; as above, fine gyp. xls; 77' top of <u>Dilworth</u> lt. gray fine sandstone; hard, indurated; 79' TD.
3/4/91						Water at 34.9' below surface; screened slty to slightly sdy interval from 33-43' (~middle of Conquista).

Table 2 (cont.)

Borehole ID 860 (#12)

Field Sample Log (Cuttings)

Dates 3/12/91 and 3/13/91

Drilling Foreman: Bill Wood

TD 83'

Date	Initials	Interval	Mineralogy	Grain size	Color	Comments/description
3-12-91 Start 3:30 pm	JGB	0-4'		Clay, silt		Black, clayey soil.
		4-10'		Silt, v.f. sand		Tan to yellowish brown clay, silty, probably oxidized <u>Dubose</u> .
		10-15'			Tan/yel. brown	Same as above w/some limonitic staining; abundant gypsum.
		15-20.5'	Gypsum, limonite	Silt, clay		Tan to light olive brown clay (silty); abundant small gyp. flakes; limonitic staining common; 15-20' was denser and less silty than 10-15' section of clay; drill cuttings from 15-20' looked like shavings; probably due to denser clay.
		20.5-25'		Fg. - Vfg. sand	Reddish brown	Hit reddish brown sand at 20.5' (<u>Deweeseville</u>); sand changed color to a lighter brown at 24' - not reddish.
		25-30'		Fg. - Vfg. sand		Light brown sand to 27.5'; hit very hard sand at 27.5' to 30.0'; cuttings were powdered by drill action.
		30-35'		Vf. - fg sand, clay		Left hard sand at 30.0'; encountered damp, light-olive gray/green sand at 32'; from 30-35' was an indurated sand.
3-13-91	JGB	35-40	Biotite flakes	Vfg. - fg sand	Light olive gray/tan	Light olive-gray/tan f.g. sand, clay, and clayey sand speckled w/dark heavy minerals; still <u>Deweeseville</u> , but getting more clay.
		40-45'		Clay, silt		Same as above, but clay content increasing transition to <u>Conquista</u> clay around 45' (estimated).
		45-50'		Silt, clay	Tan to 49'	Silty clay oxidized to 49'; at 49' encountered med. dark olive-gray clay at 49.0'
		50-55'		Clay	Dark olive gray	Dark olive-gray silty clay w/splotches of tan and clay mixed in; est. redox at 52'.
		55-60'		Silt, clay, vfg. sand		Med. dark olive-green clay; silty w/probable interbeds of tan silty, sandy clay.

Table 2 (cont.)

Borehole ID 860 (#12)

Field Sample Log (Cuttings) (cont.)

		60-65'		Clay		Produces gray-green cuttings w/tan blotches. Tan material may be from up the hole.
		65-70'		Clay, silt	Dark olive gray	Dark olive-gray slightly silty clay; some streaks of tan silty, sandy clay.
		70-75'	Calcite cement	Vfg. sand, silt clay		More of the same, except hit a hard zone at 72' - probably corresponds to <u>Conquista Sand</u> ; fossil fragments present in this interval.
		75-83'		Clay	Dark olive gray	Dark olive-green silty clay; some carbonaceous material below fossil zone after ~78'.

Table 2 (cont.)

Borehole ID 861 (#13)

Field Sample Log (Cuttings)

Dates 2/1/91 and 2/2/91
Drilling Foreman R. Papusch

TD 70'

Date	Initials	Interval	Mineralogy	Grain size	Color	Comments/description
2-1-91	RP/JB	0-5'	Qtz, clay, gyp		Med drk brn	Silty, sandy, clayey fill material. This area was mined by CONOCO and then reclaimed.
		5-10'	Qtz, clay, gyp			Fill material
		10-15'	Qtz, clay, gyp			Fill material. Stopped for day at approx. 13.5'.
2-2-91	RP/JB	15-20'	Qtz, clay, gyp		Tan- Yellow Brown	Fill material
		20-25'	Gyp, qtz sand	Fg. - vfg sand, clay	As above	Hit friable, f.g. to v.f.g. sand at approximately 23'. Possibly <u>Deweeseville</u> or very sandy fill material.
		25-30'		Fg. - vfg sand, clay	Tan sand to drk gray clay	25-26' as above. Hit reduced <u>Conquista Clay</u> at 26'. Conquista is dark greenish gray silty clay. Redox at 26'.
		30-35'	Qtz, Montmoril. clay, trace gyp	Silt, clay	Drk greenish gray	Dark greenish gray, silty, Conquista Clay. Switched to H ₂ O drilling at 35'.
		35-40'	Qtz, Montmoril. clay, trace Gyp	Clay, silt	Drk greenish gray	Dark greenish gray, silty, clay.
		40-45'	Qtz, Montmoril. clay, trace Gyp	Clay, silt	Drk greenish gray	Dark greenish gray, silty, clay.
		45-50'	Qtz, Montmoril. clay, trace Gyp	Clay, silt	Drk greenish gray	Dark greenish gray, silty, clay.
		50-55'	Qtz. Montmoril. clay, calcite	Clay, silt	Drk greenish gray	Dark greenish gray, silty, clay. Hit fossils at 52-55'. Probably shell hash zone
		55-60'	Qtz. Montmoril. clay	Clay, silt	Drk greenish gray	Dark greenish gray, silty, <u>lower Conquista Clay</u> .
		60-65'	Qtz. Montmoril. clay	Clay, silt	Drk greenish gray	Dark greenish gray, silty, clay.
		65-70'	Qtz. Montmoril. clay	Clay, silt	Drk greenish gray	Dark greenish gray, silty, clay. TD at 70'.

Table 2 (cont.)

Borehole ID 862 (#9)

Field Sample Log (Cuttings)

Date 4/1/91

TD 150'

Drilling Foreman: Bill Wood

Date	Initials	Interval	Mineralogy	Grain size	Color	Comments/description
4-1-91	RSG	0-5'	Clay/qtz. sand	Clay/f. sand	Tan/blk.	Top 3' is possibly road filler; host tan clay and sand; hit black clay (soil horizon?) @ 3' and sandy clay @ 4'.
		5-10'	Qtz., feldspar	Silt/f. sand	Lt. brown	Gypsiferous, slightly damp, sand and sandy silt; >90% qtz.
		10-15'	Qtz., rock fragments	Fine	Lt. gray	Unconsolidated sand; driller says he hit clay layer @ ~14' but not much clay in cutting.
		15-20'	Quartz	Fine sand/slt	White-lt. gray	Hard drilling 15.5-18'; silt lenses in bottom 2' of interval.
		20-25'	Qtz., rock fragments	F. sand silt	White, lt. gray	Damp; hard sand lens ~23'.
		25-30'	Quartz	V. fine silt	Lt. gray-brown	Damp.
		30-35'	Clay min.	Silt/clay	Lt. brown	Harder and darker brown clay @33'; <u>Conquista</u> contact; gypsiferous; Fe oxides.
		35-40'	Clay min.	Clay	Brown/ gray	Saturated - reduced clay @38'; Fe oxides in oxidized portion; soft clay. Redox at 38'.
		40-45'	Clay min.	Silt/clay	Dark gray	Soft; a few hard chips of red siltstone.
		45-50'	Clay min.	Silt/clay	Dark gray	As above.
		50-55'	Clay min.	Silt/clay	Dark gray	A little more silt and harder claystone.
		55-60'	Clay min.	Silt/clay	Dark gray	Silty clay and siltstone.
		60-65'	Qtz., clay minerals	V. fine sand/ silt, clay	Dark gray	Fossiliferous; very little sand (10-20%); contact with <u>Conquista Sand</u> @ 61'.
		65-70'	Clay min.	Silt/clay	Dark gray	Shell fragments sparser; siltstone and claystone lenses.
		70-75'	Clay min.	Silt/clay	Dark gray	Siltier than prev. interval; few remaining shell fragments - questionable - may have fallen in; <u>lower Conquista</u> contact @74'.
		75-80'	Clay min.	Silt/clay	Dark gray	More plastic than above; darker color, clayier.
		80-85'	Clay min.	Silt/clay	Dark gray	As above.

Table 2 (cont.)

Borehole ID 862 (#9)

Field Sample Log (Cuttings) (cont.)

		85-90'	Clay min.	Silt/clay	Dark gray	As above; some harder silt lenses; back to original gray color.
		90-95'	Clay min.	Silt/clay	Dark gray	As above, but siltier.
		95-100'	Qtz. and clay minerals	Silt/clay	Chocolate brown	Clay turned color, organic smell poorly defined, if lignite bed.
		100-105'	Qtz. and clay minerals	Silt/clay v.f. sand	Chocolate brown	Hit small hard layer ~100'; some hard sandstone chips in cutting.
		105-110'	Qtz. and clay minerals	Silt/clay	Chocolate brown	More hard drilling @~107'; lignite pieces; sandstone, siltstone chips; <u>Dilworth</u> contact @ 107'.
		110-115'	Qtz., clay minerals	V. fine sand, silt, clay	Chocolate brown, dk. green	Sandstone and siltstone chips in cuttings; clay matrix may be from up the hole.
		115-120'	Qtz., clay minerals	Silt, clay	Dark green	Less sandstone than above.
		120-125'	Qtz., clay minerals	Silt, clay	Dark green	Hard sandstone lenses.
		130-135'	Qtz., clay minerals	Silt, clay	Dark green	Occasional hard drilling.
		135-140'	Qtz., clay minerals	Silt, clay	Dark green	Sandstone layers more abundant.
		140-145'	Qtz., clay minerals	Silt, clay	Dark green	As above.
		145-150'	Qtz., clay minerals	Silt, clay	Dark green	As above.

Table 2 (cont.)
Borehole ID 863 (#1)
Field Sample Log (Cuttings)

Date 3/3/91

TD 45'

Drilling Foremen: Boyle-T. Robertson; Jacobs-R. Papusch

Date	Initials	Interval	Mineralogy	Grain size	Color	Comments/description
3/3/91	PWD	0-5'	Qtz., ?gyp.	Slt., f.-m. sd.	Lt. tan-beige	<u>Deweeseville</u> sandstone; 0-3.5' beige to lt. tan silt, unind.; some harder ochre-stained chips; light, soft material - ash? zeolite? possibly some gypsum.
			Clay, qtz., slt., carbonaceous mat.	Slt., f. sd.	Med. gray	3.5' med. gray, hard clayey siltst. to f. ss; some black carbonaceous material
		5-10'	Clay, qtz., slt., Fe oxides	Clay-silt	Yellow-tan; red-brown	5-10' Yellowish-tan clay, gummy, moist; clay to clayey silt; ochre patches, some red-stained chips of siltst.
		10-15'	Clay, qtz., silt, abund. gyp.	Silt, f.-m. sd.	Tan to red-brown	10-15' tan clayey silt becomes siltier, sandier, redder; clean qtz silt, f-m sd. 11' med. red-brown clayey siltstone; abund. gypsum
		15-20'	Qtz. sd., gyp, chert	F.-m. sd.	Beige to white	15-20' beige to white sandst., hard, gypsiferous (med. to coarsely xline gyp); chert chunks, tan, smooth; 15.5-16.5 hard, white qtz ss, f-med. grained
		20-25'	Qtz. silt. and sd., clay, chert	F.-m. sd.		20-22' clean qtz ss as above. 21' water table. 22' top of <u>upper Conquista Clay</u> , lt. beige to cream to tan gummy clay, wet; some free qtz. silt.-f. sd.. grains; occas. chert (tan) chunks as above; pale beige 25-30' sticky wet clay.
		30-35'	Clay, qtz. sd., feldspar	Clay; f.-m. sd.	Dk. gray cream to pale beige	30-33' dark gray sticky wet clay; 33' cream to pale beige f-m qtz sd, minor clay, feldspars; friable; increased water flow while drilling in ss.
		35-40'	Clay, qtz. silt.	Slt-cl	Dk. gray	35-36' as above; 36-40 dark gray silty clay, some (minor) red clay; chips of gray siltstone; possible redox boundary.
		40-45'	Qtz. silt., clay	Slt		40-45' gray silty clay to clayey silt; more indurated siltstone layers at bottom of hole.

Screened in upper Conquista from -31.71-42'; (interpreted as Conquista Sand at drill site but comparison with other nearby holes indicates that section from 22' to TD is upper Conquista).

Table 2 (cont.)

Borehole ID 864 (#2)

Field Sample Log (Cuttings)

Date 3/4/91

TD 106'

Drilling Foremen: Boyle - T. Robertson; Jacobs - R. Papusch, B. Wood

Date	Initials	Interval	Mineralogy	Grain size	Color	Comments/description
3/4/91	PWD	0-5'	Clay, qtz., silt	Clay, silt	Med. tan, with red, ochre	0-4 blk soil; <u>Dubose</u> 4-5 med. tan silty clay w/patches of hematite, limonite; gyp and carbonaceous material.
		5-10'				As above; gyp xls ((med. xline) oxidized sulfide grain, minor silt. rare yellow earthy patches.
		10-15'	Clay	Clay	Med. tan	Med. tan semi-indur. claystone, harder fragments; virtually no silt; Fe staining on clay partings; oxidized bleached Dubose.
		15-20'	Clay, qtz., silt	Clay, fine sand	As above, with white patches	Med. tan sticky clay w/patches of white silt-f.g. sd. poss. gyp sd.?
		20-25'	Qtz., Fe oxides	F-m. sand	Tan, red- and red-brown stained	20' probable top <u>Deweeseville</u> ; loose tan-red and brown-red sand f.-m.g. sand-oxidized and red stained.
		25-30'	Qtz., clay		Yellow, tan, lt. beige	Yellow-tan-lt. beige sd.; very minor clay; loose, unconsolidated; 15% dark grains.
		30-35'	Qtz., feldspar, Fe oxides		Lt. gray-beige	Hit water at ~32' - Lt. gray-beige unconsolidated sd.; predomin. qtz., minor rock frags. and dk. grains, slightly more feldspar; red grains are prob. altered sulfides.
		35-40'	Clay, qtz., Fe oxides	F. sand, clay	Lt. tan, beige	Lt. tan-beige loose f.g. sd.; some clay patches-red stained; mostly qtz, few drk. grains.
		40-45'	Qtz. silt, clay, sulfides, Fe oxides	Silt, incr. clay	Dk. tan, tannish gray	Drk. tan-tannish-gray silt; not indurated; some gypsum increasing clay content; ochre-stained patches; very fine; oxidized sulfide grains, clots of med. gray clay in lower part; top of <u>Conquista</u> at ~44'.
		45-50'	Clay, qtz. silt	Clay, silt	Med. gray	Clayey silt to silty clay; ~50% silt and 50% clay.
		50-55'			Med. gray	As above but w/more clay.
		55-60'			Med. gray	As above.
		60-65'			Med. gray	As above but more clay, ~60%.
		65-70'			Med. gray	As above.

Table 2 (cont.)

Borehole ID 864 (#2)

Field Sample Log (Cuttings) (cont.)

		70-75'	Qtz. silt, gyp., carbonate shell frags.	Silt, clay, shell frags.	Med. gray	As above but siltier, shell fragments, gypsum cemented? clean siltstone, lt. tan.
		75-80'				As above.
		80-85'				As above, ~30% silt.
		85-90'				As above, ~40% silt., thin interbeds of silt. and clay; thin silt. beds are tan.
		90-95'				As above.
		95-100'	Clay	Clay, minor slt		As above, but dominantly sticky gray clay w/minor silt; forms cohesive lumps.
		100-105'	Clay, lignite	Clay		Sticky gray clay as above; 102.5 - lignite, brown, fibrous.
		105-106'	Qtz.	F. sand	Lt. gray	<u>Dilworth</u> ss.; lt. gray, f.g. ss., indurated.

Table 2 (cont.)
 Borehole ID 865 (#5)
 Field Sample Log (Cuttings)

Date 3/31/91

TD 60'

Drilling Foreman: Bill Woods

Date	Initials	Interval	Mineralogy	Grain size	Color	Comments/description
3/31/91	RSG	0-5'	Clay-quartz	Fine	Black-yellow	1' blk. clay topsoil; fine sand and sandstone.
		5-10'	Qtz., Fspar.,	Fine	Tan-yellow	Hard streak @ 8'; poorly consolidated sand w/silicified (lenses); more of a yellowish tinge than above; Fe oxides.
		10-15'	Qtz.-clay	Very fine	Tan	Interbedded sand, siltstone and clay, dominantly silt and clay; <u>upper Conquista</u> contact ~11'.
		15-20'	Clay; qtz.	Silt/clay	Brown	Carbonaceous; Fe oxides; slightly damp silt and claystone.
		20-25'	Clays; qtz.; gypsum	Silt/clay	Darker brown	Gypsum flakes; Fe oxides; more clay than silt.
		25-30'	Clay minerals	Clay/silt	Red-brown/ gray	Becomes dk. gray; reduced silty clay @ ~28'; Fe oxides.
		30-35'	Clay minerals	Clay/silt	Dk. gray	Silty clay; gypsum flakes.
		35-40'	Clay; qtz.	Clay/v. fine snd.	Dk. gray	Hard SS ~40'; abundant fossils; <u>Conquista Sand</u> contact ~37'.
		40-45'	Clay; qtz.	Clay/silt v.f. sand	Dk. gray	Sand, siltstone; fewer fossils; <u>lower Conquista</u> contact ~43'.
		45-50'	Qtz., clay	Clay/silt, v.f. sand	Dk. gray	Dominantly silt and clay; fossils seem to have fallen in, along w/sand, from above, not abundant; different color from rest of interval.
		50-55'	Silt, clay min.	Silt/clay	Dk. gray	Hit hard streak @ 54'; silicified zone.
		55-60'	Clay	Silt/clay	Dk. gray	Silty claystone.

Table 2 (cont.)

Borehole ID 878 (#16)

Field Sample Log (Cuttings)

Dates 5/23/91 and 5/25/91

Drilling Foreman W. R. Wood

TD 122'

Date	Initials	Interval	Mineralogy	Grain size	Color	Comments/description
5/23/91 to 5/25/91						878 drilled w/mud. Cuttings very mixed, poor quality for description. Better cuttings descriptions for nearby (50') MW #856 were used for #878 to 80'. Below 80' the mud cuttings from 878 were used for description.
	RSG	0-5'	Qtz., feldspar	Fine	Lt. brown	Silty sand, some unconsolidated, some chips more indurated. <u>Conquista Sand</u>
		5-10'	Quartz	Fine	Lt. brown	Sand, silt, clay; clay starts ~7'.
		10-15'		Silt/clay	Lt. brown	Silt and clay (switch to mud).
	RSG	15-20'		Clay	Lt. brown	Clay soft but cohesive, some FeOOH.
		20-25'		Clay	Lt. brown	Same clay, more FeOOH.
		25-30'	Quartz	Clay/silt	Brown/lt. gray	Soft cohesive clay; also some silt and a very little quartz sand.
	RSG	30-35'	Quartz	Clay/silt	Brown	Clay, slightly more silty, sandy.
		35-40'	Quartz	Fg. snd, silt, clay	Brown	Fine sand, silt clay FeOOH, some carbonaceous material.
		40-45'	Qtz., feldspar	V. fine	Lt. brown	Unconsolidated sand.
		45-50'	Qtz., feldspar	V. fine	Lt. brown	Unconsolidated sand.
	RSG	50-55'	Qtz., feldspar	V. fine	Lt. brown	Unconsolidated sand.
		55-60'	Qtz., feldspar	V. fine clay	Brown, gray	Driller possibly hit clay bed ~58'; clay soft, but cohesive.
	RSG	60-65'	Quartz	Fg. snd Clay	Brown	Sand, some silicified, darker brown; some clay but not much; still Conq. sand.
		65-70'		Silt, clay	Dk. brown	Dark claystone in chips, some sand; hard drilling (<u>lower Conquista contact?</u>);
		70-75'		Clay	Chocolate brown	Chocolate-colored clay, some FeOOH; hard drilling.
	RSG	75-80'		Clay	Chocolate brown	Same as above.

Table 2 (cont.)

Borehole ID 878 (#16)

Field Sample Log (Cuttings) (cont.)

						End description of cuttings from #856.
	JB/RSG	80-97'	Lignite		Dark gray/ brown	Within lower <u>Conquista Clay</u>
	JB/RSG	97-100'			Drk. Brown	Lignite
	JB/RSG	100-122'	Qtz, clay,	Fg sand/ silt, clay		<u>Dilworth</u> starts at base of lignite; TD at 122'.

Table 2 (cont.)
 Borehole ID 879 (#17)
 Field Sample Log (Cuttings)

Date 5/25/91

TD 65'

Drilling Foreman: Richard Papusch

Date	Initials	Interval	Mineralogy	Grain size	Color	Comments/description
5-25-91	RSB/ JGB	0-5'	Clay minerals	Silt/clay	Lt. brown	0-3.5 soil; 3.5-5 is <u>Dubose</u> silty clay.
		5-10'	Clay minerals	Silt/clay	Lt brown	Silty clay, limonitic, gypsiferous; moderately plastic.
		10-15'	Clay minerals	Silt/clay	Lt. brown	Same as above.
		15-20'	Clay minerals	Silt/clay	Lt. brown	Same as above, but slightly siltier, more gypsum.
		20-25'	Clay minerals	Silt/clay	Darker brown	Silty clay w/gyp.
		25-30'	Clay minerals	Silt/clay	Darker brown	Same as above; some reduced clay; redox ~29'.
		30-35'	Clay minerals	Silt/clay	Dark gray	Reduced clay.
		35-40'	Qtz.; clay minerals	V.f./clay	Dark gray	Slightly sandy; reduced clay.
		40-45'	Qtz.; clay minerals	V.f./clay	Dark gray	Lignite from 42-44' (base <u>Dubose</u>); clayey sand from 44-45'; <u>Deweesville</u> at 44'.
		45-50'	Qtz.; clay minerals	V.f./clay	Dark green	Clayey sand, carbonaceous damp (<u>Deweesville</u>).
		50-55'	Qtz.; clay minerals	V.f./clay	Dark green	Hit indurated dark green sand at 52'; clayey.
		55-60'	Qtz.; clay minerals	V.f./clay		As above.
		60-65'	Qtz.; clay minerals	V.f./clay		As above.

Table 3. Chemical analyses of BEG monitoring wells, Falls City, Texas, UMTRA Site.

Sample location and sampling procedure

All samples (except QA sample duplicates from wells 678 and 920) are from BEG monitoring wells completed at the Falls City, Texas, UMTRA site. At least three bore volumes were pumped or bailed prior to sampling. Sampling began once pH and conductivity stabilized during pumping. Standard BEG water sampling procedures (SWI 3.1) were followed, and all samples were field filtered to 0.45 µm. Cations were preserved with 5 ml 6N HNO₃.

Analytical laboratories and methods

Major cations and selected trace elements were analyzed at the MSL by ICP-AES using the procedures described in SWI 1.5. Anions were determined at the BEG (MSL) by ion chromatography (SWI 1.15). Radium 226 and 228 were analyzed at the Texas Department of Health. U, As, and Se were analyzed by ICP-AES at the Railroad Commission of Texas laboratory. Tritium was analyzed at the University of Miami by gas counting after electrolytic enrichment.

Results

Table 1 contains the results for cations, tritium, and TDS.

Table 2 contains the results for the anionic species.

Table 3 contains the QC/QA data for this data set.

Comments

All calibration solutions at the MSL were prepared using NBS-certified elemental solutions.

All elemental data are reported as mg/L unless otherwise indicated.

Analyses of a larger trace element suite are undergoing final review and will be reported when available. Wells 864 and 855 were dry and no samples were collected.

Table explanation

[< less than indicated value]

[* reported value near detection limit]

[N.A. Not analyzed]

Table 3 (cont.)

Well ID DOE	(BEG)	Date sampled	Formation screened	U	As	Se	Ra-226 PCi/L	Ra-228 PCi/L	Tritium	Na	K
851	(6)	25-Apr-91	Deweesville	2.2	< 0.2	< 0.5	5.5 ± 0.6	6.1 ± 2.4	-.03 ± .09	722	44.6
852	(3)	25-Apr-91	Deweesville	< 2	< 0.2	< 0.5	11 ± 1	6.3 ± 1.1	-.04 ± .09	604	41.5
853	(11)	22-Apr-91	Deweesville	3.07	< 0.2	< 0.5	32 ± 2	10 ± 2	.67 ± .10	2180	67.5
854	(14)	23-Apr-91	Deweesville	< 2	< 0.2	0.37	23 ± 1	14 ± 3	4.02 ± .13	2050	99.8
856	(8)	23-Apr-91	Conquista SS	8.33	< 0.2	< 0.5	2.9 ± .4	5.9 ± 1.5	3.15 ± .11	1540	41.6
857	(7)	26-Apr-91	Conquista	< 2	< 0.2	< 0.5	1.1 ± 0.2	2.1 ± 0.7	-.13 ± .09	458	29.3
858	(10)	2-May-91	Conquista	< 2	< 0.2	< 0.5	4.3 ± 0.5	17 ± 4	.49 ± .10	1260	93.4
859	(15)	26-Apr-91	Conquista	< 2	< 0.2	< 0.5	0.7 ± 0.3	1.9 ± 1.6	.18 ± .09	1280	77.9
860	(12)	2-May-91	Conquista	< 2	< 0.2	< 0.5	0.8 ± 0.3	1.1 ± 1.3	-.09 ± .09	712	56.5
861	(13)	2-May-91	Conquista	< 2	< 0.2	< 0.5	1.0 ± 0.3	1.7 ± 1.7	-.08 ± .09	739	62.2
862	(9)	22-Apr-91	Dilworth	< 2	< 0.2	< 0.5	1.0 ± 0.3	1.5 ± 1.1	.03 ± .09	454	35.2
863	(1)	24-Apr-91	Conquista	2.69	< 0.2	< 0.5	12 ± 1	15 ± 2	.01 ± .09	1580	117
865	(5)	7-Jun-91	Conquista	< 2	< 0.2	< 0.5	N.A.	N.A.	N.A.	967	70.9
878	(16)	7-Jun-91	Dilworth	< 2	< 0.2	< 0.5	N.A.	N.A.	.19 ± .09	941	53.2
879	(17)	7-Jun-91	Deweesville	< 2	0.26	< 0.5	N.A.	N.A.	.17 ± .09	1430	123

Well ID DOE	(BEG)	Mg	Fe	Ca	Al	Si	Sr	Ba	Mn	Li	TDS
851	(6)	65.5	<0.05	677	<0.6	31.2	4.66	*0.07	*0.02	*0.1	6248
852	(3)	81.5	<0.05	762	<0.6	35.9	5.43	0.1	*0.03	*0.1	5954
853	(11)	308	0.14	1930	60	48.2	13.1	*0.04	10.6	0.5	14905
854	(14)	345	0.45	1300	33.1	47.3	19.1	<0.03	14.8	1.2	12951
856	(8)	124	*0.06	2030	< 0.6	25.7	11.1	*0.04	0.07	*0.1	12769
857	(7)	24.8	<0.05	181	<0.6	29.4	1.47	*0.06	0.09	<0.1	3798
858	(10)	200	*.10	969	* 0.7	27.3	10.4	* 0.04	5.23	0.8	8983
859	(15)	130	<0.05	910	< 0.6	21	9.43	*0.04	1.99	0.4	8594
860	(12)	58.8	*0.05	491	< 0.6	20.1	3.83	*0.04	2.13	*0.3	5836
861	(13)	88.5	*0.10	524	< 0.6	19.9	4.69	*0.03	2.93	0.3	6218
862	(9)	15.3	<0.05	238	< 0.6	21.1	1.56	<0.03	0.29	*0.1	4021
863	(1)	243	1.49	1060	49.5	38.1	11.8	0.9	13.8	1	10642
865	(5)	116	0.13	757	< 0.6	18.7	7.06	*0.04	3.05	0.7	7508
878	(16)	63.5	0.75	603	< 0.6	22.5	4.88	*0.04	5.03	*0.1	6739
879	(17)	558	49.8	1180	25.1	42.7	15.6	*0.04	40.6	2	11911

Table 3 (cont.)

Well ID		Lab ID	SO ₄	Cl	F	Br	NO ₃	HCO ₃	Anion vs.
DOE	(BEG)								cation
									(% error)
851	(6)	91-179	445	2100	1.2	5	5.4	444	-2.9
852	(3)	91-176	861	1720	<1.0	3.9	40.1	95	2.4
853	(11)	91-184	1400	7110	<1.0	14.2	56.5	0	-1.2
854	(14)	91-186	1830	5480	<1.0	11.2	10.9	0	-0.8
856	(8)	91-181	1370	5300	<1.0	10.5	73.6	530	-2.2
857	(7)	91-180	198	611	3.2	1.8	7.2	539	2.1
858	(10)	91-183	1830	2690	2.1	6.8	76.9	95	2.3
859	(15)	91-187	1770	2320	<1.0	6.9	<1.0	348	2.8
860	(12)	91-178	1560	905	<1.0	1.9	<1.0	305	-0.9
861	(13)	91-185	1500	1150	<1.0	2.6	<1.0	402	-2
862	(9)	91-182	775	340	<1.0	<1.0	<1.0	417	1.9
863	(1)	91-175	2050	3710	14.8	8.9	15.3	0	0.7
865	(5)	91-243	1730	1630	<1.0	5.2	<1.0	472	1
878	(16)	91-244	1670	1240	<1.0	3.4	<1.0	380	1.1
879	(17)	91-245	2290	4390	14.9	8.9	<1.0	0	1.5

Table 3 (cont.)

QC data for cation analyses at BEG (MSL).

Well no.	Na	K	Mg	Ca	Fe	Al	Sr	Ba	Mn	Li	SO ₄	Cl	Br	NO ₃	F
861 A	755	63	90.7	519	* 0.11	< 0.6	4.77	* 0.04	2.97	0.32	1490	1164	2.4	< 1	< 1
861 B	731	62.3	86.9	526	* 0.1	< 0.6	4.68	* 0.03	2.92	0.29	1504	1154	2.8	< 1	< 1
861 C	730	61.4	88	528	*0.09	< 0.6	4.6	* 0.03	2.91	0.29	1510	1122	2.6	< 1	< 1
Mean	739	62.2	88.5	524			4.69		2.93	0.3	1501	1147	2.6		
Std. dev.	14	0.8	2	4.7			0.08		0.03	0.02	10.3	21.9	0.2		
Rel st. dev.	2	1.3	2.2	0.9			1.71		1.1	5.77	0.7	1.9	7.8		

Blind duplicate analyses by BEG of JEG samples 678 and 920 (sampled 1/91).

Well no.	Na	K	Mg	Ca	Fe	SiO ₂	Al	Sr	Ba	Mn	SO ₄	Cl	F	Br	NO ₃
678															
(JEG)	390	50	69.7	409	1.21	68.4	0.57	3.35	0.01	3.28	1720	332	0.8	0.7	1.5
(BEG)	392	48.6	70	434	1.3	71.6	.8*	3.29	< .03	3.48	1600	351	1	< 1.0	< 1.0
920															
(JEG)	575	50	43.6	471	< .03	53.3	< .05	3.6	0.01	0.47	1890	535	0.1	1.4	1.9
(BEG)	618	49.6	49.5	518	< .05	56.2	< .6	3.9	< .03	0.53	1730	508	< 1.0	1	< 1.0

Results of quality control analyses for U, As, and Se at the Railroad Commission of Texas.

Standard	Element	Known	Observed	Element	Known	Observed	Element	Known	Observed
EPA	U	2.5	1.8	As	1	0.82	Se	0.99	0.74
WP1083	U	10	10.4	As	0.5	0.44	Se	0.495	0.42
	U	50	53.7	As	0.2	0.19	Se	0.198	N.D.
				As	0.1	ND	Se	0.099	N.D.

Table 4. BEG Core data, Falls City, Texas, UMTRA Site.

Well ID DOE	(BEG)	y	x	Land surface elevation (ft)	Surface geology	Ending unit	Total depth (ft)	Redox depth (ft)	Redox elevation (ft)
866	(22)	60374.5	67198.7	443	Deweesville	Upper Conquista	46	Not reached	
867	(24)	56764.4	65276.2	408	Backfill	Manning	168	22.8	385.2
868	(28)	60839.4	66252.9	445	Deweesville	Dilworth	117	40.7	404.3
869	(29)	61668.9	64537.9	469	Tailings	Dilworth	121.4	68.8	400.2
870	(17)	60494.5	63339.9	473	Upper Conquista	Dilworth	110	67	406
871	(20)	58672.0	68073.8	422	Dubose	Dilworth	130	54	368
872	(19)	55630.2	64917.2	420	Deweesville	Dilworth	100	35	385
873	(18)	60405.2	65278.0	456	Deweesville	Lower Conquista	75.3	37	419
874	(21)	58062.5	68789.1	441	Dubose	Dilworth	161.6	55.5	385.5
875	(30)	62304.9	64184.3	446	Conquista Sand	Manning	160	36	410
876	(16)	59175.1	64429.0	458	Upper Conquista	Manning	193.6	46.4	411.6
877	(27)	58781.7	65317.1	433	Deweesville	Conquista Sand	60	37.4	395.6

Table 5. Lithologic descriptions of 12 2-ft cores collected from January to May 1991 at the Falls City UMTRA site. Descriptions by Jon Blount and Stu Goldsmith (BEG). Coring under the supervision of JEG. General information on cores in table 4. Locations of core holes shown in location map.

Description of Core 966 (BEG #22)	
Depth/Interval (ft below surface)	
Soil	
0 - 3.0	Dark brown to brownish black clayey soil. Sand content increases significantly from 1.0 to 3.0 ft.
Deweeseville Sand	
3.0 - 11.0	Light olive gray, vfg to fg, silica-cemented sandstone. Contains minor to moderate amounts of tan bentonitic clay clasts. Yellowish-green, fluorescent autunite or meta-autunite occurs along fracture planes.
11.0 - 22.2	Light olive gray to tan, uncemented, silty, sandy clay and clayey, vfg sand. This dominantly clayey section contains burrows filled with limonite-stained vfg sand and silt. Limonite, MnO, and greenish-yellow autunite or meta-autunite along fracture and bedding planes. Calcite is abundant along a few bedding and fracture planes.
22.2 - 24.0	Pale olive green, silty sandy clay with a few reddish-brown, oxidized, carbonaceous layers.
24.0 - 27.3	Grayish-white, unconsolidated, moderately clayey, vfg sand.
27.3 - 32.3	Olive gray to light gray, silica-cemented, slightly clayey sandstone.
32.3 - 42.5	No core recovered.
Upper Conquista Clay	
42.5 - 46.0	Light olive green sandy clay to hard bentonitic clay. Dendritic MnO and trace greenish-yellow coating (autunite?) along bedding planes and fracture planes.
TD = 46 ft	

Table 5 (cont.)

Description of Core 867 (BEG #24)

**Depth/Interval
(ft below surface)**

Topsoil

0 - 3 Black sandy clay topsoil.

3 - 16.5 Olive gray sandy clay, apparently backfill. Clasts of clay, sandstone, gypsum, and limonite are unoriented. Coarsens to clayey sand by 16.5 ft.

Upper Conquista Clay

16.5 - 21.5 Abrupt change to light brown to olive green interbedded silt and clay. The clay appears to be montmorillonitic (swelling), and bedding is not always well preserved. Where bedding is preserved, and clay is hard and waxy, limonite and gypsum are abundant along fractures and bedding planes. The clay layers begin to darken at the bottom of the interval.

21.5 - 30.5
Redox at 22.8 Very dark olive gray clay, hard and waxy, interbedded with medium olive green wispy siltier beds. (Note: the irregularity of the beds may be an artifact of coring, since they all bow up towards the middle of the core.) The deepest significant appearance of limonite is at 22.8 ft. Where it is present below this, it occurs as small specks. Disseminated gypsum and occasional carbonaceous partings are present.

30.5- 47 Dark olive gray clay interbedded with medium olive gray silt. Much siltier than the previous interval, and much more fractured. Disseminated gypsum (efflorescence?) is abundant. Coarsens downward, sandy by 46.7 ft.

Conquista Sand

47 - 49.9 Medium olive gray interbedded sandy siltstone and sandy claystone . Fossiliferous: abundant gastropod and pelecypods shells. Bioturbated, with sand filling in the burrows. Sand is lenticular (2 cm maximum thickness) where not bioturbated. Calcite- and clay-cemented quartz sand, with sparse mafic grains. Gypsum is present, but sparse, usually as small crystals in the clay layers. Bioturbation and grain size decrease with depth. Lowest fossil appearance is at 49.9 ft.

Lower Conquista Clay

49.9 - 72.9 Dark brown to dark olive gray claystone with wispy sparsely sandy silt lenses (1-2 mm). Clay makes up >80% of the interval. Moderately bioturbated. Some carbonaceous stringers are present close to the overlying fossiliferous zone. Fractures and partings are abundant except in two 1 ft zones of softer clay.

72.9 - 78.5 Massive claystone: hard, waxy, sparsely fossiliferous. Sparse silt in wispy and lenticular bodies. Clay turns from dark olive gray to dark chocolate brown with depth. Becomes very carbonaceous by 78.5 ft.

78.5 - 82.3 Lignite: clay-rich at top of interval, including some irregularly shaped lenses of clay (1-2 cm). Some yellow earthy material (sulfur?) at 79.5 ft. Calcite present in partings throughout the lignite. The lignite bed grades abruptly into a moderately carbonaceous sandy clay.

Table 5 (cont.)

Dilworth Sandstone

82.3 - 92.4	Light olive gray quartz sandstone; indurated, probably quartz-cemented. Generally becomes more clay-rich with depth. Carbonaceous throughout interval. Bedding is indistinct, possibly bioturbated in top 3 ft of the interval. There is an irregularly shaped calcite nodule in this zone. Sandy clay also forms irregular shapes, filling burrows and possibly fractures. Where the sandstone becomes clay-rich, the rock becomes poorly consolidated (probably clay cemented). Limonite is abundant in this zone, with some yellow (possibly uranium) minerals associated with the limonite. Sandstone becomes a medium olive gray at 91.25 ft. This is also the lowest appearance of limonite (possibly a redox boundary?).
92.4 - 109.5	Light olive gray sandstone and siltstone interbedded with dark olive gray claystone. Bed thickness commonly <1 mm to 5 cm down to 101 ft. Below 101 ft claystone dominates, with occasional sand and silt beds. Cross-bedding is common in sand layers.
109.5 - 111	Medium olive gray limestone; vuggy, with a network of fractures filled with fibrous calcite. Yellow pyrite crystals found in vugs.
111 - 121.5	Dark gray, very fine grained quartz sandstone, moderately consolidated; possibly with clay and/or silica cement. Rip-up clasts of clay and carbonaceous material, cross-bedding present.
121.5 - 131	Medium olive gray, very fine grained quartz sandstone. Well indurated; silica and clay are the dominant cements, but there are zones of calcite cement. Cross-bedding well developed. Rip-up clasts throughout the interval. Small zone of bioturbation or soft sediment deformation.
131 - 140	Light olive gray sand and silt, interbedded with dark olive gray clay. Clay dominates except for a zone between 137 ft and 139 ft. Well consolidated. Moderately bioturbated. (Top 2.3 ft missing)
140 - 152	Light olive gray silt and very fine grained sand interbedded with dark olive gray clay. Pervasively bioturbated. Coarsening, becoming less bioturbated, and more carbonaceous with depth. Clay, and possible silica cement. Core not recovered from bottom of interval.
152 - 166.6	Chocolate colored clay interbedded with light olive gray sandy siltstone. Claystone dominates this interval. Moderately carbonaceous. Moderately to heavily bioturbated.
Manning Clay	
166.6 - 168	Abrupt change to light olive gray sandy clay, which fines downward into a silty claystone. Large burrows in the Manning are filled with dark-colored clay from the Dilworth.
TD = 168 ft	

Table 5 (cont.)

Depth/Interval (feet below surface)	Description of Core 868 (BEG #28)
Soil	
0- 1.75	Olive gray clayey sand and sandy clay. Abundant plant material
Deweesville Sandstone	
1.75-3.5	Moderately indurated light olive gray sandy clay and clayey sand. Abundant gypsum and carbonaceous material.
3.5-10.0	Whitish-gray to light olive gray vfg to fg sandy clay and clayey fg-vfg sand. Limonite and gypsum are relatively common. Minor amounts of greenish-yellow mineral coatings, possibly autunite or meta-autunite.
10.0-14.0	Dominantly indurated, olive gray sandstone. Contains a few fractures coated with Mn oxide and possible plant root casts filled with limonite.
14.0-29.0	Light olive green to light greenish-gray, clayey, unconsolidated, fg to vfg sand. Clay content increases significantly from 28 to 29 ft.
Upper Conquista Clay	
29.0- 40.7	Light olive gray clay and interlaminated silt. Section grades downward to alternating darker and lighter olive silty clay. Abundant limonite, Mn oxide and minor amounts of a fluorescent greenish-yellow uranium mineral occur along bedding and fracture planes.
Redox at 40.7	
40.7-45.0	Medium olive green, clay and interlaminated light olive green silt and vfg sand. Gypsum efflorescence is common.
45.0-57.6	Dark olive green, waxy, carbonaceous clay. Silt laminations are less abundant than above.
Conquista Sand	
57.6-63.0	Sandy, silty clayey shell hash and dark green clay.
63.0-66.0	Fossiliferous, interbedded, dark olive green, siltstone, vfg sandstone and clay. Fossils scarce by 64.7 ft. Abundant carbonaceous material from 65 to 66 ft.
Lower Conquista Clay	
66.0-78.0	Thoroughly bioturbated dark olive green, carbonaceous, clay and intermixed medium olive gray silt. Bedding is disrupted. Load structures are common. Some silt- and sand-filled burrows and load structures contain minor limonite. Minor cross-bedding.
78.0-80.6	Medium olive gray, clayey silt and vfg sand. Section is much siltier and sandier than typical Conquista. Abundant carbonaceous laminations.
80.6-91.0	Interlaminated, burrowed, dark olive green clay, lesser olive gray silt and brownish-black carbonaceous layers. Silty layers are moderately cross-bedded. Section becomes slightly fossiliferous and more clay rich with depth.
91.0-96.0	Slightly silty, massive, greenish-black, waxy clay.

Table 5 (cont.)

96.0-99.8	Lignite
Dilworth Sandstone	
99.8-114	Dark to medium olive green, carbonaceous, crossbedded fg sand, silt and interbedded clay.
114-117	Dark olive green interlaminated clayey silt and silty clay.
TD = 117 ft	

Table 5 (cont.)

Description of Core 869 (BEG #29)

Depth/Interval (feet below surface)	Soil/ Cover
0-3.0	Brownish-black clayey soil grading into a olive gray, limonite stained silty clay at 1.8 ft.
Tailings	
3.0-36.5	Interbedded sandy clay and clayey sand. Abundant limonite and gypsum throughout. Calcite present to a depth of ~15 ft.
Upper Conquista Clay	
36.5-47.0	Tailings / Conquista contact is very abrupt. Upper Conquista Clay is light olive to tan, very altered, heavily stained with limonite. Fine-grained gypsum is ubiquitous. The interval from 45 to 46 ft contains abundant gypsum nodules up to 3.2 cm in diameter.
Conquista Sand	
47.0-59.0	The Conquista Sand ranges from a gypsum-cemented, limonite-stained, sandstone with abundant fossil molds to a medium olive gray to grayish-brown, well rounded and sorted, clean, unconsolidated sand. The sand is consolidated to about 51 ft (poor recovery 51 to 59 ft). Limonite staining abundant from 49.5 ft to 50.5 ft.
Lower Conquista Clay	
59.0-64.0	Light olive tan, silty clay. Abundant limonite and pockets of gypsum.
64.0-68.8	Mottled light tan brown to medium brown, tight bentonitic clay to bioturbated clay and silt. Abundant limonite, Mn oxide and minor gypsum along bedding and fracture planes. Most of the limonite, gypsum and Mn oxide is diagenetic in origin and predates the tailings.
<u>Redox at 68.8</u>	
68.8-73.3	Mottled, greenish-black, bioturbated, carbonaceous, slightly sandy, silty clay. Abundant burrows filled with grayish-white silt and vfg sand.
73.3- 73.6	Indurated, grayish-white siltstone and vfg sandstone.
73.6-77.0	Interbedded greenish-black clay and unconsolidated, olive green, cross bedded, vfg sand.
77.0-86.5	Interlaminated greenish-black, carbonaceous clay and grayish-white siltstone. Intensely bioturbated from 83.0 to 86.5 ft.
86.5-91.6	Relatively massive, greenish-black, carbonaceous clay. Organic material increases downward.
91.6-95.2	Lignite
Dilworth Sandstone	
95.2-99.0	Medium to dark olive green, carbonaceous, silty clay. Contains clasts of clayey sand. Carbonaceous content decreases with depth.

Table 5 (cont.)

99.0-107.0	Interlaminated olive gray clayey sand and sandy, silty clay. Sand content increases with depth.
107.0-116.0	Greenish-brown to greenish-black clay interlaminated with lesser grayish-white silt and vfg sand.
116.0- 121.4	Variably indurated, locally fossiliferous, medium olive gray, slightly carbonaceous, clayey, vfg sandstone. Indurated sections are vuggy. Not calcite cemented.
TD = 121.4 ft	

Table 5 (cont.)

Description of Core 870 (BEG #17)

**Depth/Interval
(feet below surface)****Soil**

0-2.0 Dark brown clayey soil.

Upper Conquista Clay

2.0-5.5 Dark brown to light brown silty clay. The clay is waxy, dense and contains small pods of light green, waxy, bentonitic clay.

5.5-7.3 Grayish-white to light tan silty, slightly sandy, clay. This section contains minor amounts of powdery disseminated CaCO₃. Limonite staining is present along bedding and fracture planes but is not common.

7.3-15.0 Grayish-white to light tan silty clay. Limonite along bedding and fracture planes increasing in abundance with depth.

15.0-23.0 Light olive gray to tan, silty clay. Abundant limonite along bedding planes. Minor Mn oxide associated with limonite.

23.0-29.0 Same as above except the clay is slightly darker and limonite is less abundant.

Conquista Sand

29.0-33.0 Tan to light olive gray sandy clay and clayey sand. Minor limonite, sand content decreases from 31 to 33 ft.

33.0-37.0 Medium tan to light brown, sandy clay and clayey sand.

37.0-51.7 Light olive gray to light tan, limonitic, interbedded clayey, unconsolidated fg sand and lesser sandy clay. Section grades downward into an indurated sandstone with abundant fossil molds.

Lower Conquista Clay

51.7-60.0 Light olive gray to tan, silty clay.

60.0-65.0 Light medium brown silty claystone; color grades downward to reddish brown. Coarse veins of gypsum and associated limonite first encountered at 61.7 ft. Most gypsum veins are parallel to bedding, some are at low angles to bedding.

65.0-67.0 Dark reddish-brown clay. Limonite coated fractures and coarse gypsum veins are abundant.

Redox at 67 ft

67-87.4 Bioturbated greenish-black clay with interlaminated grayish-white silt. Bedding is disrupted in intensely bioturbated areas.

87.4-91.7 Lignite.

Dilworth Sandstone

91.7-93.0 Greenish-black to dark olive gray, bioturbated, interlaminated silt and clay.

93.0-98.0 Medium dark gray to olive gray, clayey, medium- to fine-grained sandstone.

Table 5 (cont.)

98.0-101.4	Similar to above, but grading to interlaminated claystone and siltstone.
101.4-110.0	Greenish-black, slightly silty, claystone.
TD = 110 ft	

Table 5 (cont.)

Depth/Interval (feet below surface)	Description of Core 871 (BEG #20)
Soil	
0-1.8	Dark, clayey, limonitic, gypsiferous soil.
Dubose Clay	
1.8-5.2	Waxy, limonitic, gypsiferous, brownish-black grading downward to light brown, silty clay.
5.2-21.8	Light brown, limonitic, gypsiferous, silty to sandy clay. Sand content increases with depth.
21.8-23.2	Yellowish-brown, limonitic, very sandy clay.
Deweesville Sandstone	
23.2-26.0	Light brown to tan, clayey, unconsolidated, sand.
26.0-30.0	Reddish-brown, silty, clayey, indurated, limonitic, carbonaceous, fg to vfg sandstone. Color of this section derived from oxidation of the relatively abundant carbonaceous material.
30.0-39.0	Light olive gray, silty clayey, fg to vfg indurated sandstone to unconsolidated sand.
39.0-41.0	Reddish-brown, limonite stained, indurated sandstone.
41.0-48.0	Light olive gray to light yellowish-tan, clayey, limonitic, carbonaceous, unconsolidated sand.
48.0-52.5	Olive gray, clayey vfg sand and sandy clay. Clay content increases with depth.
Upper Conquista	
52.5-53.5	Dark brown, carbonaceous clay. Gypsum and limonite veins common along bedding planes.
53.5-54.1	Soft greenish-gray, silty clay. Limonite common along bedding planes.
Redox at 54.1 ft	
54.1-64.0	Dark greenish-gray to greenish-black clay interlaminated with (locally abundant) greenish-gray clayey silt to grayish-white silt. Depending upon silt content, this slightly burrowed, pyritic, clayey section is massive to moderately fissile. Fine-scale cross-bedding is common in the silty layers.
64.0-80.0	Interlaminated greenish-black clay and greenish-gray to grayish-white silt. Silty layers range from < 1mm up to 16 cm in thickness. Bedding of this very silty section is partially disrupted by burrowing, cross-bedding, and load structures. Clay content increases with depth. Mostly greenish-black waxy clay with a few fossil pelecypods by 78.0 ft.
Conquista Sandstone	
80.0-82.8	Very fossiliferous, greenish-black clay and indurated clayey silt and vfg sand.

Table 5 (cont.)

Lower Conquista

82.8-105.7	Very silty, intensely biotubated, greenish-black, waxy clay. Abundant silty burrows and load structures.
105.7-107	Less silty, slightly fossiliferous sand.
107-111.5	Greenish-black, waxy, slightly silty clay. Very little evidence of bioturbation.
111.5-114.5	Lignite. Thin bentonite layer from ~112.3 to 112.45 ft.

Dilworth

114.5-115.7	Very carbonaceous/lignitic, indurated, brown to olive green interbedded clay and siltstone.
115.7-130.0	Olive green to dark olive green, interbedded clayey siltstone, sandstone, and clayey vfg sandstone.

TD = 130 ft

Table 5 (cont.)

Depth/Interval (feet below surface)	Description of Core 872 (BEG #19)
Soil	
0-1.2	Dark clayey organic soil.
Deweesville Sandstone	
1.2-13.0	Light tan to grayish-white, unconsolidated to moderately consolidated, clayey fg sand with a few thin (~2.0 inches) highly silicified layers. Limonite and, to a lesser extent, autunite/meta-autunite are common along bedding planes below 7.5 ft.
13.0-20.75	Light olive gray to grayish-white, clayey, fg-vfg sand. This material grades abruptly to Conquista clay at 20.75 ft.
Upper Conquista Clay	
20.75-35.0	Medium olive green clay with thinly interbedded silt. Abundant limonite. Mn oxide, and greenish-yellow autunite/meta-autunite along bedding planes. First gypsum veins found at 25.0 ft. Gypsum and limonite veins abundant to 35.0 ft.
Redox at 35.0 ft	
35.0-42.7	Greenish-black reducing clay with finely interlaminated olive green silty clay and silt. Load casts, cross-bedding, and burrows are not uncommon. Although bioturbation is not intense, burrowing and loading have given this section a mottled appearance.
42.7-43.0	Very hard calcite-cemented vfg sandstone. Contains a few small layers of coarsely crystalline calcite.
43.0-48.3	Interlaminated olive gray silt and greenish-black clay. Silt is much more abundant than above.
Conquista Sand	
48.3-53.0	Greenish-black to greenish-gray, very fossiliferous (pelecypods and gastropods), calcite-cemented, sandy clay to clayey sand.
Lower Conquista Clay	
53.0-73.0	Greenish-black claystone with interlaminated brownish-gray to grayish-white silt. moderately bioturbated.
73.0-79.6	Greenish-black, moderately fossiliferous, waxy, dense, claystone. Clay shows conchoidal fracture.
79.6-82.0	Lignite.
Dilworth Sandstone	
82.0-83.1	Lignitic, brownish-black, claystone.
83.1-93.0	Strongly to moderately indurated, clean to clayey olive green, vfg-fg sandstone.
93.0-97.0	Unconsolidated, greenish-gray, clayey fg-vfg sand.
97.0-98.2	Greenish-gray silty claystone, interlaminated siltstone, and indurated, calcite-cemented sandstone. Sparse fossil pelecypods.
98.2-100.0	Interbedded grayish-white siltstone, greenish-black claystone and vfg-fg greenish-gray sandstone.
TD = 100	

Table 5 (cont.)

Description of Core 873 (BEG #18)

Depth/Interval
(feet below surface)

Soil

0-2.8 Brownish-black, silty, clayey soil.

Deweesville Sandstone

2.8-5.5 Indurated, light olive gray, limonitic, vfg, clayey sandstone. Scattered patches of powdery CaCO₃.

5.5-21.8 Light olive gray to tan, clayey, vfg to fg sand. Contains a few thin layers of reddish-brown oxidized carbonaceous layers. Scattered patches of CaCO₃ to a depth of 10 ft.

Upper Conquista Clay

21.8-26.0 Light olive gray to tan/light brown, silty clay. Biotite common along bedding planes.

26.0-37.0 Finely interlaminated light to medium brown clay and tan to light olive gray, finely cross-bedded silt. Limonite and Mn oxide coatings are common along bedding planes in the clay. Gypsum and limonite veins parallel to bedding are common between 33.0 and 37.0 ft.

Redox at 37.0,

37.0-46 Greenish-black clay with interlaminated, finely crossbedded, light olive gray silt and lesser vfg sand. Bedding is partially disrupted by moderate bioturbation and possible load structures.

46-54 Same as above except clay content of section is greater and bedding is not disrupted.

Conquista Sand

54-61.1 Dark green, clayey, vfg to fg, fossiliferous, variably calcite cemented, sandstone.

61.1-69.0 Relatively unconsolidated, dark green to dark greenish-gray, clayey, fg to vfg, carbonaceous sand.

69.0-70 Moderately indurated, calcite cemented, very clayey fossiliferous sandstone.

Lower Conquista Clay

70-75.3 Dark green carbonaceous clay and interlaminated light gray silt. Bioturbation is locally intense.

TD = 75.3

Table 5 (cont.)

Description of Core 874 (BEG #21)

**Depth/Interval
(feet below surface)**

Soil

0-3.6 Brownish black, silty clay with abundant small patches of powdery white CaCO₃. Plant material locally abundant.

Dubose Clay

3.6-5.4 Dark tan sandy clay with abundant limonite and CaCO₃. Burrows filled with vfg sand and silt; load structures are common within the dominantly clayey matrix.

5.4-7.0 Light brown silty clay. The clay is waxy, dense with heavy limonite coatings along some bedding planes. Scattered patches of powdery CaCO₃.

7.0-10.0 Dark reddish-brown clay with abundant oxidized organic material. Loosely consolidated.

10.0-20.0 Light olive brown to olive tan slightly silty clay. Abundant bright yellow limonite and minor gypsum.

20.0-39.0 Light olive tan, slightly silty, dense, waxy bentonitic clay. Limonite common along bedding planes and small fractures. Minor oxidized carbonaceous material and gypsum.

39.0-49.0 Light olive tan silty clay with minor interlaminated grayish-white silt. Abundant limonite and lesser black Mn oxide along bedding planes and in small fractures perpendicular to bedding. This interval gets siltier and darker olive tan in color with depth.

49.0-55.5 Medium dark olive brown clay with very thin light gray interlaminated silt. Abundant gypsum and limonite veins between 50.4 and 55.2 ft.

Redox at 55.5 ft

55.5-58.6 Redox boundary at 55.5 ft marked by an abrupt change to dark olive green clay. The clay is interlaminated with very thin layers (1-2 mm) of light olive green silt and vfg sand.

58.6-59.0 Same as above except sand content increasing significantly with depth.

Upper Deweesville Sand

59.0-68.0 Dark olive green, very clayey, carbonaceous, pyritic fg sand.

68.0-69.3 Lignite.

Lower Deweesville Sand

69.3-77.0 Clean, vfg to fg, carbonaceous, moderately to strongly indurated, olive gray sandstone. Glauconite, zeolites, pyrite, silica cement, muscovite and biotite are important minor components.

77.0-86.0 Dark olive gray moderately to slightly clayey, unconsolidated, carbonaceous sand. Minor glauconite, pyrite, biotite, and muscovite.

86.0-94.0 Dark olive gray, unconsolidated, clayey sand. Clay content increases downward, grading to dark greenish-black sandy clay by 92.0 ft.

Table 5 (cont.)

Upper Conquista Clay

94.0-121.1 Interlaminated light gray silt and greenish-black clay and silty clay. Small-scale cross-bedding, scour structures, load structures, and minor burrowing. Typical silt laminations range from 1.0 to 10.0 mm thick.

Conquista Sand

121.1-124.1 Very clayey, calcite cemented, fossiliferous, dark greenish-gray, vfg to fg sandstone and siltstone.

Lower Conquista Clay

124.1-132.0 Bioturbated, very silty, carbonaceous, dark greenish-black to brown clay. Load structures, and silt-filled burrows are abundant. Silty zones are grayish-white in color and decrease in abundance from 129–132 ft.

132.0-136.0 Slightly silty, greenish-black, carbonaceous, bioturbated clay. The section from 130-132 is coated by a fibrous mat of greenish-yellow elongate crystalline fibers. This mineral fluoresces yellow to greenish-yellow.

136.0-148.5 Very silty, carbonaceous, bioturbated, greenish-black clay. Silty zones and silt-filled burrows are grayish-white to light gray in color.

148.5-154.0 Slightly silty, greenish-black claystone. This section is slightly fossiliferous, carbonaceous, and bioturbated.

154.0-156.5 Lignitic clay and lignite.

Dilworth Sandstone

156.5-158.0 Strongly indurated, very carbonaceous, vfg olive brown sandstone.

158.0-160.0 Indurated, dark olive greenish-gray, glauconitic, pyritic, carbonaceous sandstone.

160.0-161.6 Clayey, olive gray, carbonaceous, silt.

TD = 161.6

Table 5 (cont.)

Description of Core 875 (BEG #30)

Depth/Interval
(feet below surface)

Soil

0 - 2.3 Brownish-black to black clayey soil with abundant disseminated calcite.

Conquista Sand

2.3 - 3.5 Light olive tan, silty, vfg sandy, limonitic bentonitic clay. Abundant small veins and pods of fine-grained calcite. Sandier with depth.

3.5 - 7.0 Grayish-white to olive tan clayey fg to vfg sand. Carbonaceous material present. Limonite is common. Relatively friable; not cemented. Small amount of calcite present.

7.0 - 8.0 Light gray, very hard, CaCO₃-cemented, clayey sand and silt. Possible CaCO₃ concretion.

8.0 - 16.0 Sparsely limonitic, light olive gray to tan, unconsolidated clayey sand to sandy clay. Has a highly altered (bleached) appearance.

16.0 - 20.0 Light olive gray to tan, limonitic, indurated fg sandstone and interbedded bentonitic clay. This interval tends to form partings along the contacts of the clay and sandstone.

20.0 - 20.3 Very sandy, limonitic, olive tan to light brown clay.

Lower Conquista Clay

20.3 - 25.0 Light brown to tan brown limonitic sandy, silty, clay. This highly altered section contains abundant burrows.

25.0 - 30 Medium brown to olive gray, silty clay. Some evidence of bioturbation has been preserved. Burrows filled with light gray silt and vfg sand are not uncommon. Limonite typically coats the contact of the burrows and the surrounding clay. Coarse-veined selenite and associated limonite common below 28.5 ft.

30.0 - 36.0 Moderately bioturbated, brown, waxy, dense, clay with interlaminated light gray to grayish-white silt. Contains abundant selenite veins and associated limonite up to 1/3 inch thick along bedding planes and along fractures at a low angle to bedding. Limonite content decreases downward, relative to gypsum.

Redox at 36.0 ft

36.0 - 42.0 Dark greenish-gray to greenish-black carbonaceous clay and abundant light gray silt to vfg sand. Bedding is disrupted by loading and moderate to intense bioturbation. Silt typically occurs as thin laminae, burrows, load structures, and as swirls within the clay. No selenite veins found below the redox boundary except in a thin, partially oxidized, organic section from 36.8 to 37.4 ft.

42.0 - 50.0 Greenish-black clay with interlaminated fine-scale, cross-bedded, grayish-white silt. Some silty burrows are present but the bedding is generally not disturbed.

Table 5 (cont.)

50.0 - 54.0	Very silty, intensely biotubated, greenish-black clay. Contains abundant burrows and load structures filled with grayish-white silt.
54.0 - 59.0	Massive greenish-black clay and minor silt. Carbonaceous content increasing downward.
59.0 - 63.4	Lignite, grades to very carbonaceous clay at 63.4 ft. White bentonitic layer from approximately 60.2 to 60.4 ft.
Dilworth Sandstone	
63.4 - 68	Grayish-olive green, clayey, indurated, siltstone and lesser vfg sandstone.
68 - 74	Gray to dark olive gray indurated siltstone, vfg sandstone to soft, friable, silt and sand interbedded with silty laminated greenish-black carbonaceous clay.
74 - 84	This section is sparsely burrowed and is composed of cross-bedded, grayish-green to light gray silt and siltstone interbedded with greenish-black, carbonaceous, clay. Individual silty layers range from <1.0 mm to ~5.0 cm in thickness.
84 -106	Due to the unconsolidated nature of this section, much of it was washed out during coring. According to core recovered, this section is composed primarily of unconsolidated vfg clayey, grayish-green, carbonaceous sand locally interbedded with lesser amounts of greenish-black, waxy clay.
106 -114	Very finely interlaminated greenish-black, carbonaceous clay and grayish-white, clayey silt (typically <1.0 mm in thickness). This finely laminated silty clay locally contains interbeds of clean friable fg to vfg sandstone up to 1.0 ft in thickness.
114 -117	Bioturbated greenish-black clay and indurated, silica cemented, gray siltstone.
117-129	Strongly indurated, clean, dark olive gray fg sandstone interbedded with clayey, moderately indurated, carbonaceous, medium to dark olive green fg to vfg sand. Clay content of section increases downward.
129-139	Intensely bioturbated, greenish-black clay with abundant pods and patches of grayish-white silt and vfg sand.
139-142	Greenish-black claystone with minor silt filled burrows and grayish-white silt laminae.
142-145	Bioturbated, dark greenish-gray, carbonaceous, silty, vfg sandy clay and clayey vfg sand. Burrows contain silt and vfg sand.
145-149	Greenish-black carbonaceous clay with minor silt and vfg sand.
149-152	Intensely bioturbated, very silty, sandy greenish-black clay.
152-153.5	Greenish-black clay, increasingly carbonaceous with depth.
153.5-154.1	Lignite.
154.1-154.9	Clayey, silty, medium gray limestone.
154.9-156.6	Very carbonaceous black clay grading to a lighter bentonitic clay at 156.6 ft.

Table 5 (cont.)

Manning Formation

156.6-160

Carbonaceous, light green bentonitic clay. Dries to a light tan-beige.

TD = 160 ft

Table 5 (cont.)

Description of Core 876 (BEG #16)

**Depth/Interval
(feet below surface)**

Soil

- 0 - 2 Tan to olive tan, silty, sandy clay soil.
- 2 - 4 Grades from tan clayey sand to dark brown organic clay, with abundant plant roots, caliche veins and coatings.
- 4 - 5.5 Abundant olive gray silty clay fragments in a black organic clay matrix. Grades to an olive tan silty clay at 4.5 ft; abundant limonitic coatings along bedding planes. Caliche coatings present. Very fine grained powdery CaCO₃.

Upper Conquista Clay

- 5.5 - 10 Dense waxy olive tan slightly silty clay with a few thin silty layers. These silty layers are often limonitic. There are numerous silt-filled elongate burrows up to 1.2 inches in length, circular in cross section. The silt-filled burrows are limonitic. Abundant yellow green uranium mineral coatings associated with the limonite on bedding planes. Less commonly, this coating is also present along vertical fracture planes (limonitic plant fragments are locally abundant along a few bedding planes). Uranium coatings less abundant with depth.
- 10 - 25 Olive tan slightly silty clay darkens slightly with depth. Brown layers of clay within this overall olive tan section increase downward. Abundant limonitic veins along bedding planes and fractures at an angle to bedding. The first gypsum and limonite vein is found at 24.0 ft; above this, only limonite veins without gypsum are present. No yellow-green mineralization observed.
- 25 - 29 Olive tan to brown clay. Olive tan layers and brown layers are subequal in volume.
- 29 - 29.8 Olive brown to brown limonitic clay.

Conquista Sand

- 29.8 - 33 Olive tan to orange tan clayey fine-grained sand and sandy clay. Very abundant limonite and minor hematite. Abundant fossil molds from 29.8 ft to 31 ft. Some fossil molds filled with gypsum, which is abundant throughout the section, although it is not the dominant cement.
- 33 - 46.2 Cemented to loose limonitic clayey sand. Gypsum and limonite veins present in more clayey sections of the sandstone. Some organic-rich sections are brown. Last 0.2 ft of the Conquista Sand is silica cemented; very hard. Beginning of transition to reducing zone; cemented sand is partially altered. Color is olive gray.

Lower Conquista Clay

- 46.2 - 46.4 Oxidized olive tan lower Conquista silty clay with gypsum and limonite veins. Oxidized carbonaceous material.

Redox at 46.4 ft

Table 5 (cont.)

46.4 - 48.1	Olive gray (reduced) hard, waxy claystone, with lenticular and parallel laminations of very fine grained sand and silt (1 mm–1 cm); Silt and sand layers are light olive gray. Slightly bioturbated.
48.1 - 53.9	As above, but with convolute laminations; more bioturbation.
53.9 - 58.1	As above, but with much less silt and sand. Silt layers are wispy, lenticular (1–2 mm).
58.1 - 68.6	Olive gray claystone, but with more silt and sand than above. Laminations are convoluted as a result of bioturbation, and possibly soft-sediment deformation and flow structures. Coarsening with depth.
68.6 - 71.4	Olive gray laminated claystone as above, but with parallel to wavy silt and sand laminations (<1 mm–0.5 cm); clay and silt dominate. Some cross-bedding, and ripple marks in silt layers. Finer grained with depth. Very slightly bioturbated.
71.4 - 75	Olive gray claystone as above, with convoluted silt laminations, ripple marks, trough cross bedding, lenticular silt laminations, possible bioturbation. Finer grained with depth.
75 - 81.4	Silty claystone with very sparse lenticular silt laminations; sparsely fossiliferous: pelecypod shell fragments. Becomes increasingly carbonaceous with depth, becoming dark chocolate to black in color. Interbedded with lignite from 80.6 to 81.2 ft. Tan (bentonitic?) sandy clay nodule at 81.3 ft with abundant biotite.
81.4 - 83.5	Lignite: black, hard, dense; becoming clay rich at 82.6 ft, more lignitic at 82.9 ft, and grading abruptly into a sandy claystone.
Dilworth Sandstone	
83.5 - 86.4	Light olive gray, very fine grained quartz sandstone; well indurated. Silty and clayey laminations, commonly carbonaceous, lenticular. Small-scale cross-bedding present, as well as some bioturbation.
86.4 - 91	Medium olive gray silty and clayey very fine grained quartz sandstone, poorly consolidated. Indistinct "crenulated" silty laminations and numerous carbonaceous partings.
91 - 109.6	Dark olive gray claystone interbedded with medium olive gray siltstone and very fine grained quartz sandstone. Several 1 ft clayey sand layers; otherwise the laminations are <1–5 cm. Cross-bedding, ripples, scour marks, and lenticular sands (starved ripples) are present in sand and silt layers. Becoming finer with depth.
109.6 - 113.8	Medium olive gray very fine grained quartz sandstone, well to poorly consolidated, with <1 to 2 cm silt and clay wavy laminations, becoming more bioturbated with depth. Fossiliferous (shell fragments) and carbonaceous. Shells are replaced with a transparent, orange mineral. Indurated sand cemented with quartz and calcite. Poorly consolidated sands are cemented with clay.
113.8 - 125.3	Dark olive gray claystone interbedded with light olive gray siltstone and very fine grained quartz sandstone. Moderately to thoroughly bioturbated. Generally becoming finer with depth. Carbonaceous and fossiliferous (shell fragments), particularly in the sandy layers.

Table 5 (cont.)

125.3 - 140.4	Medium to light olive gray very fine grained quartz sandstone, well to moderately consolidated; quartz and clay cemented. Relatively massive; sparse and indistinct silt and silty clay laminations (<1 cm).
140 - 144.4	No core recovered.
144.4 - 152	(Precise depth of recovered core uncertain; only 3.7 ft recovered.) Medium to light olive gray clayey quartz sandstone. Poorly consolidated, clay cemented. Clayier layers are dark olive gray.
152 - 174.6	Medium olive gray clayey quartz sandstone. Moderately to poorly consolidated; silica and clay cement. Intensely bioturbated, but becoming less so and finer grained with depth. Carbonaceous partings present in finer grained zone.
174.6 - 184.1	Dark olive gray claystone, interbedded with light olive gray silt and very fine grained sand. Clay dominates top 2 ft of interval, with lenticular sand bodies, commonly containing carbonaceous cores. Becoming coarser and more intensely bioturbated with depth. Burrows are common. Sparsely carbonaceous. Some possible soft-sediment deformation.
184.1 - 187.1	Dark olive gray clay, as above, sparse sand and silt filling large burrows. Becomes increasingly carbonaceous with depth.
Manning Clay	
187.1 - 193.6	Olive green to olive gray silty claystone becoming grayer with depth. Carbonaceous and clay-rich burrows or roots at varying orientations. Two 10-cm lignite layers, have tops at 187.1 and 188.85 ft, respectively. A 1 ft silt-rich zone, light olive gray, from 192.5 ft to 193.5 ft grades into a sandy silt at TD
TD = 193.6 ft	

Table 5 (cont.)

Description of Core 877 (BEG #27)

**Depth/Interval
(feet below surface)**

0 - 5.5 White clayey quartz sandstone, very fine grained, clay cemented, with some limonite cement and minor biotite. Fissile, with a few 1–2 mm clay layers, but the laminations are disordered.

5.5 - 10.2 Sandy clay and siltstone; sand is very fine grained, and dominantly quartz (<5% feldspar and mafic minerals). Clay is a light olive gray; sandstone and siltstone are light tan to white. Bedding is disordered; clay, limonite and calcite follow the convolutions in the bedding, creating a marbled appearance. May be the result of loading, or perhaps this is fill material from the nearby road.

Deweeseville Sandstone

10.2 - 19 Abrupt change to a white clayey quartz sand, very fine grained. Clay and silica cemented. Bedding is convoluted to 12 ft; there are clay clasts which have no preferred orientation. Below 12 ft, there are indistinct laminations, but in general the sand is fairly massive. Limonite and yellow-green (possibly uranium) minerals are apparent, mostly along bedding planes, but also in swirls within the beds. Limonite appears more disseminated through the rest of this interval. Laminations reappear at 18 ft as 1–2 mm clay layers, some of which appear carbonaceous. Some cross-bedding is evident in the silt and sand layers.

19 - 23 (Only 1 ft recovered) Light olive gray sandstone, very fine grained. Much more clay-rich than the previous interval. Clay (and possibly gypsum) cement; friable. Cross-bedded.

23 - 27.7 White to light olive gray clayey quartz sandstone, very fine grained, probably clay cemented. Not well consolidated. Cross-bedded.

27.7 - 29.8 Light olive gray, very clayey quartz sand, grading downward into a clayey siltstone by 29 ft. Moderately well consolidated. There is abundant limonite mineralization, mostly along bedding planes, but also along fracture planes subparallel to bedding. Earthy black Mn oxide and yellow-green autunite or meta-autunite commonly present with the limonite. The limonite is generally much less common in the sandier layers.

Upper Conquista Clay

29.8 - 36.8 Clay, silt and sandstone are interbedded and cross-bedded. Individual beds range from 1mm to 4 cm; clay beds are medium olive gray, silt and sand beds are white to light olive gray. Limonite is abundant. Gypsum is present along fracture planes, but is less abundant along bedding planes. All beds darken with depth.

36.8 - 43 Interbedded silt and clay: clay is dark olive green, and silt is light olive green. Laminations range from 1 mm to 5 cm; occasional load clasts evident. Deepest appearance of limonite is at 37.4 ft. Reducing clay and silt below this.

Redox at 37.4 ft

Table 5 (cont.)

43 - 56

Olive green (reducing) interbedded silt and clay, with occasional small (1-2 cm) sandstone beds. Bedding is disrupted by loading structures and a moderate amount of bioturbation. Fossil molds of shells, infilled with gypsum are sparsely present. Laminations and cross-bedding become more distinct toward the bottom of the interval.

Conquista Sand

56 - 60

Light olive gray siltstone interbedded with dark olive gray claystone. Intensely bioturbated, although some laminations are evident at the top and bottom of the interval. Fossiliferous throughout the interval, becoming very fossiliferous by 60 ft. Fossils are present as casts and molds, but mostly as original shell material.

TD = 60 ft

Table 6. UMTRA well locations, elevations, and stratigraphic tops.

Well Id	y	x	Is	elevation	Top Tailings	Top Dubose	Top Deweesv	Top U Conq	Top Conq Sd	Top L Conq	Top Dilworth	Top Manning	Total	Depth
0601	60300.7	64293.8		463	463			443						28
0602	61610.4	65545.8		468	468			458						34
0607	61181.6	63847.9		482	482			454						40
0617	59670.0	64045.3		433				433						40
0625	60916.5	66302.3		446	446		436							37
0651	58874.3	64945.1		431	431		418							30
0662	60904.9	67576.4												
0664	51494.2	65930.0												
0665	53661.5	69447.8												
0666	61796.9	75642.5												
0676	57482.8	65996.5		407			407	388	358	354	317	236		40
0677	58605.8	68470.7		428			388	368	338	322	303			80
0678	56867.4	66425.9		410										60
0679	61878.1	60978.3		453				453	422	398	361			130
0680	60882.5	72627.2		402										
0701	62505.6	64471.5		439					439	414				40
0709	63214.4	63945.1		446					446	418				37
0712	62806.5	65662.5		433				433						38
0713	60772.9	63281.7		469				469	448	433				40
0799	61656.9	66296.5		447			447							40
0831	60573.3	65806.9		445	445		440	410	385	370	340			160
0832	63440.0	64332.4		436					436	421	366	286		152
0833	58228.7	65838.4		422	422		412	382	356	342	320			155
0834	60165.1	64892.5		464	464		462	449	417	?	346			153
0835	59347.4	65335.2		446			446	431						40
0836	60698.1	65156.8		461			461	451						40
0901	58597.7	68461.8		428		428	391	361	338	326	300			145
0902	57503.8	65983.9		407			407	379	358	350	317			152
0903	57493.3	65971.6		407			407	379	358	350	317	236		218
0904	57170.9	64874.5		399			399	388						28
0905	57169.7	64865.3		399			399	388	354	344	317			90
0906	58670.9	63758.4		419				419	419	401				30
0907	58658.6	63744.5		419				419	419	401	367	265		150
0908	61478.2	61847.5		494				494	469	445				75
0909	61497.2	61852.3		494				494	469	445	411			120
0910	61483.7	61836.1		494				494	469	445	411	323		197
0911	64502.7	64021.9		418						418	410			20
0912	64493.9	64006.8		418						418	410	336		125
0913	59086.4	67228.0		423			423	398						50
0914	61381.5	66677.1		434			434	419						20
0915	61371.9	66687.6		434			434	419	398	383	349			110
0916	62972.9	66711.4		419				419	407	385	352			35
0917	62979.9	66715.1		419				419	407	385	352			90
0918	56863.7	65174.6		403			403	393						40
0919	56737.4	64209.9		400					400	387				40
0920	56731.4	64229.0		400					400	387	352			80
0921	61389.4	66693.5		434			434	419	398	383	349			57
0922	57056.5	67960.9		441			441	393						80
0923	56118.3	63170.5		405					405	388				20
0924	55041.9	64049.8		395				395	377	366				31

Table 6 (cont.)

Well Id	y	x	Is	elevation Top	Tailings	Top Dubose	Top Deweesv	Top U Conq	Top Conq Sd	Top L Conq	Top Dilworth	Top Manning	Total	Depth
0925	64843.2	63664.0		416						416	409	336		90
0935	63088.5	70710.1		422	422		392	390	370					35
0940	62586.7	69677.9		424	424		395	393						39
0945	62071.2	67687.5		438			438	410	391	373	346			139
0951	60334.9	68978.5		436		436	403	377	363					90
0952	60339.5	68984.6		436		436	403	377	363					50
0953	62028.6	71914.1		415		415	393	363	343	332				100
0954	63162.9	71323.4		410			410	379	359	?				60
0955	63099.6	69449.2		393					388	367	340			30
0956	63104.3	69434.6		393					388	367	340			70
0957	63435.2	68807.7		387					383	365	350	255		15
0958	63430.1	68799.7		387					383	365	350	255		150
0961	63815.1	70828.5		382					382	367	333			60
0962	64140.1	70535.8		373						373	343			40
0963	64639.8	70391.3		369					369					20
0964	64926.2	69745.4		378						378	357	293		90
0965	65773.8	70672.5		367						367	361			20
0966	65378.4	70988.1		369					369	355				25
0967	66836.5	65846.0		430							430	350		110
0968	64511.4	62105.5		434						434	418			80
0969	57396.1	62190.4		440				440	425	410	373			110
0970	57410.0	62203.8		440				440	425	410	373	312		159
0971	55530.0	64106.4		390				375	360	350	322			95
0973	55362.3	66834.0		436		436	416	370	345	341	291	238		230
0974	55370.6	66813.3		436		436	416	370	345	341	291	238		170
0975	60037.0	70540.8		450		450	372	335	314	309	265			210
0976	66683.6	71637.0		359							351			100
0977	66667.7	71651.7		359							346			40
0978	64822.2	63668.7		415						415	410	320		140
0979	65119.2	65944.6		418						418	378			102
0851	59877.7	67424.6		432		428	424	395						50
0852	59902.0	66684.6		438			437	401						47
0853	58402.9	67051.2		415			410	382						40
0854	57716.3	65230.6		410			405	387						33
0855	55580.2	65392.1		412			411	393						35
0856	61631.1	65281.8		458			458	451	422	392				80
0857	60451.4	67319.2		442			437	412	377					73
0858	60184.4	65945.2		442			442	415	401	387				80
0859	58209.3	64798.2		426			425	399	391	383	349			79
0860	58361.8	67690.2		420		416	400	375	350					83
0861	56466.9	65333.3		415			392	389	363	358				70
0862	58816.9	65415.5		437			433	404	376	373	340			150
0863	57986.4	66138.6		416			416	394						45
0864	58028.6	67276.2		416		412	396	372	346	341	311			106
0865	55659.6	64803.2		415			414	404	378	372				60
0866	60374.5	67198.7		443		443	440	400						46
0867	56764.4	65276.2		408				391	361	358	326	241		168
0868	60839.4	66252.9		445			443	416	387	379	345			117
0869	61668.9	64537.9		469	466			432	422	410	374			121
0870	60494.5	63339.9		473				471	444	421	381			110

Table 6 (cont.)

Well Id	y	x	ls elevation	Top Tailings	Top Dubose	Top Deweesv	Top U Conq	Top Conq Sd	Top L Conq	Top Dilworth	Top Manning	Total	Depth
0871	58672.0	68073.8	422		420	399	381	342	339	307			130
0872	55630.2	64917.2	420			419	399	372	367	338			100
0873	60405.2	65278.0	456			453	434	402	386				75
0874	58062.5	68789.1	441		437	382	347	320	317	284			162
0875	62304.9	64184.3	446					444	426	383	289		160
0876	59175.1	64429.0	439				433	409	393	355	252		194
0877	58781.7	65317.1	433			423	403	377					60
878	61659.2	65240.8	458	458			451	418	388				122
879	57625.5	67600.5	422		418	378							65
nl 65	61291.0	62511.0	488				488	463	441	406	302		
nl 77	60112.0	62136.0	468				468	458	431	390	307		
nl 81	58982.0	61701.0	494			494	481	466	452	414	311		
nl 67	58601.0	62479.0	467				467	454	435	398	295		
nl 68	58226.0	62486.0	475			475	458	441	425	383	282		
nl 70	57453.0	62459.0	435				435	422	405	365	269		
nl 186	57053.0	62865.0	420				420	413	399	335	252		
nl 179	57856.0	63627.0	418				418	411	392	360			
nl 177	57116.0	63577.0	416				416	405	390	354	246		
nl 172	57501.0	63970.0	408				408	403	390	355			
nl 180	56310.0	63586.0	410				406	362	350	337			
nl 113	56699.0	63991.0	402					395	391	353	268		
nl 176	55938.0	64001.0	392				383	359	344	332			
sn 82	62675.0	65790.0	429				429	411	394	363	284		
sn 78	63097.0	66123.0	440				440	428	410	376	292		
sn 71	63495.0	66516.0	430				430	414	408	375	291		
sn 62	63925.0	66857.0	425				425	421	405	372	286		
sn 81	62295.0	65901.0	427				422	402	391	368	287		
sn 68	62314.0	66584.0	423				423	408	385	366	281		
sn 50	63150.0	67282.0	405				405	397	376	357	271		
sn 17	63181.0	67698.0	399					399	378	356	268		
sn 101	63607.0	68040.0	399					396	380	354	269		
sn 112	63642.0	68428.0	390					373	358	344	259		
sn 111	63296.0	68415.0	391					386	369	352	268		
sn 110	62986.0	68403.0	400				400	397	377	340	265		
sn 16	62889.0	68070.0	410				410	403	385	359	277		
sn 86	62439.0	67764.0	435			433	421	405	388	366	271		
sn 120	62325.0	66976.0	430				430	418	406	374			
sn 54	61946.0	66990.0	443			443	425	406	389	367	278		
sn 72	61524.0	66617.0	440			440	412	390	375	343	266		
sn 64	61284.0	67077.0	430			430	416	395	392	374	275		
sn 113	61780.0	68518.0	408				402	383	369	343	250		
sn 14	62206.0	68880.0	399				399	391	376	348	263		
sn 123	62492.0	69143.0	390			390	381	365	365	335	242		
sn 122	63016.0	68831.0	393					393	373	360	266		
sn 98	60993.0	67789.0	425			425	416	385	377	354	233		
sn 66	60637.0	67264.0	442		442	430	410	383	374	342	253		
sn 95	60175.0	67821.0	435		435	425	405	378	371	338	247		
sn 105	60584.0	68187.0	428		428	421	403	376	369	330	244		
sn 115	60631.0	68571.0	433		433	420	397	385	375	339	244		
sn 107	59822.0	68280.0	450		450	415	389	369	356	330	238		

Table 6 (cont.)

Well Id	y	x	Is elevation Top	Tailings	Top Dubose	Top Deweesv	Top U Conq	Top Conq Sd	Top L Conq	Top Dilworth	Top Manning	Total Depth
sn 116	60240.0	68609.0	442				442	435	417	391	309	
sn 132	60677.0	69366.0	415		415	405	381	360	350	321	229	
sn 133	60724.0	69747.0	420		420	395	372	346	339	312	218	
sn 117	59833.0	68652.0	448		448	411	382	360	347	322	230	
sn 144	59895.0	69424.0	434		434	399	371	349	345	316	227	
sn 138	60321.0	69765.0	427		427	389	361	340	334	305	216	
sn 139	60344.0	70153.0	435		435	386	357	333	324	297	209	
sn 147	59551.0	69811.0	442		442	384	353	333	320	297	215	
sl 106	65187.0	67901.0	410						410	366	265	
sl 93	64459.0	68758.0	410					410	395	363	283	
sl 81	63805.0	69117.0	384					363	355	326	240	
sl 71	63848.0	69537.0	378					365	359	346	251	
sl 62	63472	69904	400				400	393	373	353	264	
sl 64	63499	70307	410				410	404	384	364	275	
sl 21	61966	70790	409		409	406	372	348	330	310	229	
sl 20	62380	71167	405		405	399	367	343	330	306	222	
sl 34	62781	71536	409		409	401	376	352	341	316	239	
sl 12	61567	70837	417		417	397	366	342	330	316	218	
sl 14	61613	71608	417		417	391	361	338	327	297	195	
sl 3	72000	60800	430		430	379	345	323	318			
c 21	57596	65210	405			405	381	343	330	298		
c 22	57570	64907	405			405	382	346	333	299		

Table 7. Gamma-ray anomalies on borings at Falls City UMTRA site.

Well no.	Dubose	Deweeseville	Upper Conquista	Conquista sandstone	Lower Conquista	Dillworth
601						
602						
607						
625		1000				
651		1000				
671		1000				
677		1000	500			
679			-	-	600	-
701				-	250	
709				-	600	
712		-	300			
713			450	-		
831		1000		900	-	1000
832				300		
833		1000				
834		1000				
835		1000				
851	140	170				
852		1000	140			
853		160	130			
854		500	-			
856		300	300			
857	-	150				
858			130	-		
859		500	-			
860	80	120	80	-		
861		500	-	-		
862		180	370	-		
863		800	500	-		
864		170	130	-	-	-
865		300	300			
870			-	-	-	-
874	100	300	120	-	-	-
901	-	900	360	-	-	-
902		1800	-	-	-	-
903		1200	1600	-	-	-
904			800			
905		300	650			
906				240		
907				200	-	-
908		-	390	-		
909		-	300	-	-	-

Table 7 (cont.)

Well no.	Dubose	Deweeseville	Upper Conquista	Conquista sandstone	Lower Conquista	Dillworth
910		-	330	-	-	-
912			460			-
913		600	900			
915		650	1000	450		-
917		-	-	600	-	-
918		1800	-			
920				315	-	
945			1000	350	-	-
951	1400	2400	-			
953		700	-	-	-	
954		2400	2400			
956				300	-	-
958			370			-
961			330			
962				51		

Table 7 (cont.)

Well no.	Depth (ft)	Formation	Max Gamma (cps)
601		tailings	
602		tailings	1000
607		tailings	1000
625	14	Dew	1000
625	30	Dew	1000
651	12	Dew	1000
651	16	Dew	1000
676	10-25	Dew	1000
677	40	Dew top	1000
677	?	Conq	500
677	65	Conq	480
679	63-86	Conq low	580
679			600
679			550
701	25	Conq ss/l	250
709	20	Conq l	600
712	30	Conq	300
713	15	Conq u	450
831	2-5	Dew	1000
831	100	Dil	1000
831	105	Dil	1000
832	20-24	Conq ss	300
833	9-32	Dew	1000
834	13-30	Dew	1000
835	20	Dew	1000
851	10	Dub	140
851	26	Dew	170
852	14	Dew	1000
852	20	Dew	130
852	40	Conq	140
853	14	Dew	130
853	28	Dew	160
853	34	Conq	130
854	14	Dew	500
855	9	Conq	100
856	10	Dew	300
856	19	Conq	300
856	4	Dew	340
856	16-22	Dew	180
857	22	Dew	150
858	29	Conq	130
859	12	Dew	500
860	22	Dub	80
860	38-44	Dew	120

Table 7 (cont.)

Well no.	Depth (ft)	Formation	Max Gamma (cps)
860	48	Conq	80
861	10	Dew	400
861	16	Dew	500
861	24	Dew	650
862	2-8	Dew	180
862	30-40	Conq	370
863	6	Dew	200
863	14	Dew	400
863	18	Dew	800
863	29	Conq	500
864	37	Dew	170
864	45	Conq	130
865	10	Dew	300
865	18	Conq u	300
870	0-182	Conq-Dil	0
874	10	Dub	100
874	70	Dew	300
874	85	Conq u	120
901	38	Dew top	900
901	54-60	Conq up	360
902	5-30	Dew	1800
903	15	Dew	1200
903	25	Conq	1600
904	15	Conq ss?	800
905	10	Conq ss?	650
906	8	Conq ss	240
907	21	Conq ss	200
908	17	Conq	390
909	18	Conq	300
910	12	Conq	330
912	16	Conq u	460
913	10-25	Dew	600
913	28	Conq u	900
915	15	Dew	650
915	22	Conq u	1000
915	52	Conq ss	450
917	33	Conq ss	600
918	5-18	Dew-Conq	1800
919	14	Conq ss	360
920	13	Conq ss	315
945	13	Conq u	1000
945	25	Conq u	1000
951	33	Dew top	2400
951	54	Dew	360

Table 7 (cont.)

Well no.	Depth (ft)	Formation	Max Gamma (cps)
953	48	Dew	700
954	10-26	Dew	2400
956	25	Conq ss	300
958	10	Conq	370
961	25	Conq ss	330
962	13-22	Conq l	51